



Mitxitorena, Izaskun (2019) *In vitro studies on the recognition of NF- κ B p65 subunit by the deubiquitinase enzyme USP7*. PhD thesis.

<https://theses.gla.ac.uk/40917/>

Copyright and moral rights for this work are retained by the author

A copy can be downloaded for personal non-commercial research or study, without prior permission or charge

This work cannot be reproduced or quoted extensively from without first obtaining permission in writing from the author

The content must not be changed in any way or sold commercially in any format or medium without the formal permission of the author

When referring to this work, full bibliographic details including the author, title, awarding institution and date of the thesis must be given

Enlighten: Theses

<https://theses.gla.ac.uk/>
research-enlighten@glasgow.ac.uk

***In vitro* studies on the recognition of NF- κ B p65 subunit by the deubiquitinase enzyme USP7**



Submitted in fulfilment of the requirements for the degree of Doctor of Philosophy

Izaskun Mitxitorena MSc

September 2018

College of Medical, Veterinary and Life Sciences
Institute of Infection, Immunity and Inflammation
University of Glasgow

Supervisors: Dr Ruaidhrí J. Carmody (University of Glasgow)
Professor Carl S. Goodyear (University of Glasgow)

Table of Contents

Author's Declaration	7
Acknowledgements.....	8
Abstract	9
List of Tables	10
List of Figures	12
List of Abbreviations	16
1 General introduction	27
1.1 Overview	27
1.2 NF- κ B transcription factor family	27
1.2.1 NF- κ B members	28
1.2.2 NF- κ B members structure	32
1.2.2.1 p65 subunit structure	34
1.3 NF- κ B regulation	37
1.3.1 NF- κ B activation	37
1.3.1.1 Signalling pathways	38
1.3.1.1.1 Canonical pathway	38
1.3.1.1.2 Non-canonical pathway	38
1.3.2 Posttranslational modifications	40
1.3.2.1 Phosphorylation	42
1.3.2.2 Acetylation	43
1.3.2.3 Methylation	44
1.3.2.4 SUMOylation	45
1.3.2.5 Ubiquitination	45
1.3.2.6 PTMs crosstalk.....	45
1.3.3 NF- κ B inhibitors.....	46
1.4 Ubiquitination in the regulation of the NF- κ B response	54
1.4.1 The ubiquitin proteasome system	54

	2
1.4.1.1	E3 ligases 59
1.4.1.2	Deubiquitinase enzymes 59
1.4.1.3	UPS inhibitors 61
1.4.2	Ubiquitination in the NF- κ B signalling pathways..... 64
1.4.2.1	E3 ligases 69
1.4.2.2	Deubiquitinating enzymes 71
1.4.3	USP7 72
1.4.3.1	Structure 72
1.4.3.2	Function and substrates 74
1.4.3.3	USP7 inhibitors 76
1.4.3.4	Substrate specificity and binding pockets 78
1.4.3.5	p65 interaction and deubiquitination..... 79
1.5	Thesis aims 80
2	Material and Methods..... 82
2.1	Cell biology techniques 82
2.1.1	Mice..... 82
2.1.2	Cell culture 82
2.1.2.1	Maintenance 82
2.1.2.2	Bone marrow derived macrophages..... 82
2.1.2.2.1	Bone marrow isolation..... 82
2.1.2.2.2	BMDM differentiation and stimulation experiments..... 83
2.1.2.3	Cryopreservation..... 83
2.1.2.4	Plating conditions..... 83
2.2	Molecular biology techniques 84
2.2.1	DNA transformation for routine plasmid preparation 84
2.2.2	Plasmid preparation..... 84
2.2.2.1	Midiprep..... 84
2.2.2.2	Miniprep..... 84

2.2.3	Transfection	84
2.2.4	Gene expression analysis (qPCR)	85
2.2.5	Synthetic peptide arrays on membrane support (SPOT)- synthesis of peptides and overlay Analysis	86
2.2.6	Site directed mutagenesis	87
2.2.7	Cloning	87
2.2.8	DNA sequencing	90
2.3	Protein methodologies	90
2.3.1	Glutathione S-transferase (GST) - protein purification	90
2.3.2	Protein extraction	92
2.3.2.1	Non- denaturing whole cell extracts (HEK293T and RAW 264.7 cells)	92
2.3.2.2	Denaturing whole cell extracts (HEK293T cells)	92
2.3.3	Quantification	93
2.3.4	SDS-PAGE protein gels	93
2.3.5	Western blotting	93
2.4	Functional assays	94
2.4.1	GST pulldown	94
2.4.2	Immunoprecipitation	95
2.4.3	Cellular ubiquitination assay	95
2.4.4	Enzyme-linked immunosorbent assay (ELISA)	96
2.5	Bioinformatic tools	96
2.5.1	Multiple sequence alignment	96
2.5.2	Protein prediction software	96
2.5.3	Crystal structure analysis	96
2.5.4	Crystal structure alignment	96
2.5.5	Docking	97
2.5.6	Statistical analysis	97
2.6	Plasmids	97

2.7	Primers	99
2.7.1	qPCR.....	99
2.7.2	Site Directed Mutagenesis	99
2.7.3	Cloning	101
2.7.4	Sequencing	101
2.8	Antibodies	102
2.9	Buffers.....	103
2.9.1	GST-protein purification.....	103
2.9.1.1	Column wash and storage	103
2.9.2	Loading buffer	104
2.9.3	SPOT-synthesis of peptides and overlay analysis	104
2.9.4	Cell lysis buffers	105
2.9.5	Electrophoresis buffers for western blotting	106
2.9.6	Tris-glycine SDS-polyacrylamide gels	106
2.9.7	ELISA.....	107
2.10	Reagents	107
2.11	Mimetic peptides	109
2.11.1	p65 mimetic peptides	109
2.11.2	USP7 mimetic peptides.....	110
3	Characterisation of important sites of p65 involved in USP7 deubiquitinase activity	112
3.1	Abstract	112
3.2	Introduction	113
3.3	Results.....	116
3.3.1	Mutation of S269 of p65 does not affect interaction with p65.....	116
3.3.2	p65 derived peptides.....	117
3.3.2.1	Design and synthesis	117
3.3.2.2	Peptide characterisation	121
3.4	Discussion	132

4	Investigation of the molecular determinants involved in p65 recognition by USP7	136
4.1	Abstract	136
4.2	Introduction	137
4.3	Results.....	138
4.3.1	GST-p65 protein purification.....	138
4.3.2	p65 protein is recognised by the C-terminal region of USP7	139
4.3.3	p65 binds to distinct peptides on a USP7 C-terminal region peptide array	140
4.3.4	Alanine substitution arrays identify interacting residues on USP7 .	144
4.3.5	Localisation of the p65 interacting amino-acids within the USP7 sequence and structure	149
4.3.6	Suitability of the recombinant GST-p65 protein for functional GST-pull down assays	151
4.3.7	Testing the effects of USP7 mimetic peptides on USP7-p65 interaction	154
4.4	Discussion	156
5	Identification of UBL2 domain of USP7 as essential for the interaction with p65	159
5.1	Abstract	159
5.2	Introduction	160
5.3	Results.....	161
5.3.1	USP7 UBL2 is required for interaction with p65.....	161
5.3.2	USP7 Δ UBL2 does not reverse p65 ubiquitination.....	167
5.3.3	USP7 substrate specificity	168
5.4	Discussion	171
6	Structural modelling of USP7-p65 interaction	176
6.1	Abstract	176
6.2	Introduction	177
6.3	Results.....	180
6.3.1	p65 full length protein 3D structure model.....	180

6.3.2	USP7 full length protein 3D structure model	188
6.3.3	USP7-p65 complex model.....	206
6.3.3.1	No lysine specificity detected on USP7 deubiquitinase activity	206
6.3.3.2	Model of USP7-p65 interaction when p65 is ubiquitinated at K62	207
6.3.3.2.1	K62	209
6.3.3.3	Model of USP7-p65 interaction based on p65 R/KxR/KxxxR/K motif interaction with USP7 UBL2 binding pocket.....	213
6.3.3.3.1	p65 amino-acids 35-RYKCECR-41 as part of the binding interface	217
6.3.3.3.2	p65 amino-acids 295-RHRIEEK-301 as part of the binding interface	222
6.4	Discussion	227
7	General discussion	233
8	Appendixes	238
8.1	Amino-acids abbreviations	238
8.2	Cloning	240
8.3	Peptide array sequences.....	242
8.4	Alanine scanning peptide array sequences	247
8.5	Structural model of USP7-p65 complex based mutants	256
8.6	NF- κ B members sequence homology for K56, K62 and K123 of p65....	257
8.7	R/KxR/KxxxR/K motif identification within different USP7 substrates' sequences.....	259
8.8	RelB ubiquitination assay.....	262
	List of references.....	264

Author's Declaration

I hereby declare that the work described in this thesis is original and was generated as a result of my own efforts. None of the data submitted as part of this thesis has been submitted for any other degree, either at the University of Glasgow, or at any other institution. Any assistance and contribution by others to this work is duly acknowledged within the text.

Signature:



Printed name: IZASKUN MITXITORENA

Acknowledgements

Firstly, I'd like to thank my supervisors at Glasgow University Dr. Ruaidhrí Carmody and Professor Carl Goodyear for all you've provided me over the last four years. I would like to thank specially Dr. Ruaidhrí Carmody for his time, the opportunities, encouragement and guidance and for introducing me into the marvellous and interesting world of NF- κ B and DUBs. I'd also like to thank the people at AstraZeneca that helped me during my thesis; my line managers Dr. Matthew Catley and Dr. Stephen Delaney, but also Dr. Christian Tyrchan and Dr. Matti Lepistö for all your knowledge and guidance through all the computational chemistry work performed within this thesis.

Secondly, I would like to thank the GLAZgo Discovery Centre for giving me the opportunity to start my scientific career funding this PhD.

And lastly I would like to thank you all for being there for me during this loooong 4 years, in the good moments but mostly in the bad ones, you know who you are. Y por último gracias a todos por haber estado ahí en los buenos momentos pero sobre todo en los malos, vosotros sabéis quienes sois. Mila esker guztioi hor egoteagatik, momentu onetan baina bereziki momentu txarretan, zuek badakizue nortzuk zareten.

To my Glasgow little family, thank you for all the laughs, for those long nights in the lab, our karaoke times, ceilidhs, rugby games, our non-sense conversations, our weegie learning sessions, all the trips and sightseeing around UK, for housing me when I was a mice refugee and all the moments we spent together. You know you have a house in Pamplona whenever you want.

Y a vosotros gracias por hacer que las vueltas a casa fuesen cómo si el tiempo nunca hubiera pasado y no estuviese a tantos km de distancia, por esas sesiones de puesta al día y de arreglar el mundo, las conversaciones por whatsapp y todos esos momenticos a distancia o en persona. Gracias por estar ahí, por todas las horas al otro lado de la pantalla del ordenador y por todas las horas que me habéis aguantado escribiendo en casa.

Mila esker guztioi!!!

Abstract

Nuclear factor kappa-light-chain-enhancer of activated B cells (NF- κ B) transcription factor family plays a key role in the regulation of the immune response and the transcriptional response to infection through transcriptional activation of genes involved in those processes. The NF- κ B response is regulated in the nucleus by the balance between ubiquitination and deubiquitination processes. Ubiquitination of the p65 subunit of NF- κ B terminates the NF- κ B response by targeting p65 for proteasomal degradation. Nevertheless, the ubiquitin molecules can be removed from targeted proteins by the action of deubiquitinating enzymes (DUBs). Ubiquitin-specific protease 7 (USP7) is a deubiquitinase enzyme from the ubiquitin-specific protease (USP) family which deubiquitinates p65. Besides p65 deubiquitination, USP7 is involved in a huge variety of biological processes due to stabilisation or localisation of proteins involved in those processes. USP7 is a multidomain protein formed by an N-terminal Meprin and tumour necrosis factor receptor-associated factor homology (MATH) / tumour necrosis factor receptor-associated factor (TRAF) domain, a catalytic domain (CD) and five ubiquitin-like domains (UBLs) in the C-terminal region. p65 recognition by USP7 takes place through the C-terminal region, but the molecular determinants involved in the interaction are still unknown. New therapeutic compound design strategies are based on interrupting the interaction interface between both proteins involved in the interaction. Therefore, in order to design a specific inhibitor of the deubiquitinase activity of USP7 on p65 we performed a peptide array and subsequent alanine scan followed by site directed mutagenesis experiments. We concluded that UBL2 of USP7 is necessary for the interaction with p65. UBL2 deletion completely abolishes the interaction and the deubiquitinase activity of USP7 on p65. Specificity of this mutant was tested by immunoprecipitation assays with different USP7 substrates. In silico modelling revealed a putative binding pocket in USP7 UBL2 that may be targeted to inhibit the interaction with p65. Together our data suggest that a binding pocket present on UBL2 composed by amino-acids 627-ARSNGTK-633, 736-EEVKPNLTER-745 and 757-LDELMDGD-764 directs the interaction with p65, besides UBL2 when deleted inhibits the interaction with p65 and subsequently its deubiquitination in a substrate specific manner.

List of Tables

Table 1-1 p65 phosphorylation sites.	42
Table 1-2 p65 acetylation sites.	44
Table 1-3 p65 methylation sites.	45
Table 1-4 Mutations inhibiting the NF- κ B signalling pathway.....	51
Table 1-5 Compounds directly inhibiting components of the NF- κ B signalling pathway.....	51
Table 1-6 Polyubiquitin chains function in cells	55
Table 1-7 List of lysines ubiquitinated on p65	71
Table 2-1 Cell plating conditions.....	83
Table 2-2 HEK293T cells transfection conditions	85
Table 2-3 qPCR running conditions	86
Table 2-4 Cloning PCR components	87
Table 2-5 Cloning PCR running conditions	88
Table 2-6 Cloning digestion components.....	88
Table 2-7 Cloning ligation components	89
Table 2-8 Cloning colony PCR components	89
Table 2-9 Cloning colony PCR running conditions	90
Table 2-10 Non-denaturing lysis conditions	92
Table 2-11 List of plasmids.....	97
Table 2-12 List of qPCR primers.....	99
Table 2-13 List of mutagenesis primers	99
Table 2-14 List of cloning primers	101
Table 2-15 List of sequencing primers.....	101
Table 2-16 List of antibodies	102
Table 2-17 GST-protein purification buffers.....	103
Table 2-18 GST-protein purification column wash and storage buffers	103
Table 2-19 WB loading buffer.....	104

Table 2-20 SPOT-synthesis of peptides and overlay analysis buffers	104
Table 2-21 Cell lysis buffers	105
Table 2-22 Electrophoresis buffers for western blotting	106
Table 2-23 Tris-glycine SDS-polyacrylamide gels	106
Table 2-24 ELISA buffers	107
Table 2-25 List of reagents.....	107
Table 2-26 List of p65 mimetic peptides.....	109
Table 2-27 List of USP7 mimetic peptides	110
Table 3-1 CPPs classification	114
Table 3-2 CPPs cellular entry mechanisms	115
Table 4-1 Peptide location within the C-terminal region of USP7	141
Table 4-2 Peptide arrays identified within USP7 UBLs.....	144
Table 4-3 Peptide arrays selected for alanine scanning	145
Table 4-4 Amino-acids identified by the alanine scanning peptide array	146
Table 4-5 USP7 mimetic peptides sequences.....	155
Table 5-1 USP7 UBL2 new mutants	166
Table 6-1 Structures contained in each PDB file.....	189
Table 8-1 Peptide array sequences.	242
Table 8-2 Alanine scanning peptide array sequences.	247
Table 8-3 p65 K56 sequence homology within NF- κ B members.	257
Table 8-4 p65 K62 sequence homology within NF- κ B members.	257
Table 8-5 p65 K123 sequence homology within NF- κ B members.	258

List of Figures

Figure 1-1 Multifaceted roles of NF- κ B.....	28
Figure 1-2 Members of the NF- κ B family of transcription factors	31
Figure 1-3 Possible NF- κ B homo- and heterodimers.....	32
Figure 1-4 RHD 3D structures of the NF- κ B members	34
Figure 1-5 Available 3D structures of p65 protein	36
Figure 1-6 NF- κ B signalling pathways.....	39
Figure 1-7 NF- κ B members PTMs	41
Figure 1-8 NF- κ B signalling pathway inhibitors targets	50
Figure 1-9 Schematic of the UPS system	58
Figure 1-10 Schematic of the UPS system inhibitors	63
Figure 1-11 K48-linked polyubiquitin chains positive role in NF- κ B activation ...	66
Figure 1-12 K48-linked polyubiquitin chains negative role in NF- κ B activation .	67
Figure 1-13 Non-proteolytic ubiquitination of the NF- κ B signalling pathway.....	68
Figure 1-14 Nuclear NF- κ B regulation by the ubiquitination/deubiquitination balance.....	69
Figure 1-15 USP7 protein structural domains.....	73
Figure 1-16 Multifaceted USP7 role in cells	75
Figure 1-17 Schematic of the USP7 inhibitors	77
Figure 1-18 USP7 substrate binding specificity.....	78
Figure 3-1 Phosphorylation status of p65 S269 has no effect on the interaction with USP7	117
Figure 3-2 Design of p65 derived cell permeable peptides.....	118
Figure 3-3 p65 derived mimetic peptides structural localisation in a known X-Ray (PDB 1VKX)	119
Figure 3-4 p65 derived peptides structural localisation in a full length model .	120
Figure 3-5 Design of p65 derived cell permeable control peptides	122
Figure 3-6 p65 derived mimetic control peptides localisation on a known crystal structure	123

Figure 3-7 p65 derived mimetic control peptides localisation on full length p65 structural model	124
Figure 3-8 F4 p65 mimetic peptide does not inhibit LPS induced RAW 264.7 cells TNF α production	126
Figure 3-9 E4 p65 mimetic peptide does not inhibit LPS induced RAW 264.7 cells TNF α production	127
Figure 3-10 F4 p65 mimetic peptide has no effect on BMDM TNF α production upon LPS stimulation.....	128
Figure 3-11 E4 p65 mimetic peptide does not inhibit BMDM TNF α production upon LPS stimulation	129
Figure 3-12 F4 p65 mimetic peptide has no effect on RAW 264.7 cells TNF α gene expression upon LPS stimulation	130
Figure 3-13 E4 p65 mimetic peptide has no effect on RAW 264.7 cells TNF α gene expression upon LPS stimulation. A) F4 and E4 negative control (E4C1) amino-acid sequences.....	131
Figure 4-1 GST-p65 recombinant protein purification	139
Figure 4-2 p65 is recognised by the C-terminal region of USP7	140
Figure 4-3 Identification of p65 interacting regions on USP7 using peptide arrays	143
Figure 4-4 Important amino-acids of USP7 involved in p65 binding.....	148
Figure 4-5 Sequence localisation of USP7 amino-acids identified by the peptide array and subsequent alanine scan	150
Figure 4-6 Structural localisation of USP7 amino-acids identified by the peptide array and subsequent alanine scan	151
Figure 4-7 Functional GST-pulldown assay of the recombinant GST-p65 protein	153
Figure 4-8 UBL3 non-conserved loop	154
Figure 4-9 Role of USP7 mimetic peptides disrupting the interaction	156
Figure 5-1 USP7 mutants structural schematic.....	163
Figure 5-2 USP7 UBL2 deletion abolishes interaction with p65	164
Figure 5-3 Location of the important amino-acids in the linker between UBL3 and UBL4 of USP7. A) C-terminal sequence of USP7 C-terminal UBLs	165
Figure 5-4 Mutation of USP7 757-LDEL-760 762D and 764D to alanine is not sufficient to abolish USP7-p65 interaction.....	167
Figure 5-5 USP7 Δ UBL2 mutant is not able to deubiquitinate p65 protein.....	168

Figure 5-6 USP7 substrate recognition specificity	170
Figure 5-7 Structural alignment of the NF- κ B subunits	171
Figure 6-1 1VKX PDB crystal structures	181
Figure 6-2 Ribbon structures of p65 protein modelled with ROBETTA software in comparison with p65 protein structure from 1VKX.....	182
Figure 6-3 Surface structures of p65 protein modelled with ROBETTA software in comparison with p65 protein structure from 1VKX.....	183
Figure 6-4 p65 full length protein model generation.....	186
Figure 6-5 Ribbon of p65 full length protein structural model	187
Figure 6-6 Surface of p65 full length protein structural model.....	188
Figure 6-7 Crystal structures of human USP7 used to develop a USP7 full length model.....	191
Figure 6-8 USP7 NTD modelling.....	192
Figure 6-9 Structural alignment of the new modelled NTD-CD USP7 structure and 5JTJ	193
Figure 6-10 Differences between 2F1Z active CD and modelled NTD inactive CD structural conformation	194
Figure 6-11 USP7 NTD active CD structure modelling	195
Figure 6-12 Reparation of the colliding loop from the active CD with the NTD.	196
Figure 6-13 USP7 NTD-CD-UBL123 structural modelling	199
Figure 6-14 Modelled USP7 NTD-CD-UBL123 alignment with 5JTV	200
Figure 6-15 Modelled USP7 NTD-CD-UBL123 alignment with 4YOC.....	201
Figure 6-16 USP7 NTD-CD-UBL12345 structural modelling	202
Figure 6-17 USP7 CTP connection to modelled USP7 NTD, CD, UBL12345	204
Figure 6-18 Molecular Dynamics of the full length USP7 model structure in complex with ubiquitin	205
Figure 6-19 USP7 has no specificity for K56, K62 or K123. HEK293T cells were co-transfected with murine p65 WT, p65 K56R, p65 K62R and p65 K123R plasmids along with FLAG-tagged USP7	207
Figure 6-20 Definition of the interacting site of USP7 with p65 ubiquitinated lysine	208
Figure 6-21 DNA helix elongation and rearrangement	210
Figure 6-22 Interacting interface of the model based on K62-ubiquitination ...	211

Figure 6-23 Surface model of the USP7-p65/p50/DNA complex based on ubiquitination of p65 K62	212
Figure 6-24 Binding pocket on USP7	215
Figure 6-25 Binding pocket location in full length USP7 model.....	216
Figure 6-26 R/KxR/KxxxR/K motif presence on p65 human and murine sequences	217
Figure 6-27 Model based on the interaction with the motif 35-RYKECR-41 of p65	220
Figure 6-28 Surface of the USP7-p65/p50/DNA complex, modelled based on the interaction with motif 35-RYKECR-41	221
Figure 6-29 Model of p65 amino-acids 1-317 structure	223
Figure 6-30 Model based on the interaction with the motif 295-RHRIEEK-301 of p65.....	225
Figure 6-31 Surface of the USP7-p65/p50/DNA complex modelled based on the interaction with motif 295-RHRIEEK-301.....	226
Figure 8-1 p65 WT and mutants cloning into an empty pCDNA3.1 expression vector	241
Figure 8-2 USP7-p65 complex structural model.....	256
Figure 8-3 R/KxR/KxxxR/K motif presence on USP7 different substrates' sequences.....	261
Figure 8-4 USP7 Δ UBL2 mutant deubiquitinates RelB protein	263

List of Abbreviations

	Abbreviation	Name
#	3D	Three dimensional
A	AMP	Adenosine monophosphate
	AMPK	AMP-activated protein kinase
	AntP	Antennapedia
	ARH1	Adrenodoxin reductase homolog
	ATP	Adenosine triphosphate
B	BAFF	B cell activating factor
	BAFFR	B cell activating factor receptor
	Bcl-3	B cell leukaemia
	BCR	B cell receptor
	BM	Bone marrow
	BMDM	Bone marrow derived macrophages
	BSA	Bovine serum albumin
C	CBP	CREB-binding protein
	CD	USP7 catalytic domain
	cDNA	Complementary DNA
	Cezanne	Cellular zinc finger anti-NF- κ B

	Abbreviation	Name
C	chk	CSK-homologous kinase
	ciAP	Cellular inhibitor of apoptosis
	ck	Creatine kinase
	CMV	Cytomegalovirus
	CPP	Cell penetrating peptides
	CRBN	Cereblon
	CRL	Culling RING ligases
	CSK	C-terminal Src kinase
	CSN	COP9 signalosome
	CTP	USP7 C-terminal 20 amino-acids peptide
	CYLD	Deubiquitinase cylindromatosis protein
D	DAXX	Death domain-associated protein
	DD	Death domain
	DHMEQ	Dehydroxymethyl Epoquinomicin
	DMEM	Dulbecco's Modified Eagle Medium
	DMSO	Dimethyl sulfoxide
	DNA	Deoxyribonucleic acid
	DNMT1	DNA (cytosine-5)-methyltransferase 1

	Abbreviation	Name
D	DUB	Deubiquitinating enzyme
E	E1	Ubiquitin activating enzyme
	E2	Ubiquitin conjugating enzyme
	E3	Ubiquitin protein ligase
	EBNA1	Epstein-Barr nuclear antigen 1
	EBV	Epstein-Barr virus
	ECS	Cullin-5-RING ubiquitin ligase
	EDTA	Ethylenediaminetetraacetic acid
	ELISA	Enzyme-linked immunosorbent assay
	ER	Endoplasmic reticulum
	ERAD	Endoplasmic reticulum-associated degradation
	ERK	Extracellular signal-regulated kinase
F	FBS	Fetal bovine serum
	FDA	United States food and drug administration
	FOXO4	Forkhead box protein O4
	FT	Flow through
G	GMPS	Guanosine monophosphate synthetase
	GRR	Glycine rich region

	Abbreviation	Name
G	GSH	Glutathione
	GSK	Glycogen synthase
	GST	Glutathione S-transferase
H	HDAC	Histone deacetylase
	HECT	Homology to E6-AP C-terminal
	HEK293T	Human embryonic kidney 293T cells
	HIV-1 TAT	TAT protein of human immunodeficiency virus 1
	HP	High performance
	HRP	Horseradish peroxidase
	HSV-1	Herpes simplex virus 1
	HUBL	HAUSP/USP7 UBLs
	I	ICP0
I κ B		Inhibitor of κ B
IKK		I κ B kinase
IL-1		Interleukin 1
IL-1R		Interleukin 1 receptor
IMiDS		Immunomodulatory drugs
ING4		Inhibitor of growth family member 4

	Abbreviation	Name
I	IPTG	Isopropyl β -D-1-thiogalactopyranoside
J	JAMM	JAB/MPN/Mov34
	JNK	c-Jun N-terminal kinase
	Josephins	Machado-Joseph diseases proteases
L	LB	Luria Bertani
	LPS	Lipopolysaccharide
	LT β R	Lymphotoxin β receptor
	LZ	Leucine zipper
M	MATH	Meprin and tumour necrosis factor receptor-associated factor homology
	MD	Molecular dynamics
	MDM2	Mouse double minute 2
	MSK	Mitogen and stress-activated protein kinase
	NAE	NEDD8 activating enzyme
	NAK	Numb-associated kinase
	NBD	NEMO binding domain
	NEM	N-ethylmaleimide
	NEMO	NF- κ B essential modulator
	NES	Nuclear export sequence

	Abbreviation	Name
N	NF- κ B	Nuclear factor kappa-light-enhancer of activated B cells
	NIK	NF- κ B inducing kinase
	NLS	Nuclear localisation sequence
	NMR	Nuclear magnetic resonance
	NSD1	Nuclear receptor-SET domain-containing protein 1
	NTD	USP7 N-terminal domain
O	ODN	Decoy oligonucleotide
	ORF73	LANA from human herpes virus 8
	OTU	Ovarian tumour proteases
	OTUB1	OTU ubiquitin aldehyde binding 1
P	PAGE	Polyacrylamide gel electrophoresis
	PBS	Phosphate-buffered saline
	PBS-T	PBS 0.05% tween 20
	PCAF	p300/CBP-associated factor
	PCR	Polymerase chain reaction
	PDLIM	PDZ and LIM domains protein 2
	Peli-1	Pellino E3 ubiquitin ligase 1

	Abbreviation	Name
P	PAMP	Pathogen-associated molecular pattern
	Pim	Proviral integration site for moloney murine leukaemia virus
	PK	Protein kinase
	PPAR γ	Peroxisome proliferator-activated receptor γ
	PTD	Protein transduction domain
	PIAS3	Protein inhibitor of activated signal transducer and activator of transcription 3
	PTEN	Phosphatase and tensin homolog
	PTM	Posttranslational modification
Q	qPCR	Quantitative PCR
R	RANK	Receptor activator of nuclear factor κ B
	RBR	RING between RING
	RHD	REL homology domain
	RING	Really interesting new gene
	RIP1	Receptor interacting protein 1
	RIPA	Radioimmunoprecipitation assay
	RITA	Reactivating p53 and inducing tumour apoptosis
	RNA	Ribonucleic acid

	Abbreviation	Name
R	RSK	Ribosomal s6 kinase
S	SCF	Skp, cullin, F-box containing complex
	SDM	Site directed mutagenesis
	SDS	Sodium dodecyl sulphate
	SET	Suppressor of variegation-enhancer of zeste-trithorax
	SFM	Serum free media
	siRNA	Small interfering RNA
	SL	Sesquiterpene lactones
	SOC	Super optimal broth with catabolite repressor
	SOCS1	Suppressor of cytokine signalling 1
	SPOT	Synthetic peptide arrays on membrane support
	SUMO	Small ubiquitin-like modifier
T	TAB	TAK1 binding protein
	TAD	Transcription activating domain
	TAK1	TGFB activated kinase 1
	TAT	Transactivating transcription protein
	TBK	TANK binding kinase
	TBP	TATA binding protein

	Abbreviation	Name
T	TBS	Tris-buffered saline
	TBS-T	TBS with 0.05% Tween 20
	TCR	T cell receptor
	TE	Tris, EDTA
	TEMED	Tetramethylethylenediamine
	TIR	Toll/Interleukin 1 receptor
	TIRAP	TIR domain containing adaptor protein
	TLR	Toll-like receptor
	TNF	Tumour necrosis factor
	TNF-RSC	TNFR1-associated signalling complex
	TNFR	Tumour necrosis factor receptor
	TRADD	Tumour necrosis factor receptor type 1-associated death domain protein
	TRAF	Tumour necrosis factor receptor-associated factor
	U	UBA1
UBL		Ubiquitin-like domain
UBL12		USP7 ubiquitin-like domains 1 and 2
UBL123		USP7 ubiquitin-like domains 1, 2 and 3

	Abbreviation	Name
U	UBL12345	USP7 ubiquitin-like domains 1, 2, 3, 4 and 5
	UBL125	USP7 ubiquitin-like domains 1, 2 and 5
	UBL145	USP7 ubiquitin-like domains 1, 4 and 5
	UBL34	USP7 ubiquitin-like domains 3 and 4
	UBL345	USP7 ubiquitin-like domains 3, 4 and 5
	UBL45	USP7 ubiquitin-like domains 4 and 5
	UCH	Ubiquitin carboxy-terminal hydrolases
	UHRF1	Ubiquitin-like with PHD and RING finger domains 1
	UPS	Ubiquitin proteasome system
	USP	Ubiquitin-specific protease
	USP7	Ubiquitin-specific protease 7
W	UV	Ultraviolet
	WB	Western Blot
	WT	Wild type

Chapter One

Introduction

1 General introduction

1.1 Overview

As this study focussed on the regulation of the NF- κ B transcription factor family by the ubiquitin proteasome system (UPS), the introduction of this thesis will provide a broad overview of the NF- κ B transcription factor family and the UPS components regulating the NF- κ B signalling pathway and activity and will include; i) reviewing the characteristics of NF- κ B protein members, ii) describing the tight regulation of NF- κ B activation, iii) exploring the role of the UPS on NF- κ B regulation, and lastly iv) a broad overview of USP7 and its role recognising and deubiquitinating p65 subunit of NF- κ B.

1.2 NF- κ B transcription factor family

NF- κ B is an evolutionary conserved inducible transcription factor family [1-3]. Despite its discovery as a protein bound to 5'-GGGACTTCC-3' DNA sequence in the intronic enhancer of the B-lymphocyte-specific immunoglobulin κ chain [4, 5], it is ubiquitously expressed in all mammalian cell types [1, 2, 6]. A wide range of stimuli such as inflammatory cytokines (tumour necrosis factor (TNF) α , interleukin 1 (IL-1)), bacterial products (lipopolysaccharide (LPS), double stranded deoxyribonucleic acid (DNA)) and pro-apoptotic stimuli (ultraviolet (UV) light, γ irradiation and oxygen free radicals) [7-10] lead to the activation of NF- κ B. NF- κ B has a fundamental role in a number of biological processes such as cell survival, proliferation, differentiation and apoptosis [2, 11, 12]; as well as a key role in the control of immunity by controlling the immune innate and adaptive responses and immune homeostasis [7, 13, 14]. NF- κ B is involved in those processes through the transcriptional induction of genes involved in them, e.g. chemokines, cytokines, adhesion molecules [6, 7, 15, 16] (for a more precise description and list of NF- κ B target genes see Boston University NF- κ B transcription factors' web page, <http://www.bu.edu/nf-kb/>) (see Figure 1-1). Due to such wide effects on physiology, its dysregulation is associated with numerous pathological states including (but not restricted to) cancer, autoimmune diseases, neurodegeneration and inflammatory diseases [12, 17, 18].

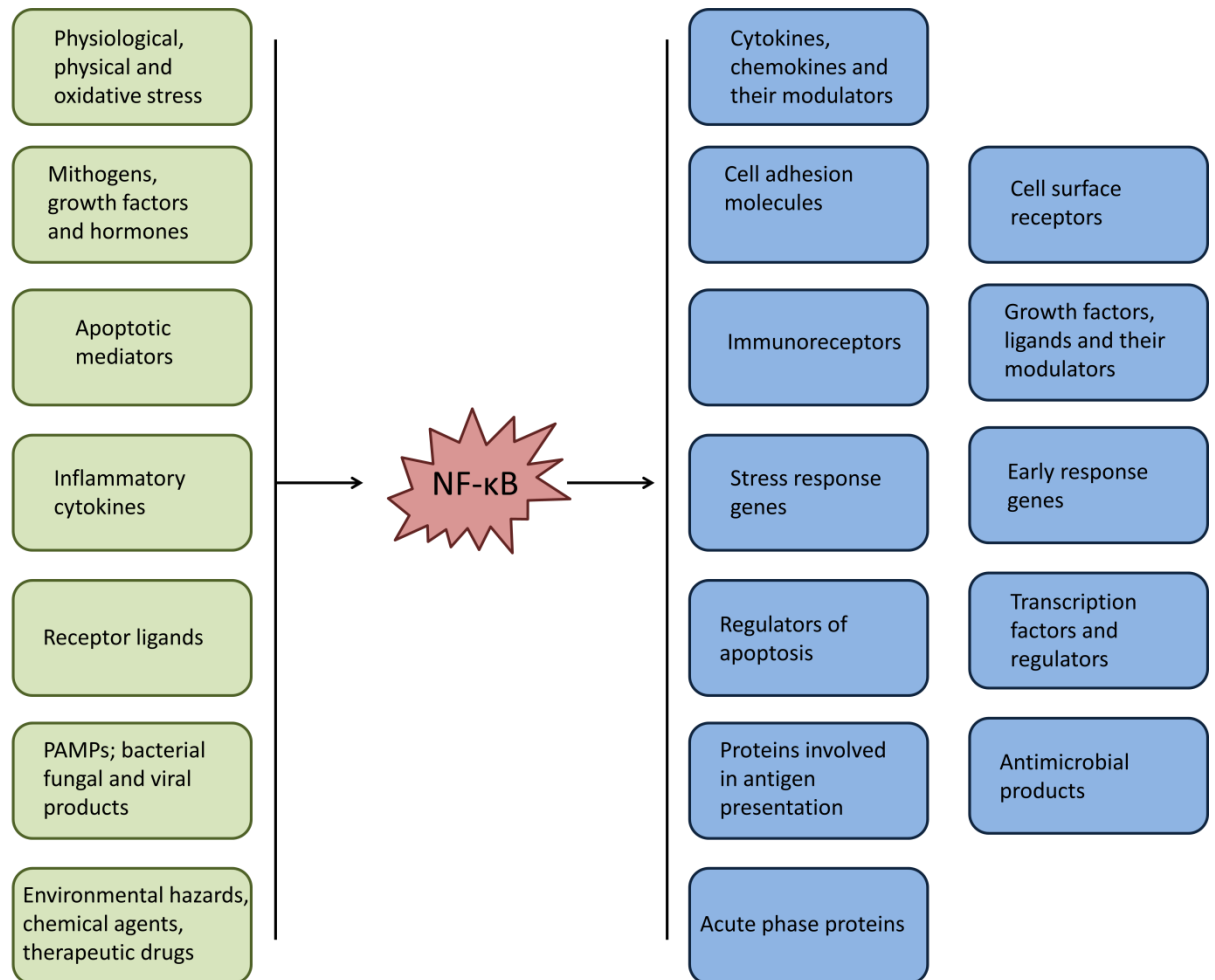


Figure 1-1 Multifaceted roles of NF- κ B. NF- κ B response is activated upon a wide variety of stimuli (green boxes) which induces the expression of hundreds of genes involved in different cellular processes (blue boxes). For a full list see <http://www.bu.edu/nf-kb> webpage. *PAMP: Pathogen-associated molecular pattern.

1.2.1 NF- κ B members

The NF- κ B family is encoded by 5 genes; NFKB1, NFKB2, RELA, RELB and cREL [15, 19] which code for 7 proteins p105 (precursor protein of p50), p100 (precursor protein of p52), p50, p52, p65 (RelA), RelB and c-Rel [15] that through the formation of homo- and heterodimers generate 15 NF- κ B species [19, 20]. Each NF- κ B protein or subunit carries out specific biological roles depending on their co-factors and dimer specific affinities for DNA binding sequences [1, 19]. Once the dimers are formed, they bind to κ B sites in promoters or enhancers of their target genes regulating their transcription by the recruitment of transcriptional co-activators or transcriptional co-repressors [21]. NF- κ B specifically recognises and binds κ B DNA elements with a consensus sequence as follows 5'-GGGRNYYYCC-3', where R is an unspecified purine, Y is an unspecified pyrimidine and N is any nucleotide [22].

All 5 NF- κ B subunits share a 300 amino-acids length N-terminal REL homology domain (RHD) [1, 15]. The RHD domain is responsible of the dimerisation of NF- κ B subunits, DNA binding, and binding to the inhibitory inhibitor of κ B (I κ B) protein family [1, 7, 16, 23]. The C-terminal region of the RHD is composed of a series of positively charged amino-acids which form a nuclear localisation sequence (NLS) [1]; while the N-terminal region contains an immunoglobulin like domain which regulates the DNA binding selectivity for each κ B site [23] (see Figure 1-2).

NF- κ B subunits are divided into two groups depending on their ability to activate transcription. p65, RelB and c-Rel contain a C-terminal transcription activating domain (TAD) enriched in abundant serines, acidic and hydrophobic amino-acids, which when mutated reduce or inhibit the transcriptional activity of these subunits [24]. c-Rel transactivating activity is weaker than p65 activity, but when there are increased levels of c-Rel, p65 activity is attenuated [1]. RelB, besides the TAD domain, requires the presence of an N-terminal Leucine Zipper (LZ) domain for transactivation activity, and only binds the DNA in complex with p50 or p52 [1]. p50 and p52, which are generated by the limited proteasomal degradation of p105 and p100 respectively, lack the TAD domain [15, 19, 21], thereby they do not have transactivational activity when present as homodimers [19] (see Figure 1-2). p50 and p52 can act via 3 different ways: 1) by altering the I κ B-site specificity when forming a heterodimer with p65, RelB or c-Rel, 2) by repressing the transcription when bound to κ B sites as homodimers, or 3) by promoting transcription by the recruitment of other TAD-containing proteins to the κ B sites [21]. Therefore, dimerisation of the NF- κ B subunits generates 15 possible dimers, from which 12 are able to bind the DNA and potentially activate transcription of target genes [25]. The most common dimer in physiological conditions is p50-p65 [2, 20, 22, 26] which controls the immune response and cellular growth and development [22]. All subunits can homodimerise or heterodimerise with each other except for RelB, which is only able to form stable heterodimers with p50 and p52 [7, 24] (see Figure 1-3).

Besides its specific activity on κ B promoter sites, NF- κ B has different DNA binding specificity and affinity depending on the dimer composition [1, 14]. These differences on DNA binding and specificity to interact with other

neighbouring factors of homo- and heterodimers allow them to have distinct biological functions, being able to target selective genes depending on the stimuli [1, 14].

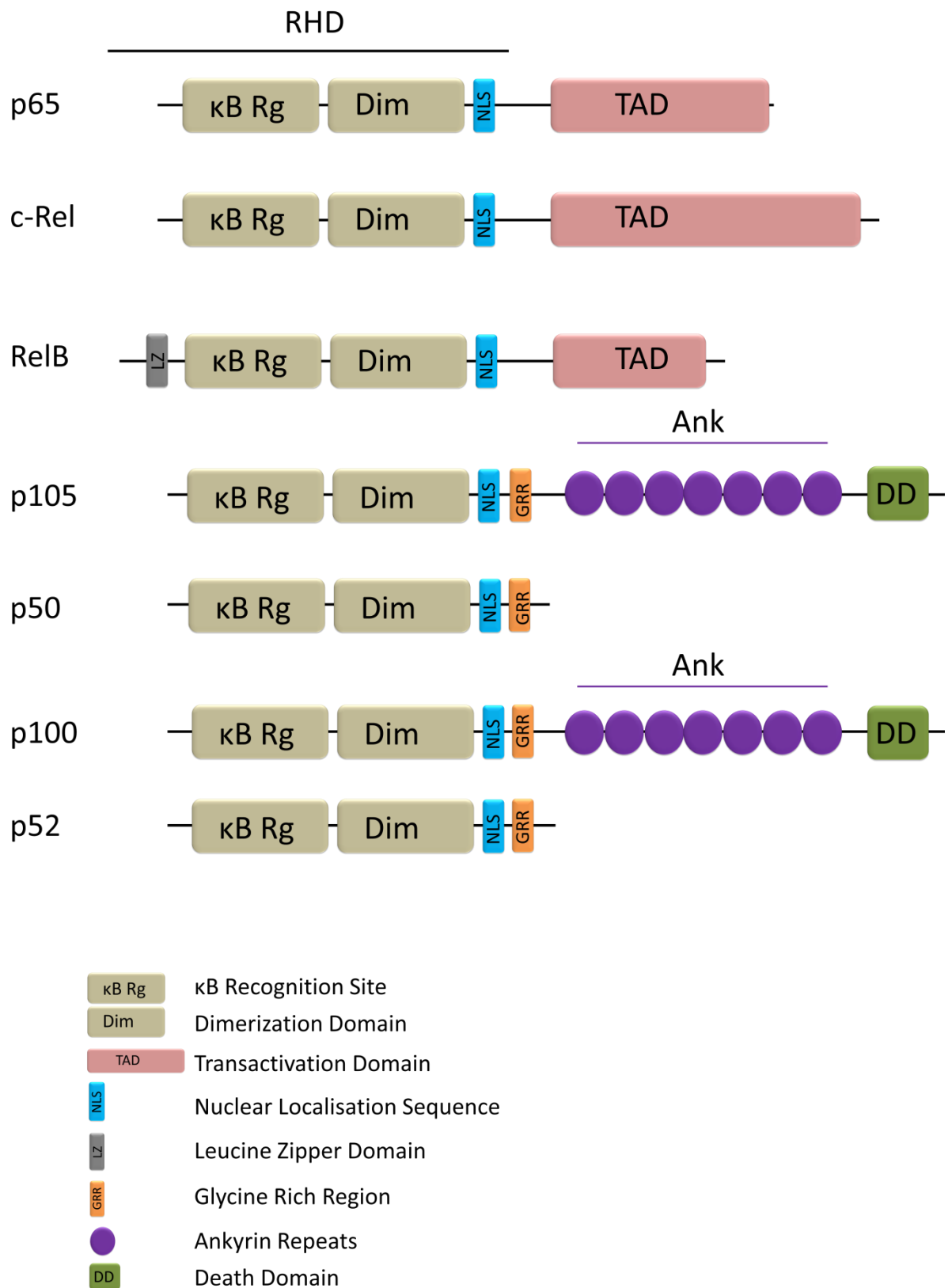


Figure 1-2 Members of the NF-κB family of transcription factors. Schematic representation of the NF-κB family members indicating their structural domains. All NF-κB members share a RHD in their N-terminal region, composed by an N-terminal region in charge of DNA binding followed by a region controlling the dimerisation and a NLS in its C-terminal region. p65, c-Rel and RelB contain a TAD in their C-terminal region. The precursor proteins p100 and p105 contain a C-terminal glycine rich region (GRR), an ankyrin repeat domain and a death domain (DD). The limited proteolytic degradation occurs after the GRR region, generating p50 and p52.

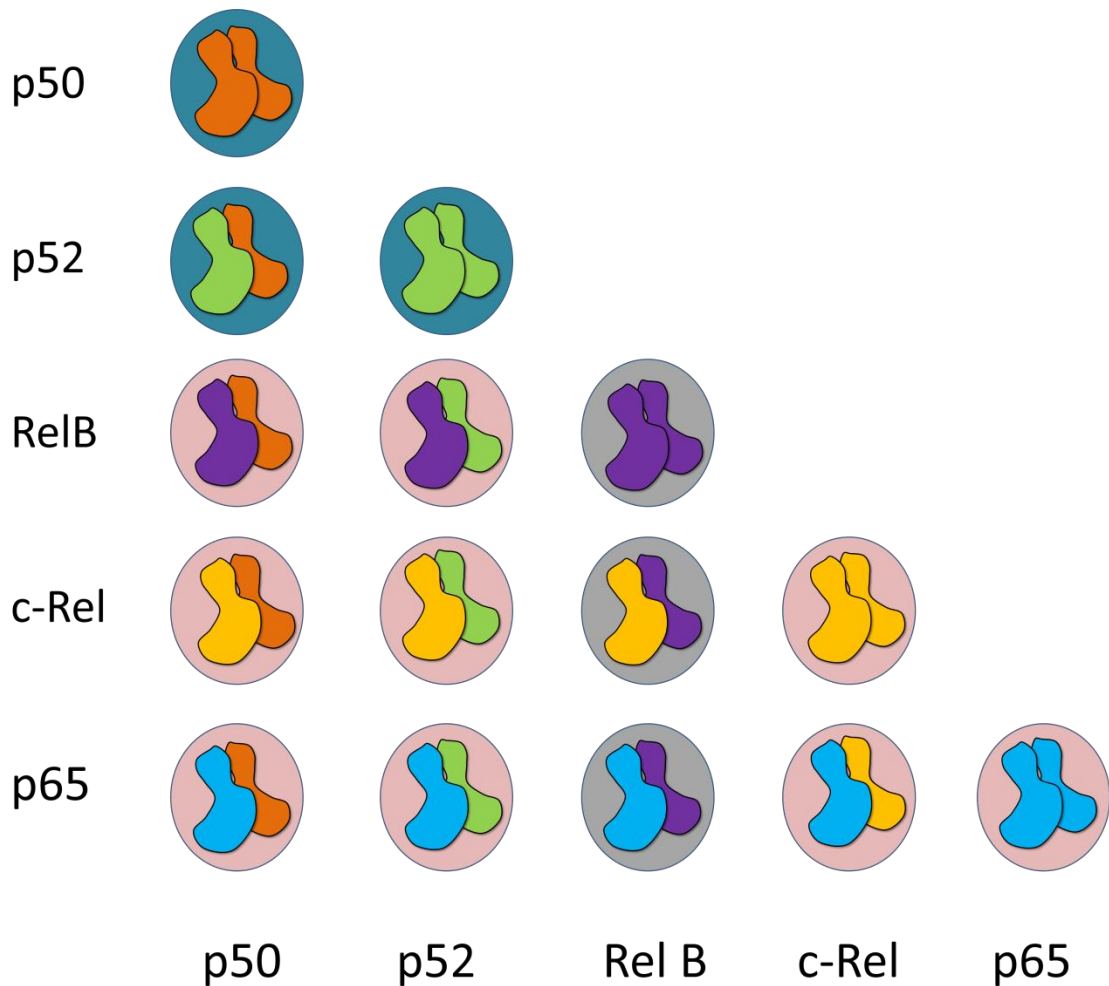


Figure 1-3 Possible NF- κ B homo- and heterodimers. NF- κ B subunits are able to form dimers via their RHDs. Only p65, RelB and c-Rel contain transactivating activity, therefore homodimers and heterodimers containing any of these subunits contain transactivating ability (pale pink circles). On the other hand, p50 and p52 lack the TAD domain and are not able to activate transcription, thus p50-p52 heterodimer and p50 or p52 homodimers have no transactivating ability (blue circles). However, not all dimer combinations are found in vivo (grey circles), RelB is only known to dimerise with p50 and p52.

1.2.2 NF- κ B members structure

The interest during the past decades of knowing how NF- κ B members dimerise and bind to the DNA promoter of their target genes has resulted in a number of solved X-Ray structures. A number of these solved structures are formed by the dimerisation of the NF- κ B members in complex with the DNA helix but there are as well, structures of the NF- κ B members in complex with interacting partners. The majority of the structures present on the Protein Data Bank are truncated versions of the NF- κ B members containing their RHD. However there are also two three dimensional (3D) structures of a partial TAD region of the p65 subunit [27, 28].

NF- κ B members' 3D structure is highly similar among them (see Figure 1-4). Each subunit is formed by an N-terminal β -barrel, folded into an immunoglobulin like module and linked by a flexible linker to a C-terminal β -barrel, folded into an immunoglobulin like module [22, 29-34]. There are a few structural differences within subunits. p50 and p52 share strong similarity [34] and differ with p65 secondary structure by the presence of a second α -helix on the N-terminal region of p50 [22]. RelB linker's conformation differs with the linker conformation of the other subunits. RelB linker's helical conformation is more prominent than in the other subunits [31]. The N-terminal β -barrel regulates DNA binding, while the C-terminal β -barrel is the most invariant part of the NF- κ B sequence and controls NF- κ B dimerisation [29]. The dimerisation interface is similar in all NF- κ B members and is composed by a central hydrophobic core surrounded by hydrogen bonds [22, 30, 31]. Differences in dimers stability is due to slight differences in this interface [22, 30, 31]. NF- κ B dimers differ in their relative orientation of the N-terminal and C-terminal regions of the RHDs [29, 34-39], even when they bind κ B sites with the same core sequence [29].

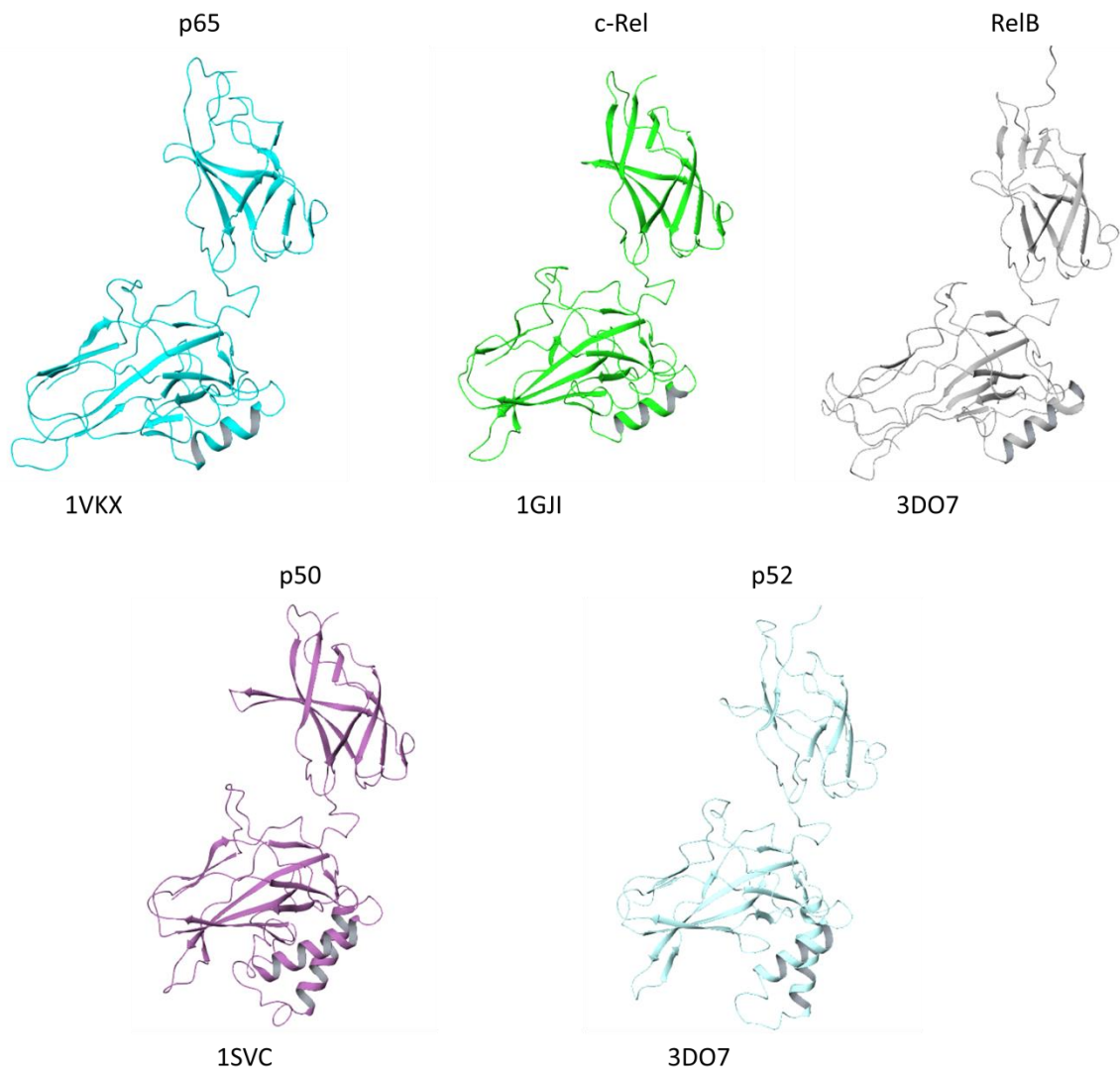


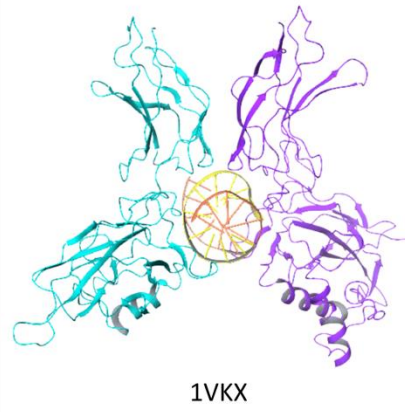
Figure 1-4 RHD 3D structures of the NF- κ B members. p65 subunit from 1VKX is coloured in blue (amino-acids 19-291 of the murine protein), c-Rel from 1GJI in green (amino-acids 7-281 from *Gallus gallus*), RelB from 3DO7 in grey (amino-acids 1-400 of the murine protein), p50 from 1SVC in purple (amino-acids 2-366 from *Homo sapiens*) and p52 from 3DO7 in light blue (amino-acids 35-341 from *Mus musculus*).

1.2.2.1 p65 subunit structure

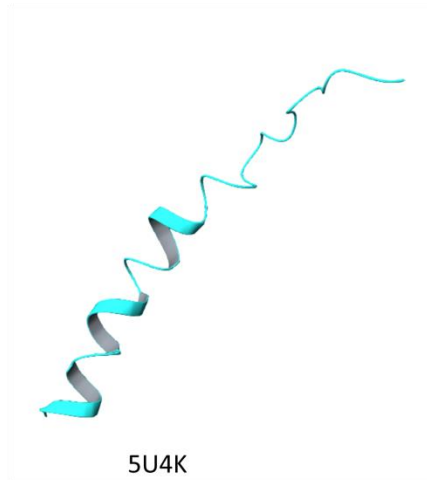
The most common dimer in cells is p50-p65 heterodimer [22]. p50-p65-DNA complex structure is available on the Protein Data Bank (PDB: 1VKX) [22]. 1VKX PDB file is composed of the 3D structure of p50-p65 heterodimer bound to the κ B DNA of the intronic enhancer of the immunoglobulin light chain gene [22]. Despite being able to solve the 3D structure of the complex; p65 and p50 proteins are truncated and correspond to the murine sequence of these proteins. p65 truncated protein in 1VKX is formed by amino-acids 19-291 [22]. Amino-acids 19-291 are located within the RHD; while the TAD of p65 is not present on the structure (amino-acids 428-551) (see Figure 1-5) [40]. However, regions of the

p65 TAD 3D structure in complex with protein interactors are also available which were solved through nuclear magnetic resonance (NMR) experiments (see Figure 1-5) [27, 28]. p65 TAD is divided into two domains TAD1 and TAD2, which are required for full transcriptional activity of p65 [40]. TAD1 is located in the C-terminal region of p65 TAD (amino-acids 521-551) and restores a 95% of the full transactivating potential of p65 [40]. TAD1 contains a highly conserved region in 542-546 and a short transient helical conformation in 534-546. There is a conformational change between the unbound and the bound state of p65, because of which this helical conformation turns into a clear α -helix conformation in the bound state [28]. On the other hand, TAD2 is located in the preceding region (amino-acids 428-521) in an extended conformation containing an N-terminal α -helix, a dynamically disordered C-terminal α -helix and two additional helical turns (449-452 and 465-468) which regulate the electrostatic contacts with interacting proteins. The region prior to one of these helical turns, D444-D448, is highly acidic containing 4 out of 5 negatively charged residues [27], contributing to the interaction with different proteins. On the other hand, TAD2 restores a 30% of the full transactivation ability of p65 [40]. However, p65 TAD is a highly flexible region [27], which may undergo conformational rearrangements upon substrate binding. p65 is known to undergo conformational rearrangements of the RHD domain upon I κ B α binding [36]. The N-terminal region of the RHD rotates, due to the flexibility of the linker, from an open unbound conformation to a close conformation [41]. These rearrangements allow variability in the DNA sequence recognition [36]. The flexibility of p65 makes difficult to solve the full length p65 3D structure.

A



B



C



Figure 1-5 Available 3D structures of p65 protein. A) 1VKX 3D structure of the p50-p65 heterodimer RHDs in complex with the DNA helix. p65 is coloured in blue, p50 in purple and the DNA helix in yellow and pink. **B)** 5U4K 3D structure of the TAD1 of p65. **C)** 2LWW 3D structure of the TAD2 of p65. All 3D structures were analysed with Maestro Schrodinger Software.

1.3 NF- κ B regulation

NF- κ B activity is tightly regulated [2]. This regulation is performed through several posttranslational modifications (PTMs) which control the activity of the central components in the NF- κ B signalling [12, 42] such as phosphorylation, ubiquitination, acetylation and SUMOylation [42]. Of these PTMs ubiquitination of NF- κ B subunits is a critical factor in the termination of the NF- κ B response and is a major limiting factor in the expression of pro-inflammatory genes [15]. One key protein family in the regulation of the NF- κ B response is the I κ B family [6, 8]. The I κ B family is formed by three different groups of proteins, the classical I κ B proteins, the NF- κ B precursor proteins and the atypical I κ B proteins [43]. The classical I κ Bs are I κ B α , I κ B β and I κ B ϵ , which sequester NF- κ B dimers in the cytoplasm [43]. The NF- κ B precursor proteins are p105 and p100, which following a limited proteolytic degradation, form p50 and p52 subunits respectively [43]. And the atypical I κ B proteins, localised in the nucleus, are B-cell leukaemia 3 (Bcl-3), I κ BNS and I κ B ζ [15, 19, 43], which function is to modulate transcription of NF- κ B genes by acting as transcriptional co-activators [15, 21, 43]. These I κ B members share a series of ankyrin repeats which regulate binding of NF- κ B dimers through their RHD domains [43, 44].

1.3.1 NF- κ B activation

Several pathways lead to NF- κ B activation as a consequence of changes in the intracellular microenvironment [12], the majority of which converge on the I κ B kinase (IKK) complex activation, which is composed by two catalytic subunits (IKK α and IKK β) and a regulatory subunit (IKK γ /NF- κ B essential modulator (NEMO)) [15, 17, 20], and subsequent I κ B degradation [12]. Different receptor signalling such as TNF receptors (TNFR), Toll-like receptors (TLR), Interleukin 1 receptor (IL-1R), T cell receptors (TCR), B cell receptors (BCR), receptor activator of nuclear factor κ B (RANK) and B cell activating factor (BAFF) receptor (BAFFR) results in the activation of the NF- κ B response [12]. Signalling intermediates upstream of the IKK complex are shared between different NF- κ B pathways; however, differences between pathways are based on conformational changes, protein-protein interactions and assembly of large protein complexes at those early steps of the NF- κ B signalling pathways [12].

1.3.1.1 Signalling pathways

NF- κ B activation is generally considered to take place through either the canonical or the non-canonical pathways [45, 46] (see Figure 1-6).

1.3.1.1.1 Canonical pathway

Typically in resting cells, NF- κ B dimers are bound to I κ B proteins in the cytoplasm. Activation of receptors including TLRs, TNFR and IL-1R [20, 46, 47], through TNF α , IL-1 β , LPS [20, 46, 47] stimuli, leads to the activation of the IKK complex [7-10, 15]. The active IKK complex phosphorylates I κ B proteins, leading to its ubiquitination by the E3 ligase SCF^{TRCP} complex and consequent proteasomal degradation [7-10, 15, 48, 49]. Then, the NF- κ B dimers are free to translocate to the nucleus by their NLS, where they bind to different promoters to induce the transcription of various genes such as pro-inflammatory cytokines and chemokines, and initiate the immune response. An important NF- κ B target gene is I κ B α , which binds to the NF- κ B dimers sequestering them back to the cytoplasm through a nuclear export sequence (NES), in a negative feedback loop [7-10, 15]. See Figure 1-6.

1.3.1.1.2 Non-canonical pathway

This pathway is activated mainly through a small number of members of the TNF receptor superfamily; such as lymphotoxin B receptor (LTBR), CD40, BAFFR and RANK [6, 7, 22, 42]. In this pathway p100 acts as an I κ B protein and binds the RelB subunit masking its NLS domain, thereby sequestering it in the cytoplasm [6, 7, 22, 42]. Activation requires p100 processing to form p52 by proteasomal partial degradation [6, 7, 22, 42]. IKK α phosphorylates p100 targeting it for ubiquitination by the E3 ligase SCF^{TRCP} complex and subsequent proteasomal degradation [6, 7, 22, 42, 50, 51]. This pathway controls genes important in the regulation of homeostatic processes like lymphoid organogenesis, bone metabolism and B cell survival [2]. See Figure 1-6.

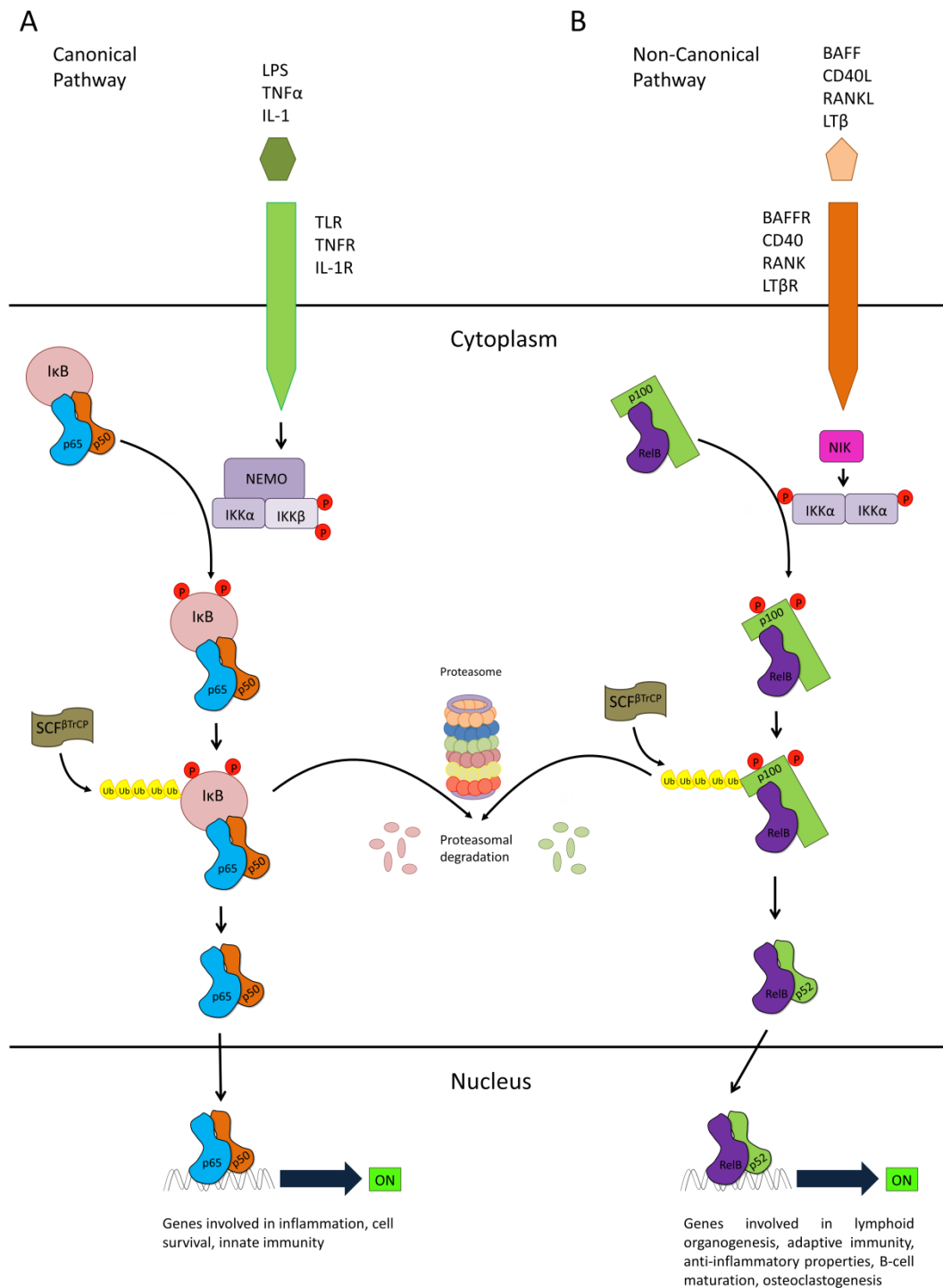


Figure 1-6 NF- κ B signalling pathways. A) Canonical pathway. In resting cells NF- κ B dimers are sequestered in the cytoplasm by the I κ B protein family. Once the cell receives a stimuli, such as TNF α , IL-1 or LPS; the IKK complex is activated and phosphorylates the I κ B proteins, tagging them for ubiquitination by the SCF- β TrCP E3 ligase complex and subsequent proteasomal degradation. NF- κ B dimers are then free to translocate to the nucleus where they bind to the promoter of their target genes transcribing them including genes involved in inflammation, cell survival and innate immunity. **B)** Non-canonical pathway. In resting cells, RelB is bound to p100 precursor protein. Upon stimuli such as CD40L, LT β , RANK ligand (RANKL) and BAFF, NF- κ B inducing kinase (NIK) is activated and subsequently the IKK complex. IKK α phosphorylates p100, tagging it for ubiquitination by the SCF- β TrCP E3 ligase complex and subsequent controlled proteolytic degradation by the proteasome. As a result, RelB-p52 dimers are free to translocate to the nucleus where they bind their target genes promoters including genes involved in the lymphoid organogenesis, adaptive immunity, anti-inflammatory properties, B-cell maturation and osteoclastogenesis, transcribing them.

1.3.2 Posttranslational modifications

A number of PTMs of different components of the NF- κ B signalling pathway, not only of NF- κ B members, influences NF- κ B activity at different levels. These PTMs include phosphorylation, acetylation, methylation, SUMOylation, glycosilation, nitrosilation and ubiquitination among others [52-54]. See Figure 1-7.

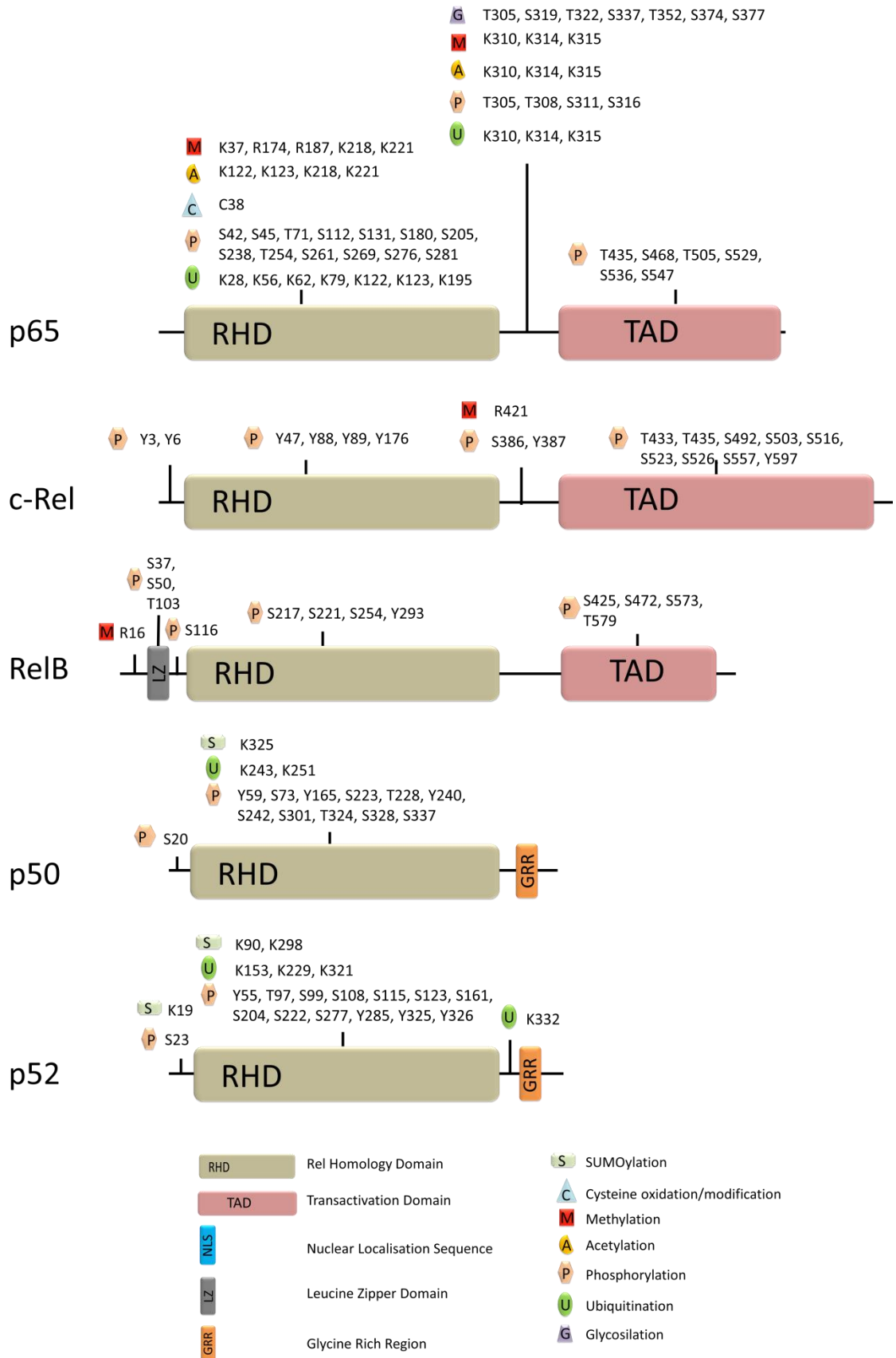


Figure 1-7 NF-κB members PTMs. Location of the different PTMs (SUMOylation, cysteine oxidation/modification, methylation, acetylation, phosphorylation, ubiquitination and glycosylation) described within the structural domains of each NF-κB member. The PTM data are taken from the PhosphoSite webpage and corresponds to the human proteins of the NF-κB family members.

1.3.2.1 Phosphorylation

Regulation of the NF- κ B members through phosphorylation has been extensively studied and it has a critical role on regulation of the NF- κ B activity [55]. There are several phosphorylation sites in all NF- κ B members (see Figure 1-7) and some of these sites regulate the transcriptional activity of NF- κ B dimers in a gene specific manner [56-61]. These phosphorylations are either a consequence of signalling from upstream components or they work as a crosstalk within different signalling pathways [17].

Phosphorylation of p65 induces a conformational change on p65 which has effects on protein ubiquitination and stability, and protein-protein interactions [62, 63]. It contains several phosphorylation sites within its whole sequence (see Table 1-1). S276 and S536 are the most studied phosphorylation sites but they are not the only ones. The different phosphorylations can enhance transactivation, promote the degradation of the subunit, regulate DNA binding specificity, stimulate dimerisation, inhibit the transactivation activity and facilitate other PTMs [57, 64-67] (see Table 1-1).

Table 1-1 p65 phosphorylation sites.

Site	Kinase	Effect	Reference
S42	Unknown	Inhibition, regulation of molecular association	[64, 68]
S45	PKA	Inhibition, regulation of molecular association	[64, 68-70]
T71	Unknown	Unknown	PhosphoSite
S112	Unknown	Unknown	[64]
S131	IKKB	Unknown	[68]
T136	IKKB	Unknown	[68]
S180	Unknown	Unknown	[64]
S205	Unknown	Transactivation	[58]
S238	PKA	Unknown	[64, 68, 70-73]
T254	Unknown	Prolyl isomerisation, transactivation	[65]
S261	Unknown	Unknown	[68]

Site	Kinase	Effect	Reference
S269	Unknown	Unknown	[68]
S276	PKA-C, MSK1, MSK2, Pim-1, RSKp90, PKCζ	Transactivation, K310 acetylation Unknown Unknown Unknown Unknown Unknown	[63, 66, 74] [75-77] [78] [79] [80] [81]
S281	Unknown	Transactivation	[58, 82]
T305	Unknown	Unknown	[83]
Y306	Unknown	Unknown	PhosphoSite
T308	Unknown	Unknown	[83]
S311	PKCζ	K310 acetylation, transactivation	[84-87]
S316	Unknown	Transactivation	[88]
T435	Unknown	Transactivation	[89, 90]
S468	GSK3B IKKε IKKB	Inhibition Transactivation Slight inhibition	[67] [56] [91]
S472	Unknown	Unknown	[68]
T505	Chk 1	Transactivation	[56, 92, 93]
S529	CK2	Transactivation, K310 acetylation	[94-97]
S536	IKKε, IKKB, IKKα, RSK1, NAK/TBK1	Transactivation, K310 acetylation Unknown Unknown Unknown Unknown	[57, 98-101] [57] [57, 98, 99] [57, 102] [57]
S547	Unknown	Unknown	PhosphoSite

*Protein kinase (PK), mitogen and stress-activated protein kinase (MSK), proviral integration site for moloney murine leukaemia virus (Pim), ribosomal s6 kinase (RSK), glycogen synthase kinase (GSK), C-terminal Src kinase (CSK)-homologous kinase (Chk), creatine kinase (CK), numb-associated kinase (NAK)/TANK binding kinase (TBK).

1.3.2.2 Acetylation

Acetylation of p65 is a reversible process which takes place in the nucleus [103, 104]. p65 subunit could be acetylated through a reversible process at seven

lysine residues (K122, K123, K218, K221, K310, K314 and K315) [103]. Acetylation of the majority of p65 acetylated lysines takes place through the activity of the p300/CREB-binding protein (CBP) acetyltransferases [103] and the effect depends on the lysine residues acetylated. Acetylation regulates the transcriptional activation of NF- κ B, the DNA binding affinity, the subcellular localisation and the ability to associate with I κ B α (see Table 1-2) [103-106]. Acetylation can be reversed by the action of histone deacetylases (HDACs). HDAC3 deacetylates the acetylated forms of p65 at K218 and K221 promoting its interaction with I κ B α and subsequent cytoplasmic translocation, repressing the transactivating activity of NF- κ B; while deacetylation of K122 and K123 increases the DNA binding of p65, activating the transcriptional activity of p65 [103, 104].

Table 1-2 p65 acetylation sites.

Site	Acetyltransferase	Effect	Reference
K122	p300/CBP PCAF	Reduces DNA binding	[103]
K123	p300/CBP PCAF	Reduces DNA binding	[103]
K218	p300/CBP	Impairs I κ B association	[103, 104]
K221	p300/CBP	Enhances DNA binding	[103-105]
K310	p300/CBP	Transactivational activity	[105]
K314	p300/CBP	Transactivational activity	[103, 106]
K315	p300/CBP	Transactivational activity	[103, 106]

* p300/CBP-associated factor (PCAF)

1.3.2.3 Methylation

The functional result of NF- κ B methylation varies depending on the methylated site and the methylation state (mono-, di- or trimethylation) [107-109]. Several methylation sites has been identified on p65 subunit such as, K37 [108], K218, K221 [107], K314 and K315 [109]. Some of these methylations induce the ubiquitination and degradation of p65 terminating the NF- κ B response [109], while others enhance the transcriptional activity of NF- κ B [107, 108]. However, as it happens for the phosphorylation and acetylation, methylation is also a reversible process by the action of histone demethylases [107]. See Table 1-3.

Table 1-3 p65 methylation sites.

Site	Methyltransferase	Effect	Reference
K37	Set9	Transactivational activity	[108]
K218	NSD1	Transactivational activity	[107]
K221	NSD1	Transactivational activity	[107]
K314	Set9	Ubiquitination and degradation	[109]
K315	Set9	Ubiquitination and degradation	[109]

* Nuclear receptor-SET domain-containing protein 1 (NSD1), suppressor of variegation-enhancer of zeste-trithorax (SET).

1.3.2.4 SUMOylation

SUMOylation occurs through the activity of the small ubiquitin-like modifier (SUMO) family of proteins [110, 111]. SUMOylation requires the action of a set of enzymes, SUMO activating protein, SUMO conjugating protein UBC9 and SUMO ligases [112]. It affects protein stability and promotes the nuclear translocation of the cytoplasmic dimers [111]. For example, SUMOylation of RelB subunit reduces RelB activity while its DNA binding capacity is intact [112]. p65 SUMOylation by the SUMO ligase protein inhibitor of activated signal transducer and activator of transcription 3 (PIAS3) acts also as a repression mechanism, it prefers DNA bound p65 and is induced by NF- κ B activation [113].

1.3.2.5 Ubiquitination

Ubiquitination is crucial not only for the activation of the NF- κ B response but also for the termination of it. Ubiquitin direct proteasomal degradation is required in the cytoplasm to free the NF- κ B dimers from the I κ B proteins and activate the NF- κ B response, but also in the nucleus to terminate the NF- κ B response [2, 42]. However, non-proteolytic ubiquitination is also required upstream of the IKK complex for the recruitment of necessary proteins. The regulation of the NF- κ B activity through ubiquitination will be further detailed in section 1.4.

1.3.2.6 PTMs crosstalk

Besides the regulation through different PTMs, there is a crosstalk among them [114, 115]. For example phosphorylation of certain p65 serines promotes binding

of p300/CBP and subsequently, acetylation of p65. Phosphorylation also mediates ubiquitination of different proteins, as for example I κ B proteins. On the other hand, p65 acetylation at K310 inhibits p65 methylation of K314, K315 [114]. Several lysines on p65 could be methylated, acetylated or ubiquitinated, the mechanism by which one or the other PTM occurs remains unclear [114].

1.3.3 NF- κ B inhibitors

Inhibition of the NF- κ B signalling pathway has been broadly studied. Here we summarise the strategies developed to target the NF- κ B signalling pathway and give some examples of inhibitors of each strategy. The majority of the inhibitors target upstream components of the NF- κ B signalling pathway such as the IKK complex or I κ B proteins degradation. NF- κ B inhibitors encompass a variety of natural products, chemicals, peptide proteins, synthetic compounds and cell penetrating peptides (CPPs). The CPP strategy is based on the ability of certain peptidic sequences, formed by 5-30 amino-acid residues rich in basic amino-acids, to cross the cellular membrane and enter into the cell [116-123]. These CPPs present a high transduction efficiency and low cytotoxicity [119, 120] and are able to deliver a large variety of cargoes into the cell [116, 120, 121, 124]. NF- κ B inhibitors can be classified, according to at which level of the signalling pathway they act, into the following groups; upstream IKK complex, IKK complex or I κ B phosphorylation, I κ B degradation, nuclear translocation of NF- κ B, DNA binding of NF- κ B and NF- κ B transactivation (see Figure 1-8, Table 1-4 and Table 1-5).

The IKK complex is the first common level for the integration of many NF- κ B activating pathways [7]. The strategy of NF- κ B inhibitors targeting upstream the IKK complex is to block a signal before it activates this first common level. The targets of these inhibitors are the receptors receiving the stimuli, the adaptor molecules recruited to the receptors or the kinases activating the IKK complex. For example, TNFR inhibition by antibodies or blocking agents leads to the inhibition of TNF induced NF- κ B response [125]. Within the adaptor molecules recruited to TNFR, we find tumour necrosis factor receptor type 1-associated death domain protein (TRADD), TRAF2 and TRAF6 [126]. ARH1 compound binds to TRADD and inhibits TRADD-TRAF2 interaction, therefore the activation of the NF- κ B response [127]. A dominant negative mutant of TRAF2 inhibits the CD40

and TNF α mediated NF- κ B activation [128], while a dominant negative mutant of TRAF6 blocks the IL-1 induced NF- κ B activation [129]. On the other hand, Toll/interleukin 1 receptor (TIR) domain containing adaptor protein (TIRAP) is recruited to TLR4 following LPS stimulation [130]; a CPP containing the sequence of TIRAP, antennapedia (AntP)-TIRAP has been described to inhibit LPS induced NF- κ B response [130, 131]. Additionally, a kinase deficient mutant of NF- κ B inducing kinase (NIK) has been reported [132, 133]. NIK phosphorylates IKK α leading to the activation of the non-canonical pathway [42, 134]; this kinase deficient mutant of NIK, inhibits IL-1 and TNF α induced NF- κ B activation [132, 133].

The IKK complex and subsequent phosphorylation of I κ B proteins is the prime target of NF- κ B signalling pathway inhibitors. These inhibitors can be classified into five groups depending on their mechanism of action. The first group are gene based inhibitors; dominant negative forms of IKK α and IKK β are shown to block the NF- κ B response [135-141]. These dominant negative mutants can be created by mutations on the adenosine triphosphate (ATP) binding site or by mutations on the kinase activation loop [136-141]. The second group is formed by ATP analogues with some specificity to interact with IKK such as β -carboline and SC-839 [142, 143]. Both ATP analogues have a preference for IKK β . The third group is composed by allosteric inhibitors of IKK like BMS-345541 [144]. These inhibitors bind to an allosteric site on both IKK α and IKK β leading to conformational rearrangements of their structure [144]. The fourth group contains compounds that interact with C179 of IKK β like thiol reactive compounds (parthenolide, arsenite, and some epoxyquinoids) [145-148]. C179 is located in the activation loop of IKK β between S177 and S181 which phosphorylation is required for IKK β activation [42, 134]. This interaction might interfere with IKK β phosphorylation and subsequent activation. And lastly, the fifth group is formed by CPPs targeting the interaction of NEMO with IKK α and IKK β . The most studied peptide inhibits the NEMO binding domain (NBD). NEMO is a scaffolding protein [149] which does not contain a catalytic domain but is critical for IKK activation [150]. Cells lacking NEMO fail to respond to any inducers of the canonical pathway [150]. NEMO associates with IKK α and IKK β through the NBD which is formed by a hexa-peptide sequence (LDWSWL) within the C-terminal region of IKK α and IKK β [150]. Disruption of the interaction

between NEMO and IKK β blocks TNF α induced NF- κ B activation in cells [150]. Several CPPs directly target NBD; AntP-NBD [151, 152], transactivating transcription (TAT)-NBD [152-155] and protein transduction domain (PTD) 5-NBD [152, 156]. They interact with IKK β and IKK α , although the function on IKK α is still unknown and they have a higher preference for IKK β [152]. These CPP inhibitors effectively block TNF α induced IKK and NF- κ B activation specifically [152].

Inhibitors of I κ B ubiquitination and degradation consist of inhibitors of the ubiquitination step and inhibitors of the proteasomal degradation. The synthetic compound Ro196-9920, has been described to inhibit I κ B α ubiquitination in mouse models, subsequently blocking the NF- κ B response [157]. Some phosphopeptides corresponding to the I κ B α phosphorylation sites have also been shown to inhibit NF- κ B signalling [158]. These phosphopeptides act as competitive inhibitors for binding the E3 ligase of I κ B α , thus blocking the NF- κ B response [158]. CPPs mimicking serine to alanine mutations of the phosphorylation sites of I κ B α S32 and S36 have also been reported. TAT-I κ B α (S32A, S36A) is known as TAT super repressor [116]. Inhibitors of the proteasome system include compounds like Bortezomib [159-161] and will be described in section 1.4.1.3.

The nuclear translocation step has an important role in NF- κ B activation. Several CPPs have been shown to inhibit p50 translocation. The best described CPP inhibiting nuclear translocation is SN50 [162, 163]. SN50 contains the NLS of p50 subunit and blocks p50 nuclear translocation by binding the importin complex. However, it also inhibits the nuclear translocation of other transcription factors which used this system [162, 163].

Targeting the NF- κ B DNA binding ability is a more specific strategy in order to inhibit the NF- κ B response. Novel compounds from clary sage (*Salvia Sclarea*) [164] and triterpene derivatives [165] are competitive inhibitors of the NF- κ B proteins by binding to κ B sites. Decoy oligonucleotides (ODNs) used this mechanism of action; they usually have modifications to increase their stability and affinity for κ B sites [166-168]. Their therapeutic potential has been demonstrated in a number of animal models of inflammation and cancer [166-168]. On the other hand, several compounds have been described to impaired

NF- κ B DNA binding ability by forming covalent bonds with the NF- κ B proteins. For example, sesquiterpene lactones (SL) inhibit NF- κ B binding ability by interaction with C38 of p65, which is located in the DNA binding loop of p65 [169, 170]. Some SLs are able to interact with homologous C residues of c-Rel and p50 [148]. However some SL like parthenolide, inhibit IKKB as well [146]. Dehydroxymethylepoxiquinomicin (DHMEQ) forms adducts with C38 of p65, C62 of p50, C144 of RelB and C27 of c-Rel impairing their DNA binding ability, thus inhibiting the NF- κ B response [171-174].

The last step of the NF- κ B signalling pathway that can be targeted is the transactivation of NF- κ B proteins. PTMs of the NF- κ B proteins have effects on their transactivating activity [52-54]. Therefore, there are some CPPs designed to inhibit NF- κ B p65 subunit phosphorylation [175, 176]. Phosphorylation of S276, S529 and S536 of p65 are required for normal transactivating ability of p65 [66, 96, 99]. AntP-peptide containing p65 S276 and AntP-peptide containing S529 and S536 effectively block TNF α , LPS and IL-1 induced NF- κ B activation [175, 176].

Besides the above inhibitors directly targeting specific steps of the NF- κ B pathway, bacterial [177-179], fungal [180, 181] and viral proteins [182], antioxidants [183, 184] and anti-inflammatory [185, 186] and immunosuppressive agents [187-189] have been described to inhibit the NF- κ B response through different mechanisms like inhibition of the IKK complex, impairing the DNA binding, blocking I κ B degradation and inhibiting the transactivation of NF- κ B proteins. Additionally some United States food and drug administration (FDA) approved drugs have been demonstrated to inhibit NF- κ B activity for example aspirin [185] and Bortezomib [190]. On the other hand, several compounds like D609, R031-8220, SB203580 [191], wortmannin and LY294,002 [192, 193] have been shown to indirectly inhibit NF- κ B transactivation ability.

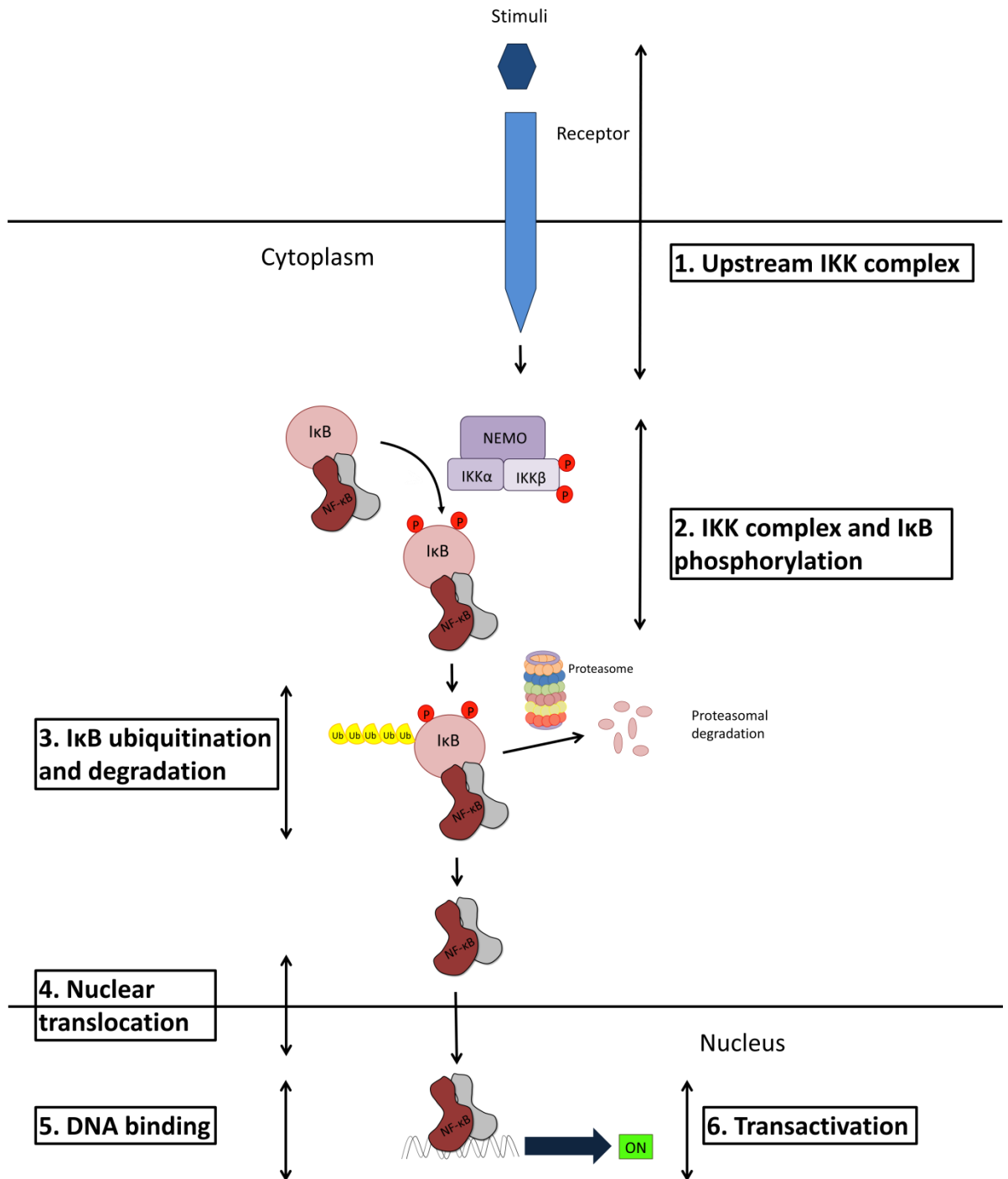


Figure 1-8 NF-κB signalling pathway inhibitors targets. Inhibitors of the NF-κB signalling pathway target different levels of the signalling cascade. These inhibitors are classified into different groups depending on which level of the signalling pathway they target. The first group targets components upstream the IKK complex, second group targets directly the IKK complex or IκB phosphorylation, the third group targets the IκB ubiquitination and degradation, fourth group the nuclear translocation of the NF-κB dimers, fifth group the ability of NF-κB dimers to bind the DNA, and lastly the sixth group targets the transactivation of the NF-κB dimers.

Table 1-4 Mutations inhibiting the NF- κ B signalling pathway

Target	Mutant	Function	Reference
Upstream IKK complex	TRAF2 dominant negative mutant	Inhibits CD40 and TNF α induced NF- κ B response at receptor associated proteins level	[128]
Upstream IKK complex	TRAF6 dominant negative mutant	Inhibits IL-1 induced NF- κ B response at receptor associated proteins level	[129]
Upstream IKK complex	NIK kinase deficient mutant	Inhibits IKK activation by NIK	[132, 133]
IKK complex	IKK α dominant negative mutant	Inhibits IKK α kinase activity	[135-141]
IKK complex	IKK β dominant negative mutant	Inhibits IKK β kinase activity	[135-141]

Table 1-5 Compounds directly inhibiting components of the NF- κ B signalling pathway

Target	Compound	Function	Reference
Upstream IKK complex	Anti-TNFR antibody or agent	Inhibits TNF α signalling at receptor level	[125]
Upstream IKK complex	AntP-TIRAP	Inhibits TLR4 signalling at receptor associated proteins level	[130, 131]

Target	Compound	Function	Reference
Upstream IKK complex	ARH1	Inhibits TRADD-TRAF2 interaction	[127]
IKK complex	β -carboline	ATP analogue of IKK	[142, 143]
IKK complex	SC-839	ATP analogue of IKK	[142, 143]
IKK complex	BMS-345541	Allosteric inhibitor of IKK	[144]
IKK complex	Thiol reactive compounds	Interaction with C179 of IKK, inhibiting IKK phosphorylation and activation	[145-148]
IKK complex	AntP-NBD TAT-NBD PTD5-NBD	Inhibits the interaction of IKK α and IKK β with NEMO, thus its activation	[151, 152] [152-155] [152, 156]
I κ B ubiquitination and degradation	Ro196-9920	Inhibits I κ B α ubiquitination	[157]
I κ B ubiquitination and degradation	Phosphopeptides	Competitive inhibitors of I κ B α E3 ligase, thus inhibiting I κ B α ubiquitination	[158]
I κ B ubiquitination and degradation	TAT-I κ B α (S32A, S36A)	Inhibits I κ B α phosphorylation and subsequent ubiquitination	[194, 195]

Target	Compound	Function	Reference
NF- κ B nuclear translocation	SN50	Inhibits p50 nuclear translocation	[162, 163]
NF- κ B DNA binding ability	Compounds from <i>Salvia Sclarea</i>	Competitive inhibitors of κ B sites	[164]
NF- κ B DNA binding ability	Triterpene derivatives	Competitive inhibitors of κ B sites	[165]
NF- κ B DNA binding ability	Decoy oligonucleotides	Competitive inhibitors of κ B sites	[166-168]
NF- κ B DNA binding ability	Sesquiterpene lactones	Covalent binding with C residue on the active loop of the DNA binding domain	[148, 169, 170]
NF- κ B DNA binding ability	DHMEQ	Covalent binding with C residue on the active loop of the DNA binding domain	[171-174]
NF- κ B transactivation	AntP- p65 S276	Inhibits p65 S276 phosphorylation	[175]
NF- κ B transactivation	AntP- p65 S529 and S536	Inhibits p65 S529 and S536 phosphorylations	[175, 176]

However, most of these strategies are not totally NF- κ B specific and have also effects on other signalling pathways. Some targets of these inhibitors are shared members of different signalling pathways. Inhibition of these shared members may inhibit NF- κ B response as well as PKR, c-Jun N-terminal kinase (JNK) and extracellular signal-regulated kinase (ERK) 1/2 [196-198]. As for other inhibitors the mechanism of action is not completely elucidated, additional investigation of the potential effects is needed [152]. Further investigation on NF- κ B specific inhibition is required to properly develop a new specific NF- κ B inhibitory compound.

1.4 Ubiquitination in the regulation of the NF- κ B response

Ubiquitination has a key role in the activation and termination of the NF- κ B response.

1.4.1 The ubiquitin proteasome system

The UPS is key for most of the regulated proteolysis in the cells [199] but it also has non-degradative functions. Some of these functions are; regulation of the cell cycle [200]; cancer and cell survival [200]; immune response by the digestion of external or internal proteins into peptides which are presented by antigen presenting cells [201]; protein misfolding, it collaborates in the elimination of misfolded proteins [202]; endoplasmic reticulum (ER) associated degradation (ERAD) by its involvement on the degradation of misfolded proteins [203, 204]; and inflammatory responses by its role on the NF- κ B response [205] (see section 1.4.2). It has a huge variety of substrates and malfunction of the UPS is involved in several pathologies such as cancer [206, 207], cardiovascular disease [208], viral diseases [209] and neurodegenerative disorders [210] among them.

Proteins targeted for proteasomal degradation by the proteasome are tagged by the addition of ubiquitin molecules [211, 212]. Ubiquitin is a small molecule of 76 amino-acids which is covalently attached to the target proteins by an isopeptide bond between the carboxy terminal of the C-terminal glycine (G76) and the primary amine of a lysine of the target protein or the ubiquitin itself

[213, 214]. Ubiquitin contains 7 lysines (K6, K11, K27, K29, K33, K48 and K63) and the N-terminal methionine (M1) which can serve as an additional ubiquitination site [215-217]. The different polyubiquitin chain linkages lead to different structural conformations and different biological roles [215-217] (see Table 1-6). K11 and K48 linkages promote proteasomal degradation of target proteins [218-221]. The other K-linked polyubiquitin chains are involved in non-proteolytic functions; such as, DNA damage response (K6, K27, K63) [222-226], adenosine monophosphate (AMP)-activated protein kinase (AMPK) related kinase signalling (K29, K33) [227], mitochondrial biology (K6, K27) [228-231], endocytosis (K63) [232] and NF- κ B signalling (K63, M1) [226, 233-238] among others.

Table 1-6 Polyubiquitin chains function in cells

K-linkage	Function	Reference
M1	NF- κ B activation	[233-238]
K6	DNA damage response Parkin mediated mitophagy	[222, 223] [228, 229]
K11	Cell cycle regulation Proteasomal degradation ERAD Wnt/ β -catenin signalling	[239] [221] [240-242] [243]
K27	PKC signalling pathway DNA damage response Parkin mediated mitophagy Differentiation and tolerance of T cells	[244] [224] [230, 231] [245]
K29	Differentiation and tolerance of T cells AMPK-related kinases regulation Wnt/ β -catenin signalling	[246] [227] [243]
K33	Differentiation and tolerance of T cells AMPK-related kinases regulation Post-Golgi trafficking	[247] [227] [248]
K48	Proteasomal degradation Lysosomal degradation	[218-220] [249]
K63	DNA damage response Stress response	[225, 226] [250]

K-linkage	Function	Reference
K63	NF- κ B signalling	[226]
	Endocytosis	[232]
	Lysosomal targeting	[249]

The ubiquitination process is regulated by a three step enzymatic cascade that involves the ubiquitin activating enzyme E1, a ubiquitin conjugating enzyme E2 and a ubiquitin protein ligase E3 [211, 214]. The first step requires the activation of the ubiquitin molecule in an ATP dependent manner. This activated ubiquitin molecule is bound to the E1 enzyme by the formation of a thioester bond and is passed onto one E2 conjugating enzyme as an activated moiety. Lastly, the E2-ubiquitin binds the E3 ligase bound to the target substrate forming a complex and the ubiquitin molecule is then transferred onto the target protein [212, 214, 251]. In order to mark these target proteins for proteasomal degradation addition of several ubiquitin molecules by a K48-linkage occurs [212, 251]. See Figure 1-9.

Polyubiquitinated substrates are delivered to the proteasome [251]. The proteasome is a ~2.5MDa multimeric subunit composed by two components, the 20S core particle and the 19S regulatory particle [213, 214, 251, 252]. The 20S is organised in a barrel structure formed by 4 heptameric rings. The inner two are the β -rings formed by β type subunits, and the outer two are the α -rings formed by α type subunits. The active site is in the centre of the barrel and located in the β -rings, while the α -rings are more conserved forming a selective barrier between the catalytic site and the cytoplasm or nucleus of the cell [213, 214, 252]. This active site contains different catalytic activities, trypsin like, chemotrypsin like and peptidyl-glutamyl-peptide bond hydrolysing activities [213]. This barrel is capped at either sides or single end by the regulatory particle 19S [213, 214, 252]. The 19S regulates the gate opening for substrate proteasomal degradation. It contains several enzymatic activities and ubiquitin receptors promoting deubiquitination of substrates, unfolding of the target proteins and translocation into the 20S interior [213, 214, 252]. The deubiquitination of tagged substrates support the ubiquitin recycling within the cell [214]. This deubiquitination of the target protein takes place through the

activity of several DUBs such as RPN11, USP14 and UCH37 [253-256]. Once the target protein is in the interior of the 20S particle, is cleaved and degraded [213, 214, 252]. See Figure 1-9.

However, ubiquitination is a reversible process, ubiquitin molecules can be removed by DUBs [257, 258] (see Figure 1-9). There is a balance between ubiquitination and deubiquitination; and depending on which activity level is higher, the result will be the ubiquitination of target proteins and subsequent proteasomal degradation or maintenance of the target protein [257, 259]. Thus, the importance of E3 ligases and DUBs in NF- κ B response.

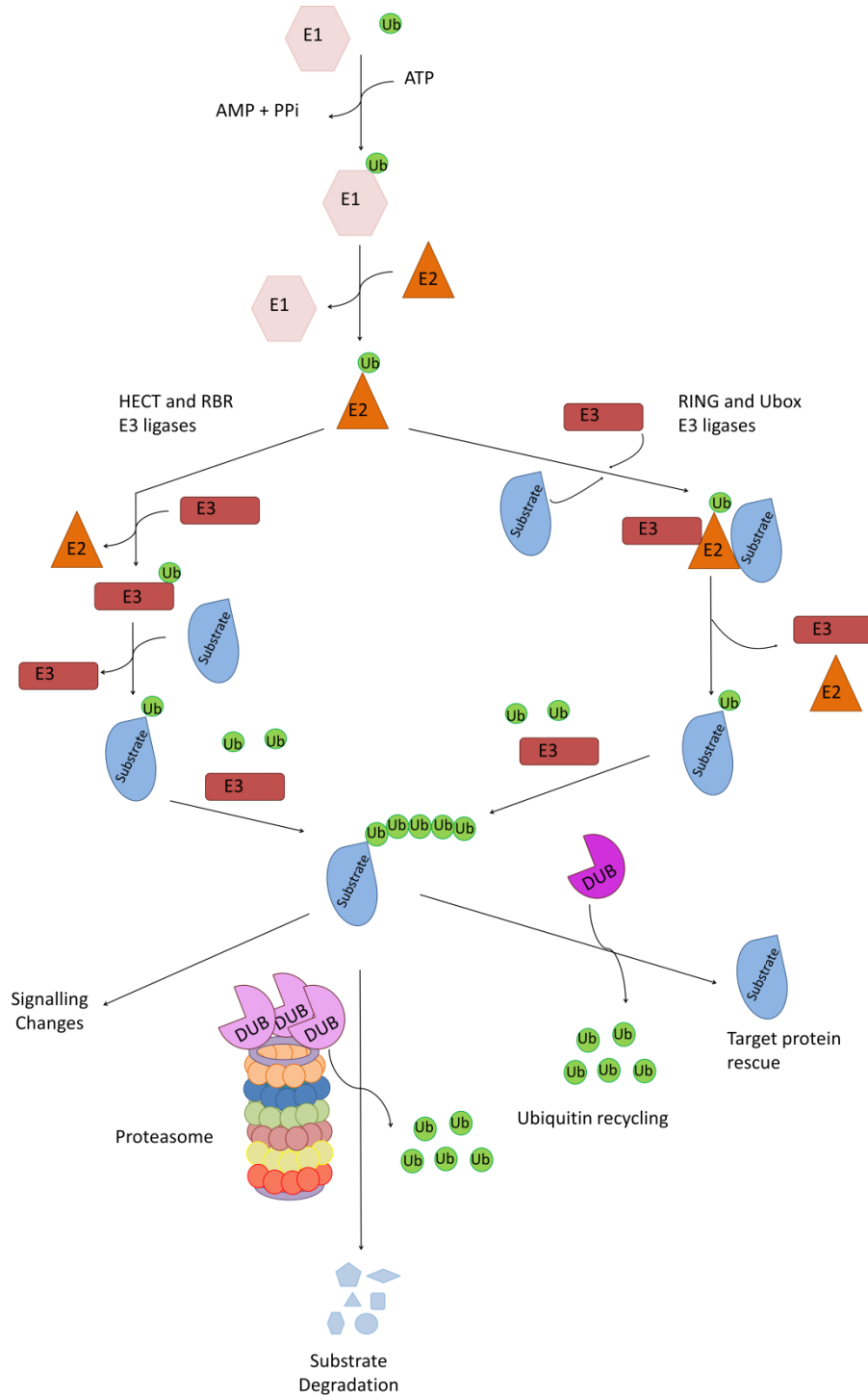


Figure 1-9 Schematic of the UPS system. The protein ubiquitination process is regulated by a three step enzymatic cascade that involves the ubiquitin activating enzyme E1, a ubiquitin conjugating enzyme E2 and a ubiquitin protein ligase E3. Firstly the ubiquitin molecule is activated in an ATP dependent manner and is subsequently bound to the E1 enzyme. Secondly, the active ubiquitin is transferred to the E2 enzyme. And lastly, the ubiquitin molecule is transferred onto the target protein via two different ways depending on the E3 ligase transferring the ubiquitin. RING and Ubox E3 ligases bind to the E2 enzyme and to the substrate directly transferring the ubiquitin from the E2 to the substrate. While for HECT and RBR E3 ligases the ubiquitin is firstly transferred from the E2 enzyme to the E3 ligase and then onto the target protein. Subsequently, addition of several ubiquitin molecules could occur. This protein ubiquitination could lead to proteasomal degradation prior ubiquitin molecules removal, cellular signalling or the ubiquitin molecule could be removed by DUBs rescuing the tagged protein from degradation.

1.4.1.1 E3 ligases

Protein degradation selectivity by the UPS is controlled by E3 ligases [214]. While there are only two E1 enzymes, there are around 40 E2 enzymes and more than 600 E3 ligases; hence, substrate recognition and specificity is determined by E3 ligases [214], proving the important role of E3 ligases within the UPS system. There are four different subfamilies of E3 ligases; Really interesting new gene (RING) E3 ligases, Homology to E6-AP C-terminal (HECT) E3 ligases, Ubox E3 ligases and RING between RING (RBR) E3 ligases [260-264]. These subfamilies differ in their E2 binding domains and substrate recognition domains, determining the specificity of the UPS action [260-264]. E3 ligases are helped by co-factors which modify E3 ligases' intracellular localisation and subsequently localisation of the ubiquitinating activity [260-264]. The transfer of ubiquitin from the E2 enzyme to the substrate occurs via two different mechanisms [214, 252]. RING and Ubox subfamilies bind to both, E2 and substrate, at the same time catalysing the transfer of ubiquitin directly from the E2 to the substrate [214, 252]. While HECT and RBR subfamilies require a two-step reaction process. Firstly, the ubiquitin is transferred from the E2 to the active cysteine of the E3 and subsequently transferred from the E3 ligase to the substrate [214, 252].

1.4.1.2 Deubiquitinase enzymes

Ubiquitin can be removed from target proteins by the action of deubiquitinating enzymes [257, 258]. It is an essential mechanism in ubiquitin-mediated signalling networks [258]. For many proteins addition of a ubiquitin molecule supposes a decrease in their stability [259]; however, protein stability is restored by the removal of the ubiquitin molecule by DUBs [257]; hence, it is not only important the ubiquitination process but also the deubiquitination process. DUBs specifically cleave the isopeptide bond at the c-terminus of ubiquitin [265-267]. By this reaction, DUBs add an additional posttranslational regulation level. The cleavage of the isopeptide bond is made by a nucleophilic attack to the carbonyl group of the isopeptide bond, resulting in the hydrolysis of the bond linking the ubiquitin to the target protein or to itself [268, 269]. As a consequence of the reaction, a polyubiquitin chain or monoubiquitin chain and a non-ubiquitinated target protein are obtained.

There are 95 putative DUBs encoded in the human genome, from which only 79 are functional [270]. DUBs are divided into five families according to their protease domain. The majority of them are cysteine proteases but there is a small group which are zinc metalloproteases. The five cysteine protease families are; ubiquitin carboxy-terminal hydrolases (UCHs), USPs, ovarian tumour proteases (OTUs), Machado-Joseph diseases proteases (Josephins) and the MIU-containing novel DUB family (MINDY); and the zinc metalloprotease family is formed by the JAB1/MPN/Mov34 (JAMMs) [258, 266, 267, 269, 271].

The purposes of DUBs' activity are; processing of the ubiquitin precursors [272] and recycling of attached ubiquitin from molecules committed to degradation and consequently generating free ubiquitin, maintaining the ubiquitin homeostasis [273-275]; rescuing ubiquitinated proteins from proteasomal and lysosomal degradation [276, 277]; controlling protein trafficking [278, 279]; increasing target protein expression [280]; editing the ubiquitin chains [265] and regulating intracellular processes such as, cell cycle progression [281], apoptosis [268, 282], reproduction [283], gene transcription [268], DNA damage and repair [281] and immunity [284-288]. DUBs carry out their function by; interaction and co-regulation of E3 ligases; hydrolysis and re-organisation of poly- and monoubiquitinated proteins; being active at certain localisations in the cell and facilitating or inhibiting proteolysis [269]. In order to act in the correct localisation and recognise the specific substrate, the activity of these DUBs has to be strictly regulated [266]. Therefore, action of DUBs is tissue specific and context-dependent [282]. Apart from substrate protein specificity, DUBs are able to distinguish between different ubiquitination chains and linkages [267, 289], adding an extra regulatory level of their activity.

The mechanisms regulating DUBs deubiquitinating activity are; PTMs [290, 291]; protein interaction and allosteric activation [290, 292, 293]; redox regulation by reactive oxygen species [294]; specific subcellular localisation [295-298]; and in final instance, reactivity and conformation of their active site residues' [299-301].

1.4.1.3 UPS inhibitors

The ubiquitin and proteasome system has been an interesting subject for research in order to find novel therapeutic drugs. Several steps can be targeted within the proteasomal degradation pathway [302, 303] (see Figure 1-10). The proteasome itself can be directly inhibited. MG132 is the best known proteasome inhibitor and it is frequently used in research. MG132, also called carbobenzoxy-L-leucyl-Leucyl-L-leucin, is a peptide aldehyde proteasome inhibitor [304] able to inhibit different types of proteases [304]. It covalently binds the active site of the β subunits of the proteasome effectively blocking the proteolytic activity of the 26S proteasome complex [305]. It has never been clinically tested due to rapid oxidation, but is a valuable tool in research [302]. Due to the proteasome being key in the cellular function, blocking its activity leads to cellular toxicity and cell death after prolonged treatment or high concentrations [306, 307]. However, only two proteasome inhibitors have been approved by the FDA; Bortezomib [159, 308-310] and Carfilzomib [311-314], both of them approved for the treatment of cancer. Several drugs have been discovered but due to toxicity, poor specificity or drug activity, none have been approved by the FDA yet, although some are currently in clinical trials [306, 307, 315].

Components of the three enzymatic steps in the ubiquitination process can be targeted. Several E1 inhibitors have been developed. PYR-41 is an irreversible inhibitor of ubiquitin-like modifier activating enzyme 1 (UBA1) blocking its catalytic cysteine [316]. But it can also partially inhibit HECT E3 ligases activity [316]. PYDZ-4409 is also a UBA1 inhibitor [317]. JS-K is a nitric oxide producing prodrug which inhibits the ubiquitin binding to E1 enzymes [318]. Finally, MLN4924 inhibits the E1 NEDD8 activating enzyme (NAE) [319, 320]. NEDD8 is required for the activation of Cullin RING ligases (CRL) an E3 ligases subfamily [321-323]. MLN4924 inhibitor binds to the binding pocket of NEDD on NAE and subsequently all the CRL E3 enzymes stay in their inactive conformation [324].

Drugs targeting different E2 enzymes have also been developed, which is a more specific strategy than targeting E1 enzymes [325]. Different strategies have been used, either directly inhibiting E2 enzymes or blocking the transfer of ubiquitin to substrates [326-328]. As an example, CC0651 is an allosteric inhibitor of cell division cycle 34 (CDC34) E2 enzyme [326]. It binds into a pocket far from its

catalytic domain inducing conformational rearrangements which make it unable to transfer the ubiquitin into the target protein [326]. On the other hand, two different compounds have been designed to inhibit UBE2N-UBE2V1 E2 enzyme activity [327, 328]. UBE2N is the active subunit and the target for these two compounds [327-329]. NSC607923 is a small molecule compound which inhibits the UBE2N-ubiquitin binding [328]. BAY 117082 covalently modifies the reactive cysteine of UBE2N and possibly of several other E2 enzymes [327].

Inhibitors of the ubiquitin ligation step target E3 ligases or their interaction with their target proteins. These include inhibitors of the Skp, cullin, F-box containing complex (SCF)^{SKP2} E3 ligase complex, by the disruption of the interaction between its components [330-332]. Three inhibitors of Cereblon (CRBN), an E3 ligase enzyme component of the complex CRL4^{PDB1} have been approved by the FDA for multiple myeloma cancer treatment [333-335]. Thalidomide, Lenalidomide and Pomalidomide alter CRBN substrate preference and are called immunomodulatory drugs (IMiDs) [333-335]. Inhibitors of the mouse double minute 2 (MDM2) E3 ligase and p53 complex include Nutlins [336], MI219 [337] and reactivating p53 and inducing tumour apoptosis (RITA) [338]. RITA binds to p53 inhibiting its interaction with MDM2 [338], while Nutlins and MI219 bind to MDM2 inhibiting its interaction with p53 [336, 337]. Ubiquitin chains are also target of some inhibitory compounds [306, 339]. Ubistatins are small molecules which specifically bind to K48 linked ubiquitin chains changing the conformation of ubiquitin and impairing its recognition by polyubiquitin receptors of the proteasome [339].

DUBs have also been the subject of research in the field of UPS inhibitors [302, 303]. All patented deubiquitinating enzyme inhibitors are largely reviewed in *Deubiquitinases (DUBs) and DUB inhibitors: a patent review* (Farshi et al, 2016). DUB enzymes inhibition shifts the ubiquitination-deubiquitination equilibrium towards ubiquitination and subsequent proteasomal degradation of the substrate proteins [302].

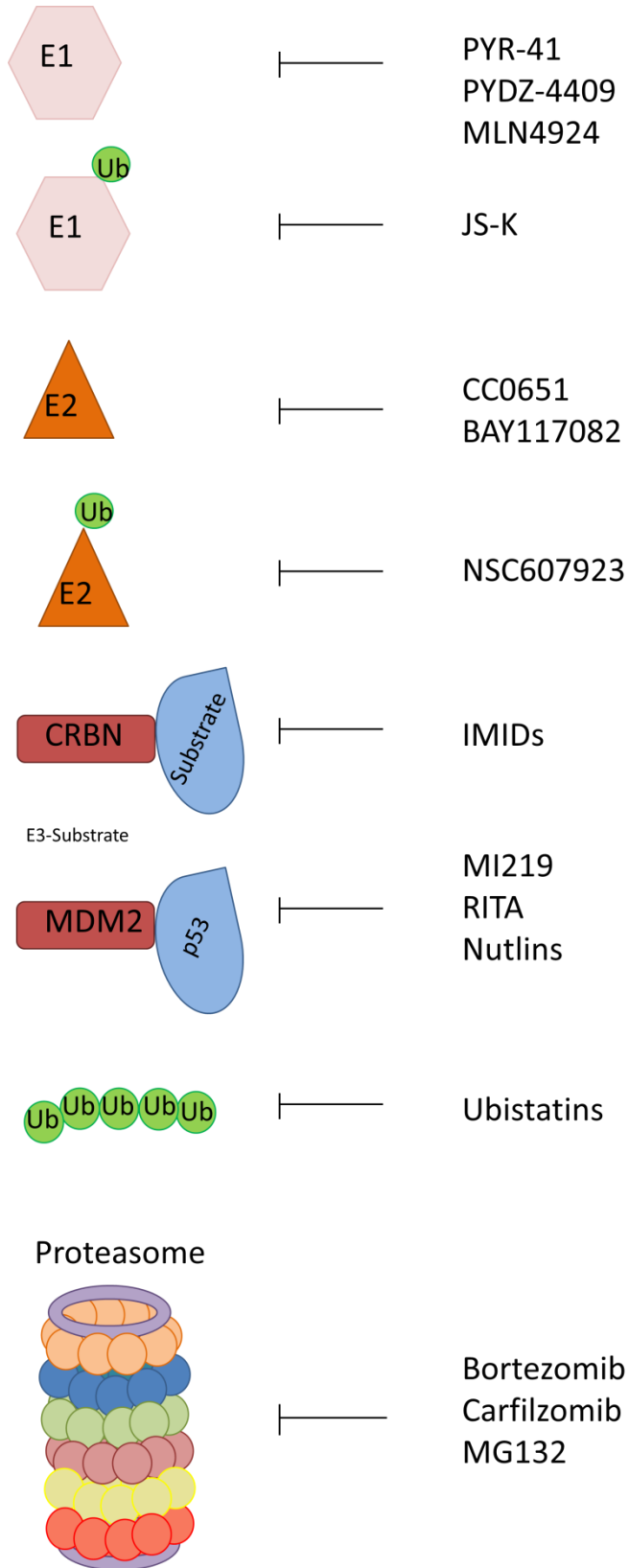


Figure 1-10 Schematic of the UPS system inhibitors. Inhibitors blocking different steps of the ubiquitination process. PYR-41, PYDZ-4409 and MLN4924 compounds inhibit E1 enzymes activity while JS-K compound inhibits the binding of E1 enzyme to the active ubiquitin molecule. Similarly, CC0651 and BAY117082 inhibit E2 enzymes activity while NSC607923 inhibits the binding of the ubiquitin molecule to the E2 enzyme. IMiDs directly inhibit CRBN E3 ligase, however there are compounds inhibiting the E3-substrate interaction such as MI219, RITA and Nutlins which inhibit MDM2-p53 interaction. Ubistatins, on the other hand, inhibit the recognition of polyubiquitin chains. And lastly, Bortezomib, Carfilzomib and MG132 compounds inhibit the proteasome activity.

1.4.2 Ubiquitination in the NF- κ B signalling pathways

Ubiquitination of different components of the NF- κ B signalling pathway is required for NF- κ B activation. Different polyubiquitin chains play an important role in the activation and termination of the NF- κ B activity. K48 polyubiquitin chains are essential for the activation of the NF- κ B response in the canonical pathway but they also play an inhibitory role in the non-canonical pathway. Processing of the p100 and p105 proteins is required for p52 and p50 formation respectively [43]. p100 and p105 precursor proteins phosphorylation by the IKK complex is recognised by the E3 ligase complex SCF^{BTrCP}. SCF^{BTrCP} polyubiquitinates, with K48-linked polyubiquitin chains, p100 and p105 leading to their partial degradation and subsequent p52 and p50 formation respectively [42, 340, 341]. In the canonical pathway, ubiquitination and subsequent proteasomal degradation of the I κ B proteins is required to free the NF- κ B dimers leading to their nuclear translocation [7-10, 15]. Phosphorylation of I κ Bs by the IKK complex is also recognised by SCF^{BTrCP}, which K48 polyubiquitinates the I κ B proteins leading to their proteasomal degradation [341]. In this way, K48 polyubiquitination is exerting its NF- κ B signalling pathway activator role. Besides, the K48 polyubiquitination plays a positive role in the activation of the non-canonical pathway as well. In CD40 signalling, cellular inhibitor of apoptosis protein (cIAP) 1/2, which are recruited to CD40, ubiquitinate proteins associated to CD40 like TRAF2 and TRAF3, which leads to their proteasomal degradation and subsequent activation of the NF- κ B activity [342]. See Figure 1-11. However, in the absence of a stimulus K48 polyubiquitination restricts the constitutive activation of NF- κ B non-canonical pathway. In this case cIAP1/2 ubiquitinate NIK, leading to its proteasomal degradation and inhibiting the NF- κ B constitutive activation [343-345]. See Figure 1-12.

Addition of non-proteolytic polyubiquitin chains is also crucial for activation and/or termination of the NF- κ B response. In the TNFR signalling, components of the TNFR1-associated signalling complex (TNF-RSC) undergo K63 and linear ubiquitination. The TNF-RSC is composed of proteins such as receptor interacting protein 1 (RIP1), cIAP1/2, TGF β activated kinase 1 (TAK1) [346]. K63- and linear polyubiquitination of RIP1 by cIAP1/2 recruits TAK1 binding protein (TAB)-TAK1 complex and activates its kinase activity phosphorylating and activating the IKK

complex, subsequently activating the NF- κ B response [346-351]. Besides cIAP1/2 ubiquitination, RIP1 could be linearly ubiquitinated by the LUBAC complex [352]. In the same way, K63-polyubiquitination by TRAF6 and linear polyubiquitination by LUBAC of NEMO promotes IKK activation [233, 351-358]. However, these linkages also play a role in the termination of the NF- κ B response by the recruitment of negative regulators of NF- κ B activity leading to its inhibition [359-361]. It has also been described that TNF α stimulation leads to K11 polyubiquitination of RIP1 by cIAP1 leading to IKK activation and subsequent NF- κ B activation [236, 362]. K6- and K27-polyubiquitination of NEMO activates the NF- κ B pathway in response to TNF α stimulation or virus infection respectively [363, 364]. K33-linked polyubiquitination of PKC ζ inhibits the TCR signalling, thus inhibiting the NF- κ B response [247]. Moreover, mixed polyubiquitin chains have been discovered, which can carry multiple recognition signals [365]. See Figure 1-13.

Ubiquitination of NF- κ B subunits is also critical in the termination of the NF- κ B response and is a major limiting factor in the expression of pro-inflammatory genes [366, 367]. NF- κ B ubiquitination and deubiquitination are DNA binding dependent [287, 366, 368]. DNA has a role as an allosteric regulator of NF- κ B, inducing a conformational change in NF- κ B structure [369, 370]. This change is recognised by the proteins of the ubiquitination apparatus, that differentially interact with DNA-bound versus nucleoplasmic NF- κ B [369, 370]. This will be further described in section 1.4.2. See Figure 1-14.

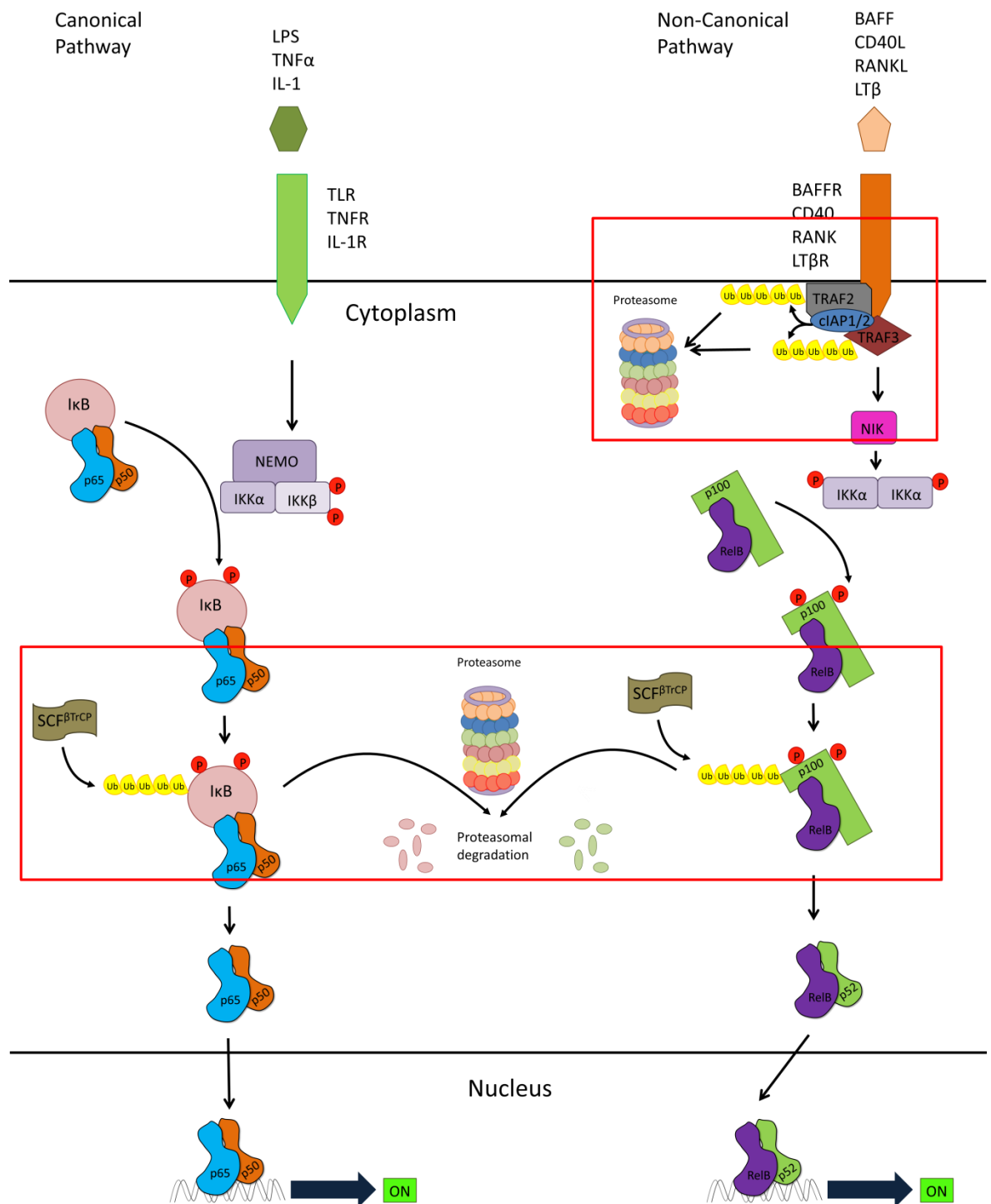


Figure 1-11 K48-linked polyubiquitin chains positive role in NF- κ B activation. During the NF- κ B signalling cascade, K48 ubiquitination and subsequent proteasomal degradation of proteins is required (highlighted in red boxes). In the canonical pathway, I κ B proteins sequester NF- κ B dimers in the cytoplasm, but K48 ubiquitination by the SCF- β TrCP E3 ligase complex and subsequent proteasomal degradation of these I κ B proteins leads to translocation of the dimers into the nucleus. In the non-canonical pathway, receptor associated protein cIAP1/2 K48 ubiquitinates other receptor associated proteins such as TRAF2 and TRAF3 leading to their proteasomal degradation and subsequent NF- κ B activation. Besides, K48 polyubiquitination by the SCF- β TrCP E3 ligase complex and controlled proteasomal degradation of p100 leads to the formation of RelB-p52 dimers able to translocate to the nucleus and activate the NF- κ B response.

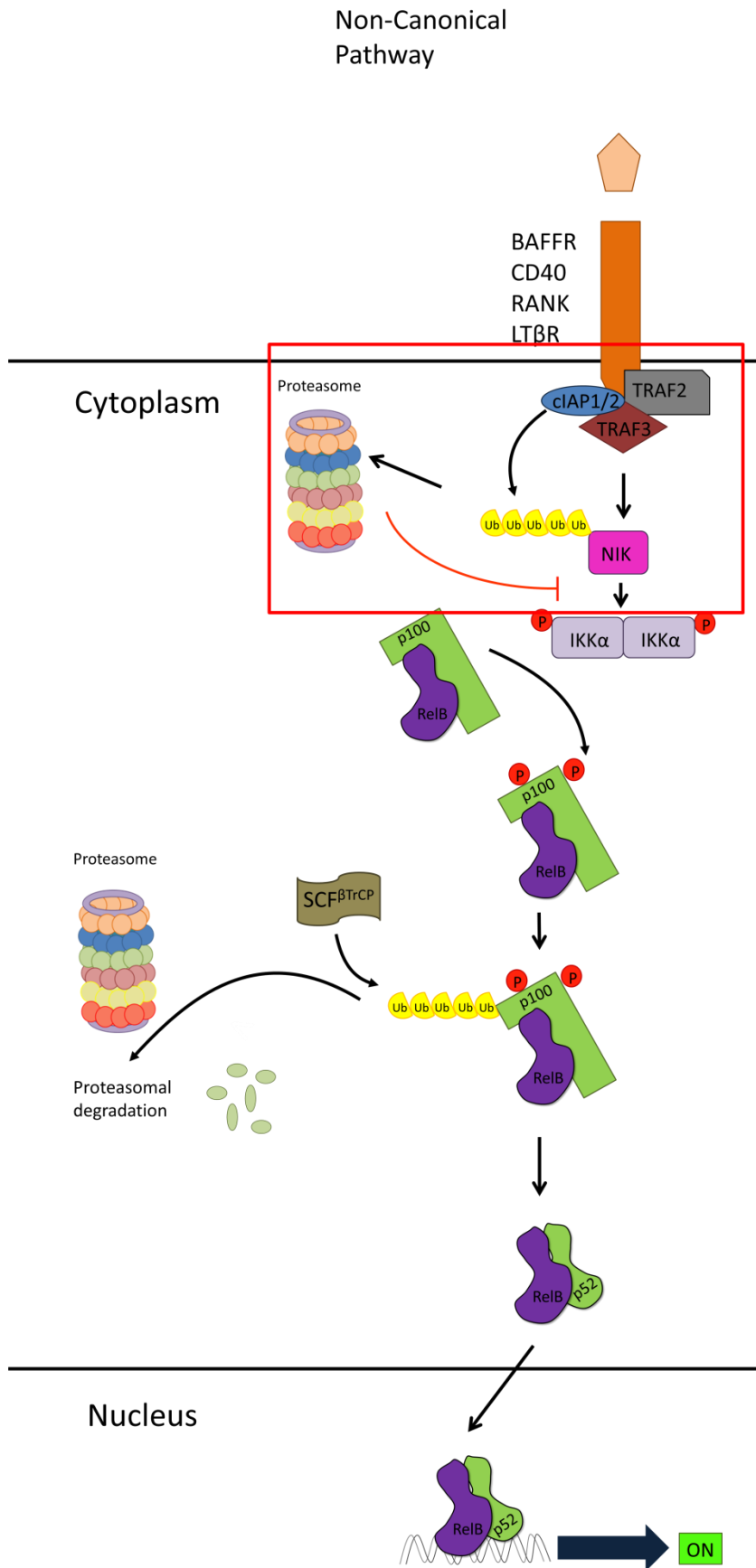


Figure 1-12 K48-linked polyubiquitin chains negative role in NF-κB activation. In the non-canonical pathway in the absence of a stimulus the receptor associated protein cIAP1/2 K48 polyubiquitinates NIK leading to its proteasomal degradation and subsequent restriction of the NF-κB constitutive activation (highlighted in the red box).

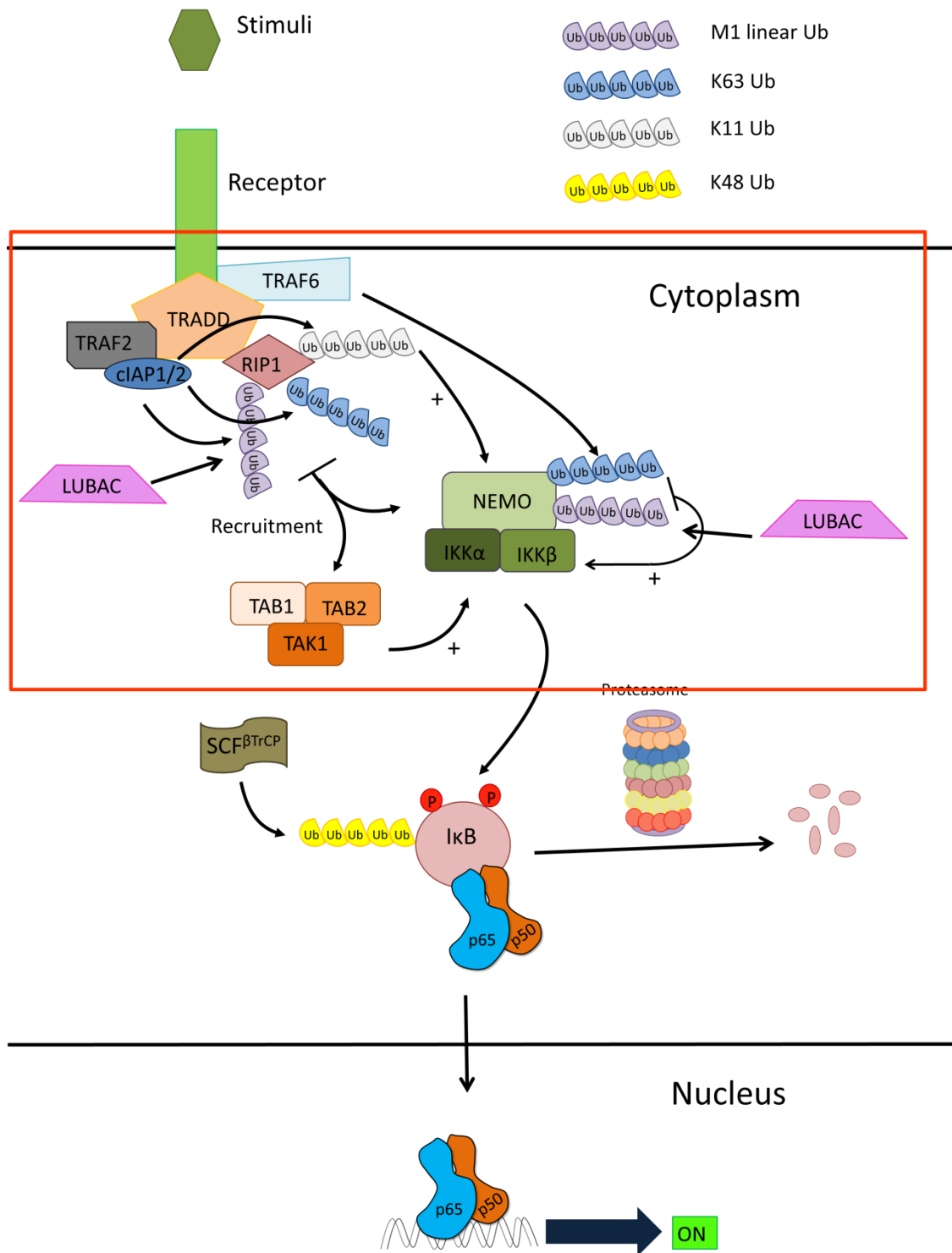


Figure 1-13 Non-proteolytic ubiquitination of the NF-κB signalling pathway. Receptor associated RIP1 protein could be K63 and K11 polyubiquitinated by cIAP1/2 and M1 polyubiquitinated by cIAP1/2 and LUBAC. K11 polyubiquitination of RIP1 activates the IKK complex. K63 and M1 polyubiquitination of RIP1 recruits NEMO and subsequently activates the IKK complex, and TAB-TAK1 complex which phosphorylates and activates the IKK complex. NEMO protein, component of the IKK complex, could be M1 polyubiquitinated by LUBAC and K63 polyubiquitinated by TRAF6 which leads to IKK activation. M1 polyubiquitin chains are coloured in grey, K11 polyubiquitin chains in blue, K48 polyubiquitin chains in yellow and K63 polyubiquitin chains in light purple. Non-proteolytic ubiquitination within the NF-κB signalling pathway is highlighted in the red box.

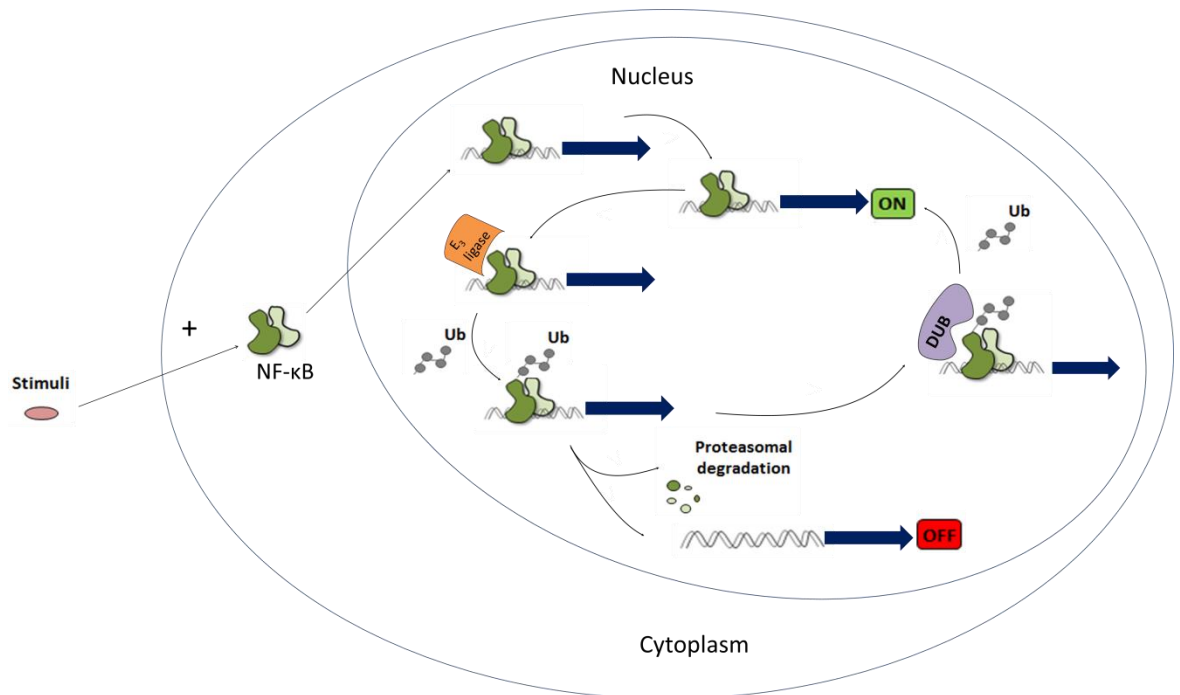


Figure 1-14 Nuclear NF-κB regulation by the ubiquitination/deubiquitination balance. NF-κB response is regulated in the nucleus by the ubiquitination/deubiquitination balance. Once the cell receives an stimuli it activates the NF-κB response, NF-κB dimers are free in the cytoplasm and translocate to the nucleus where they bind to their target gene promoters and transcribed them. In the nucleus, NF-κB dimers can be ubiquitinated by E3 ligases and subsequently degraded by the proteasome, terminating the NF-κB response. This ubiquitin process is reversible and ubiquitin molecules can be removed from target proteins by the action of DUBs. Removal of the ubiquitin molecules maintains an active NF-κB response.

1.4.2.1 E3 ligases

E3 ligases have an important role inducing NF-κB degradation. Almost all NF-κB subunits are known to be ubiquitinated and subsequently degraded by the proteasome system but the main focus is on p65 ubiquitination. The mechanism of action and the specific E3 ligase ubiquitinating each ubiquitination site on p50, p52, c-Rel and RelB are poorly understood.

p52 is known to be ubiquitinated at K153, K229, K319 but no further information of the ubiquitination process on p52 is available [71, 371, 372]. p50 ubiquitination is induced in response to TLR and TNFR activation and it requires p50 DNA binding [368]. Two ubiquitination sites have been identified K243 and K251 [71, 372, 373]. Herpes simplex virus 1 (HSV-1) infected cell protein 0 (ICP0) and it has been identified to interact with p50 and deubiquitinate it [374]. However the specific p50 ubiquitinating mechanism is still unknown. RelB

ubiquitination promotes transcriptional activity and it consists on different K-linkages of polyubiquitin chains [375-377]. This suggests that RelB ubiquitination does not have a proteolytic role, although the different polyubiquitination chain types may have different functions. c-Rel ubiquitination sites have not yet been identified, although two E3 ligases interacting with c-Rel have been identified, pellino E3 ubiquitin ligase 1 (Peli-1) [378] and cIAP [344, 379]. Both proteins when overexpressed induce c-Rel ubiquitination, however, no evidence of direct ubiquitination of c-Rel by Peli-1 and cIAP has yet been reported [344, 378, 379].

p65 protein is known to be ubiquitinated by several E3 ligases such as peroxisome proliferator-activated receptor γ (PPAR γ) [380], inhibitor of growth family member 4 (ING4) [381-383], suppressor of cytokine signalling 1 (SOCS1) [384], ORF73 (LANA from human herpesvirus 8) [385], PDZ and LIM domains protein 2 (PDLIM2) [386] and HERC3-Ubiquilin1 [387], at several ubiquitination sites including K28, K56, K62, K79, K122, K123, K195, K310, K314 and K315 [380-383] (see Table 1-7). HERC3 E3 ligase overexpression leads to p65 ubiquitination and degradation. However, this p65 ubiquitination requires the action of a second E3 ligase, ubiquilin1 [387]. PDLIM2 is a member of the actinin associated LIM protein family which interacts and promotes p65 ubiquitination, although *in vitro* p65 ubiquitination ability has yet not been demonstrated [386]. ORF73 is a cullin-5-RING ubiquitin ligase (ECS) type ligase complex which increases p65 ubiquitination and subsequent degradation [385]. SOCS1 is also an E3 ligase forming part of a multisubunit ECS complex, ECS^{SOCS1} [384]. It was the first NF- κ B E3 ligase identified, binding and ubiquitinating p65 promoting its proteasomal degradation [384]. PPAR γ is a member of the superfamily of nuclear hormone factors which contains a RING finger domain acting as an E3 ligase inducing ubiquitination and degradation of p65 at K28 [380]. ING4 is a member of the ING family of chromatin modifying proteins which together with E2 enzyme Ubch3, induces K48-linked polyubiquitination of p65 at K62 [381-383].

Existence of several ubiquitin sites may be explained by the different binding requirements of distinct E3 ligases. Various p65 E3 ligases have been identified and although the ubiquitination site of all the identified E3 ligases has not been determined, the established ones do not overlap [380-383]. This suggests specificity of E3 ligases for p65 ubiquitination sites.

Table 1-7 List of lysines ubiquitinated on p65

Amino acid	Enzyme	Function	Reference
K28	PPAR γ	Degradation	[380]
K56	Unknown	Unknown	[381, 382]
K62	ING4	Degradation	[381-383]
K79	Unknown	Unknown	[381, 382]
K122	Unknown	Unknown	[381]
K123	Unknown	Unknown	[381, 382]
K195	Unknown	Degradation	[381, 388]
K310	Unknown	Unknown	[381, 382]
K314	Unknown	Unknown	[381]
K315	Unknown	Unknown	[381, 382]

1.4.2.2 Deubiquitinating enzymes

Several DUBs are indirectly involved in NF- κ B regulation by deubiquitination of different molecules upstream the NF- κ B signalling pathway leading to activation or inactivation of the NF- κ B response; such as deubiquitinase cylindromatosis protein (CYLD) [284, 389, 390], A20 [391-393], cellular zinc finger anti NF- κ B (Cezanne) [286, 394], USP2 [395], USP11 [396, 397], USP14 [398], USP15 [399], USP18 [398], USP21 [400], USP22 [398] and USP35 [401]. In addition USP7 [287] and USP31 [402] deubiquitinate the p65 NF- κ B subunit. p65 deubiquitination increases protein stability [287, 402]. The action of USP7 [287] and USP31 [402] is a mechanism for the control of transcription through the active recycling of ubiquitinated NF- κ B.

USP31, later called USP48, was discovered in 2004 [403]. This protein contains a conserved ubiquitin hydrolase region, a ubiquitin protease region and a ubiquitin-like domain [402, 403]. This enzyme inhibits TNF α -induced ubiquitination of p65 acting downstream of IKK β [404]. It is located in the nucleus [402, 404] where it indirectly interacts with the p65 subunit of NF- κ B through COP9 signalosome (CSN) association [402]. Inhibition of USP31 decreases NF- κ B target gene expression while p65 expression is intact [402]. It

preferentially trims long ubiquitin chains and is selectively activated through association with K48-linked ubiquitin [402].

1.4.3 USP7

USP7 (previously called HAUSP) was discovered in 1997 [405]. USP7 is a cysteine protease [406-408] that is located in the nucleus [409]. USP7 has a family conserved CD shared with the rest of USPs [406, 410, 411]. This conserved CD shares homology in its amino-acid sequence surrounding the catalytic triad, but also shares structural homology arranged in three architecture domains resembling the palm, fingers and thumb of a hand [406, 410-412]. While areas outside the CD are very divergent in their sequence and structure, leading to substrate specificity of each protein within the USPs [406, 411, 412]. USP7 preferentially cleaves substrate-attached monoubiquitin and short polyubiquitin chains [413].

USP7 interacts with different subunits of NF- κ B transcription factor; c-Rel, p50, p52, p65 and RelB subunits [287]. Interaction between USP7 and NF- κ B is DNA dependent [282, 287]. USP7 binds p65 at the promoter of NF- κ B target genes, regulating p65 ubiquitination and its stability at sites of transcription [282, 287]. The interaction with p65 is through the C-terminal region of USP7 [287]. Because of this, USP7 deubiquitinating activity is critical in determining the duration and strength of the NF- κ B transcriptional response by opposing promoter associated ubiquitin activities [282, 287].

1.4.3.1 Structure

There has been a huge effort elucidating the 3D structure of USP7, and USP7-substrates complexes. USP7 is a 1103 amino-acid multidomain protein. USP7 is formed by an N-terminal MATH/TRAF domain, a CD containing the amino-acids forming the catalytic triad (Cys223, His 464, Asp 481), and a C-terminal region composed of five ubiquitin like domains (UBLs) and referred as HAUSP (USP7) ubiquitin-like domains (HUBL) (see Figure 1-15) [267, 414-417]. The MATH/TRAF domain is involved in substrate recognition, [414, 415, 417-419]. The UBLs present in the C-terminal region have two different functions. UBL 1, 2 and 3 (UBL123) are involved in substrate recognition [41, 406, 408, 420, 421]. While

UBL 4 and 5 (UBL45) are essential, along with the C-terminal 20 amino-acids peptide (CTP), for full USP7 deubiquitinase activity [299, 408]. These structural domains are arranged in a way in which the fingers, palm and thumb [269, 411], create the ubiquitin binding pocket [408, 411].



Figure 1-15 USP7 protein structural domains. USP7 is a multidomain protein composed of an N-terminal MATH/TRAF domain, a catalytic domain in charge of the deubiquitinase activity of USP7 and 5 UBLs located in the C-terminal region, which is called HUBL.

When looking for USP7 3D structure on the Protein Data Bank server, there are around 50 available structures. But none of them is formed by the full length USP7 protein. Recent studies have modelled a USP7 full length molecule [299]. Unluckily this model is not available on the PDB server. This lack of a full size USP7 X-Ray structure is probably due to the size of USP7 (130KDa). Within all the available USP7 structures the whole USP7 is covered. For example; USP7 N-terminal domain (NTD) and CD (PDB: 2F1Z); CD and CTP (PDB: 5JTJ); CD and UBL123 (PDB: 5J7T); and UBL domains 1, 2, 3, 4 and 5 (UBL12345) (PDB: 4YOC).

On the other hand, USP7 is a flexible molecule, which is known to undergo conformational rearrangements when binding its substrates [299-301, 408]. The catalytic triad of USP7 is misaligned in the apo conformation of the protein; that is, when USP7 is not bound to its substrate. The loops close to the catalytic triad are in such conformation that the ubiquitin binding is not possible due to steric impediments [299-301]. When ubiquitin is covalently bound to USP7, USP7 undergoes conformational rearrangements leading to its active state [299-301]. In this active state the catalytic triad is aligned and there are no steric obstacles for ubiquitin binding [299-301]. The loop hindering the catalytic triad undergoes these conformational rearrangements making ubiquitin binding possible; this loop is called the switching loop [300, 408] and it is in charge of the active and inactive state of USP7. The conformational rearrangement of the switching loop results in the creation of an active cleft in which the CTP binds, stabilising the active conformation [299, 300]. The conformational rearrangements to mediate the shift between the apo and the active conformation are partly mediated by

the HUBL. The HUBL is formed by three modules; UBL 1 and 2 (UBL12) dimer, UBL3 and UBL45 dimer [300, 418, 422]. These modules are connected through flexible regions [300, 418, 422]. HUBL are also connected to the CD through a flexible α -helix [300]. Flexibility of these areas allows the appropriate position of UBL domains in order to be able to position the CTP on the active cleft and activate USP7. Flexibility of molecules is important in the regulation of substrate recognition and protein complexes formation, therefore the importance of a whole picture of the protein structure.

1.4.3.2 Function and substrates

USP7 acts on a variety of substrates, such as the p65 subunit of NF- κ B [287], MDM2 [417], p53 [417], phosphatase and tensin homolog (PTEN) [423, 424], DAAX [423], caspin [425], forkhead box protein O4 (FOXO4) [426], DNA (cytosine-5)-methyltransferase 1 (DNMT1) [420], ICP0 [41], ubiquitin-like with PHD and RING finger domains 1 (UHRF1) [427], N-Myc proto-oncogene protein [428] and Epstein-Barr nuclear antigen 1 (EBNA1) [429, 430]. In this way, USP7 has an effect in different biological processes such as apoptosis and senescence [300, 418, 422, 431, 432], stress response [432, 433], DNA repair [300, 407, 418, 432, 434, 435], epigenetic regulation [407, 422, 431], viral infection [407], tumourigenesis [407, 422, 431, 435], cell cycle control [431, 433], cell survival [422, 431, 432] and inflammatory response [407]. The ability of USP7 to control such a range of different processes relies on the variety of different substrates which targets. See Figure 1-16.

USP7 targets a series of viral proteins such as ICP0 from HSV-1, EBNA1 from Epstein-Barr virus (EBV), vIRF4 and ORF73 from human herpes virus 8, UL35 from cytomegalovirus (CMV) and E1B-55K from adenovirus [435]. From these proteins, the most studied ones are ICP0 and EBNA1. USP7 was firstly discovered bound to ICP0 [405, 429]. ICP0 is crucial for effective lytic infection through the activation of viral genes during early stages of infection and alteration of the cellular levels of different proteins in the host [41]. On the other hand, EBNA1 regulates viral gene transcription maintaining EBV in latently proliferating cells [436]. p53 is the best studied substrate of USP7 [407, 418, 422, 435]. However, it is not the only member of the p53 pathway which interacts with USP7. MDM2 E3 ligase ubiquitinates p53 protein but is also a USP7 substrate [407, 418, 422, 435].

The p53 pathway is involved in apoptosis and senescence, the stress response, DNA repair process, tumourigenesis and cell survival [431, 437, 438]. USP7 effects on these processes are mainly through its activity on p53 and MDM2. In addition, DAXX, which is involved in apoptosis, cell survival and tumourigenesis processes [439, 440], is also a USP7 substrate [441]. Besides its activity on tumourigenesis through p53, MDM2 and DAXX it is also involved in neuroblastomas through its interaction with N-Myc [428]. USP7's role in chromatin modification is through the action of substrates such as DNMT1 [41, 300, 422, 433] and UHRF1 [41, 422]. DNMT1 is essential for the maintenance of methylation patterns in the genome [420, 442], while UHRF1 is an E3 ligase which recognises hemi-methylated DNA and recruits DNMT1 [41, 443]. In addition, UHRF1 [443], claspin [407] and p53 [431] are also involved in cell cycle control. Claspin controls the DNA damage checkpoint [407], while UHRF1 is required for the G1/S phase transition [443]. Finally, USP7 is involved in the inflammatory response by interaction with all NF- κ B members [287]. USP7 is able to interact with all subunits of the NF- κ B family but its deubiquitinase activity has only been studied on p65 subunit [287].

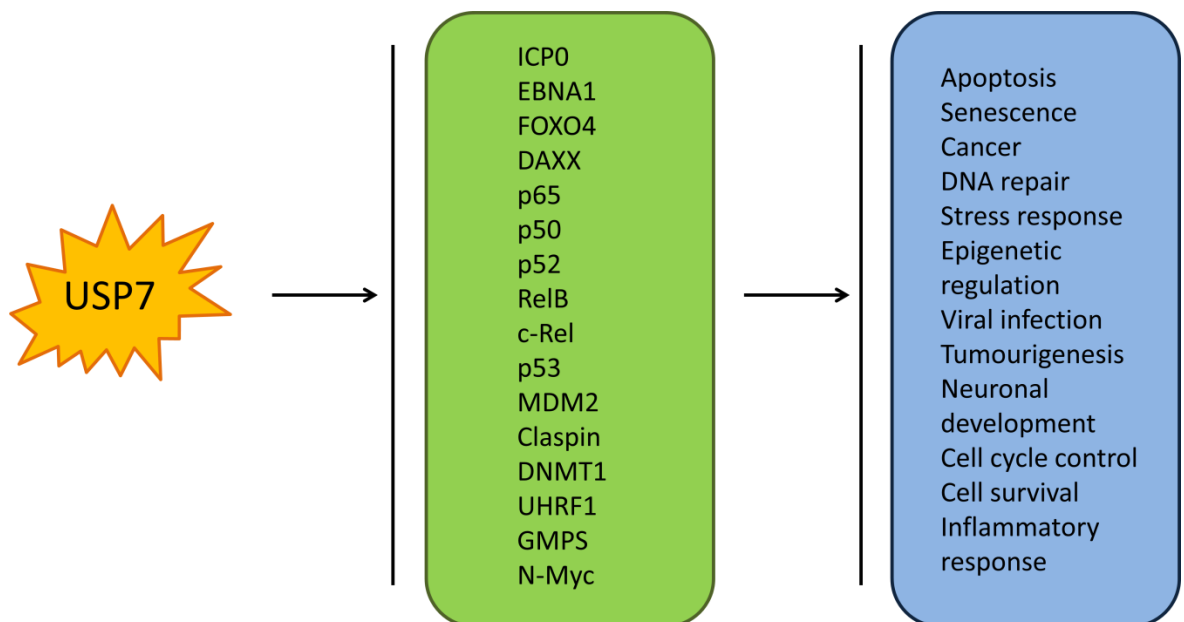


Figure 1-16 Multifaceted USP7 role in cells. USP7 interacts with a broad variety of substrates (green box) and thus, it acts in a variety of biological processes (blue box).

The importance of USP7 in various biological processes in the cell is reflected in the lethality of USP7 knockout mice [444]. USP7 is essential for early embryonic development in mice, USP7 knockout mice show deficiency in cell proliferation,

due to a failure of its blastocyst to proliferate [444]. Homozygous embryos at E6.5 are smaller and contain disorganised cells with no pro-amniotic cavity formation; at E7.5 they do not contain a recognisable structure and embryonic cells were reduced in number. USP7 knockout embryos die between E6.5 and E7.5 [444]. Therefore, USP7 plays a crucial role within cellular biological processes.

The crucial role of USP7 within different cellular biological processes makes it an interesting target for new therapeutic drugs. Although the main focus at the moment is at p53 pathway inhibition for different cancer treatments [445], the fact that it is able to interact with such different proteins as EBNA1, ICP0, DNMT1, UHRF1 and NF- κ B members, has increased its therapeutic potential for treatment of different diseases e.g. arthritis, infectious diseases and epigenetic disorders among others.

1.4.3.3 USP7 inhibitors

One of the first USP7 inhibitors developed is HBX 19,818 which forms a covalent bond with Cys223 in the catalytic site, blocking USP7 in a non-substrate specific manner [446]. More USP7 inhibitors were developed including P22077 [447], P509 [448] and HBX 41,108 [446, 449]. These four inhibitors show similar effects on cells, on stability of p53, on transcription of p53 target genes and on p21 protein levels [446-449]. However, these inhibitors are not USP7 specific, having a broader effect on different cysteine protease DUBs such as USP9, USP5, OTU ubiquitin aldehyde binding 1 (OTUB1), UCH-L3, UCH-L1, USP8, USP14 and USP15 [450-452]. Four recent studies developed specific inhibitors of USP7 [445, 453-455]. The studies performed by Turnbull et al. and by Lamberto et al. are based on the conformational rearrangements underwent by the switching loop of USP7 after ubiquitinated substrate binding [445, 454]. USP7 has a switching loop located in close proximity to the catalytic triad which has an active and an inactive state. The inhibitors XL-188, FT671 and FT827 bind into a pocket located in that switching loop in its inactive conformation, inhibiting the binding of USP7 to the ubiquitin molecule present in its substrate and keeping its enzymatic activity off [445, 454]. On the other hand GNE-6640 and GNE-6776 non-covalently bind USP7 in close proximity to the catalytic triad attenuating the ubiquitin binding to the catalytic triad [453]. Similarly, oxadiazole

compounds recognize a binding pocket overlapping the catalytic pocket and therefore inhibiting substrate binding; and aminopyridine compounds bind to a functional site on the palm of USP7 CD impeding the binding of the target protein to the catalytic site [455]. These more selective inhibitors have similar *in vivo* effects to those less selective inhibitors. FT671 increases p53 level and MDM2 degradation leading to induction of p53 target genes, and promotes degradation of UHRF1 and DNMT1 in colorectal carcinoma HCT116 and bone osteosarcoma U2OS cell lines [445]. It also stabilises p53 levels on human neuroblastoma IMR-32 cell line and MM.1S multiple myeloma cell line [445]. FT671 shows a dose-dependent inhibition of tumour growth on MM.1S cell line [445]. GNE-6776 and GNE-6640 have similar effects *in vivo*, they stabilise p53, promote MDM2 ubiquitination, upregulate p21, and decrease proliferation and caspase activation on TP53 wild type (WT) cell lines [453]. XL-188 increase p53 and p21 proteins level and promotes HDM2 loss in MCF7 cells and MM.1S myeloma cells [454]. Oxadiazole and aminopyridine compounds increase p53 level on SJSA osteosarcoma cells and reduce cell viability by cell cycle arrest on EOL-1, increasing the caspase activity [455]. See Figure 1-17.

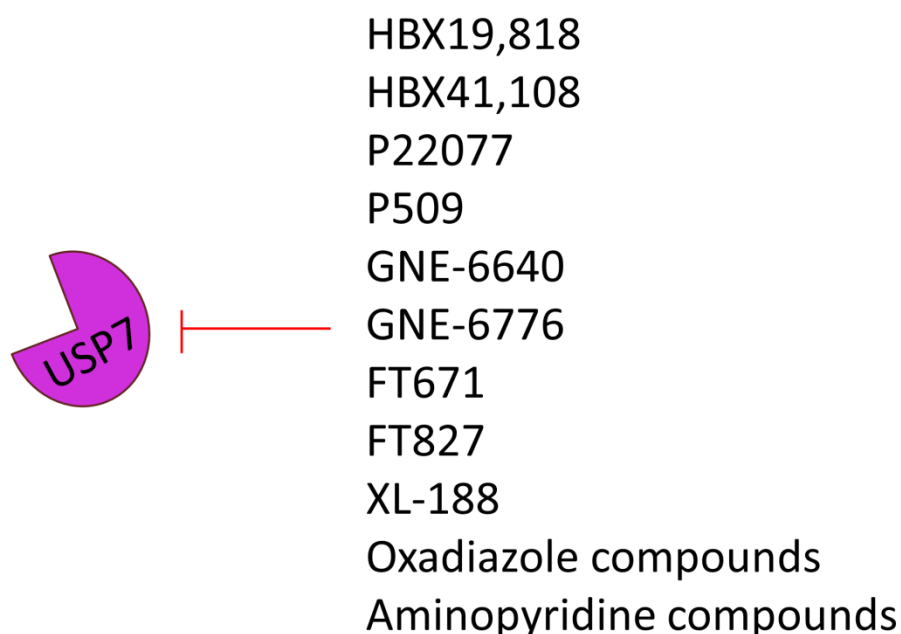


Figure 1-17 Schematic of the USP7 inhibitors. Chemical compounds developed to inhibit the deubiquitinase activity of USP7. HBX19,818, HBX41,108, P22077 and P509 inhibitors directly inhibit the catalytic activity of USP7 by the direct binding to the catalytic triad. GNE-6640, GNE-6776, oxadiazole compounds and aminopyridine compounds by to a site in close proximity to the active site impeding the binding of the ubiquitin molecule to the catalytic triad. However, FT671, FT827 and XL-188 inhibitors bind to the switching loop in the apo conformation blocking the active state of USP7.

These approaches are USP7 specific but not substrate specific and would be expected to promote the ubiquitination of all USP7 substrates equally. These inhibitors inhibit the deubiquitinase activity equally in all its substrates; therefore, USP7 is not able to specifically deubiquitinate p53, MDM2, EBNA1, DAXX, DNMT1, UHRF1, p65 among other substrates.

1.4.3.4 Substrate specificity and binding pockets

Some of the crystallised USP7 components are solved in complex with USP7 substrates, such as DNMT1 (4YOC), UHRF1 (5C6D), MDM2 (2F1X) p53 (2FOO) and ICPO (5C56) among others. There is an increasing interest to discover the molecular determinants of USP7 involved in the recognition of its substrates. As USP7 is involved in a variety of biological processes, information on the specific residues involved in substrate recognition provides a unique target for each of USP7 substrates. USP7 substrates can be divided into two groups depending on the region of USP7 required for the interaction, the N-terminal or C-terminal region. p65 protein is known to be recognised by the C-terminal region of USP7 (see Figure 1-18) [287].

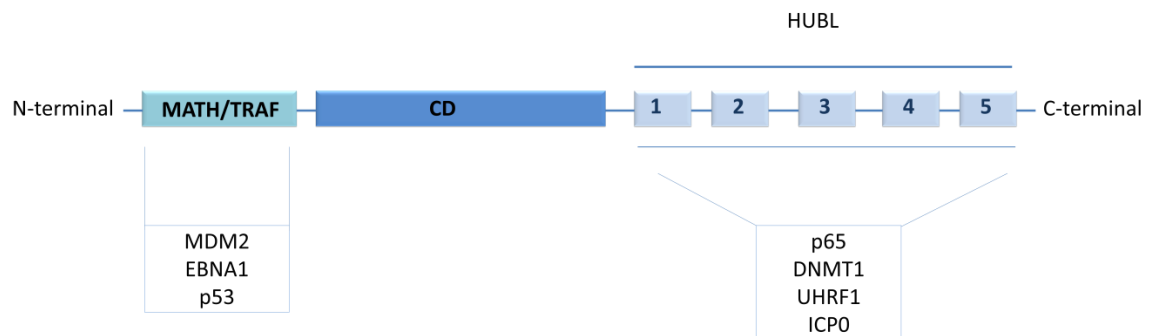


Figure 1-18 USP7 substrate binding specificity. Substrate recognition is performed by two different regions of USP7, the MATH/TRAF domain and the C-terminal HUBL. Several of its substrates are recognised by the N-terminal MATH/TRAF domain as it is the case of MDM2, EBNA1 and p53. On the other hand, the C-terminal HUBL is in charge of recognition of substrates such as p65, DNMT1, ICPO and UHRF1. There are still several substrates which binding specificity has not been elucidated.

ICPO was the first USP7 substrate discovered and it is recognised by the C-terminal region of USP7 [41]. Using a peptide binding technique, Pfoh et al, narrowed the interacting amino-acids involved in the sequence of USP7 [41]. They discovered that the peptidic sequence of ICPO binds in a predominantly

negatively charged region of USP7 located on UBL2. This region of USP7 is 758-DELMDGD-764, and the peptidic sequences used from ICP0 contain two lysines which interact with the negatively charged aspartate residues of USP7. Mutation of USP7 D762 and D764 decrease the interaction with ICP0 and also with guanosine monophosphate synthetase (GMPS) and UHRF1, two other known substrates of USP7 [41]. Following this advance on discovering the amino-acids of USP7 involved in the recognition of its substrates by the C-terminal region, Kim and Sixma analysed the pattern motif recognised by USP7 [418]. They used peptidic sequences of each substrate (DNMT1, GMPS, ICP0, UHRF1) and co-crystallised them with USP7 UBL12 for substrates recognised by the C-terminal region [418]. They used the same approach to co-crystallised substrates recognised by the N-terminal region (MDM2, p53, EBNA1) with USP7 MATH/TRAF domain [418]. They identified the amino-acid motifs recognised by USP7. In the N-terminal region the consensus motif is formed by P/A/ExxS [418]. A region containing that motif in substrates recognised by USP7 is more likely to be part of the binding interface. While for the C-terminal region of USP7, the motif recognised on the substrates is a positively charged motif K/RxKxxxK [418]. This positively charged motif is recognised by a region located on UBL2 of USP7 containing the 758-DELMDGD-764 area identified by Pfoh et al as an important region involved in the interaction with ICP0, UHRF1 and GMPS [41, 418]. While characterisation of the binding interface of these substrates has been identified, there are still substrates whose binding sites are still unknown.

1.4.3.5 p65 interaction and deubiquitination

USP7 has been identified as an NF- κ B deubiquitinase, critical for NF- κ B transcriptional activity [287]. Inhibition of the deubiquitinating activity of USP7, blocks the pro-inflammatory effectors transcription induced by the NF- κ B response [287]. USP7 recognises p65 subunit through its C-terminal region and deubiquitinates it, but the specific molecular determinants involved in the binding interface are still unknown [287].

1.5 Thesis aims

- Identification of the molecular determinants involved on USP7-p65 interaction.
- Investigation of the interaction mechanism of USP7-p65 by the elaboration of a USP7-p65 structural model.
- Identification of possible inhibitory peptides of USP7 deubiquitinase activity on p65.

Chapter Two

Material and methods

2 Material and Methods

2.1 Cell biology techniques

2.1.1 Mice

C57BL/6 WT mice were used for extraction of bone marrow (BM). All animals were housed within the Biological Central Research Facility at Glasgow University. Animals had access to food and water *ad libitum*. All experiments received ethical approval and were performed under the auspices of a UK Office License.

2.1.2 Cell culture

2.1.2.1 Maintenance

Human embryonic kidney 293T (HEK293T) and RAW 264.7 (murine macrophages) cell lines were cultured in high glucose Dulbecco's Modified Eagle Medium (DMEM) (Sigma, D6429) containing 10% heat inactivated fetal bovine serum (FBS) (Gibco 10500-064), 2mM glutamine (Sigma, G7513), and 100U/ml penicillin/streptomycin (Sigma, P0781). All cells were maintained at 37°C in a humidified environment with 5% CO₂. Cells were sub-cultured three times per week following mechanical (RAW 264.7 cells) or enzymatic detachment (HEK293T) with 0.05% Trypsin ethylenediaminetetraacetic acid (EDTA) solution (Gibco, 25300-054).

2.1.2.2 Bone marrow derived macrophages

2.1.2.2.1 Bone marrow isolation

BM was isolated from C57BL/6 mice for generation of primary bone marrow derived macrophages (BMDM) *in vitro*. Mice were sacrificed by CO₂ asphyxiation and cervical dislocation. Hind legs were removed at the hip joint and excess tissue removed from the femur and tibia bones. In sterile culture conditions, bones were cleaned in sterile DMEM. Bones were then cut at each extremity and the BM was flushed with DMEM using a 21-gauge needle and a 10ml syringe. Isolated BM was collected and resuspended in sterile DMEM and filtered through a 40µm cell strainer to generate a single cell suspension. The BM suspension was

centrifuged for 5 minutes at 400g and resuspended in DMEM 10% FBS supplemented with glutamine and penicillin/streptomycin or freezing media (10% dimethyl sulfoxide (DMSO), FBS) for cryopreservation.

2.1.2.2.2 BMDM differentiation and stimulation experiments

Following isolation or cryopreservation, bone marrow was cultured in DMEM 10% FBS supplemented with glutamine, penicillin/streptomycin and 30% L929 conditioned media (BMDM differentiation media) in sterile petri dishes, for seven days. Differentiation media was replaced on day 3 and any non-adherent cells were removed. By day 7, adherent monocytes/macrophage progenitors were differentiated into BMDMs. BMDMs were removed from petri dishes by incubating them with 5mM EDTA in sterile phosphate-buffered saline (PBS) at 37°C for 2 minutes. Cells were washed in DMEM 10% FBS supplemented with glutamine and penicillin/streptomycin by centrifugation at 300rpm for 5 minutes and resuspended in DMEM 10% FBS supplemented with glutamine and penicillin/streptomycin. BMDMs were replated overnight in tissue culture treated dishes for subsequent experiments.

2.1.2.3 Cryopreservation

Cells were centrifuged for 5 minutes at 300rpm and pellets were resuspended in FBS containing 10% DMSO. Resuspended cells were frozen at -80°C for one day and then stored in liquid nitrogen.

2.1.2.4 Plating conditions

The number of cells plated in each tissue culture plate or dish depends on the cellular type cultured (see Table 2-1).

Table 2-1 Cell plating conditions

Plate/Dish	Media volume	No. HEK293T	No. RAW 264.7	No. BMDM
24 well	500µl	0.1 x10 ⁶	0.2 x10 ⁶	1 x10 ⁶ /ml
12 well	1ml	0.25 x10 ⁶	0.5 x10 ⁶	1 x10 ⁶ /ml
6 cm	5ml	2 x10 ⁶	4 x10 ⁶	1 x10 ⁶ /ml
10 cm	10ml	5 x10 ⁶	10 x10 ⁶	1 x10 ⁶ /ml

2.2 Molecular biology techniques

2.2.1 DNA transformation for routine plasmid preparation

XL-1 Blue Competent cells (Agilent technologies, 200249) were used for transformation of DNA for routine plasmid preparation. 10ng of the desired DNA was added to 20 μ l of cells and incubated for 30 minutes on ice. Cells were subjected to a heat shock, 45 seconds at 42°C, and recovered from it for 2 minutes on ice before the addition of 300 μ l of super optimal broth with catabolite repressor (SOC) media (Invitrogen, 5544-034, P/N 46-0700) for 1 hour at 37°C. Cells were plated in Luria-Bertani (LB) agar plates supplemented with their corresponding antibiotic (ampicillin 100 μ g/ml -Sigma Aldrich, A9518- and Kanamycin 50 μ g/ml -Melford, K0126-), and incubated overnight at 37°C.

2.2.2 Plasmid preparation

2.2.2.1 Midiprep

A single bacterial colony was picked and inoculated into 5ml LB-Broth media supplemented with the corresponding antibiotic as explained above for a starter culture. The starter culture was incubated for several hours at 37°C shaking at 150rpm. Afterwards, the starter culture was added to a 100ml culture supplemented with the respective antibiotic and incubated at 37°C shaking at 150rpm overnight. Plasmid DNA was prepared following the Pure Yield Plasmid Midiprep System kit (Promega, A2495) protocol. Plasmid concentration was measured using a NanoDrop spectrophotometer.

2.2.2.2 Miniprep

5ml of LB-Broth media supplemented with the respective antibiotic was inoculated with a single colony and incubated overnight at 37°C shaking at 150rpm. DNA was extracted using Qiaprep Spin Miniprep kit (Qiagen, 27104) following manufacturer's instructions.

2.2.3 Transfection

HEK293T cells were transiently transfected using Turbofect transfection reagent (Thermo Scientific, R0531). Plasmids were incubated with serum free media

(SFM) and turbofect for 15 minutes at room temperature and added dropwise to the cells. The transfection ratios are as follows; 100:1:2 (SFM (μl): DNA (μg): Turbofect (μl)) (see Table 2-2). Within each experiment total plasmid concentrations were kept constant between samples by the addition of an empty expression vector. For a list of used plasmids see Table 2-11.

Table 2-2 HEK293T cells transfection conditions

Dish size	#Cells	SFM	DNA	Turbofect
10cm	5×10^6	400 μl	4 μg	8 μl
6cm	2×10^6	300 μl	3 μg	6 μl

2.2.4 Gene expression analysis (qPCR)

For real time polymerase chain reaction (PCR) or quantitative PCR (qPCR) analysis, ribonucleic acid (RNA) was extracted using RNeasy kit (Qiagen, 74104), QiaShreders (Qiagen, 79654) and RNase Free DNase Set (Qiagen, 79254) following manufacturer's instructions. The RNA was reversed transcribed to complementary DNA (cDNA) using nanoScript RT Kit (Primer Design, RT nanoscript) following its protocol. qPCR was performed with Perfecta SYBR Green FastMix Rox (Quanta Bioscience, 95073-012) using QuantiTect Primer Assays (Qiagen) in a 384 well plate using QuantStudio 7 Flex (Applied Biosystems by Life Technologies) with the running conditions as described in Table 2-3.

Data was normalised to TATA binding protein (TBP) and gene expression changes calculated using the $2^{-\Delta\Delta\text{CT}}$ method [456].

Table 2-3 qPCR running conditions

Stage	Cycle	Rate	Temperature	Time
Hold	1	(1.6° C/s)	50° C	2 minutes
		(1.6° C/s)	95° C	10 minutes
PCR	40	(1.6° C/s)	95° C	15 seconds
		(1.6° C/s)	60° C	1 minute
Melt Curve	1	(1.6° C/s)	95° C	15 seconds
		(1.6° C/s)	60° C	1 minute
		(1.6° C/s)	95° C	15 seconds

TBP primers were resuspended in Tris, EDTA (TE) buffer (Tris/HCl 1M pH8, EDTA 0.5M pH8, H₂O). Sequences and/or catalogue numbers of each primer are listed in Table 2-12.

2.2.5 Synthetic peptide arrays on membrane support (SPOT)-synthesis of peptides and overlay Analysis

SPOT-synthesis of peptides was performed by Dr. Kiely, (University of Limerick, Limerick, Ireland). Arrays were activated by incubation in 100% ethanol for 5 minutes. The excess of ethanol was cleaned with tris-buffered saline (TBS) with 0.05% Tween-20 (TBS-T) for 5 minutes. Arrays were then equilibrated in TBS-T for 10 minutes and blocked with 5% non-fat milk (Marvel) in TBS-T for 1 hour at room temperature. The interaction of glutathione S-transferase (GST) and GST-p65 proteins with the peptide array was investigated by overlying the cellulose membrane with 10µg/ml of each protein in 1% milk/TBS-T overnight at 4° C. Arrays were washed three times for 5 minutes in TBS-T before immunoblotting with anti-GST primary antibody (Sigma G7781) for 2 hours at 1:2,000 dilution in 5% Milk TBS-T. Arrays were washed as previously described and incubated for 1 hour with anti-Rabbit horseradish peroxidase (HRP) conjugated secondary antibody (GE Healthcare NA934V). Arrays were washed as previously described and bound protein was detected with Western Bright ECL chemiluminescence substrate (Advansta K-12045-D50). Arrays were incubated in peptide array stripping buffer (buffer composition listed in Table 2-20) for 30 minutes at 70° C and washed twice for 10 minutes with TBS-T. Arrays were developed in the dark room and scanned on the Li-cor c-Digit machine to detect bound protein.

2.2.6 Site directed mutagenesis

Site directed mutagenesis (SDM) of USP7 was performed using Quick Change Lightning Site Directed Mutagenesis Kit (Agilent Technologies, 210518-5) and Q5 Site Directed Mutagenesis Kit (New England Biolabs, E05545) as per instructions. SDM primers were designed using NEBase Changer online tool (<https://nebasechanger.neb.com/>) from NEB and PrimerX online bioinformatic tool (<http://www.bioinformatics.org/primerx/>).

High-performance liquid chromatography (HPLC) grade oligonucleotides were purchased from IDT Integrated DNA Technologies.

Oligonucleotides sequences are displayed in Table 2-13.

2.2.7 Cloning

To remove and insert different epitope tags from previous plasmids from the group, human p65 WT, mouse p65 WT and mutants were sub-cloned into pCDNA 3.1 vector (kindly donated by Graham Milligan's Lab). Proteins' cDNA was amplified from existing plasmids following the PCR amplification conditions describe in Table 2-4 and Table 2-5. See Table 2-14 for a list of used primers.

Table 2-4 Cloning PCR components

Product	Concentration	Volume	Supplier	Catalogue Number
DNA	100ng/ μ l	1 μ l	N/A	N/A
Primer F	100 μ M	5 μ l	N/A	N/A
Primer R	100 μ M	5 μ l	N/A	N/A
Q5 High Fidelity 2X Master Mix	2X	12.5 μ l	NEB	M0492S
H ₂ O	N/A	1.5 μ l	Qiagen	1039480
Total	N/A	25 μ l	N/A	N/A

Table 2-5 Cloning PCR running conditions

Cycles	Temperature	Time
1	98 °C	30 seconds
35	98 °C	10 seconds
	Tm	30 seconds
	72 °C	1 minute
1	72 °C	2 minutes
1	4 °C	∞

Amplification products were run in a 1% agarose gel, with the addition of 1/10,000 gel red (PAGE Gel Red Nucleic Acid, Biotium, 41008). Samples were loaded on loading buffer (10X Blue Juice Gel Loading Buffer, Invitrogen, 10816-015) and their size was measured by the addition of a 1Kb DNA Ladder (Promega, G571A). Proteins were extracted from the gel with Pure Link Quick Gel Extraction Kit, according to manufacturer's conditions (Invitrogen by Thermo Fisher Scientific, K210012).

Purified proteins were digested overnight at 37 °C, using the corresponding restriction enzymes following the conditions described in Table 2-6.

Table 2-6 Cloning digestion components

Product	Volume	Supplier	Catalogue Number
CutSmart Buffer	2µl	NEB	B7204S
Restriction Enzyme 1 HindIII	1µl	NEB	R0104S
Restriction Enzyme 2 XbaI	1µl	NEB	R0145S
Purified protein //	16µl	N/A	N/A
// Purified Vector	10µl + 6µl H ₂ O		

Digested products were run on an agarose gel and extracted from the gel as previously described.

Purified digested products were ligated overnight at 16°C following the conditions described in Table 2-7.

Table 2-7 Cloning ligation components

Product	Volume	Supplier	Catalogue Number
Construct	6µl	N/A	N/A
pCDNA3.1	2µl	N/A	N/A
10X Buffer for T4 DNA ligase with 10mM ATP	1µl	NEB	B0202S
T4 DNA ligase	1µl	NEB	M0202S
Total	10µl	N/A	N/A

20µl of XL-1 Blue Competent cells were transformed with 2µl of the ligation product following the protocol explained in section 2.2.1.

12 colonies of each ligation product bacterial transformation were picked for colony PCR amplification following the conditions in Table 2-8 and Table 2-9.

Table 2-8 Cloning colony PCR components

Product	Concentration	Volume	Supplier	Catalogue Number
DNA	N/A	Colony	N/A	N/A
Primer F	10µM	1µl	N/A	N/A
Primer R	10µM	1µl	N/A	N/A
Q5 High Fidelity 2X Master Mix	2X	10µl	NEB	M0492S
H₂O	N/A	8µl	N/A	N/A
Total	N/A	20µl	N/A	N/A

Table 2-9 Cloning colony PCR running conditions

Cycles	Temperature	Time
1	98 °C	30 seconds
35	98 °C	10 seconds
	Tm	30 seconds
	72 °C	1 minute
1	72 °C	2 minutes
1	4 °C	∞

From the positively amplified colonies, 5 were selected for subsequent miniprep preparation (as explained in section 2.2.2.2), and sent for sequencing to ensure the success of the cloning.

2.2.8 DNA sequencing

Plasmid DNA sequencing was performed by GATC-Biotech LTD (Germany), using on site primers or specifically designed primers by GATC-Biotech LTD (Germany). See list of primers on Table 2-15. Sequencing results were analysed using Geneious Molecular Biology and NGS Analysis Tools (Biomatters LTD, New Zealand).

2.3 Protein methodologies

2.3.1 Glutathione S-transferase (GST) - protein purification

BL21 DE3 cells (Agilent Technologies, 200131) were transformed with GST-p65 mouse pET-42a(+) (GenScript, Lot.552515 S-2 S26776) by the addition of 150ng of DNA to the cells. Cells were incubated on ice for 30 minutes, and then exposed to a heat shock (45 seconds at 42 °C), followed by incubation on ice for 2 minutes and the addition of 100µl SOC medium (Invitrogen, 5544-034, P/N 46-0700) for an hour at 37 °C and shaking at 150rpm. Cells were plated onto LB agar plates containing 50µg/ml kanamycin. Plates were incubated overnight at 37 °C. A single colony was isolated and incubated overnight in 5ml LB-Broth containing 50µg/ml kanamycin. Cultures were incubated shaking at 150 rpm and 37 °C. 1.4ml of the overnight culture was added to 200ml LB-Broth containing 50µg/ml

kanamycin in a conical flask. Cultures were grown shaking at 150rpm and 37°C for 3 hours. Before induction, a 200µl aliquot was mixed with 200µl of 2X sodium dodecyl sulphate (SDS) loading buffer (buffer composition listed in Table 2-19), boiled for 5 minutes at 95°C and stored at -20°C (uninduced sample). Cultures were induced with 0.5mM isopropyl β-D-1-thiogalactopyranoside (IPTG) and incubated for 3 hours shaking 150rpm at 37°C. Following induction, a 200µl aliquot was prepared as explained above for uninduced sample. Cultures were centrifuged at 18,000g for 25 minutes at 4°C. Pellets were frozen at -20°C for 30 minutes. Pellets were transferred to 50ml tubes and frozen at -80°C. Pellets were thawed on ice and resuspended in 35ml of cold lysis buffer supplemented with two complete, mini, EDTA-free protease inhibitor cocktail tablets (Roche Diagnostics GmbH) (for buffer composition see Table 2-17). The resuspended pellet was sonicated for 25 minutes with 15 second pulses, and 45 second rest between each pulse (Soniprep 150 MSE SANYO). Lysates were cleared by centrifugation at 15,000g for 30 minutes at 4°C (Sigma Laboratory Centrifuges, 4K15). Supernatant was transferred to a cold 50ml tube. 200µl of supernatant was added to 200µl 2X SDS loading buffer, boiled at 95°C for 5 minutes and stored at -20°C (crude lysate). GSTrap high performance (HP) column (GE Healthcare, Bioscience AB) was used to purify the GST recombinant p65. The column was firstly equilibrated with 5 volumes of binding buffer at a flow rate of 5ml/min (for buffer composition see Table 2-17). The cleared supernatant was added to the column at a flow rate of 0.5ml/min and the flow through (FT) was collected. A 200µl aliquot of FT was prepared as previously described for the uninduced sample. Collected FT was re-run through the column at the same rate. The column was washed by the addition of 10 volumes of binding buffer at a flow rate of 5ml/min. First and last washes were collected and prepared as the uninduced sample described above. Protein was eluted by the addition of 10 volumes of elution buffer at a flow rate of 3ml/min (for buffer composition see Table 2-17). Six elution samples were collected and prepared as describe above for the uninduced sample. Elutions were snap frozen and stored at -80°C. All prepared samples were analysed by SDS polyacrylamide gel electrophoresis (PAGE). Afterwards, column was washed and kept on storage buffer (for buffer composition see Table 2-18).

2.3.2 Protein extraction

2.3.2.1 Non- denaturing whole cell extracts (HEK293T and RAW 264.7 cells)

Cell culture media was aspirated from the plates and cells were gently washed with PBS 4°C. Cells were detached from the plate with PBS 4°C and pelleted at 11,000g 4°C for 1 minute. Pellets were resuspended in 20µl-500µl radioimmunoprecipitation assay (RIPA) buffer (see Table 2-10 for RIPA buffer volumes and Table 2-21 for RIPA buffer composition). Resuspended pellets were incubated on ice for 30 minutes and the lysates were cleared by centrifugation at 16,000g for 10 minutes at 4°C. Supernatants were collected and quantified as explained in section 2.3.3 (Bradford Assay).

Table 2-10 Non-denaturing lysis conditions

Plate/dish	RIPA buffer volume
24 well plate	20µl
12 well plate	50µl
6cm dish	200µl
10cm	500µl

2.3.2.2 Denaturing whole cell extracts (HEK293T cells)

Cells were incubated with 10mM N-ethylmaleimide (NEM) for 30 seconds prior to harvest. Cell culture media was aspirated from the plates and cells were gently washed with 4°C PBS containing 10mM NEM. Cells were detached from the pellets using 4°C PBS containing 10mM NEM and pelleted at 11,000g for 1 minute at 4°C. Pellets were resuspended in 100µl 1% SDS and boiled for 5 minutes at 95°C. Cell pellets were disrupted by sonication, 5 cycles of 30 seconds at 30% amplitude, using Bandelin Sonopuls ultrasonic homogeniser HD 2070 with MS 73 microtip. Lysates were cleared by centrifugation at 16,000g for 10 minutes at 4°C.

2.3.3 Quantification

Cellular protein extracts were quantified by Bradford Assay technique. 1µl of protein extracts was diluted in 1ml of 1X Bradford assay reagent (Protein Assay Dye Reagent Concentrate, Bio-Rad, 500-0006). A triplicate of each sample was measured using a spectrophotometric 96 well plate reader at 595nm absorbance (Tecan Sunrise, Magellan Software). An 8-point standard curve between 0-10.5µg/ml of bovine serum albumin (BSA) was generated to determine unknown sample protein concentrations.

2.3.4 SDS-PAGE protein gels

Protein samples were denatured and separated by SDS-PAGE using the miniProtean Tetra Cell System from Bio-Rad. Cell extracts were diluted in 2X or 4X SDS loading buffer and boiled for 5 minutes at 95°C to be denatured and samples were resolved in 8% acrylamide gels (see Table 2-23). Gels were run at 120V for 60-100 minutes in 1X Tris-glycine running buffer (for buffer composition see Table 2-22). Resolved proteins were then detected by Western Blot (WB) (explained in section 2.3.5).

2.3.5 Western blotting

Proteins were denatured and separated as explained above in sections 2.3.2 and 2.3.4. Resolved proteins were transferred to Amersham Protan 0.45µm NC Nitrocellulose Blotting membrane (GE Healthcare, Life Science, Amersham, 10600007) using the Mini Trans-Blot Electrophoretic Transfer System from Bio-Rad and 1X Tris-glycine Transfer Buffer (for buffer composition see Table 2-22). Nitrocellulose membranes were incubated in Ponceau solution (Sigma Aldrich, P7170) and washed with PBS-Tween-20 0.05% (PBS-T) to confirm proper transfer of the proteins from the gel to the nitrocellulose membrane. Membranes were incubated in 5% non-fat milk (Marvel)/PBS-T solution to block any non-specific binding of the antibodies to the membrane. Nitrocellulose membranes were then probed with primary antibodies in 5% milk/PBS-T overnight at 4°C and secondary antibodies in 5% milk/PBS-T for 1 hour at room temperature. After each antibody's incubation, membranes were washed 3 times for 5 minutes in PBS-T. Secondary antibodies used were horse radish peroxidase (HRP) conjugated. Protein was detected with Western Bright ECL (Advansta, K12045-D50) or

Western Bright Sirius (Advansta, K12043-D20) chemiluminescent substrates. Membranes were scanned using the LI-COR c-Digit Model 3600 (USA). When multiple antibody reprobings for protein of the same or similar size were required, membranes were stripped using Restore Plus Western Blot Stripping Buffer (Thermo Scientific, 46430) as manufacturer's instructions. Protein sizes were confirmed by the addition of a protein ladder (Thermo Scientific, 26616) and subsequent use of a chemiluminescent marker from Li-cor or a biotinylated protein ladder (Cell Signalling Technologies, 07/2017) and the addition of an anti-biotin antibody (Cell Signalling, 02/2017).

2.4 Functional assays

2.4.1 GST pulldown

HEK293T cells were transiently transfected with the appropriate plasmid and transfection reagent amount (see Table 2-2). DMEM 10% FBS supplemented with glutamine and penicillin/streptomycin media was discarded from the dishes and cells were washed with cold PBS. Cells came off from the dish by the addition of cold PBS and pelleted by centrifugation for 1 minute at 11,000g at 4°C. Pellets were resuspended in 500µl pulldown lysis and binding buffer and incubated for 30 minutes on ice. Cells were extracted by centrifugation for 10 minutes at 16,000g at 4°C. Protein amount was quantified by the Bradford method described in section 2.3.3. Equal amounts of samples were transferred into a clean eppendorf and were diluted to a final volume of 1ml with pulldown lysis and binding buffer (see Table 2-21 for buffer composition). Diluted samples were precleared with 50µl of glutathione (GSH) agarose beads (Sigma Aldrich, G4510) for 2 hours in a rotator at 4°C and centrifuged at 14,000g 4°C for 2 minutes. Cleared samples were incubated for 2 hours with 50µl of GSH agarose beads and 150nM of the purified recombinant GST-p65 or with 5µg of the commercially available GST-p65 (Enzo, BML UW9990-0050). Pulled down proteins were washed three times for 5 minutes on PBS-T and eluted by the addition of 30µl 2X SDS loading buffer, boiled for 5 minutes at 95°C. Samples were frozen at -20°C or subsequently analysed by WB.

2.4.2 Immunoprecipitation

Non-denaturing whole cell extracts were prepared as explained in section 2.3.2.1 and quantified as explained in section 2.3.3. Equal amount of protein (60µg) was diluted in RIPA buffer (0.1% Igepal) up to 20µl and 20µl of 2X SDS loading buffer, boiled at 95°C for 5 minutes and kept frozen for subsequent analysis. To immunoprecipitate the desired protein, equal amounts of proteins (1mg) were diluted in a final volume of 1ml with RIPA buffer (0.1% Igepal). Samples were precleared for 1 hour at the rotator at 4°C by the addition of 20µl of protein G agarose beads (EMD Millipore 16-266). Beads were discarded by centrifugation of the samples at 14,000g 4°C for 2 minutes. Samples were incubated with 20µl of protein G agarose beads and 1µl of the respective antibody, overnight on the rotator at 4°C. Immunoprecipitated proteins were washed three times with 1ml RIPA buffer and centrifugation at 11,000g 4°C for 1 minute. Proteins were eluted from the beads by the addition of 30µl of 2X SDS loading buffer and boiling at 95°C for 5 minutes, incubation on ice for 2 minutes and centrifugation at 14,000g 4°C for 2 minutes. Samples were kept at -20°C or analysed via WB.

2.4.3 Cellular ubiquitination assay

Denatured whole cell extracts were prepared as describe in section 2.3.2.2. Equivalent volumes of lysates (10µl) were diluted in 10µl of RIPA buffer (1% Igepal CA-630, 20mM NEM) and 20µl of 2X SDS loading buffer. Lysates were boiled for 5 minutes at 95°C, incubated on ice for 2 minutes and centrifuged for 2 minutes at 14,000g 4°C. They were kept at -20°C for subsequent analysis. The remaining volume of lysates (90µl) was resuspended in 900µl of RIPA buffer (1% Igepal, 20mM NEM). Samples were precleared for 30 minutes at 4°C in a rotator by the addition of 20µl of Protein G agarose beads (EMD Millipore 16-266). After centrifugation for 2 minutes at 14,000g 4°C, supernatants were transferred to a clean eppendorf and 20µl protein G agarose beads and 1µl of p65 antibody was added. Samples were immunoprecipitated overnight at 4°C on a rotator. Immunoprecipitated protein was washed 3 times on 1ml RIPA buffer followed by centrifugation at 11,000g and 4°C for 1 minute. Protein was eluted by the addition of 30µl of 2X SDS loading buffer, boiling for 5 minutes at 95°C,

incubation on ice for 2 minutes and centrifugation for 2 minutes at 14,000g 4° C. Samples were analysed by WB.

2.4.4 Enzyme-linked immunosorbent assay (ELISA)

The TNF α ELISA assay (TNF α ELISA, BD Bioscience, BD OptEIA, set mouse TNF α , 555268) was performed according to manufacturer's protocol. Absorbance was read at 450nm using Tecan Sunrise Plate reader and Magellan software. See Table 2-24 for buffer composition.

2.5 Bioinformatic tools

2.5.1 Multiple sequence alignment

Multiple sequence alignment of the family members of the NF- κ B family was performed using multiple alignment tool from Geneious R9 (Biomatters Ltd) software.

2.5.2 Protein prediction software

Prediction of the full-length structure of the p65 NF- κ B member was performed by ROBETTA Software from the Baker Lab (<http://robetta.bakerlab.org/>).

2.5.3 Crystal structure analysis

Crystal structures were analysed with Maestro Schrodinger software and MOE software. Full length p65 was modelled using 1VKX PDB file and ROBETTA models of full length p65 protein, with Maestro Schrodinger software. Full length USP7 was modelled using the following PDB files 5J7T, 4YOC, 5JTJ, 2F1Z, 5JTV, with Maestro Schrodinger software and MOE software. Full complex of the interaction was modelled by the addition of the heterodimer of p50-p65 from 1VKX PDB file.

2.5.4 Crystal structure alignment

3D structural alignments of the different members of the NF- κ B family as well as USP7 alignment of different PDB files, was performed by Maestro Schrodinger software and MOE software.

2.5.5 Docking

Modelled docking of the complex was performed with the help of Dr Matti Lepistö and Dr Christian Tyrchan (AstraZeneca, Gothenburg, Sweden) using Maestro Schrodinger software and MOE software.

2.5.6 Statistical analysis

Shapiro Wilk normality test and Mann Whitney test were performed with GraphPad Software.

2.6 Plasmids

Table 2-11 List of plasmids

Protein	Species	Backbone	Tag	Tag position	Antibiotic resistance
USP7	Human	pRK5	Flag	N-terminal	Ampicillin
USP7 Δ Math	Human	pRK5	Flag	N-terminal	Ampicillin
USP7 Δ HUBL	Human	pRK5	Flag	N-terminal	Ampicillin
USP7 Δ UBL2345	Human	pRK5	Flag	N-terminal	Ampicillin
USP7 Δ UBL345	Human	pRK5	Flag	N-terminal	Ampicillin
USP7 Δ 45	Human	pRK5	Flag	N-terminal	Ampicillin
USP7 Δ 5	Human	pRK5	Flag	N-terminal	Ampicillin
USP7 Δ 4	Human	pRK5	Flag	N-terminal	Ampicillin
USP7 Δ 3	Human	pRK5	Flag	N-terminal	Ampicillin
USP7 Δ 2	Human	pRK5	Flag	N-terminal	Ampicillin
USP7 Δ 1	Human	pRK5	Flag	N-terminal	Ampicillin
USP7 Δ Loop	Human	pRK5	Flag	N-terminal	Ampicillin
USP7 LoopSubs	Human	pRK5	Flag	N-terminal	Ampicillin
USP7 P804A	Human	pRK5	Flag	N-terminal	Ampicillin

Protein	Species	Backbone	Tag	Tag position	Antibiotic resistance
USP7 K869A	Human	pRK5	Flag	N-terminal	Ampicillin
USP7 DE	Human	pRK5	Flag	N-terminal	Ampicillin
USP7 DD	Human	pRK5	Flag	N-terminal	Ampicillin
USP7 DEDD	Human	pRK5	Flag	N-terminal	Ampicillin
USP7 LDEL	Human	pRK5	Flag	N-terminal	Ampicillin
USP7 LDELDD	Human	pRK5	Flag	N-terminal	Ampicillin
p65	Human	pEF	Ha	C-terminal	Ampicillin
p65	Human	pCDNA3.1			Ampicillin
p65	Mouse	pCMV	Flag	N-terminal	Ampicillin
p65	Mouse	pCDNA3.1	Flag	N-terminal	Ampicillin
p65	Mouse	pCDNA3.1			Ampicillin
p65 267A	Mouse	pCDNA3.1	Flag	C-terminal	Ampicillin
p65 267A	Mouse	pCDNA3.1			Ampicillin
p65 269A	Mouse	pCDNA3.1	Flag	C-terminal	Ampicillin
p65 269A	Mouse	pCDNA3.1			Ampicillin
p65 269D	Mouse	pCDNA3.1	Flag	C-terminal	Ampicillin
p65 269D	Mouse	pCDNA3.1			Ampicillin
p65 K56R	Mouse	pCDNA3.1	Flag	N-terminal	Ampicillin
p65 K56R	Mouse	pCDNA3.1			Ampicillin
p65 K62R	Mouse	pCDNA3.1	Flag	N-terminal	Ampicillin
p65 K62R	Mouse	pCDNA3.1			Ampicillin
p65 K123R	Mouse	pCDNA3.1	Flag	N-terminal	Ampicillin
p65 K123R	Mouse	pCDNA3.1			Ampicillin
Empty		pCDNA3.1	Flag	N-terminal	Ampicillin
Empty		pCDNA3.1			Ampicillin
Empty		pRK5	Flag	N-terminal	Ampicillin
Bcl3	Mouse	pRK5	Flag	N-terminal	Ampicillin
p50	Mouse	pRK5	Flag	N-terminal	Ampicillin
c-Rel	Mouse	pRK5	Flag	N-terminal	Ampicillin

Protein	Species	Backbone	Tag	Tag position	Antibiotic resistance
RelB	Mouse	pEF4	Flag	N-terminal	Ampicillin
DAXX	Mouse	pRK5	Flag	N-terminal	Ampicillin
EBNA1	H. Herpes Virus4 (EBV)	MSCV	Flag/Ha	N-terminal	Ampicillin
p53	Human	pCMV			Kanamycin
Ubiquitin*	Human		Ha	N-terminal	Ampicillin
GST-p65	Mouse	pET 42 a+	GST	N-terminal	Kanamycin

*Ubiquitin Ha plasmid (Matt Walsh Lab).

2.7 Primers

2.7.1 qPCR

Table 2-12 List of qPCR primers

Primer	Sequence	Supplier	Catalogue Number
mTBP 1	TGTTGGTGATTGTTGGT	Eurofins	N/A
mTBP 2	AACTGGCTTGTGTGGGAAAG	Eurofins	N/A
TNF α	Quantitect Primer Assay Hs_TNF_1_SG	Qiagen	QT00029162

2.7.2 Site Directed Mutagenesis

Table 2-13 List of mutagenesis primers

Primer	Sequence	Supplier
USP7 Δ UBL2345 F	CGAGCTGGCTGCTAGTGGATGAACCTTACCCAA G	IDT
USP7 Δ UBL2345 R	CTTGGGTAAGGTTTCATCCACTAGCAGCCAGCTC G	IDT
USP7 Δ UBL345 F	GATAACAGTGAATTACCCTGAGCAAAGGAGTAT TTCCGAG	IDT

Primer	Sequence	Supplier
USP7 ΔUBL345 R	CTCGGAAATACTCCTTTGCTCAGGGTAATTCAC TGTTATC	IDT
USP7 Δ45 F	CAGCTTAAGATGAAAATCACATGATTTGAGAAC AGGCGAAG	IDT
USP7 Δ45 R	CTTCGCCTGTTCTCAAATCATGTGATTTTCATCT TAAGCTG	IDT
USP7 Δ5 F	GAAATCCCTTTGGACCAGGTGTGAATAGACAAA GAGAATGAGATG	IDT
USP7 Δ5 R	CATCTCATTCTCTTTGTCTATTCACACCTGGTCC AAAGGGATTTT	IDT
USP7 Δ4 F	ATCCCTTTGGACCAGGTG	IDT
USP7 Δ4 R	ACTTCGCCTGTTCTCAAAG	IDT
USP7 Δ3 F	CTTAAGATGAAAATCACAGACTTTG	IDT
USP7 Δ3 R	GTGGTAGAGATCTCGGAAATAC	IDT
USP7 Δ2 F	GATGACCCTGAAAATGATAAC	IDT
USP7 Δ2 R	ATGATCTTTATCAAACCTGGG	IDT
USP7 Δ1 F	GTTGATCCCGAGCTGGCTG	IDT
USP7 Δ1 R	GAGATGGGCTTCCTGCCG	IDT
USP7 ΔLoop F	AGGCGAAGTTTTAAATGTATATG	IDT
USP7 ΔLoop R	TTTCATCTTAAGCTGCTG	IDT
USP7 LoopSubs F	GCTGCGGCCAGGCGAAGTTTTAAATGTATATG	IDT
USP7 LoopSubs R	GGCTGCGGCTTTCATCTTAAGCTGCTG	IDT
USP7 P804A F	CATTTTCTGTGATAAAACAATCGCTAATGATCCT GGATTTGTGG	IDT
USP7 P804A R	CCACAAATCCAGGATCATTAGCGATTGTTTTAT CACAGAAAATG	IDT
USP7 K869A F	GAGATCTTCTACAGTTCTTCGCGCCTAGACAAC CTAAGAAAC	IDT
USP7 K869A R	GTTTCTTAGGTTGTCTAGGCGCGAAGAACTGTA GAAGATCTC	IDT
USP7 DE F	TAAAGCCCTTGCTGCACTAATGGATG	IDT
USP7 DE R	TCAAGAGACACGTCATAG	IDT
USP7 DD F	TGCCATCATAGATTTTCAGAAGGATG	IDT

Primer	Sequence	Supplier
USP7 DD R	CCAGCCATTAGTTCATCAAGGGC	IDT
USP7 DD (DEDD) F	TAAAGCCCTTGATGAACTAATGGCTG	IDT
USP7 DD (DEDD) R	TCAAGAGACACGTCATAGTC	IDT
USP7 DEDD F	TGCCATCATAGTATTTTCAGAAGGATGAC	IDT
USP7 DEDD R	CCAGCCATTAGTGCAGCAAGGGC	IDT
USP7 LDEL F	GCAGCAATGGATGGTGACATCATAG	IDT
USP7 LDEL R	AGCAGCGGCTTTATCAAGAGACAC	IDT
USP7 LDELDD F	GCAGCAATGGCTGGTGCCATCATA	IDT
USP7 LDELDD R	AGCAGCGGCTTTATCAAGAGACACG	IDT

2.7.3 Cloning

Table 2-14 List of cloning primers

Primer	Sequence	Supplier
P65 F	CCCAAGCTTGGGGCCACCATGGACGATCTGTTTCCCCTC	IDT
P65 R	GCTCTAGAGCTTAGGAGCTGATCTGACTCAAAG	IDT
P65- Flag F	CCCAAGCTTGGGGCCACCATGGATTACAAGGATGACGACGATAAG GACGATCTGTTTCCCCTC	IDT

2.7.4 Sequencing

Table 2-15 List of sequencing primers

Primer	Sequence	Supplier
T7	TAATACGACTCACTATAGGG	GATC
BGH-Reverse	TAGAAGGCACAGTCGAGG	GATC
CMV-F	CGCAAATGGGCGGTAGGCGTG	GATC
EBV-RP	GTGGTTTGTCCAAACTCATC	GATC
hUSP7-300	GGTGATGCCACGCTTTTA	GATC
hUSP7-699	TTTCACGAATCAGCTACG	GATC
hUSP7-1396	GTGGTTTATCTAAACCC	GATC
hUSP7-2099	ATTACTGTGGGCATATC	GATC

Primer	Sequence	Supplier
hUSP7-2700	CAGCCAATTTAGGGAAGAGG	GATC
mp65-Cterminal	GAGCCCATGCTGATGGAGTA	GATC
mp65-Nterminal	GCATTTATAGCGGAATCGCA	GATC

2.8 Antibodies

Table 2-16 List of antibodies

Antibody	Company	Catalogue Number
p65	Santa Cruz Biotechnologies	Sc-8008
p65	Bethyl	A301-824A
p65	Santa Cruz Biotechnologies	Sc-372
GST	Sigma Aldrich	G7781
FLAG	Sigma	F1804
USP7	Bethyl	A300-033A
p53	Santa Cruz Biotechnologies	Sc-6243
Ha	Santa Cruz Biotechnologies	Sc-805
β -Actin	Sigma	SAB 1305567
c-Rel	Santa Cruz Biotechnologies	Sc-71
RelB	Santa Cruz Biotechnologies	Sc-226
DAXX	Santa Cruz Biotechnologies	Sc-7152
Mouse	GE Healthcare	NXA931V
Rabbit	GE Healthcare	NA934V
Biotin HRP Linked	Cell Signalling Technologies	02/2017

2.9 Buffers

2.9.1 GST-protein purification

Table 2-17 GST-protein purification buffers

Buffer	Composition
Lysis buffer	Tris HCl 50mM pH 8.5 NaCl 150mM DTT 10mM
Binding buffer	PBS pH7.3 {NaCl 140mM, KCl 2.7mM, Na ₂ HPO ₄ 1.8mM, KH ₂ PO ₄ 10mM} DTT 10mM
Elution buffer	Tris HCl 50mM pH 8 Reduced Glutathione 10mM DTT 10mM

2.9.1.1 Column wash and storage

Table 2-18 GST-protein purification column wash and storage buffers

Buffer	Composition
Removal of precipitated or denatured substances	2 Volumes of 6M Guanidine Hydrochloride 5 Volumes of PBS
Removal of hydrophobically bound substances	4 Volumes of EtOH 70% 5 Volumes of PBS
Storage	EtOH 20%

2.9.2 Loading buffer

Table 2-19 WB loading buffer

Buffer	Composition
2X SDS loading buffer	20% Glycerol 0.2% bromophenol blue 4%SDS 200mM B-mercaptoethanol 100mM Tris/HCl pH6.8 H ₂ O
4X SDS loading buffer	40% Glycerol 240mM Tris/HCl pH 6.8 8% SDS 0.04% Bromophenol Blue 5% B-mercaptoethanol H ₂ O

2.9.3 SPOT-synthesis of peptides and overlay analysis

Table 2-20 SPOT-synthesis of peptides and overlay analysis buffers

Buffer	Composition
10X TBS 1litre	1M Tris-Cl pH 7.5 100ml NaCl 87.8g H ₂ O up to 1 litre
TBS-T	TBS 1X 0.05% Tween20
Peptide array stripping buffer	2% SDS 62mM Tris pH6.8 20mM DTT

2.9.4 Cell lysis buffers

Table 2-21 Cell lysis buffers

Buffer	Composition
Radioimmunoprecipitation assay (RIPA)	50mM Tris/HCl pH7.4 0.1-1% Igepal 0.25% Sodium deoxycholate 150mM NaCl 1mM EDTA pH8 1mM PMSF* 1mM NaF* 1mM Na ₃ VO ₄ * 2µg/ml aprotinin* 1µg/ml pepstatin* 2µg/ml leupeptin*
Pull down lysis and binding buffer	20mM Tris/HCl pH8 200mM NaCl 1mM EDTA pH8 0.5% Igepal 1mM PMSF* 2µg/ml aprotinin* 1µg/ml pepstatin*

*Added to the buffer immediately prior to use.

2.9.5 Electrophoresis buffers for western blotting

Table 2-22 Electrophoresis buffers for western blotting

Buffer	Components
1X Tris-glycine running buffer	25mM Tris/HCl 250mM glycine 0.1% SDS H ₂ O
1X Tris-glycine transfer buffer	48mM Tris/HCl 39mM glycine 0.0375% SDS 20% methanol H ₂ O

2.9.6 Tris-glycine SDS-polyacrylamide gels

Table 2-23 Tris-glycine SDS-polyacrylamide gels

Gel	Volume	Components	
5% Stacking	1ml	H ₂ O	680μl
		30% Acrylamide	170μl
		1M Tris/HCl pH6.8	130μl
		10% SDS	10μl
		10% ammoniumpersulfate	10μl
		TEMED	1μl
8% Resolving	5ml	H ₂ O	2.3ml
		30% Acrylamide	1.3ml
		1.5M Tris/HCl pH8.8	1.3ml
		10% SDS	50μl
		10% ammoniumpersulfate	50μl
		TEMED	3μl

2.9.7 ELISA

Table 2-24 ELISA buffers

Buffer	Composition
Coating buffer	0.2M Na ₃ PO ₄ pH6.5
Assay diluent	10% FBS PBS, pH7
Wash buffer	PBS Tween-20 0.05%
Stop solution	2N H ₂ SO ₄

2.10 Reagents

Table 2-25 List of reagents

Reagent	Company	Catalogue #
Acrylamide/Bis-acrylamide Solution	30% Sigma	A3574
Agarose Ultrapure	Invitrogen Life technologies	16500
Ammonium persulfate	Sigma	A3678
Ampicillin sodium salt	Sigma Aldrich	A9518
Aprotinin from bovine lung	Sigma Life Science	A1153
B-mercaptoethanol	Sigma Aldrich	M6250
Bovine Serum Albumin	Sigma Aldrich	A7906
Bromophenol Blue	Sigma Aldrich	B8026
DMSO (Dimethyl sulfoxide)	Fisher chemical	D/4120/PB08
DPBS 1X	Gibco	14190-094
DTT (Dithiothreitol)	Melford Biolaboratories	MB1015
Dulbecco's Modified Eagle's Medium-high glucose	Sigma	D6429
EDTA (Ethylenediaminetetraacetic acid)	Fisher chemical	D/0700/60

Reagent	Company	Catalogue #
Ethanol	VWR AnalaR Normapur	20821-330
GHS beads	Sigma Aldrich	G4510
L-glutamine solution	Sigma	G7513
L-Glutathione reduced	Sigma Aldrich	G4251
Glycerol	Fisher Scientific	G/0650/17
Glycine	Fisher Chemical	G/0800/60
Guanidine Hydrochloride	Sigma Life Science	G3272
Heat inactivated FBS	Gibco	10500-064
Hydrochloric acid S.G	Fisher Chemical	H/1200/PB17
Igepal CA-630	Sigma	18896
IPTG (Isopropyl beta-D-1-thiogalactopyranoside)	Sigma	16758
Isopropanol	Sigma	24137
Kanamycin	Melford Laboratories	K0126
Potassium chloride	Analar Normapur	26764
Leupeptin	Sigma Life Science	L2884
Lipopolysaccharides from Escherichia Coli 055:B5	Sigma Aldrich	L2880
Methanol	Fisher chemical	M/4000/PC17
Nuclease free water	Qiagen	1039480
Penicillin-Streptomycin	Sigma	P0781
Pepstatin A	Sigma Life Science	P5318
Phenylmethanesulfonyl fluoride	Sigma	P7626
Potassium dihydrogen phosphate	Analar Normapur	26936
Protease inhibitor cocktail tablets Complete	Roche Diagnostics GmbH	11697498001
Protein Assay Dye Reagent Concentrate	Bio-Rad	500-0006
Protein G agarose beads	EMD Millipore	16-266
Ponceau S Solution	Sigma Aldrich	P7170
Restore Plus Western Blot Stripping Buffer	Thermo Scientific	46430

Reagent	Company	Catalogue #
Sodium chloride	VWR BDH Prolabo	27810.295
Sodium deoxycholate	Sigma Aldrich	D6750
Sodium dihydrogen phosphate dihydrate	Riedel de Haen	04269
SDS (Sodium Dodecyl Sulphate)	VWR	UN1325
Sodium fluoride	Sigma Aldrich	S7920
Sodium hydrogen phosphate	AnalaR Normapur	102494C
Sodium hydroxide pellets	Fisher chemicals	S/4920/53
Sodium orthovanadate	Sigma	S6508
Sulfuric acid	Sigma Aldrich	258105
TEMED (Tetramethylethylenediamine)	Sigma	T9281
TMB 1X Substrate Solution	eBioscience	00-4201-56
Tris HCl	Fisher Scientific	BP 152-1
0.05% Trypsin-EDTA 1X	Gibco	25300-054
Tween-20	Sigma Life Science	P2287
Western Bright ECL	Advansta	K12045
Western Bright Sirius	Advansta	K12043

2.11 Mimetic peptides

2.11.1 p65 mimetic peptides

Table 2-26 List of p65 mimetic peptides

Peptide	Sequence	Modification	Supplier
E4	YGRKKRRQRRPYADPSLQAPVRVSMQLR	N/A	GenScript
E4 Control 1	YGRKKRRQRRPYADPSLQAPVAVSMQLR	R267A	GenScript
E4 Control 2	YGRKKRRQRRQQPRDSLVPVAVSMRLPYA	Scrambled	GenScript
F4	YGRKKRRQRRSPFNGPTEPRPPTTRIAV	N/A	GenScript
F4 Control	YGRKKRRQRRSPFNGPTEPRPPTAAIAV	R329A, R330R	GenScript

2.11.2 USP7 mimetic peptides

Table 2-27 List of USP7 mimetic peptides

Peptide	Sequence	Supplier
Upep1	GYRDGPGNPLR	GenScript
Upep2	LRHNYEGT	GenScript
Upep3	RDGPGNPLRHNYEGT	GenScript

Chapter Three

Characterisation of important sites of p65 involved in USP7 deubiquitinase activity

3 Characterisation of important sites of p65 involved in USP7 deubiquitinase activity

3.1 Abstract

The NF- κ B transcription factor family is fundamental for the regulation of inflammation and the response to infection by directly controlling the transcription of genes involved in these processes. Due to its key role in these processes, NF- κ B activity is highly regulated. The balance between ubiquitination and deubiquitination is a critical factor in the control of NF- κ B mediated responses. USP7 is a DUB known to deubiquitinate the p65 subunit of the NF- κ B transcription factor family. However, the molecular determinants of p65 recognition as a substrate by USP7 are currently unknown. Based on a peptide analysis of p65 and USP7 interaction, we generated two cell permeable peptides mimicking regions of p65 previously identified as mediating interaction with USP7. These p65 mimetic peptides were not able to inhibit the NF- κ B response. Further investigation on the specific recognition of p65 by USP7 is needed in order to develop a mimetic peptide able to inhibit USP7 activity on p65. A recently discovered phosphorylation site on p65 at S269 is in close proximity to R267. R267 of p65 is known to inhibit the interaction when mutated to alanine. We studied the effect of the phosphorylation status of p65 S269 on the interaction with USP7. However, mutation of S269 does not interfere with USP7-p65 interaction.

3.2 Introduction

The transcription factor NF- κ B is a key regulator of the immune response. Aberrant NF- κ B activity leads to the development of a number of human diseases; for instance, different types of cancer (for example leukaemia, lymphoma) [457-459], autoimmune diseases (such as, lupus, diabetes, arthritis, multiple sclerosis) [2, 457, 458], neurodegenerative diseases (like Alzheimer, Parkinson, Huntington) [458], and viral infection diseases (e.g. AIDS, infection skin diseases) [457, 458]. Therefore the tight regulation of the NF- κ B response is important for human health.

NF- κ B activity is regulated by different PTMs such as phosphorylation and ubiquitination among others [42]. Phosphorylation of NF- κ B subunits plays a key role controlling their stability, degradation, interaction with other factors and transcription activity [17]. Certain phosphorylation events regulate the NF- κ B transcriptional activity in a gene specific manner [17]. p65 is the most studied subunit and the main focus has been placed on S276 and S536 phosphorylation sites. Phosphorylation of these sites leads to transactivation of the NF- κ B response and K310 acetylation [17]. However, there are various phosphorylation sites like S269, whose function in p65 regulation is still unknown [68]. On the other hand, ubiquitination of NF- κ B subunits is the major limiting factor of pro-inflammatory genes expression [15]. USP7 DUB deubiquitinates p65 subunit of NF- κ B, leading to the termination of the NF- κ B response [287]. As explained in section 1.4.3.3, huge efforts have been made on the generation of USP7 inhibitors. All the inhibitors developed are based on a catalytic inhibition of USP7 but are not substrate specific and would be expected to promote the ubiquitination of all USP7 substrates equally. Therapeutic targeting of USP7 to inhibit NF- κ B in the context of inflammation will require much greater substrate selectivity in order to minimise the potential for toxicity.

In this chapter we investigated the ability of p65 mimetic peptides to inhibit USP7-p65 interaction. In order to test these peptides, we used a peptide transduction strategy which is based on the ability of certain peptidic sequences to cross the cellular membrane and enter into the cell, as explained in section 1.3.3. Cargo molecules can be attached to the CPPs by different methods; chemical crosslinking, cloning and chemical synthesis [116, 122]. Among these

cargoes are proteins, nanoparticles, oligonucleotides and small interfering RNAs (siRNAs) [118, 120-122]. Once the cargoes have been taken up, they are able to act on their cellular targets [116].

CPPs can be classified by their origin or their physicochemical properties. According to their origin there are three groups of CPPs; natural CPPs, chimeric CPPs and synthetic CPPs (see Table 3-1) [119, 124, 460]. On the other hand, according to their physicochemical properties they are divided in 3 different groups; cationic CPPs, amphipathic CPPs and hydrophobic CPPs (See Table 3-1) [116, 118, 120].

Table 3-1 CPPs classification

Classified by	Group	Description
Origin	Natural CPPs	Derived from natural proteins
Origin	Chimeric CPPs	Fusion of two natural proteins or peptide sequences
Origin	Synthetic CPPs	Peptides based on natural proteins designed to mimic their activity
Physicochemical properties	Cationic CPPs	High content of positively charged residues e.g. NLS
Physicochemical properties	Amphipathic CPPs	Chimeric peptides formed by the covalent bond of an hydrophobic patch to an NLS
Physicochemical properties	Hydrophobic CPPs	Contain apolar residues

CPPs enter into the cells through different mechanisms. These mechanisms are independent but can occur at the same time [118, 119]. Cellular uptake mechanisms can be classified as energy independent and energy dependent. Energy independent mechanisms are known as direct translocation and include inverted micelle formation, adaptive translocation, pore formation model, carpet like model and membrane thinning model [117, 119, 460]. Whereas CPPs entering the cells through energy dependent mechanisms, do so through endocytosis, including micropinocytosis, clathrin and/or caveolae mediated

endocytosis and clathrin and/or caveolae independent mediated uptake [117-121]. See Table 3-2. All these mechanisms are based on interactions between positively charged residues in the CPP sequence and negatively charged components of the lipid bilayer, leading to rearrangements in the membrane which result is the uptake of the peptide into the cell.

Table 3-2 CPPs cellular entry mechanisms

Group	Type
Energy independent or direct translocation	Inverted micelle formation, adaptive translocation, pore formation model, carpet-like model, membrane thinning model
Energy dependent or endocytosis	Micropinocytosis, clathrin and/or caveolae mediated endocytosis, clathrin and/or caveolae independent endocytosis

The first CPP discovered was part of the TAT protein from human immunodeficiency virus 1 (HIV-1 TAT) [124, 461-464]. A basic region composed by 10 amino-acids containing 2K and 6R promotes HIV-1 TAT protein cellular uptake [118, 124, 461-463]. TAT protein when added exogenously to cells in culture is uptaken by adsorptive endocytosis [461, 464]. Once in the cell it localises predominantly in the nucleus and nucleoli [462, 463]. TAT protein is also able to carry other molecules into the cells [118, 124, 463, 464], an important fact for drug therapies. The ability of CPPs to deliver a wide variety of cargoes into the cells makes them a really interesting tool for researching purposes. The most important one is their ability of therapeutic drug delivery. CPPs have been used to target the NF- κ B signalling pathway as explained in section 1.3.3. However, these CPPs are not totally NF- κ B specific, and have also effects on other signalling pathways [116].

A peptide array and subsequent alanine scan analysis to determine the specific residues of p65 involved in the interaction with USP7 was previously performed [287]. Using these data we designed a mimetic peptide derived from the amino-acids of p65 that interact with USP7. We hypothesised that a p65 mimetic

peptide may block the interaction of p65 and USP7, thereby promoting p65 ubiquitination and proteasomal degradation, and inhibiting NF- κ B mediated inflammatory responses. The mimetic peptide was fused to the TAT sequence of the HIV-1 TAT protein, in order to deliver the peptide to the nucleus. Several phosphorylation sites on p65 have been described to play an important role on the NF- κ B response [17], including S536 and S468 which regulate p65 ubiquitination through interaction with E3 ligases [17]. A recently described phosphorylation site at S269 is in close proximity to R267 a residue previously identified as critical for interaction with USP7 [287]. In this chapter we also investigated the potential role of S269 phosphorylation in regulating the interaction of p65 with USP7.

3.3 Results

3.3.1 Mutation of S269 of p65 does not affect interaction with p65

S269 is located in close proximity to R267, which when mutated to alanine inhibits the interaction of p65 with USP7. In order to study the potential role of S269 phosphorylation in the interaction, two different mutants were created, S269D and S269A. S269D mimics the phosphorylation of WT p65 protein at S269 by the presence of the negative charge contained by the aspartic acid, while S269A mimics the non-phosphorylated status by the absence of the negative charge. These mutants were previously created in the Carmody group. Original p65 mutants were C-terminal FLAG-tagged in a pCDNA3.1 vector, while WT p65 was N-terminal FLAG-tagged in a pCMV vector. Firstly, p65 WT and mutants were sub-cloned into pCDNA3.1 vector. Cloning was performed in order to reduce the variability of the interaction due to the presence of the FLAG-tag in a different site and/or due to different expression of each expression vector. See appendix 8.2.

p65 WT, p65 R267A, p65 S269A and p65 S269D plasmids were co-transfected with USP7 FLAG-tagged plasmid in HEK293T cells. Cells were harvested and lysates were immunoprecipitated with anti-p65 antibody. Protein levels were analysed by western blotting with anti-p65 and anti-FLAG antibodies. R267A mutation is known to inhibit the interaction between USP7 and p65 [287], therefore, it was used as a negative control for the interaction. There are no visible differences in

the protein level of USP7 when immunoprecipitated with p65 S269A and p65 S269D in comparison to WT p65 (see Figure 3-1). From these results, we can conclude that the phosphorylation status of p65 S269 has no effect on the interaction of p65 with USP7.

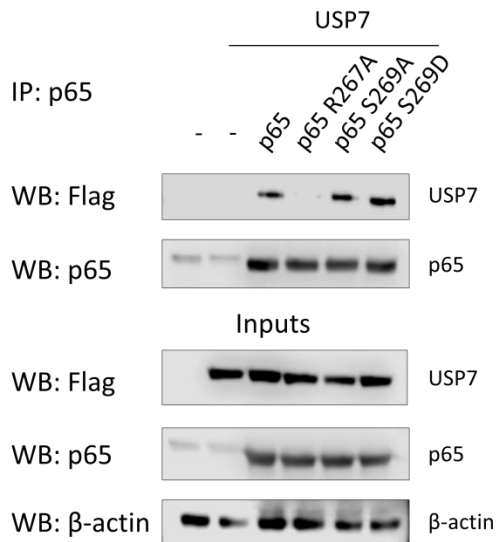


Figure 3-1 Phosphorylation status of p65 S269 has no effect on the interaction with USP7. HEK293T cells were co-transfected with p65 WT, p65 R267A, p65 S269A and p65 S269D along with USP7 FLAG-tagged plasmids. Cells were lysed and immunoprecipitated with anti-p65 antibody. The immunoprecipitations were immunoblotted with antibodies anti- p65 and anti-FLAG. The figure is a representative of three independent experiments.

3.3.2 p65 derived peptides

3.3.2.1 Design and synthesis

Two p65 derived mimetic peptides, designated E4 and F4, were designed according to the results obtained from a p65 peptide array and subsequent alanine scan previously performed in the lab [287] (see Figure 3-2). Peptide E4 contains amino acids 256-273 of p65 and includes R267 (see Figure 3-2). In addition to the inhibitory role of R267A mutation [287], substitution of R273 with an alanine highly decreases the interaction with USP7 in peptide array experiments, indicating that 273 residue is also important for interaction. The E4 peptide is contained within the available crystal structure of p65 subunit (PDB 1VKX), where it corresponds to an accessible site for the interaction with USP7 (see Figure 3-3).

Peptide F4 comprises amino-acids 316-333 of p65 (see Figure 3-2). This peptide contains two arginine residues (R328, R329) which when mutated to alanine highly reduce the interaction with USP7 in peptide array experiments [287]. We were not able to analyse F4 position in the crystal structure of p65 as the PDB 1VKX model covers only amino acids 19-291. Transactivation domains are difficult to crystallise due to the instability of the domain, so we created a full length p65 structural model using ROBETTA software (<http://robetta.bakerlab.org/>) and the truncated p65 3D structure from 1VKX (see section 6.3.1). This software was developed by Baker Lab and it uses available X-Ray crystal structures to predict structures. As we can see in the model, the missing part of the subunit in 1VKX is formed by flexible loops, which are more likely to move than to stay immobile. According to this model both mimetic peptides, E4 and F4 are accessible for potential interaction with USP7 (see Figure 3-4).

The final peptides consisted of the selected p65 sequence with the addition of the cell permeable HIV-TAT cargo carrying peptide sequence (YGRKKRRQRR). This 10 amino acid HIV-TAT sequence mediates the cellular uptake and nuclear localisation of fused peptides [465]. Previous work in the group confirmed the cellular uptake and nuclear localisation of peptides fused to this HIV-TAT sequence with no transfection required [466].

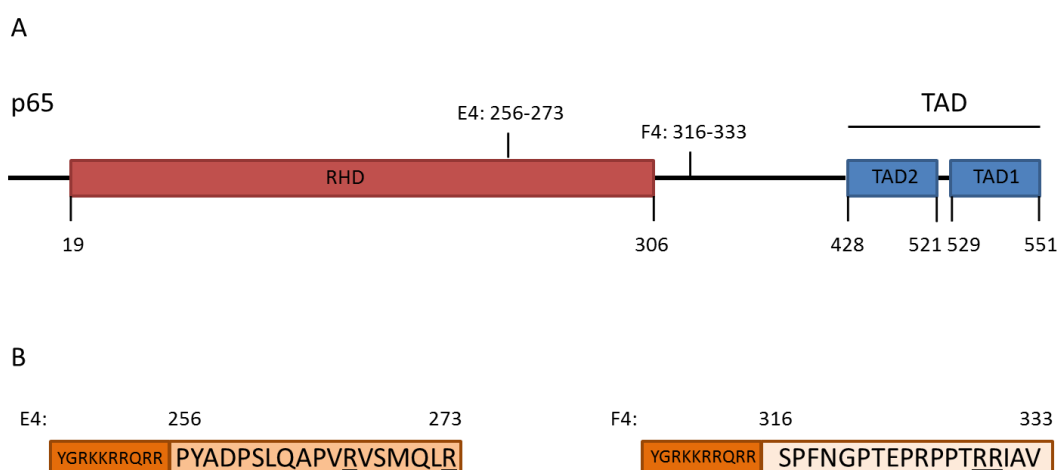


Figure 3-2 Design of p65 derived cell permeable peptides. A) Schematic representation of p65 subunit of NF- κ B with the corresponding p65 derived mimetic peptides E4 and F4. Position of both peptides within the p65 protein is indicated. **B)** Schematic of the p65 derived mimetic peptides fused to the HIV-TAT cargo protein construct (YGRKKRRQRR). Sequences of each peptide are noted. R267, R273 and R329 and R330 are underlined in E4 and F4 respectively.

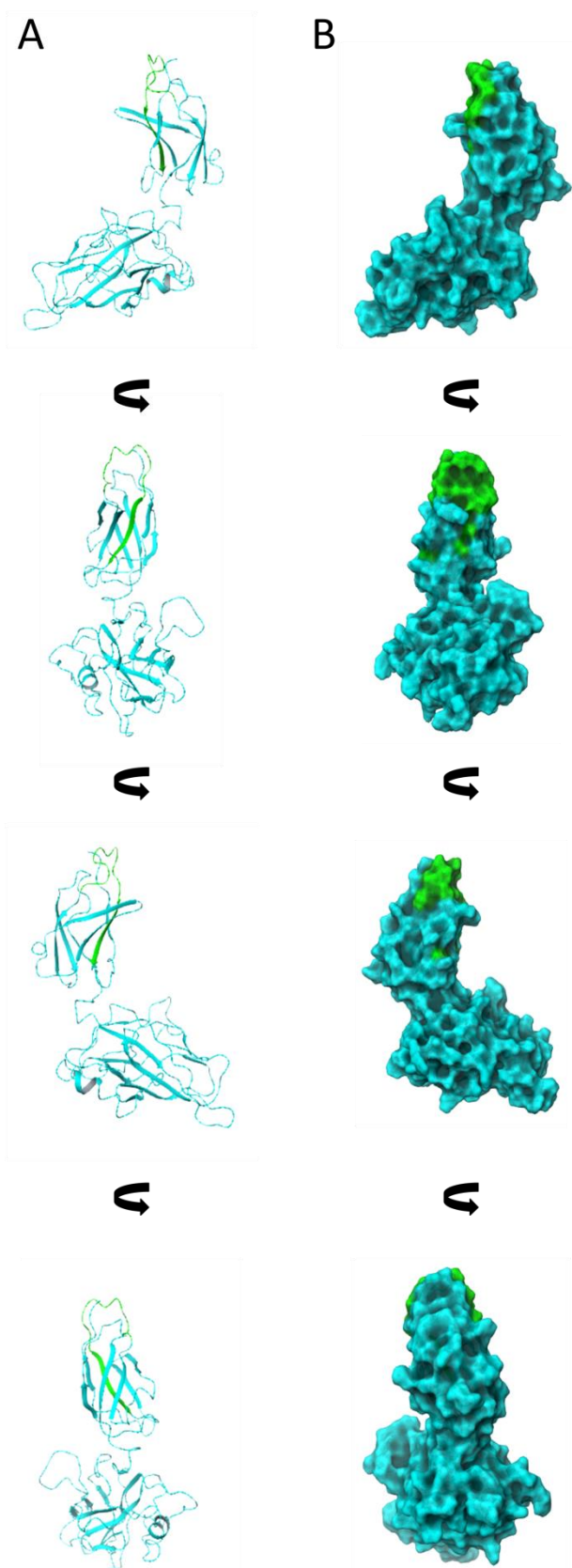


Figure 3-3 p65 derived mimetic peptides structural localisation in a known X-Ray (PDB 1VKX). A) Ribbon of the crystal structure of p65 from PDB 1VKX (amino-acids 19-291, RHD {amino-acids 19-306}). E4 peptide is marked in green. F4 is not present in the in 1VKX. **B)** Surface of the crystal structure of p65 from PDB 1VKX (amino-acids 19-291, RHD {amino-acids 19-306}). E4 peptide is marked in green. F4 is not present in the X-Ray. All structures were analysed with Maestro Schrodinger software.

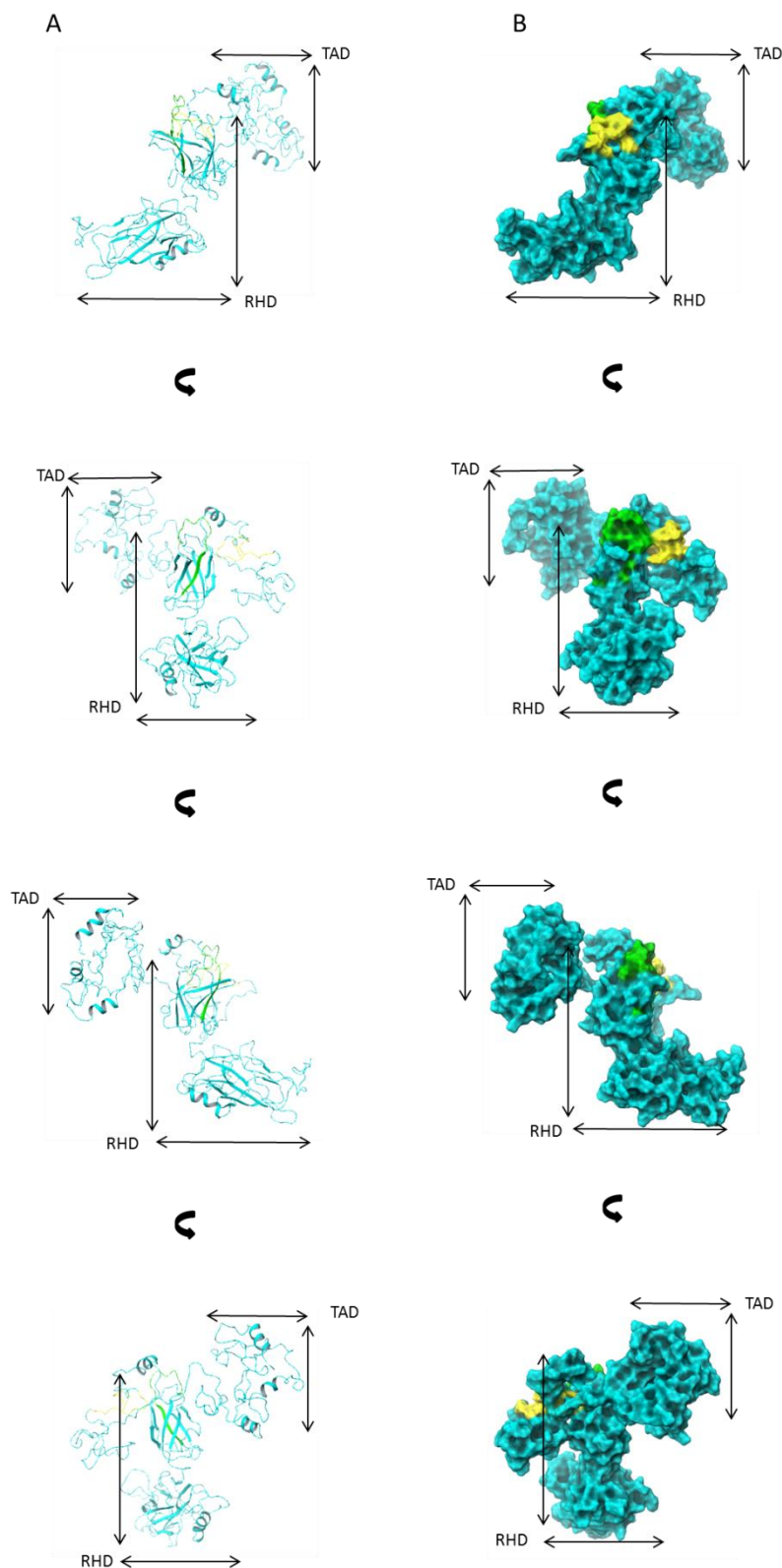


Figure 3-4 p65 derived peptides structural localisation in a full length model. A) Ribbon of the full length model of p65 created by ROBETTA Software. E4 peptide is marked in green. F4 is coloured in yellow. The RHD and TAD domains of p65 are labelled in each of the structure views. **B)** Surface of the full length model of p65 created by ROBETTA Software. E4 peptide is marked in green. F4 is coloured in yellow. The RHD and TAD domains of p65 are labelled in each of the structure views. All structures were analysed with Maestro Schrodinger software.

3.3.2.2 Peptide characterisation

Two control peptides were also designed to be used as a negative control for the effects of E4 and F4 on signalling in vitro. These control peptides will confirm that the effects on the NF- κ B response are due to the activity of the specific test peptide and not due to the presence of a CPP. The control peptides E4C1 and F4C were based on the E4 and F4 sequence but containing alanine substitutions of essential p65 interacting amino-acids [467] previously identified by peptide array [287] (E4C1: YGRKKRRQRRPYADPSLQAPVAVSMQLR; F4C: YGRKKRRQRRSPFNGPTEPRPPTAAIAV) (see Figure 3-5). In the case of E4C1 R267 was mutated to alanine and in the case of F4C R328 and R329 were mutated to alanine. The mutated amino acids on each peptide control are highlighted on the crystal structures of p65 (PDB 1VKX and ROBETTA p65 full length model) (see Figure 3-6 and Figure 3-7). In addition, a second control peptide was designed for E4 mimetic peptide (E4C2). The design was performed using the bioinformatic tool Scrambled from Mimotopes, The Peptide Company. This second peptide control consisted of a scrambled E4 peptide sequence and the addition of the HIV-TAT cargo protein (E4C2: YGRKKRRQRRQQPRDSLVPVAVSMRLPYA) (see Figure 3-5). Previous work in the group confirmed that following 2 hours of peptide treatment, the mimetic peptides are effectively internalised by cells and translocated to the nucleus [466], where USP7 and p65 interaction takes place [287]. To investigate the effect of these peptides on TLR signalling regulation in vitro, ELISA and qPCR analysis were performed.

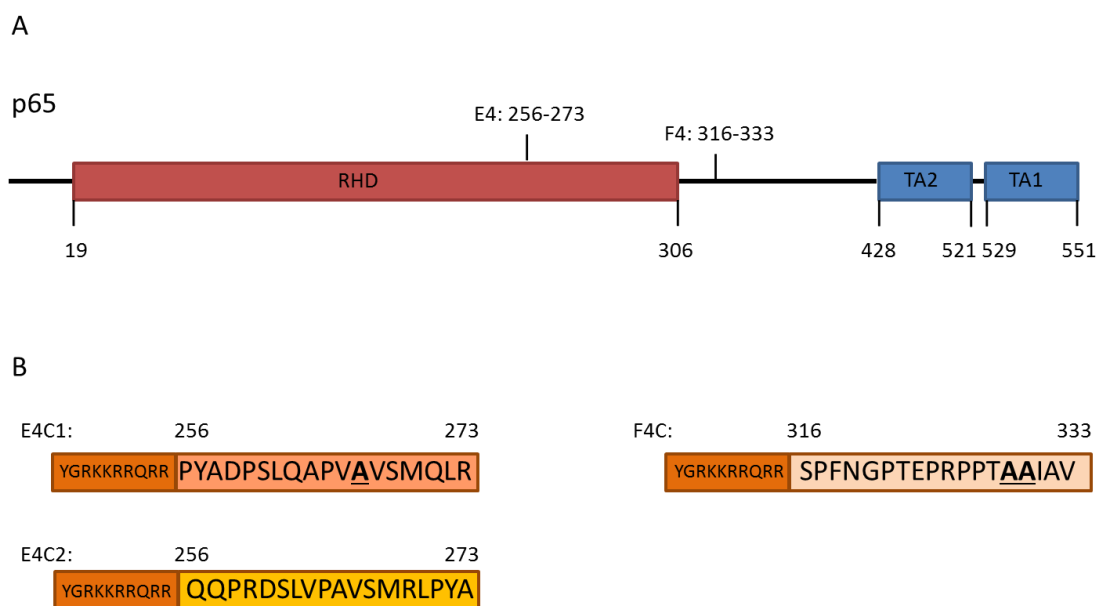


Figure 3-5 Design of p65 derived cell permeable control peptides. A) Schematic representation of p65 subunit of NF- κ B. The corresponding p65 derived mimetic peptides E4 and F4. Position of both peptides within the molecule is indicated. **B)** Schematic of the p65 derived mimetic control peptides fused to the HIV-TAT cargo protein construct. Sequences of each peptide are noted. Residue sites mutated to alanine compared to the WT sequence are underlined and marked in bold. E4C2 is a scrambled peptide, designed from the WT sequence.

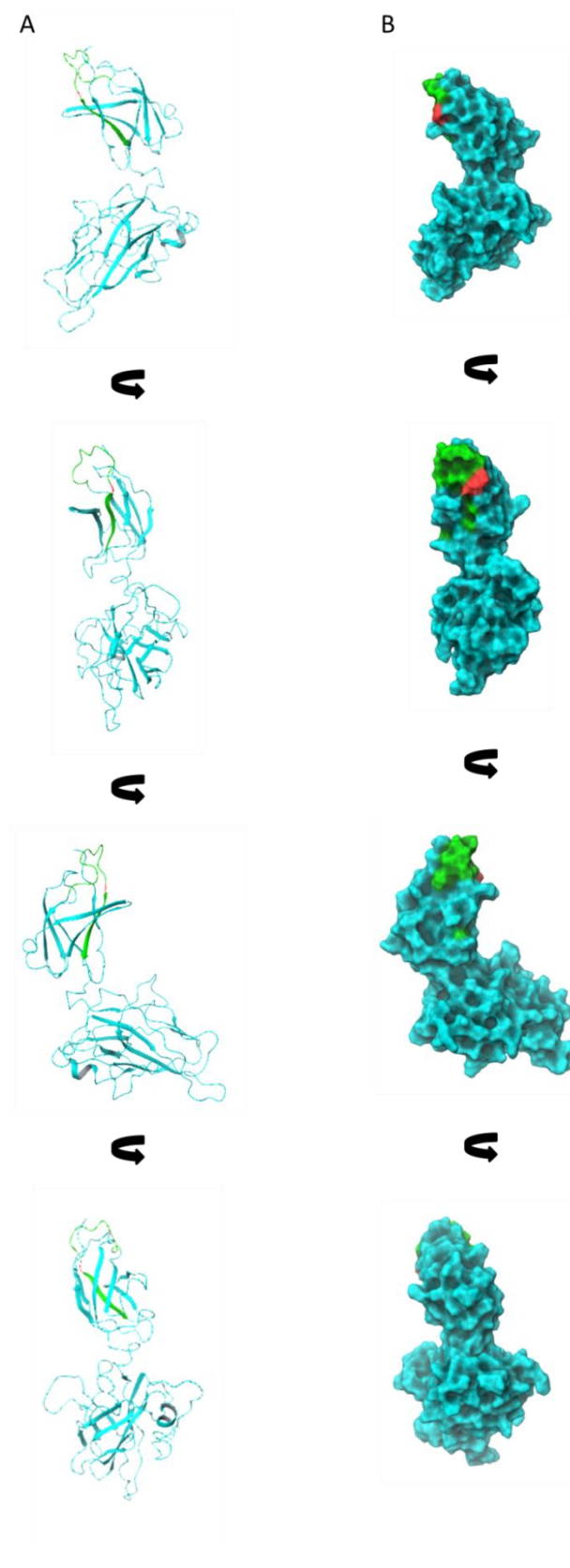


Figure 3-6 p65 derived mimetic control peptides localisation on a known crystal structure. A) Ribbon of the crystal structure of p65 from PDB 1VKX (amino-acids 19-291, RHD {amino-acids 19-306}). E4 peptide is marked in green. Amino-acids mutated to alanine are coloured in red. F4 is not present in the structure. **B)** Surface of the crystal structure of p65 from PDB 1VKX (amino-acids 19-291, RHD {amino-acids 19-306}). E4 peptide is marked in green. Amino-acids mutated to alanine are coloured in red. F4 is not present in the structure. All structures were analysed with Maestro Schrodinger software.

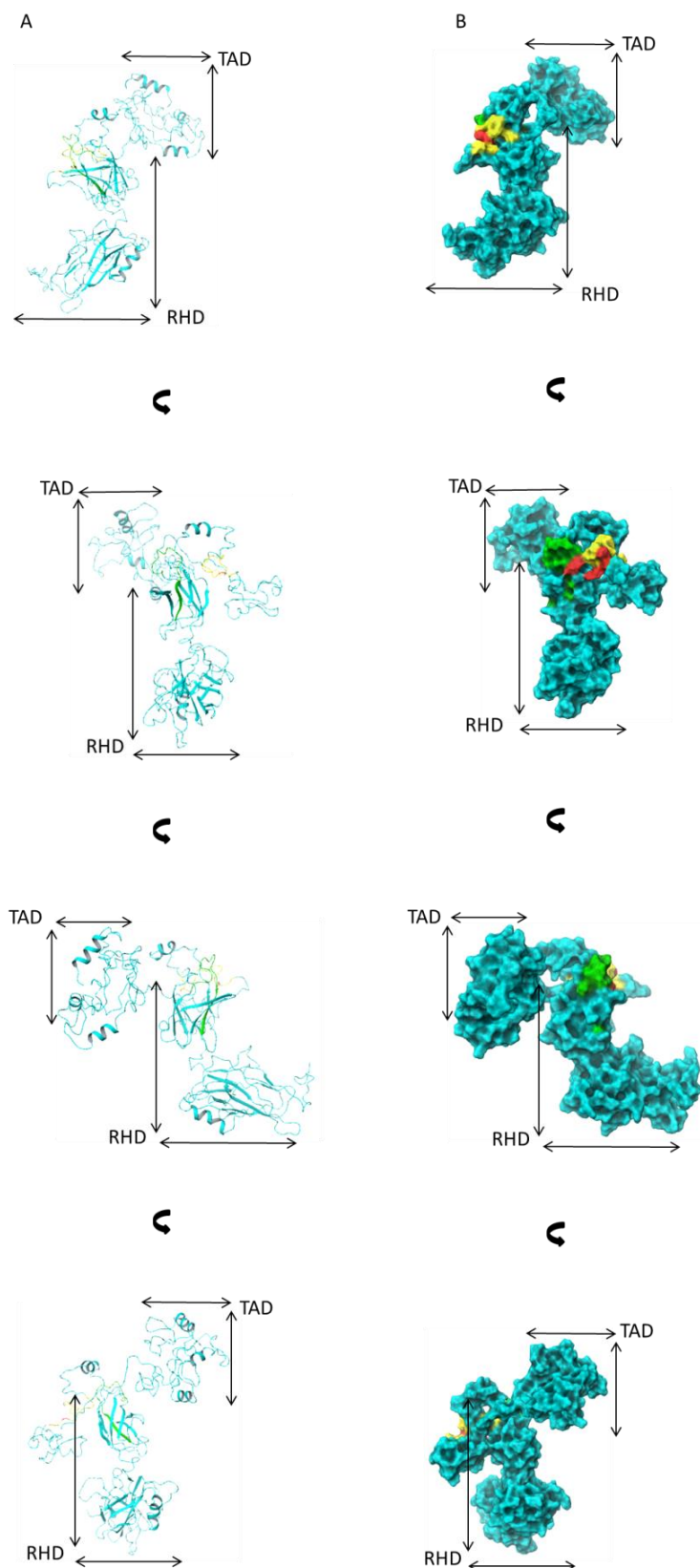


Figure 3-7 p65 derived mimetic control peptides localisation on full length p65 structural model. A) Ribbon of the full length model of p65 created by ROSETTA Software. E4 peptide is marked in green. F4 is coloured in yellow. Amino-acids mutated to alanine are coloured in red. The RHD and TAD of p65 are labelled in each of the structure views. **B)** Surface of the full length model of p65 created by ROSETTA Software. E4 peptide is marked in green. F4 is coloured in yellow. Amino-acids mutated to alanine are coloured in red. The RHD and TAD of p65 are labelled in each of the structure views. All structures were analysed with Maestro Schrodinger software.

A TNF α ELISA assay was performed to detect the effect of the peptide on LPS induced TNF α production. Experiments were carried out in RAW 264.7 cells and BMDM. Cells were incubated with different peptide concentrations (3 μ M, 10 μ M, 30 μ M and 100 μ M) for 2 hours and followed by 4 hours or 8 hours LPS stimulation (100ng/ml) (see Figure 3-8, Figure 3-9, Figure 3-10 and Figure 3-11). No statistically significant differences were shown between peptide and control peptide treatments (non-parametric Mann Whitney test), suggesting that the p65 mimetic peptides E4 and F4 do not inhibit the interaction of USP7 on p65; and therefore, p65 mimetic peptides E4 and F4 are not able to inhibit the LPS induced TNF α production.

qPCR analysis was performed to detect differences at TNF α gene transcription level. qPCR analysis was completed in RAW 264.7 cells. Cells were incubated for 2 hours with increasing concentrations of the peptides (3 μ M, 10 μ M, 30 μ M and 100 μ M) followed by a 2 hours LPS (100ng/ml) stimulation to activate the NF- κ B pro-inflammatory response (see Figure 3-12 and Figure 3-13). No statistically significant differences were found between peptide and control peptide treatments (non-parametric Mann Whitney test), suggesting that the p65 mimetic peptides E4 and F4 do not inhibit the interaction of USP7 with p65; and therefore, p65 mimetic peptides E4 and F4 are not able to inhibit p65 mediated TNF α expression. These results corroborate the results obtained in the ELISA assay.

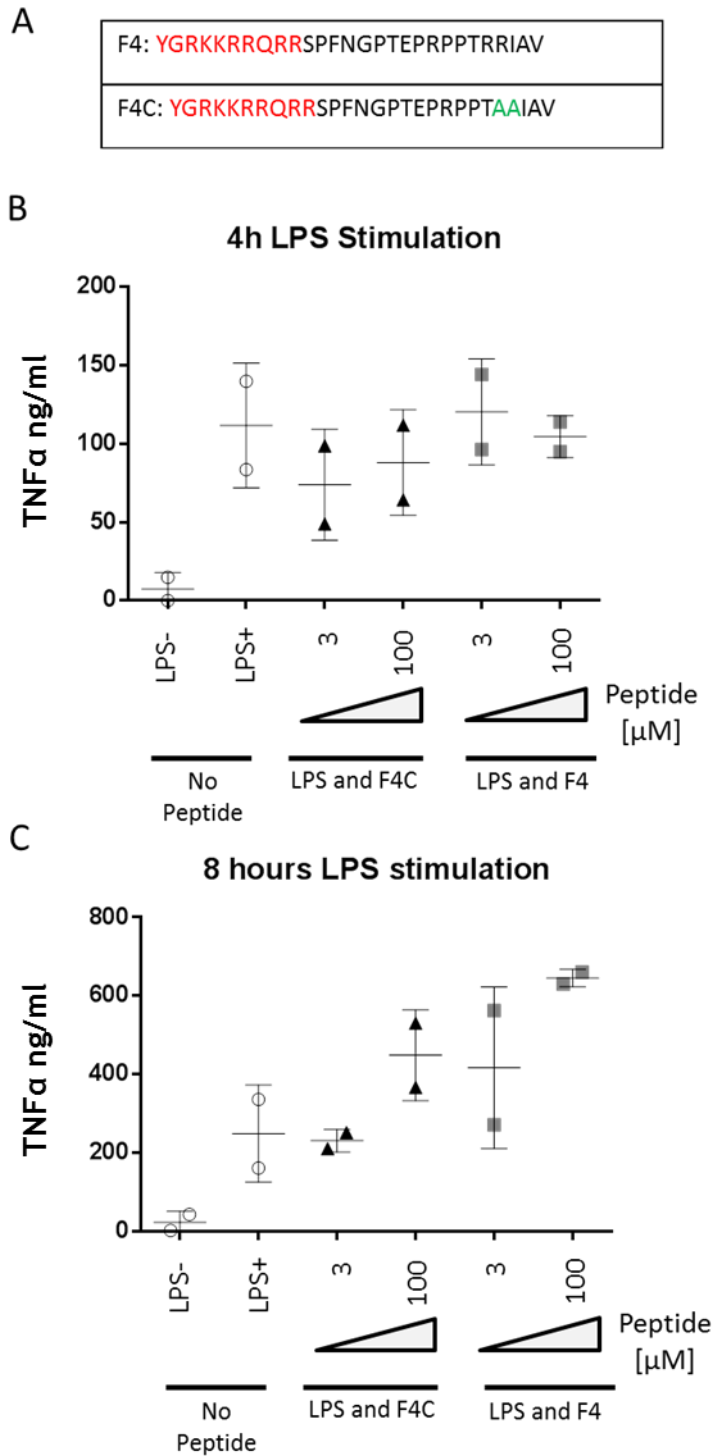


Figure 3-8 F4 p65 mimetic peptide does not inhibit LPS induced RAW 264.7 cells TNF α production. **A)** F4 and F4 negative control (F4C) amino-acid sequences. Marked in red is the HIV-TAT cargo protein sequence. Labelled in green, the amino-acids mutated in order to create the negative control. **B)** RAW 264.7 cells were left untreated or pre-treated for 2h with increasing concentrations (3 μ M-100 μ M) of either F4 or F4C peptide before stimulation with 100ng/ml of LPS. Supernatants were harvested 4h after stimulation and the concentration of TNF α was determined by ELISA. Data shown are the medians of the technical triplicates from different independent experiments with the corresponding standard deviation. **C)** RAW 264.7 cells were left untreated or pre-treated for 2h with increasing concentrations (3 μ M-100 μ M) of either F4 or F4C peptide before stimulation with 100ng/ml of LPS. Supernatants were harvested 8h after stimulation and the concentration of TNF α was determined by ELISA. Data shown are the medians of the technical triplicates from different independent experiments with the corresponding standard deviation.

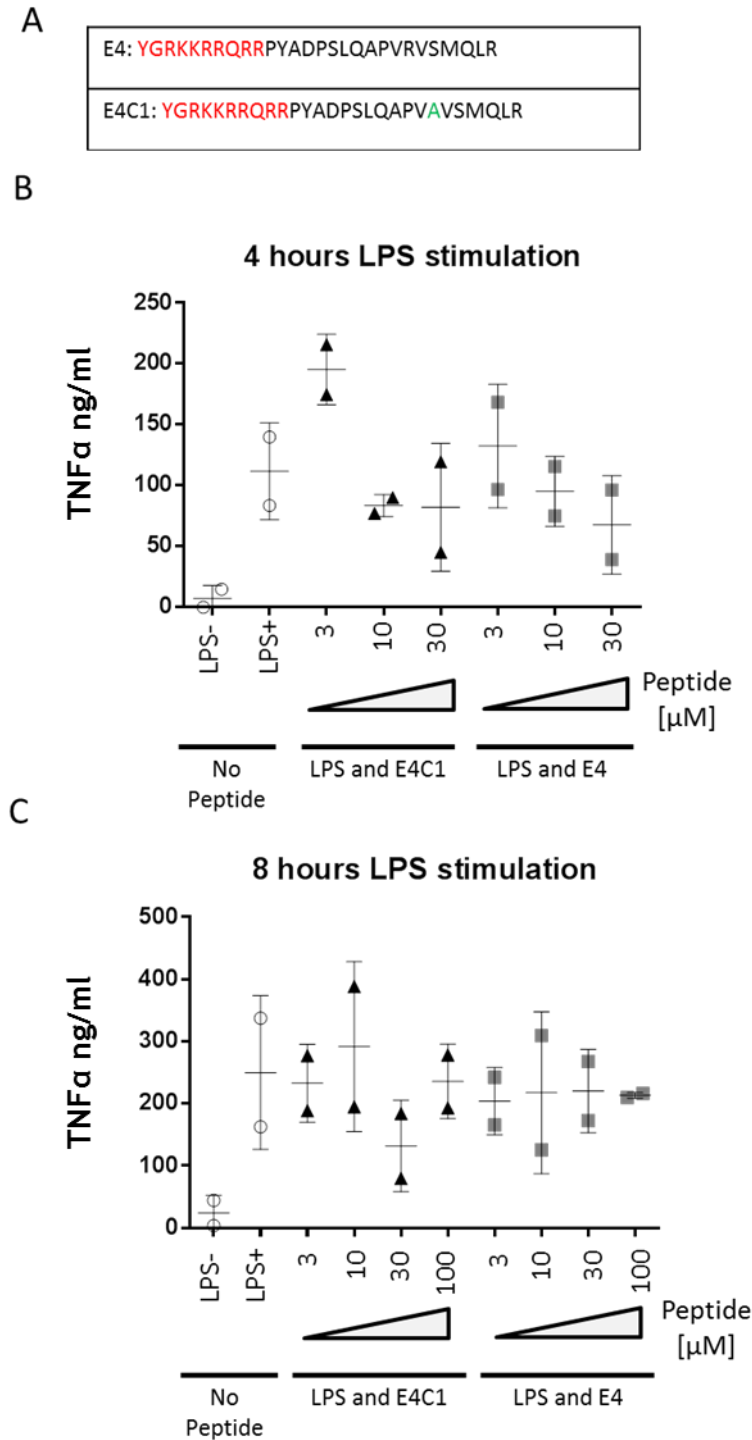


Figure 3-9 E4 p65 mimetic peptide does not inhibit LPS induced RAW 264.7 cells TNF α production. **A)** E4 and E4 negative control (E4C1) amino-acid sequences. Marked in red is the HIV-TAT cargo protein sequence fused to the mimetic peptides. Labeled in green, the amino-acids mutated in order to create the negative control. **B)** RAW 264.7 cells were left untreated or pre-treated for 2h with increasing concentrations (3 μ M-30 μ M) of either E4 or E4C1 peptide before stimulation with 100ng/ml of LPS. Supernatants were harvested 4h after stimulation and the concentration of TNF α was determined by ELISA. Data shown are the medians of the technical triplicates from different independent experiments with the corresponding standard deviation. **C)** RAW 264.7 cells were left untreated or pre-treated for 2h with increasing concentrations (3 μ M-100 μ M) of either E4 or E4C1 peptide before stimulation with 100ng/ml of LPS. Supernatants were harvested 8h after stimulation and the concentration of TNF α was determined by ELISA. Data shown are the medians of the technical triplicates from different independent experiments with the corresponding standard deviation.

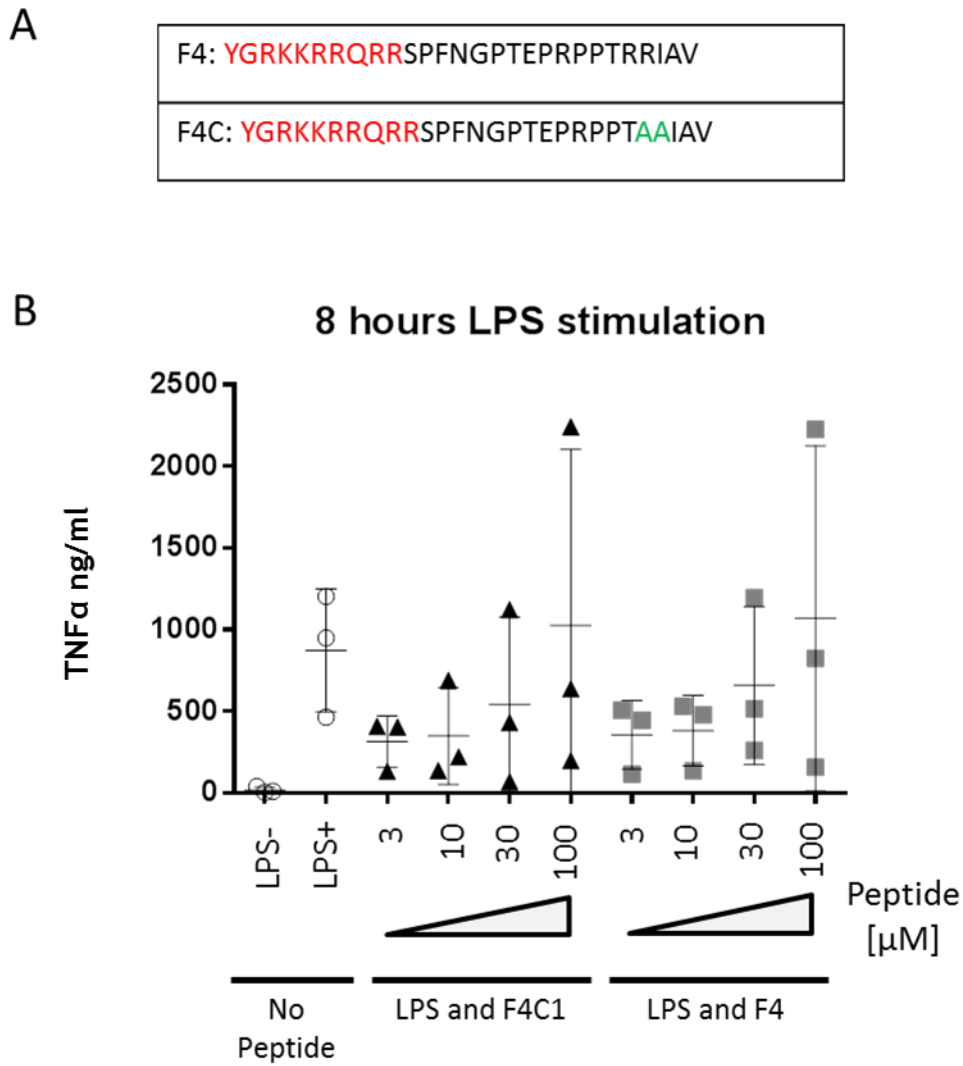


Figure 3-10 F4 p65 mimetic peptide has no effect on BMDM TNF α production upon LPS stimulation. **A)** F4 and F4 negative control (F4C) amino-acid sequences. Marked in red is the HIV-TAT cargo protein sequence fused to the mimetic peptides. Labelled in green, the amino-acids mutated in order to create the negative control. **B)** Mouse BMDM were left untreated or pre-treated for 2h with increasing concentrations (3 μ M-100 μ M) of either F4 or F4C peptide before stimulation with 100ng/ml of LPS. Supernatants were harvested 4h after stimulation and the concentration of TNF α was determined by ELISA. Data shown are the medians of the technical triplicates from different independent experiments with the corresponding standard deviation.

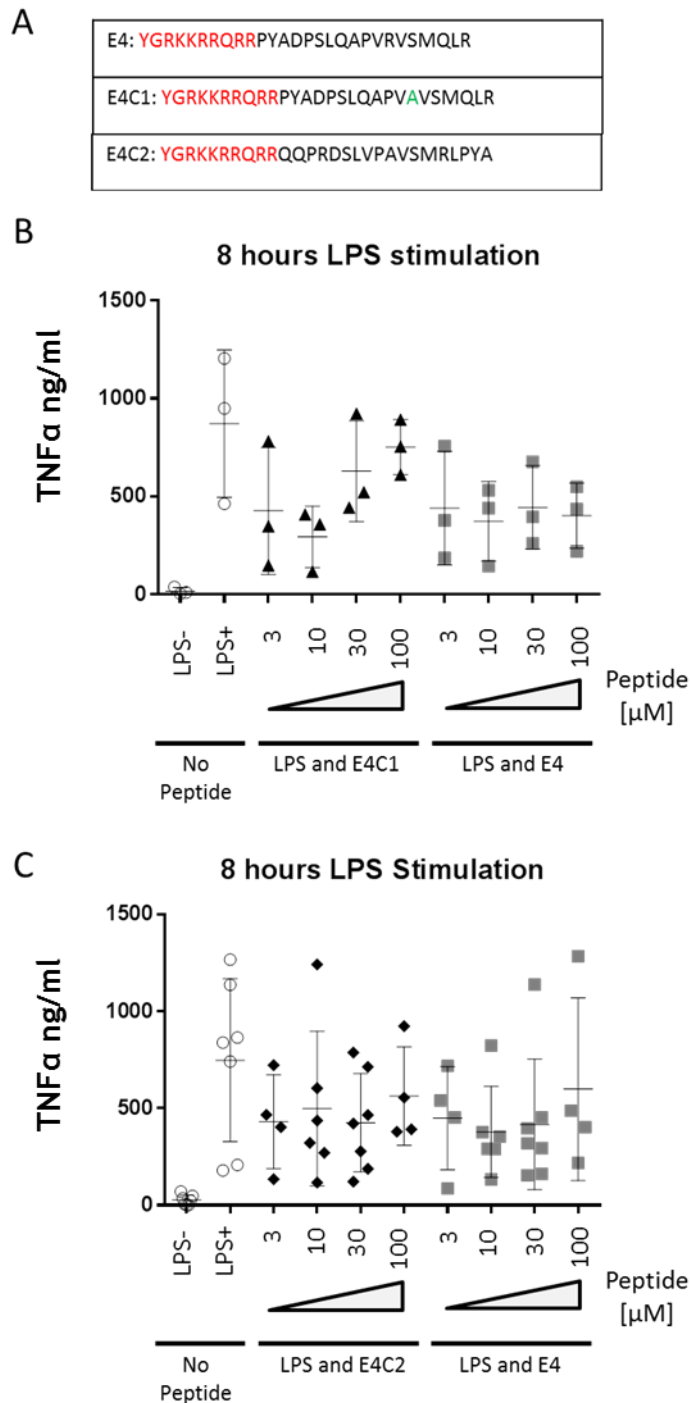


Figure 3-11 E4 p65 mimetic peptide does not inhibit BMDM TNF α production upon LPS stimulation. **A)** E4 and E4 negative control (E4C1 or E4C2) amino-acid sequences. Marked in red is the HIV-TAT cargo protein sequence fused to the mimetic peptides. Labelled in green, the amino-acids mutated in order to create the negative control. **B)** Mouse BMDMs were left untreated or pre-treated for 2h with increasing concentrations (3 μ M-100 μ M) of either E4 or E4C1 peptide before stimulation with 100ng/ml of LPS. Supernatants were harvested 4h after stimulation and the concentration of TNF α was determined by ELISA. Data shown are the medians of the technical triplicates from different independent experiments with the corresponding standard deviation. **C)** Mouse BMDM were left untreated or pre-treated for 2h with increasing concentrations (3 μ M-100 μ M) of either E4 or E4C1 peptide before stimulation with 100ng/ml of LPS. Supernatants were harvested 4h after stimulation and the concentration of TNF α was determined by ELISA. Data shown are the medians of the technical triplicates from different independent experiments with the corresponding standard deviation.

A

F4: YGRK KRRQRR SPFNGPTEPRP PTR RIAV
F4C: YGRK KRRQRR SPFNGPTEPRP PTA IAIV

B

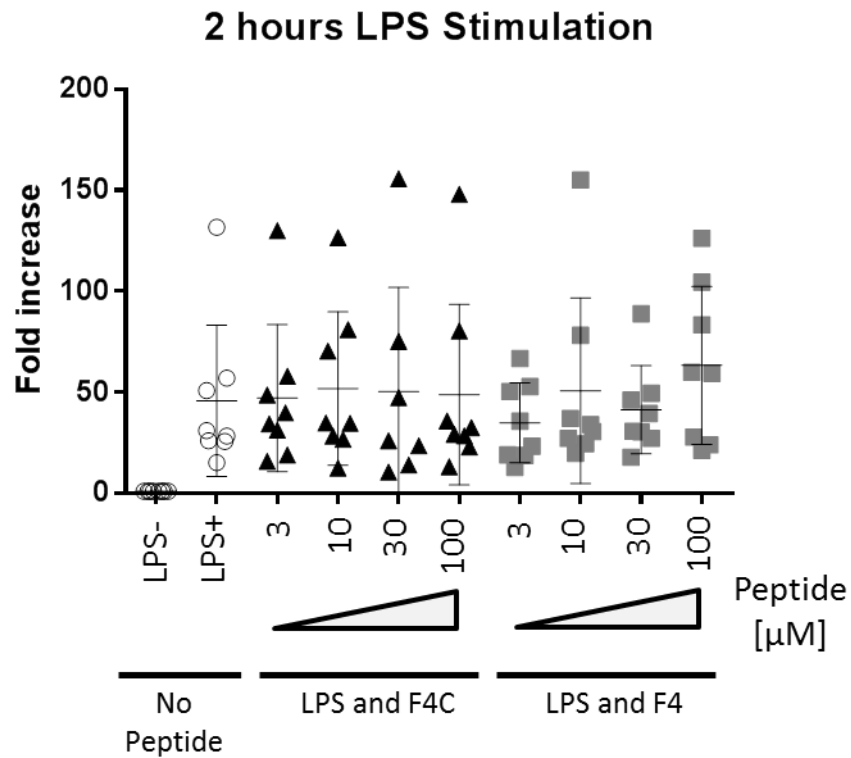


Figure 3-12 F4 p65 mimetic peptide has no effect on RAW 264.7 cells TNF α gene expression upon LPS stimulation. **A)** F4 and F4 negative control (F4C) amino-acid sequences. Marked in red is the HIV-TAT cargo protein sequence fused to the mimetic peptides. In green are shown the amino-acid mutated in order to create the negative control are shown in green. **B)** RAW 264.7 cells were left untreated or pre-treated for 2h with increasing concentrations (3 μ M-100 μ M) of either E4 or E4C1 peptide before stimulation with 100ng/ml of LPS. Cells were harvested 2h after stimulation and the TNF α gene expression was determined by qPCR. Data shown are the medians of the technical triplicates from different independent experiments with the corresponding standard deviation.

A

E4: YGRKKRRQRRPYADPSLQAPVRVSMQLR
E4C1: YGRKKRRQRRPYADPSLQAPVAVSMQLR

B

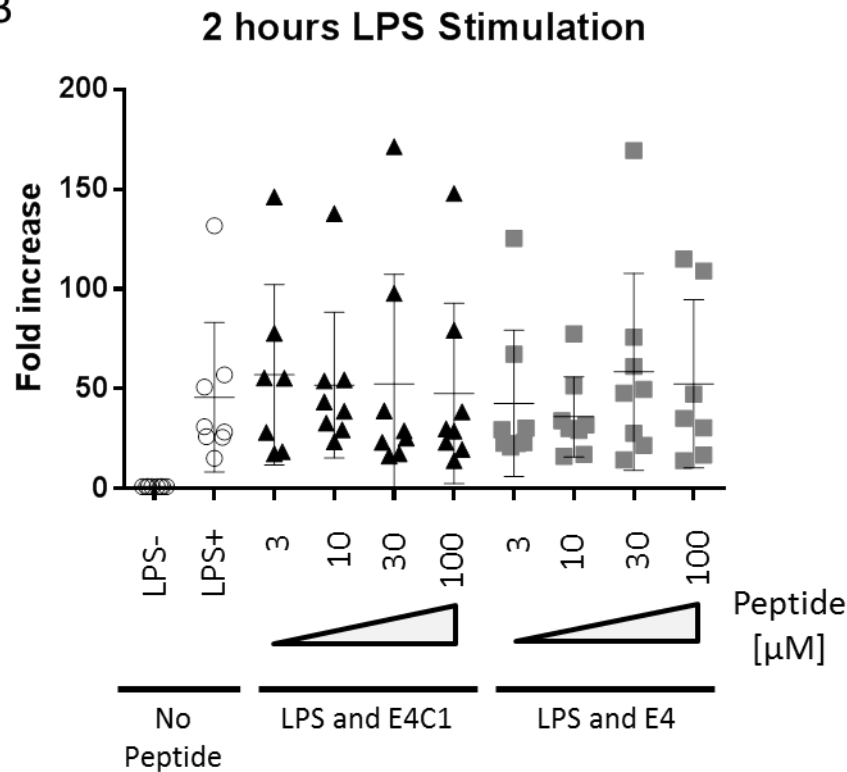


Figure 3-13 E4 p65 mimetic peptide has no effect on RAW 264.7 cells TNF α gene expression upon LPS stimulation. **A)** F4 and E4 negative control (E4C1) amino-acid sequences. Showing in red the HIV-TAT cargo protein sequence fused to the mimetic peptides. The amino-acids mutated in order to create the negative control are marked in green. **B)** RAW 264.7 cells were left untreated or pre-treated for 2h with increasing concentrations (3 μ M-100 μ M) of either E4 or E4C1 peptide before stimulation with 100ng/ml of LPS. Cells were harvested 2h after stimulation and TNF α gene expression was determined by qPCR. Data shown are the medians of the technical triplicates from different independent experiments with the corresponding standard deviation.

3.4 Discussion

The NF- κ B response is regulated by a number of PTMs of which, ubiquitination plays a key role in the nuclear regulation of the NF- κ B family members. The balance between ubiquitination and deubiquitination is crucial for the NF- κ B transcriptional response. A higher level of ubiquitination will lead to proteasomal degradation and thereby, reduced NF- κ B activity; while a higher level of deubiquitination will lead to an increase in the NF- κ B response. USP7 binds to NF- κ B at the promoters of NF- κ B target genes, regulating p65 ubiquitination and its stability at sites of transcription [287]. Thus, USP7 deubiquitinase activity is critical in determining the duration and strength of the NF- κ B transcriptional response by opposing promoter associated ubiquitination [287, 468]. Targeting USP7-NF- κ B interaction provides a novel therapeutic opportunity in the treatment of chronic inflammatory diseases. The blockade of this interaction will inhibit the expression of pro-inflammatory effectors, key mediators of inflammation [287].

The mechanism by which USP7 recognises p65 as a substrate and interacts with it is still unknown. However, previous studies have identified important sites in p65 for the interaction with USP7, such as R267 and S536 phosphorylation [287]. R267 when mutated to alanine inhibits USP7-p65 interaction and decreases USP7 deubiquitinase activity [287] and S536 when mutated to alanine decreases USP7-p65 interaction [287].

Combining the importance of phosphorylation on p65 activation and ubiquitination on the termination of the NF- κ B response, we studied the role of p65 S269 phosphorylation [68] on USP7 interaction. S269 is in close proximity to R267, thus we hypothesised the possibility of a crosstalk between phosphorylation and the UPS. The phosphorylation status of S269 was analysed by the creation of two different mutants S260D and S269A. These mutants are based on the forces generated by the presence of a negative charge when the amino-acid is phosphorylated and the absence of charge when is not phosphorylated. This is a common tool in research to study the interaction between proteins which considers the physicochemical properties of the interaction. The fact that both p65 S269 mutants do not inhibit the interaction with USP7 means that a disruption of the force field by the presence of a

negative charge in that area has no effect on the interaction with USP7. The phosphorylation itself could be important for the activation of p65, but our data show it is not important for the interaction with USP7.

Previous work identified a number of amino-acids of p65 as important for the interaction with USP7 [287]. Due to the lack of a full length elucidated 3D structure of p65, we modelled a full length p65 structure using ROBETTA software (see Figure 3-4 and Figure 3-7) to gain more detail about location of the identified amino-acids. This model revealed that peptides of p65 that interact with USP7 are localised quite close together in the 3D structure of p65. On the one hand, conformational rearrangements which molecules undergo in nature after protein-protein interactions are one of the problems when trying to solve the full length p65 protein 3D structure. Proteins in nature are flexible, in a changing conformation; and when binding to their substrates, they change into a stable state. When purifying a protein, the resulting solved structure is the result of the properties applied and the stability of the protein in such conditions. It might be probable that full length p65 protein on its own is not stable enough to be crystallised and it would require of a protein interaction to stabilise it. However, even if the protein is stable enough to be solved; it is possible that in nature the protein is found in a different conformation able to recognised different parts of p65. For these reasons, structural models are a useful tool. Our p65 full length model is the first model covering the full length of p65 protein. The flexibility of the TAD domain makes it a very difficult target to model. Peptide E4 is present in the actual crystal structure PDB 1VKX, but that structure is missing the TAD of p65. The TAD of p65 is a really flexible part of p65, which is probably formed by a flexible loop. This loop could actually hide E4 peptide in nature. Whereas F4 is present on a flexible loop, models of this part vary quite a lot. From the ROBETTA model, the F4 peptide is accessible to be recognised by USP7 but it could be possible that another 3D structure is formed in nature.

We hypothesised that a mimetic peptide containing R267 or a mimetic peptide containing R328 and R329 will compete with endogenous p65 in USP7 interaction; and therefore decrease the NF- κ B inflammatory response via the inhibition of USP7 deubiquitination of p65. Both peptides were attached to the

cargo carrying peptide sequence of TAT protein. The effect of the peptides on the NF- κ B response was studied at target gene expression level by qPCR and pro-inflammatory cytokines production level by ELISA. In both cases, the results were negative; the designed p65 mimetic peptides did not have any effect on the NF- κ B response. There were no significant differences on gene expression or cytokine production, when comparing peptide treatment to untreated cells. This absence of significant differences in TNF α expression and production could be because the mutated amino-acids on p65 sequence are important and contribute to the interaction but are not enough to disrupt the interaction with USP7. In protein-protein interactions electrostatic intermolecular interactions are the strongest bond between proteins. When molecules are small, disruption of a few electrostatic interactions might be enough to abolish the interaction, but within two proteins we also encounter van der Waal forces. Van der Waal forces are the weakest interaction between two proteins, but are the most common attractive forces between two proteins. The force field created by the Van der Waal forces could be stronger than the electrostatic interaction and even disrupting the electrostatic interaction might not be sufficient to disrupt the Van der Waal force field. The mimetic peptide might be binding to USP7 but not inhibiting the interacting site with p65, which would explain why USP7 is still able to create an adequate attractive force field and bind to p65 even in the presence of the mimetic peptide. For this reason we suggest that the targeted area is important for the interaction but it is not sufficient to disrupt the interaction. Taking all these into account, further investigation on the molecular determinants involved in the interaction is needed to be able to create a p65 mimetic peptide able to inhibit specifically USP7's activity on p65 subunit of NF- κ B.

Chapter Four

Investigation of the molecular determinants involved in p65 recognition by USP7

4 Investigation of the molecular determinants involved in p65 recognition by USP7

4.1 Abstract

The NF- κ B transcription factor family is a key regulator of inflammation and orchestrates the transcriptional response to infection by directing the transcription of genes involved in these processes. Ubiquitination, and subsequent proteasomal degradation, of NF- κ B subunits is a critical factor in the termination of NF- κ B mediated responses. However, ubiquitin chains can be removed by DUBs. USP7 is a crucial DUB for NF- κ B subunits deubiquitination. USP7 is known to deubiquitinate the p65 subunit of NF- κ B; however, the molecular determinants of p65 recognition as a USP7 substrate are currently unknown. The blockade of this interaction inhibits the expression of pro-inflammatory effectors. USP7 is involved in several biological processes, such as cell cycle, apoptosis, stress response, DNA repair, cell survival, tumourigenesis, epigenetic regulation and viral infection due to its interaction with substrates involved in those processes. For this reason, targeting the catalytic deubiquitinase activity of USP7 leads to a variety of effects in many different biological processes. Therefore, we need to study the molecular determinants involved in USP7-p65 interaction in order to target p65 specifically. To understand the binding interface of USP7-p65 interaction, we performed a peptide array and subsequent alanine scanning array to identify the amino-acids of USP7 required for p65 recognition. Amino-acids within the C-terminal UBL12345 of USP7 were identified, the majority of the amino-acids being localised in a non-conserved loop of UBL3. Most of the amino-acids identified were charged, which is crucial in the generation of electrostatics interactions between proteins. Further investigation on the specific contribution of each UBL domain is required to identify the interaction binding pocket.

4.2 Introduction

USP7 has been identified as an NF- κ B deubiquitinase, critical for NF- κ B transcriptional activity [287]. Inhibition of USP7 deubiquitinase activity inhibits the NF- κ B response and it also affects several different biological processes. USP7 acts in various biological processes; such as apoptosis, DNA damage repair, cell cycle, transcription regulation, neuronal development, tumourigenesis, viral infection, epigenetic regulation and stress response [300, 418, 422, 433]; through the stabilisation or cellular localisation of proteins involved in those processes, for example, DNMT1, p53, caspase [300, 422, 433] and ICP0 [300, 422]. Knowledge of the specific binding site with each target would enable strategies to target specific substrates of USP7.

USP7 contains an N-terminal MATH/TRAF domain involved in substrate recognition [408, 411]; a C-terminal domain containing five UBLs [300, 418, 422] essential for an effective catalytic activity [408]; and a conserved CD [406, 408, 411]. p65 is known to be recognised by the C-terminal region of USP7 [287]. Nevertheless, the molecular determinants involved in USP7-p65 interaction are still unknown. Peptide arrays are a useful tool to study protein-protein interactions [469, 470]. The peptide array method consists in the synthesis of a library of overlapping peptides covering the whole target sequence. The most common procedure to prepare the peptide library on a solid support is the SPOT-synthesis technique. The SPOT-synthesis method is a rapid and inexpensive way of simultaneous chemical synthesis of large numbers of predefined peptides on a variety of solid supports [470-473]. SPOT-synthesis of peptide libraries for peptide arrays is commonly used to map protein-protein interactions [469, 471, 474]. Other uses of peptide arrays are extensively described in *Applications of peptide arrays prepared by the SPOT-technology* [471].

Peptide arrays when used for protein-protein interaction mapping are incubated with the binding protein (cell extract or recombinant protein) and detected through different techniques. Typically a primary antibody against the binding protein or the recombinant tag and a secondary antibody coupled to HRP are used [287, 475].

Based on the knowledge that USP7 C-terminal region is essential for the recognition of p65 as a substrate, we performed a USP7 C-terminal region peptide array. Interacting peptides were selected for subsequent alanine scanning array to determine the important amino-acids involved in the interaction. Those amino-acids are located within the 5 UBLs but a great number of them are located in a loop on UBL3 not conserved in the other UBLs. Amino-acids identified in UBL1 correspond to positively charged amino-acids, while amino-acids identified in UBL2 are located in a negatively charged patch. However, amino-acids identified within UBL3, 4 and 5 (UBL345) are not in an overall negative or positive patch. Charged amino-acids form electrostatic interactions between proteins and are potential targets for drug discovery strategies.

4.3 Results

4.3.1 GST-p65 protein purification

A recombinant GST-p65 protein was purified in order to perform a peptide array analysis. Recombinant GST-p65 plasmid was synthesised by GenScript. The murine p65 protein sequence was cloned into pET42a(+) expression vector. pET42a(+) vector allows inducible expression of GST fusion proteins in *E.coli*. Expression of GST-p65 protein requires the addition of IPTG to induce the activation of the promoter controlling the protein expression. *E.coli* BL21 DE3 cells were transformed with pET42a(+)-GST-p65. The recombinant protein was induced with an optimised concentration of 0.5mM IPTG for 3 hours at 37°C. GST-p65 protein was subsequently purified through a GSTrap HP column (GE Healthcare, Bioscience AB). See Figure 4-1.

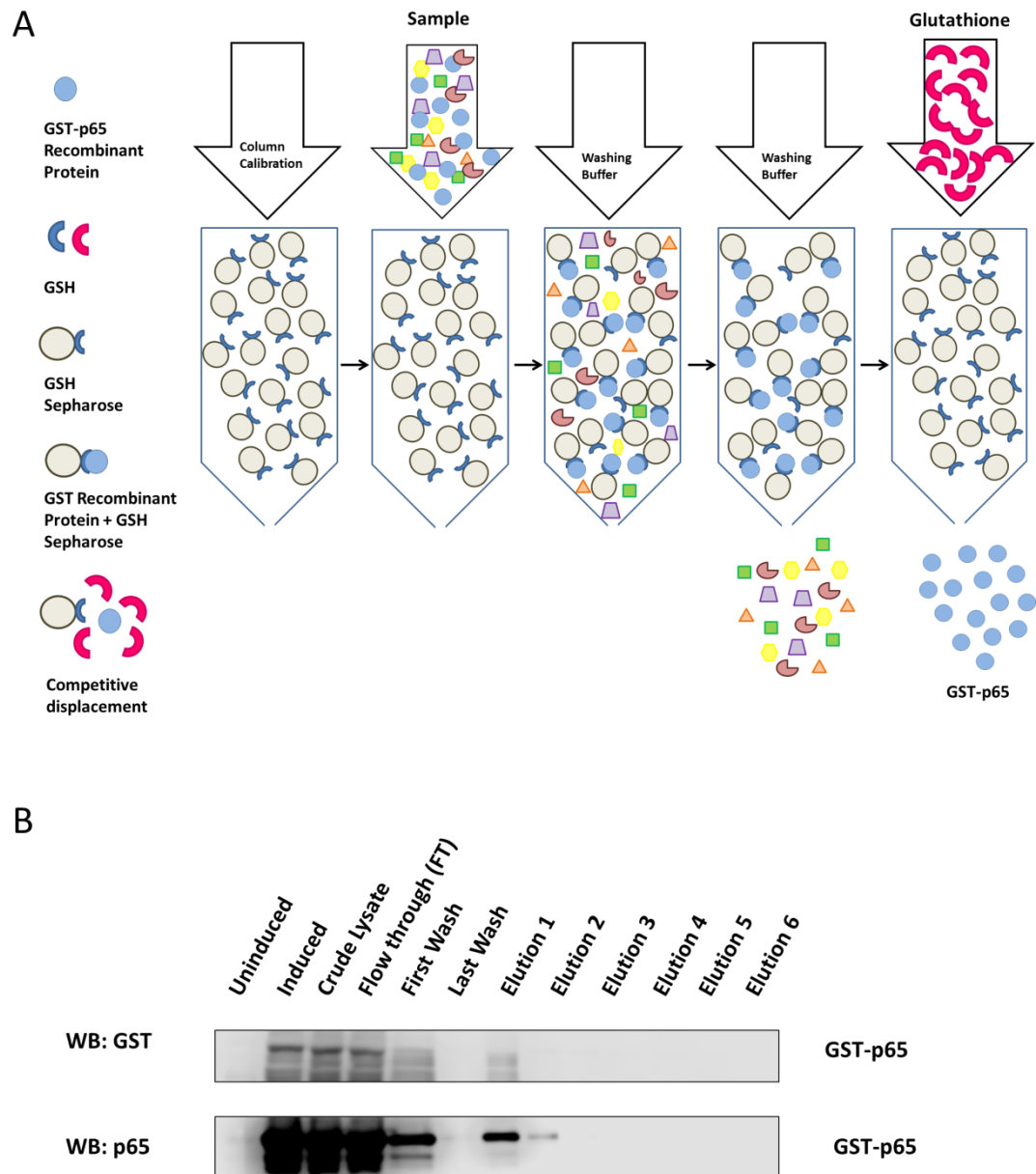


Figure 4-1 GST-p65 recombinant protein purification. **A)** GST-p65 recombinant protein purification process through the GSTrap HP column schematic. Firstly, the GSTrap HP column is calibrated by the addition of binding buffer. Subsequently the sample goes through the column, and the GST-p65 binds to the GSH sepharose beads. Addition of the washing buffer clears the column just maintaining the GST-p65 protein bound to the GSH sepharose beads. Lastly, addition of glutathione to the column competes for the GST-p65 protein binding and elutes it from the column. **B)** *E. coli* BL21 DE3 were transformed with pET42a(+) GST-p65 plasmid. GST-p65 protein expression was induced with the addition of 0.5mM IPTG. The induced recombinant protein was affinity purified with a GSTrap HP column. Samples of each step of the process were analysed by western blotting for GST and p65.

4.3.2 p65 protein is recognised by the C-terminal region of USP7

Previous studies discovered USP7 as a deubiquitinase enzyme of p65 [287]. p65 protein is recognised as a substrate of USP7 by its HUBL [287]. In order to confirm these findings a immunoprecipitation assay in HEK293T cells transfected with USP7 WT, a USP7 mutant lacking the MATH/TRAF domain (USP7 Δ MATH) and

a USP7 mutant with the C-terminal HUBL deleted (USP7 Δ HUBL) FLAG-tagged plasmids along with p65-HA was performed. Following cellular lysis, USP7 was immunoprecipitated with anti-FLAG antibody. Immunoprecipitated proteins were immunoblotted with anti-p65 and anti-FLAG antibodies. This analysis confirmed that deletion of the C-terminal region of USP7 is sufficient to inhibit p65 interaction, while deletion of the MATH/TRAF domain has no effect on the interaction. See Figure 4-2.

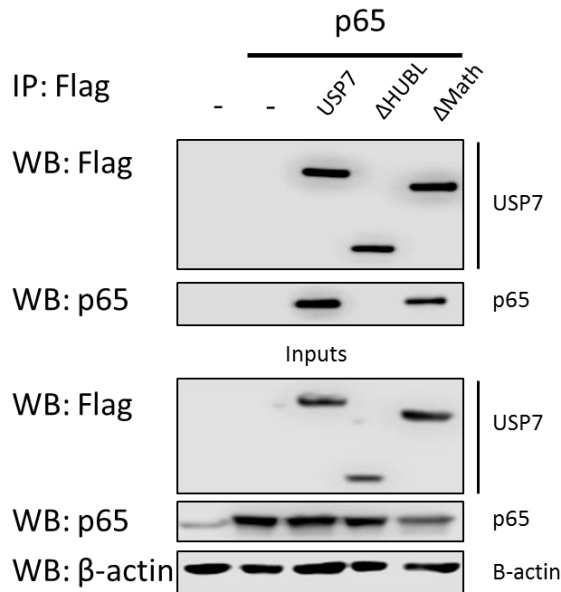


Figure 4-2 p65 is recognised by the C-terminal region of USP7. HEK293T cells were transfected with USP7, USP7 Δ MATH and USP7 Δ HUBL FLAG-tagged plasmids along with p65-HA. Cell lysates were immunoprecipitated with an anti-FLAG antibody and immunoblotted with anti-FLAG and anti-p65 antibodies. Deletion of the C-terminal region of USP7 is sufficient to inhibit the interaction with p65, while deletion of the N-terminal MATH/TRAF domain has no effect on p65 recognition. The figure is a representative of three independent experiments.

4.3.3 p65 binds to distinct peptides on a USP7 C-terminal region peptide array

C-terminal region of USP7 is essential for the interaction with p65 [287]. This C-terminal region of USP7 is formed by 5 UBLs. In order to experimentally identify the molecular determinants of USP7 mediating the interaction with p65, an immobilised peptide array based technique was performed. The peptide array consisted on a library of overlapping (4 amino-acids overlap) peptides of 18 amino-acids in length covering amino-acids 541-1101 of the C-terminal region of USP7 (see appendix 8.3). USP7 overlapping peptides were SPOT-synthesised on nitrocellulose membranes (see Figure 4-3 and Table 4-1). USP7 peptide arrays

were then probed with either GST (previously purified by Dr. Patricia Collins) or GST-p65 proteins. Bound protein was detected by immunoblotting with anti-GST antibody (see Figure 4-3).

GST-p65 protein specifically binds to a number of USP7 peptides suggesting that p65 likely makes contacts throughout the C-terminal region of USP7, not just specifically in one of the UBLs (see Table 4-2). The majority of the peptides identified were located within UBL3 and 4 (UBL34), with peptides identified in UBL3 more positively charged due to the presence of K and R amino-acids, and peptides identified in UBL4 more negatively charged due to the presence of D and E amino-acids. These domains may interact extensively with p65 protein. On the other hand, peptides identified on UBL 1, 2 and 5 (UBL125) are not as numerous but contain charged amino-acids within their sequences. Electrostatic interactions are the basis of protein-protein interactions. From this data it appears that UBL34 form more contacts with p65 than the rest of the UBLs; but interactions formed within UBL125 may be due to electrostatic forces which have an important role in the interaction. Electrostatics interactions within any of the UBLs and the substrate proteins may be important in the interaction. It is important to take into account that a greater number of identified peptides does not mean that those identified amino-acids are more important than amino-acids identified on any of the other UBLs. Based on the presence of negatively or positively charged amino-acids in those binding peptides, various peptides were selected for subsequent alanine scan analysis.

Table 4-1 Peptide location within the C-terminal region of USP7

Peptides	Amino-acids	USP7 region
A1-A2	541-562	N-terminal
A3-A6	549-578	N-terminal-Ubl1
A7-A27	565-662	Ubl1
A28-B1	649-678	Ubl1-linker
B2	665-682	Linker
B3-B6	669-698	Linker-Ubl2
B7-B24	685-770	Ubl2
B25-B28	757-786	Ubl2-linker

Peptides	Amino-acids	USP7 region
B29	773-790	Linker
B30-C3	777-806	Linker-Ubl3
C4-C21	793-878	Ubl3
C22-C24	865-890	Ubl3-linker
C25	877-894	Ubl3-linker-Ubl4
C26-C29	881-910	Linker-Ubl4
C30-D9+F1-F6	897-972	Ubl4
F7+D14-D15	959-984	Ubl4-linker
D16	971-988	Ubl4-linker-Ubl5
D17-D19	975-1000	Linker-Ubl5
D20-E9	987-1080	Ubl5
E10-E13	1067-1096	Ubl5-C-terminal
E14-E15	1083-1101	C-terminal

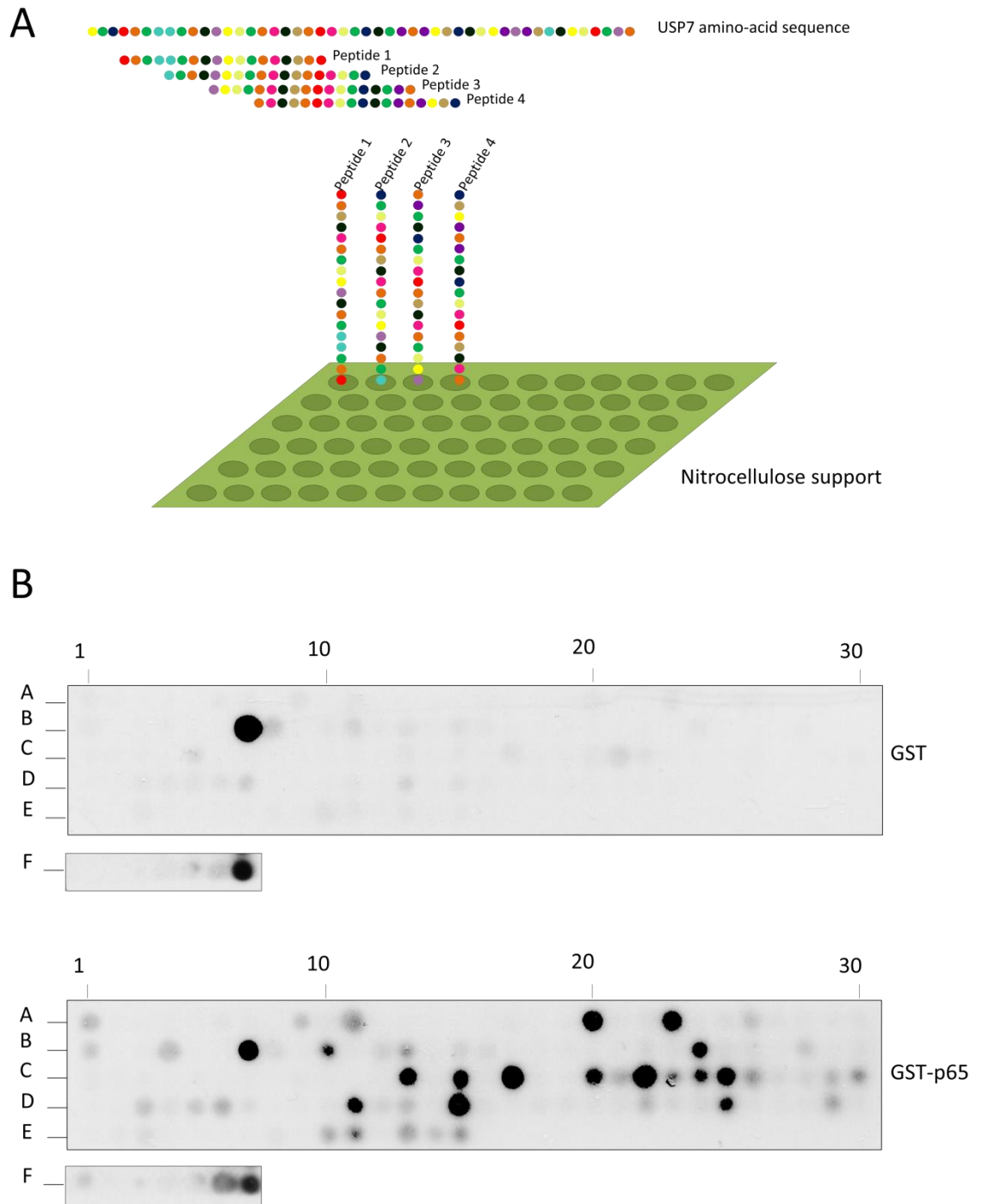


Figure 4-3 Identification of p65 interacting regions on USP7 using peptide arrays. A) Peptide array of immobilised 18-mer peptides overlapping by 4 amino-acids schematic. **B)** Peptide arrays of immobilised overlapping 18-mer peptides, each shifted to the right by 4 amino-acids encompassing the full C-terminal region of USP7 were generated. Arrays were probed with GST or GST-p65 and immunoblotted with anti-GST antibody. Each dot represents binding of the protein to the peptide arrays. Each peptide array is labelled by a letter followed by a number. Sequences of the peptides are shown on section 8.3.

Table 4-2 Peptide arrays identified within USP7 UBLs

USP7 UBL Domain	Identified peptide array
UBL1	A20
	A23
UBL2	B7
	B10
	B24
UBL3	C13
	C15
	C17
	C20
	C23
	C24
	C25
UBL4	C25
	D11
	D15
	F6
	F7
UBL5	D25
	E11

4.3.4 Alanine substitution arrays identify interacting residues on USP7

In order to identify individual amino-acids essential for p65 binding within the regions of USP7 identified by the peptide array, a series of alanine-scanning arrays were generated. Alanine scanning arrays were derived from the 18-mer nucleotides parent peptide by subsequent single alanine substitutions (see appendix 8.4); in other words, each amino-acid was sequentially mutated to an alanine, whereas alanine residues were not mutated to a different amino-acid. Protein interactions are more likely to happen through electrostatic interactions between opposite charges. Thus, peptides were selected based on the peptide array results and on their amino-acidic composition. Peptides containing a high

charged amino-acid content were selected for subsequent alanine scan (see Table 4-3). The alanine scanning array was incubated with GST-p65 and immunoblotted with anti-GST antibody. GST-p65 bound to the alanine scanning arrays was detected by HRP-conjugated antibody. For each alanine substitution, the binding of GST-p65 was calculated in comparison to the binding of the parent peptide. Substitutions with less than a 60% binding of the parent peptide were considered as important amino-acids for p65 recognition as a substrate (see Table 4-4). These data indicated a number of key amino-acids within all five UBLs, but mostly located on UBL3 (see Figure 4-4). Most of the amino-acids identified as important within all UBLs are K, R, D or E. Taking this into account, contribution of each UBL to the interaction must be studied; a greater number of contacts within a UBL does not mean that UBL drives the interaction, it may be important but not essential for the interaction.

Table 4-3 Peptide arrays selected for alanine scanning

Peptide	Sequence
A23	SNGTKRPAMLDNEADGNK
B24	LDKALDELMDGDIIVFQK
C13	RLNTDPMLLQFFKSQGYR
C15	LQFFKSQGYRDGPGNPLR
C17	YRDGPGNPLRHNYEGTLR
C20	YEGTLRDLLQFFKPRQPK
C25	YYQQLKMKITDFENRRSF
C30	IWLNSQFREEEITLYPDK
D25	FLLRIHQGEHFREVMKRI
E10	PGNMSHPRPWGLDHFNK
E15	APKRSRYTYLEKAIKIH

Table 4-4 Amino-acids identified by the alanine scanning peptide array

Amino-acid	Position	Domain	Peptide
K	633	UBL1	A23
R	634	UBL1	A23
K	646	UBL1	A23
L	757	UBL2	B24
D	758	UBL2	B24
E	759	UBL2	B24
L	760	UBL2	B24
D	833	UBL3	C13
M	835	UBL3	C13
F	839	UBL3	C13
G	844	UBL3	C15
Y	845	UBL3	C13
R	646	UBL3	C15/C17
D	847	UBL3	C15/C17
G	848	UBL3	C17
P	849	UBL3	C15
G	850	UBL3	C15/C17
N	851	UBL3	C15/C17
L	853	UBL3	C15/C17
R	854	UBL3	C15/C17
N	855	UBL3	C17
Y	856	UBL3	C17
E	857	UBL3	C17
G	858	UBL3	C17
T	859	UBL3	C17
L	860	UBL3	C17
R	861	UBL3	C17
Q	872	UBL3	C20
D	887	Linker	C25
F	888	Linker	C25
L	899	UBL4	C30

Amino-acid	Position	Domain	Peptide
F	903	UBL4	C30
E	905	UBL4	C30
K	914	UBL4	C30
E	1019	UBL5	D25
R	1023	UBL5	D25
I	1024	UBL5	D25
R	1074	UBL5	E10
P	1075	UBL5	E10
W	1076	UBL5	E10
L	1079	UBL5	E10
D	1080	UBL5	E10
H	1081	C-terminal	E10
F	1082	C-terminal	E10
K	1084	C-terminal	E10
N	1102	C-terminal	E15

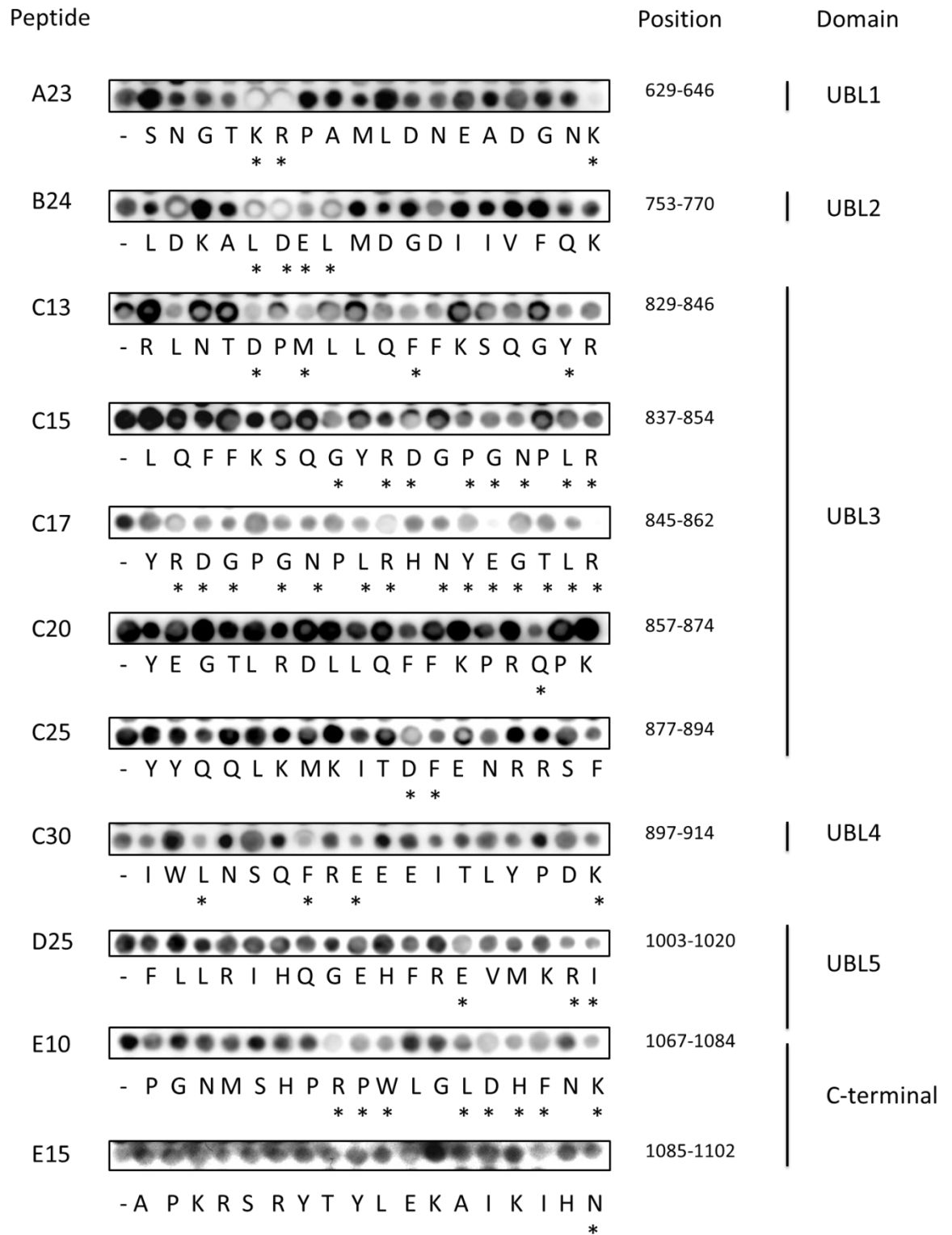


Figure 4-4 Important amino-acids of USP7 involved in p65 binding. Selected 18 amino-acids length peptides from USP7 sequentially substituted with alanine, probed with GST-p65 and immunoblotted with anti-GST antibody. Binding of GST-p65 protein to each substituted alanine peptides was compared to the binding of the parent peptide. Each peptide is labelled on the left of the image, their sequences are marked under the peptide array. The first peptide in each array corresponds to the parent peptide. Amino-acids included in the array and their location within the C-terminal region is indicated in the right side of the image. Amino-acid substitutions leading to a 40% reduction compared to parent peptides are marked with an asterisk.

4.3.5 Localisation of the p65 interacting amino-acids within the USP7 sequence and structure

The C-terminal region of USP7 is formed by five UBLs which share the ubiquitin β -grasp fold [299, 408, 418]. Despite sharing the ubiquitin fold, they are not more similar to each other than to UBL domains from different proteins [408, 418]. The 5 UBLs are very divergent in sequence [408, 418]. Here, we localised the important amino-acids identified by the peptide array and subsequent alanine scan in USP7 sequence and structure of USP7 C-terminal region (see Figure 4-5 and Figure 4-6). Most of the identified amino-acids are located on UBL3, specifically in a loop not conserved among the UBLs. Moreover, most of the identified amino-acids correspond to charged amino-acids (K, R, D, E), which are more likely to be important for protein-protein interactions through the formation of electrostatic interactions. Some of the amino-acids identified are located in an internal area of the protein, which is not able to interact with other proteins. Amino-acids identified on UBL1 are positively charged, creating a positive patch which might interact with a negative patch on p65. Whereas, amino-acids identified on UBL2 are in a negative patch and might be identified by a positive charged motif on p65. These amino-acids are also located on a groove which is suitable to form a binding pocket for protein recognition. In the case of UBL345, positive and negatively charged amino-acids are recognised in the same way, so their charges may be neutralised, not forming a positive or negative patch (see Figure 4-6). Besides amino-acids on UBL3 which are located in a non-conserved loop and amino-acids on UBL2 which are located on a possible binding pocket groove; amino-acids on UBL1, 4 and 5 (UBL145) are not located on a specific structural position which would indicate substrate recognition and binding. Contribution of each domain to the interaction is still unknown.

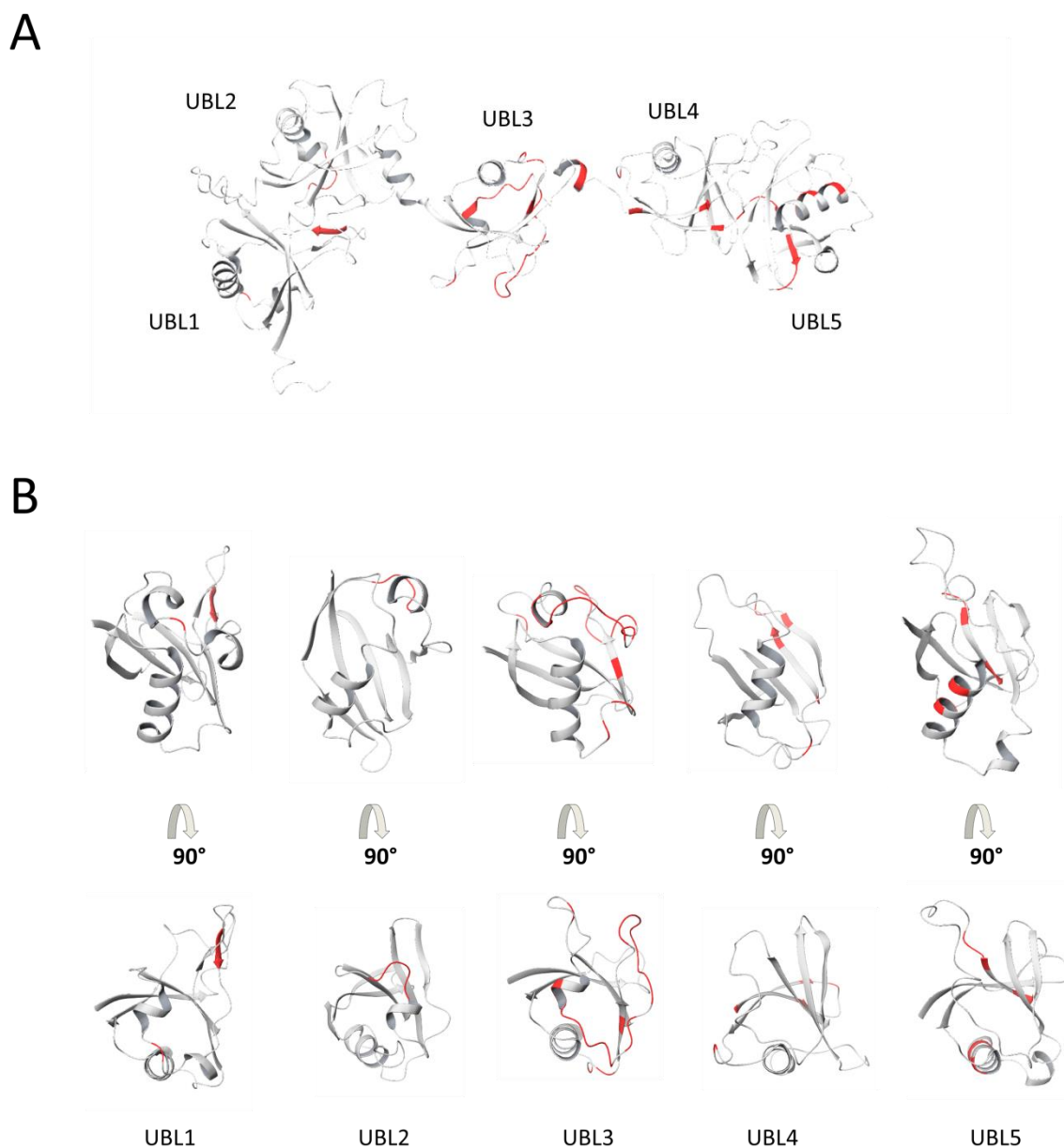


Figure 4-6 Structural localisation of USP7 amino-acids identified by the peptide array and subsequent alanine scan. A) 3D structure of the C-terminal region of USP7 in white with the identified amino-acids in red (PDB: 2YLM). **B)** UBL domains 3D structure from the front of the domain and from the top. UBLs are coloured in white and identified amino-acids in red.

4.3.6 Suitability of the recombinant GST-p65 protein for functional GST-pull down assays

GST-pull down assays can be used to detect protein complexes formation. We performed this technique in order to subsequently evaluate the effect of inhibitory peptides on USP7-p65 complex formation. GST or GST-p65 recombinant proteins were incubated with a whole HEK293T cell lysate overexpressing FLAG-tagged USP7 and affinity purified with GSH agarose. USP7 did not co-purify with either GST-p65 recombinant protein laboratory purified or

commercial one (see Figure 4-7). GST-p65 laboratory purified protein is a full length p65 murine protein, while commercial GST-p65 is a truncated version of p65 human protein, containing amino-acids 12-317. GST-p65 purified protein is very unstable and 2 hours at 4°C was sufficient for degradation of p65 protein (see Figure 4-7). On the other hand, commercial GST-p65 is a truncated version of p65 human protein. It might be possible that amino-acids interacting with USP7 are missing on the truncated version of the protein. Both experiments were carried out at the same time as a positive technical control with a GST-p50 protein and an overexpressed Bcl-3 FLAG-tagged protein. GST-p50 is known to be able to pull down overexpressed Bcl-3 [466]. GST protein and GST-p50 recombinant protein were previously purified by Dr Patricia Collins. See Figure 4-7. To test the commercial GST-p65 truncated protein we added another control. p65 protein dimerises with p50 protein through the C-terminal region of their RHD domains which is contained in the truncated version of the GST-p65 commercial protein. Thus, we overexpressed p50 FLAG-tagged protein in order to analyse the ability of GST-p65 truncated protein to bind to overexpressed p50 protein. However, GST-p65 truncated protein is not able to interact with p50. These data indicate that recombinant p65 is not suitable for pulldown experiments to investigate interaction with USP7.

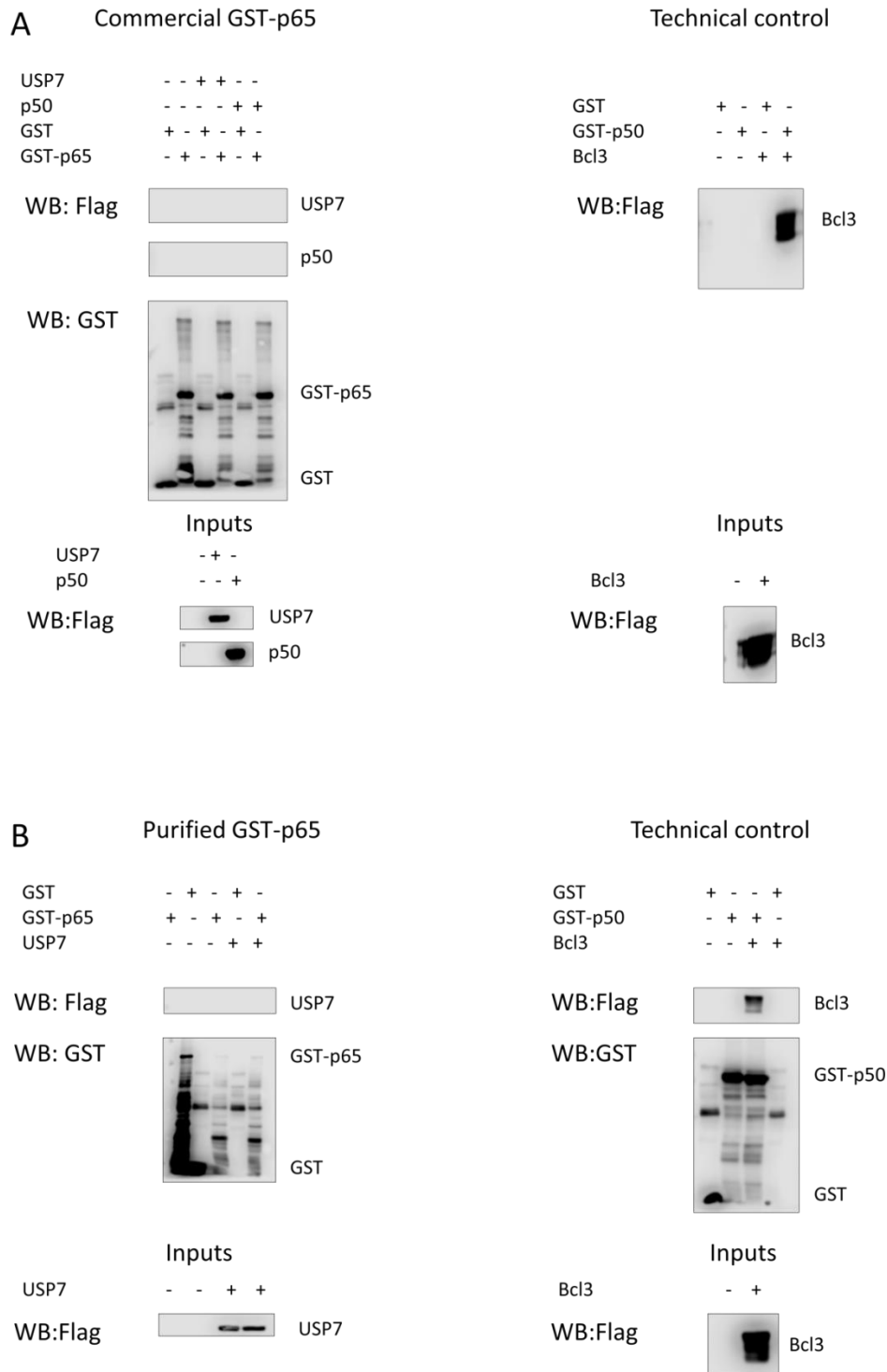


Figure 4-7 Functional GST-pulldown assay of the recombinant GST-p65 protein. A) GST or GST-p65 recombinant proteins were incubated with a whole HEK293T cell lysate overexpressing FLAG-tagged USP7 and FLAG-tagged p50 and affinity purified with GSH agarose. Commercial GST-p65 is not able to bind USP7 or p50 protein. GST or GST-p50 recombinant proteins were incubated with a whole HEK293T cell lysate overexpressing FLAG-tagged Bcl3 and affinity purified with GSH agarose as a technical control. The technical control shows interaction between GST-p50 and Bcl3. **B)** GST or GST-p65 recombinant proteins were incubated with a whole HEK293T cell lysate overexpressing FLAG-tagged USP7 and affinity purified with GSH agarose. Purified GST-p65 is not able to bind USP7. By the end of the experiment the recombinant protein is degraded. GST or GST-p50 recombinant proteins were incubated with a whole HEK293T cell lysate overexpressing FLAG-tagged Bcl3 and affinity purified with GSH agarose as a technical control. The technical control performed with a GST-p50 and Bcl3 FLAG-tagged protein shows interaction between GST-p50 and Bcl3.

4.3.7 Testing the effects of USP7 mimetic peptides on USP7-p65 interaction

As most of the identified amino-acids are located in a non-conserved loop on UBL3 (amino-acids 844-860), we decided to design USP7 mimetic peptides to determine if these mimetic peptides could disrupt the interaction with p65. Three USP7 mimetic peptides were designed based on the USP7 sequence of UBL3, which were designated as Upep1, Upep2 and Upep3. Upep1 covers amino-acids 844-854, Upep2 amino-acids 853-860, and Upep3 encompasses both of them (see Figure 4-8 and Table 4-5).

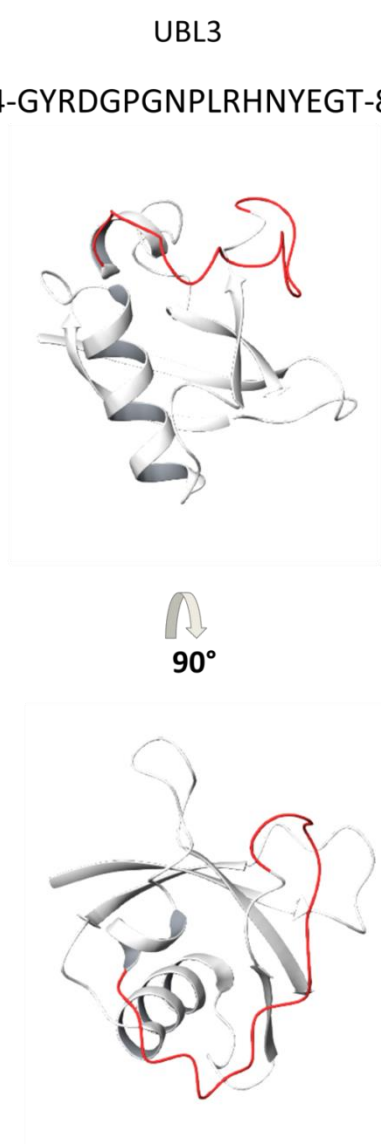


Figure 4-8 UBL3 non-conserved loop. Sequence of the UBL3 non-conserved loop and structural location on USP7 UBL3 3D structure (PDB: 2YLM).

Table 4-5 USP7 mimetic peptides sequences.

Peptide	Sequence	Amino-acids location
Upep1	GYRDGPGNPLR	844-854
Upep2	LRHNYEGT	853-860
Upep3	RDGPGNPLRHNYEGT	846-860

Since GST pulldown is not suitable to assess the interaction between USP7 and p65, we decided to perform a immunoprecipitation assay with the addition of the USP7 mimetic peptides. In order to study the ability of USP7 mimetic peptides to disrupt an already bound USP7-p65 complex, we co-transfected HEK293T cells with USP7-FLAG and p65-HA proteins. Lysates were immunoprecipitated with an anti-FLAG antibody in the presence of individual peptides (100 μ M) overnight at 4°C. Proteins were detected by western blotting and immunoblotted with anti-FLAG and anti-p65 antibodies. None of the peptides was able to disrupt the USP7-p65 complex (see Figure 4-9). To investigate the ability of the peptides to prevent USP7-p65 interaction, we transfected HEK293T cells with p65-HA plasmid and different HEK293T cells with USP7-FLAG. Cellular p65 lysates were combined with cellular USP7 lysates and immunoprecipitated with an anti-FLAG antibody in the presence of individual USP7 peptides (100 μ M) overnight at 4°C. However, USP7 and p65 when transfected separately and mixed are not able to form an interacting complex (see Figure 4-9). These data demonstrated that mutational approaches would be required to identify the role of UBL3 domain in the interaction.

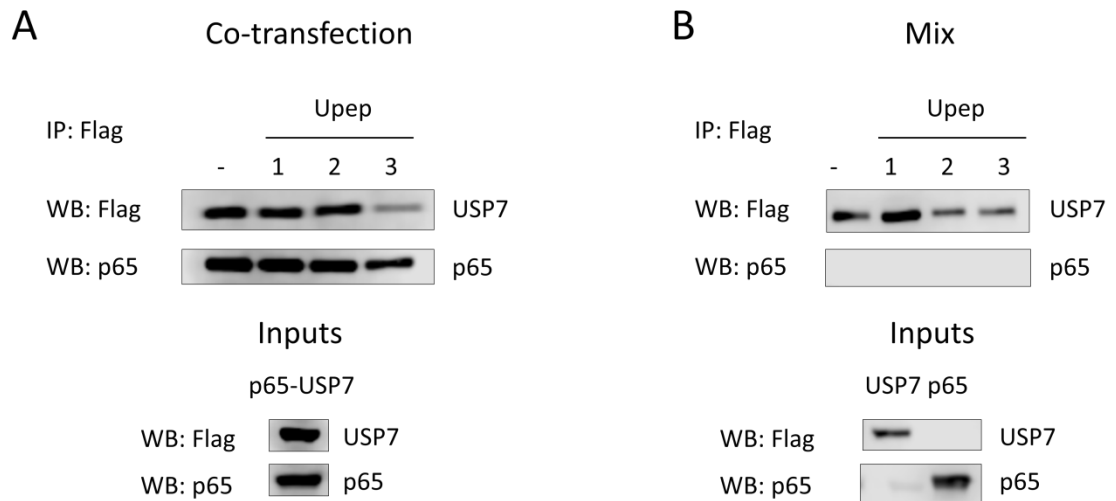


Figure 4-9 Role of USP7 mimetic peptides disrupting the interaction. A) Co-transfection of HEK293T cells with USP7-FLAG and p65-HA plasmids. Lysates were immunoprecipitated with an anti-FLAG antibody in the presence of individual USP7 mimetic peptides (100 μ M). There is no disruption of the interaction due to the presence of any USP7 mimetic peptide. The figure is a representative of three independent experiments. **B)** Transfection of HEK293T cells with USP7-FLAG and p65-HA plasmid separately. Cellular lysates were mixed and immunoprecipitated with an anti-FLAG antibody in the presence of individual USP7 mimetic peptides (100 μ M). Lysates containing USP7 and p65 separately are not able to form a USP7-p65 interacting complex. The figure is a representative of three independent experiments.

4.4 Discussion

The p65 subunit is recognised as a USP7 substrate by USP7 C-terminal region [287]. The C-terminal region of USP7 is composed of five UBLs which share the ubiquitin β -grasp fold [299, 300]. Despite very low sequence similarity their structures share homology [418]. These 5 UBLs are arranged in an elongated 2+1+2 conformation (UBL12 + UBL3 + UBL45). UBL12 and UBL45 form stable dimers and are connected to UBL3 through small linkers. These linkers give some flexibility to the C-terminal region of USP7 [299, 300, 408, 418, 422]. We performed a peptide array and subsequent alanine scan analysis to further investigate the amino-acids in charge of the interaction. Most of the amino-acids identified are localised in UBL3, specifically in a loop not present in the other UBLs. UBL45 are required for full deubiquitinase activity of USP7, while UBL123 are in charge of substrate recognition [299, 300, 408, 418, 422]. Flexibility of UBL3 is required for the structural rearrangements of USP7 leading to its active state [299, 300, 408, 418, 422]. We hypothesised an important role of UBL3 in p65 recognition, which is supported by the presence of a non-conserved crystal structure formed by several positively charged amino-acids. The presence of

positively charged amino-acids gives the possibility of forming electrostatic interactions with a negatively charged area of p65 protein.

To further assess the role of the non-conserved loop on UBL3 we tried to perform a functional analysis. Commonly, interaction of proteins is studied by a GST-pulldown. Recombinant protein of interest is incubated with a cellular lysate and pulldown by affinity binding. For p65 protein this approach was not possible due to the instability of the protein, which is degraded after 2h at 4°C. On the other hand, commercially available p65 is truncated; it lacks the TAD domain.

We tested the contribution of UBL3 amino-acids 844-860 located in a non-conserved loop to USP7-p65 interaction; by generation of USP7 mimetic peptides and immunoprecipitation assays but no inhibition of the interaction was found. These results may be due to the technique performed not being suitable enough to study the contribution of the UBL3 non-conserved loop, or due to that loop not being essential for the interaction. A protein may be recognised by a specific binding pocket, but that does not mean that region is the only region making contacts with the target protein. Proteins in nature are flexible, and upon binding, they undergo conformational rearrangements in order to form a stable complex [476]. It could be possible that the binding site is not localised on UBL3 non-conserved loop, but those contacts are required upon recognition and binding to stabilise the complex.

Amino-acids throughout the entire C-terminal sequence of USP7 were identified as important amino-acids for the interaction. Despite localising a very promising binding area on a non-conserved loop with several positively charged amino-acids on UBL3; none of the methods used detected an effect on USP7-p65 interaction. Further experiments to elucidate the contribution of each UBL domain to the interaction are required.

Chapter Five

**Identification of UBL2 domain of
USP7 as essential for the
interaction with p65**

5 Identification of UBL2 domain of USP7 as essential for the interaction with p65

5.1 Abstract

USP7 deubiquitinase enzyme controls the deubiquitination of p65 subunit of NF- κ B. Inhibition of USP7 deubiquitinase activity blocks pro-inflammatory gene expression. USP7 has a broad range of substrates involved in different biological processes. Thus, selective inhibition of USP7 activity towards p65 is required in order to harness the therapeutic potential of USP7 inhibition in inflammatory disease. USP7 multidomain protein recognises substrates by different regions. The N-terminal MATH/TRAF domain recognises substrates such as EBNA1, p53 and MDM2, while substrates like DNMT1, UHRF1, ICP0 and p65 are recognised by the C-terminal region. Within the C-terminal region a pocket in UBL2 generates the binding site for a number of substrates, as for example, ICP0, DNMT1 and UHRF1. This binding pocket located in UBL2 recognises a positively charged motif K/RxKxxxK in substrates like DNMT1 and UHRF1. We performed a series of mutational experiments followed by immunoprecipitation assays to study the role of each UBL in the interaction and the possibility of a binding pocket for p65 recognition. Our data identified that deletion of UBL2 inhibits interaction of USP7 with p65 and thereby, USP7 deubiquitination of p65. However, UBL2 is not required for interaction with a series of substrates such as DAXX, p53, EBNA1 and RelB. These data suggest that substrate specific inhibition might be possible, which is crucial for therapeutic purposes as substrate selective inhibition of USP7 activity enables the targeting of the pro-inflammatory effects of p65 while maintaining the biological roles of USP7 through different substrates.

5.2 Introduction

As explained in section 1.2, NF- κ B transcription factor family regulates inflammation and transcriptional response upon infection [287] and is tightly regulated. NF- κ B nuclear regulation occurs by the balance between ubiquitination and deubiquitination. USP7 recognises the p65 subunit through its C-terminal region and deubiquitinates it [287]. Inhibition of the deubiquitinating activity of USP7 blocks pro-inflammatory gene transcription [287]. However, USP7 is involved in several biological processes in pathology and physiology such as inflammation, tumourigenesis, cell cycle, apoptosis, DNA repair and viral infection; through the stabilisation and localisation of proteins involved in those processes like DNMT1, p53, UHRF1, MDM2, ICP0, NF- κ B family members [287, 418, 431, 477]. Identification of the specific molecular determinants involved in p65 recognition by USP7 is required in order to develop specific inhibitors of the NF- κ B response.

Protein-protein interactions are defined by the structural arrangements of the proteins involved in the interaction [476]; thereby, USP7 structure plays a key role to understand substrate recognition. As explained in section 1.4.3.1, USP7 is composed of an N-terminal MATH/TRAF domain, a catalytic domain and a C-terminal domain composed by 5 UBLs, the HUBL [287, 299, 418]. The N-terminal MATH/TRAF domain and UBL12 domains are involved in substrate recognition [41, 418]. USP7 is known to interact with all NF- κ B members [287], but the interacting region has only been studied for p65. Interaction of USP7 with p65 requires the C-terminal region but not the N-terminal region [287]. Homology between the NF- κ B subunits might suggest similar mechanisms for recognition by USP7. The five NF- κ B subunits share an N-terminal RHD but only p65, RelB and c-Rel contain a C-terminal TAD domain. RelB also incorporates an N-terminal LZ domain. [1, 40, 52, 478-481]. These structural differences might lead to different interacting mechanisms with USP7.

In this chapter, we investigated the contribution of each UBL domain of USP7 to the interaction with p65, identifying UBL2 of USP7 as the domain in control of p65 recognition. Furthermore, we studied the effect of UBL2 deletion on the recognition of different USP7 substrates such as DAXX, EBNA1, p53, c-Rel and RelB, detecting effects only on c-Rel recognition. To further analyse the

inhibition of USP7 deubiquitinase activity on p65 we explored the effect of USP7 UBL2 deletion on its deubiquitinase activity, confirming that inhibition of the interaction correlates with inhibition of the deubiquitinase activity.

5.3 Results

5.3.1 USP7 UBL2 is required for interaction with p65

To further analyse the binding site of USP7-p65 interaction we created a series of USP7 mutants through site directed mutagenesis (explained in section 2.2.6). In order to investigate the contribution of each UBL domain to the interaction with p65 we created a series of C-terminal truncated USP7 mutants lacking one or more UBLs. As a result, we obtained USP7 Δ UBL5 in which UBL5 is deleted, USP7 Δ UBL45 in which UBLs 4 and 5 are deleted, USP7 Δ UBL345 in which UBLs 3, 4 and 5 are deleted and USP7 Δ UBL2345 in which UBLs 2, 3, 4 and 5 are deleted (see Figure 5-1). Mutant USP7 Δ HUBL in which all five UBLs are deleted, was previously generated in the group [287]. HEK293T cells were co-transfected with USP7 WT, USP7 Δ UBL5, USP7 Δ UBL45, USP7 Δ UBL345, USP7 Δ UBL2345 and USP7 Δ HUBL FLAG-tagged plasmids along with p65-HA plasmid. Cellular lysates were immunoprecipitated with an anti-FLAG antibody and immunoblotted with anti-FLAG and anti-p65 antibodies (see Figure 5-2). USP7 Δ UBL2345 and USP7 Δ HUBL totally abolish the interaction with p65, while USP7 Δ UBL45 and USP7 Δ UBL345 decrease the level of interacting p65 protein.

As USP7 Δ UBL45 and USP7 Δ UBL345 demonstrated decreased interaction with p65, we decided to further study the effect of UBL4 and UBL3 by deletion of each domain (see Figure 5-1). HEK293T cells were co-transfected with USP7 WT, USP7 Δ UBL4, USP7 Δ UBL3, USP7 Δ UBL45 and USP7 Δ HUBL FLAG-tagged plasmids along with p65-HA plasmid. Cellular lysates were immunoprecipitated with an anti-FLAG antibody and immunoblotted with anti-FLAG and anti-p65 antibodies (see Figure 5-2). USP7 Δ UBL4 and USP7 Δ UBL3 are able to interact with p65, thus neither UBL3 nor UBL4 are required for p65 interaction.

As mutant USP7 Δ UBL45 decreases the interaction with p65, we decided to study the effect of the UBL3 and UBL4 linker. The peptide array analysis identified two amino-acids D887 and F888, which are located in an α -helix within the linker

between both domains (see Figure 5-3). Those amino-acids were not present in USP7 Δ UBL45 mutant, so we decided to analyse the contribution of this linker to the interaction with p65, by deletion or mutation to alanine of the amino-acids forming the α -helix, 885-ITDFEN-890. HEK293T cells were co-transfected with USP7 WT, USP7 Δ UBL3-4Linker, USP7 UBL3-4Linker to alanine, USP7 Δ UBL45 and USP7 Δ HUBL FLAG-tagged plasmids along with p65-HA plasmid. Cellular lysates were immunoprecipitated with an anti-FLAG antibody and immunoblotted with anti-FLAG and anti-p65 antibodies (see Figure 5-2). Both mutants were able to interact with p65, suggesting that the linker is not required for p65 interaction.

Further investigation of possible structural models of the interacting USP7-p65 complex was performed during a stay in AstraZeneca (described on section 6.3.3). Based on these analyses we created two possible mutants located on UBL3 and UBL3-4 linker region which could affect the interaction with p65, USP7 K869A and USP7 P884A respectively. K869 mutation to alanine could affect the potential formation of a salt bridge with D94 of p65 and P884 mutation to alanine could change the conformation of the loop coordinating the DNA-p65 interaction. The model also suggested possible contacts with UBL1 and UBL2 (see appendix 8.5); thus we created two more mutants, USP7 Δ UBL1 in which UBL1 is deleted and USP7 Δ UBL2 in which UBL2 is deleted (see Figure 5-1). HEK293T cells were co-transfected with USP7 WT, USP7 Δ UBL1, USP7 Δ UBL2, USP7 K869A, USP7 P884A and USP7 Δ UBL2345 FLAG-tagged plasmids along with p65-HA plasmid. Cellular lysates were immunoprecipitated with an anti-FLAG antibody and immunoblotted with anti-FLAG and anti-p65 antibodies (see Figure 5-2). Deletion of UBL2 domain was sufficient to inhibit USP7-p65 interaction, while the rest of the mutations did not prevent interaction with p65.

To study the contribution of amino-acids within UBL2 of USP7 to the interaction with p65, we designed several mutants. These mutants were based on the peptide array data (see section 4.3.5) and knowledge of the USP7 binding pocket for its interaction with ICP0, DNMT1 and UHRF1 [41]. The peptide array data identified amino-acids 757-LDEL-760 as potentially involved in p65 recognition (see Figure 4-4). D762 and D764 have previously been implicated as mediators of USP7 interaction with ICP0, UHRF1 and GMPS [41]. To investigate the role of these amino-acids in the interaction with p65 we created several mutants, USP7

DE758-759AA, USP7 D762A D764A, USP7 LDEL757-760AAA, USP7 LDEL757-760AAA D762A D764A and USP7 DE758-759AA D762A D764A (denominated USP7 DE, USP7 DD, USP7 LDEL, USP7 LDELDD and USP7 DEDD respectively) (see Table 5-1). HEK293T cells were co-transfected with USP7 WT, USP7 DE, USP7 DD, USP7 DEDD, USP7 LDEL, USP7 LDELDD and USP7 Δ UBL2 FLAG-tagged plasmids along with p65-HA plasmid. Cellular lysates were immunoprecipitated with anti-FLAG antibody and immunoblotted with anti-FLAG and anti-p65 (see Figure 5-4). There are no significant differences in the interaction of the mutants with p65.

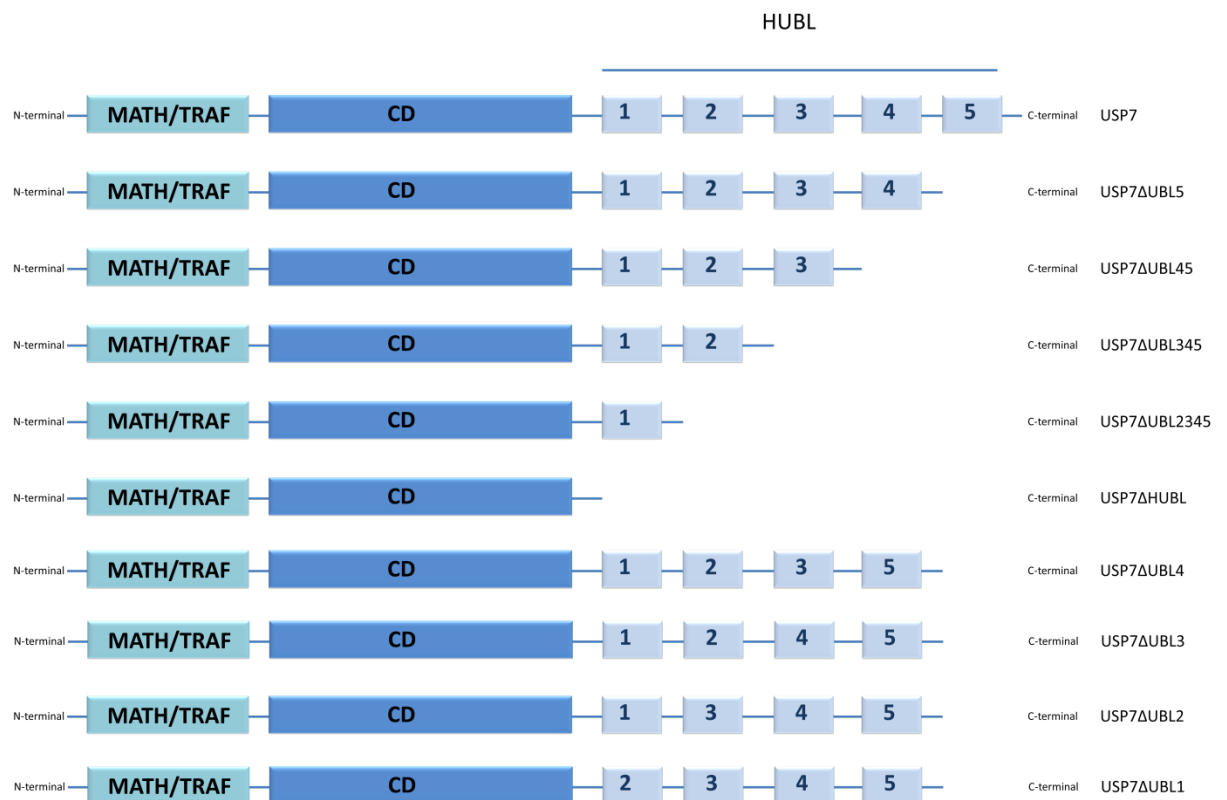


Figure 5-1 USP7 mutants structural schematic. Schematic representation of USP7 Δ UBL5, USP7 Δ UBL45, USP7 Δ UBL345, USP7 Δ UBL2345, USP7 Δ HUBL, USP7 Δ UBL4, USP7 Δ UBL3, USP7 Δ UBL2 and USP7 Δ UBL1 USP7 mutants used for the immunoprecipitation assays.

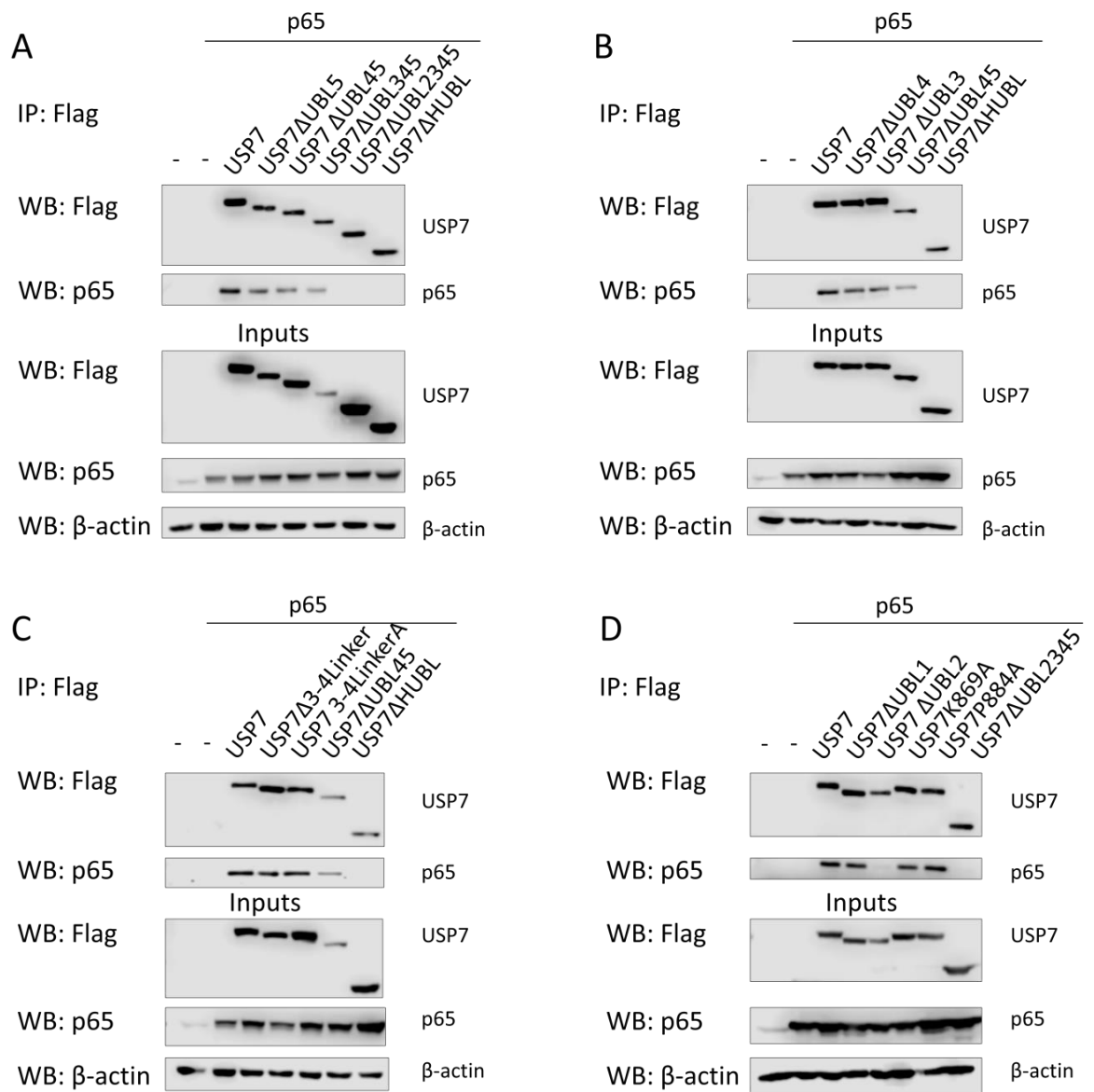


Figure 5-2 USP7 UBL2 deletion abolishes interaction with p65. **A)** HEK293T cells were co-transfected with USP7 WT, USP7ΔUBL5, USP7ΔUBL45, USP7ΔUBL345, USP7ΔUBL2345 and USP7ΔC FLAG-tagged plasmids along with p65-HA plasmid. Cellular lysates were immunoprecipitated with an anti-FLAG antibody and immunoblotted with anti-FLAG and anti-p65 antibodies. USP7ΔUBL2345 abolishes USP7-p65 interaction. The figure is a representative of three independent experiments. **B)** HEK293T cells were co-transfected with USP7 WT, USP7ΔUBL4, USP7ΔUBL3, USP7ΔUBL45 and USP7ΔC FLAG-tagged plasmids along with p65-HA plasmid. Cellular lysates were immunoprecipitated with an anti-FLAG antibody and immunoblotted with anti-FLAG and anti-p65 antibodies. Deletion of UBL3 or UBL4 did not inhibit USP7-p65 interaction. The figure is a representative of three independent experiments. **C)** HEK293T cells were co-transfected with USP7 WT, USP7ΔUBL3-4Linker, USP7 UBL3-4Linker to alanine, USP7ΔUBL45 and USP7ΔHUBL FLAG-tagged plasmids along with p65-HA plasmid. The amino-acids mutated to alanine or deleted in the linker between UBL3 and UBL4, are 885-ITDFEN-890. Cellular lysates were immunoprecipitated with an anti-FLAG antibody and immunoblotted with anti-FLAG and anti-p65 antibodies. The linker between UBL3 and UBL4 is not required for USP7-p65 interaction. The figure is a representative of three independent experiments. **D)** HEK293T cells were co-transfected with USP7 WT, USP7ΔUBL1, USP7ΔUBL2, USP7 K869A, USP7 P884A and USP7ΔUBL2345 FLAG-tagged plasmids along with p65-HA plasmid. Cellular lysates were immunoprecipitated with an anti-FLAG antibody and immunoblotted with anti-FLAG and anti-p65 antibodies. Deletion of UBL2 prevents USP7-p65 interaction. The figure is a representative of three independent experiments.

A

VERLQEEKRIEAQKRKERQEAHL YMQVQIVAEDQFCGHQGNMYDEEKVKYTVFKVLKNS
SLAEFVQSLSQTMGFPQDQIRLWPMQARSNGT PAMLDNEADGN TMIELSDNENPWTI
FLETVDPELAASGATLPKFDKDH DVMLFLKMYDPKTRSLNYCGHIYTPISCKIRDLLPVM
 CDRAGFIQDTSLILYEEVKPNLTERIQDYDVSLDKA LDK IMDGDIVFQKDDPENDNSEL
 PTAKEYFRDLYH RVDVIFCDKTIPNDPGFVVTLSNRMNYFQVAKTVAQRLNT PLLQF
KSQGYRIGGGPLHMYETLDLLQFFKPRPKKLYYQQLKMKITDFENRRSFKCIWLN
SQFREEEITLYPDKHGCVRDLLEECKKAVELGEKASGKLRLLEIVSYKIIGVHQEDELLE
CLSPATSRTFRIEEIPLDQVDDIKENEMLVTVAHFHKEVFGTFGIPFLLRIHQGEHFRV
MKQSLLDIQEKEFEKFKFAIVMMGRHQYINEDEYEVNLKDFEPQPGNMSHPLG
HNKAPKRSRYTYLEKAKIHN

B

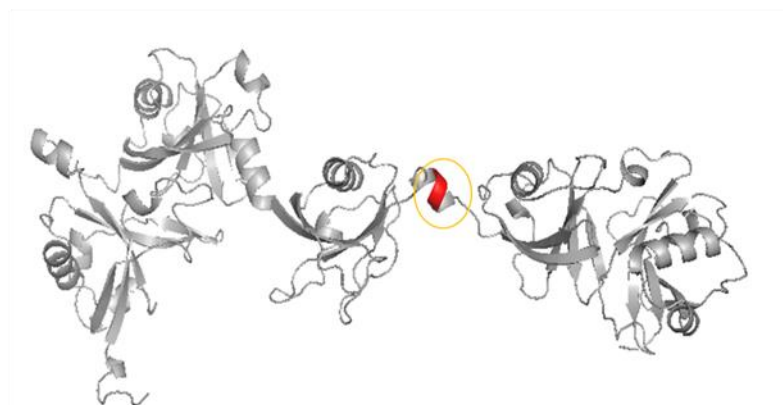


Figure 5-3 Location of the important amino-acids in the linker between UBL3 and UBL4 of USP7. A) C-terminal sequence of USP7 C-terminal UBLs. Important amino-acids identified in the peptide array analysis and subsequent alanine scan are underlined, in italics and marked in red. UBL1 is coloured in purple, UBL2 is coloured in blue, UBL3 is coloured in green, UBL4 in yellow and UBL5 in maroon. Amino-acids D887 and F888 are marked in an orange circle. **B)** USP7 C-terminal region 3D structure with amino-acids ITDFEN 885-890 coloured in red. Amino-acids 885-ITDFEN-890 were mutated to alanine or deleted in order to study the contribution of UBL3-UBL4 linker to the interaction with p65. PDB: 2YLM.

Table 5-1 USP7 UBL2 new mutants

Mutant Name	Mutation
USP7 DE	D758A E759A
USP7 DD	D762A D764A
USP7 LDEL	L757A D758A E759A L760A
USP7 LDELDD	L757A D758A E759A L760A D762A D764A
USP7 DEDD	D758A E759A D762A D764A

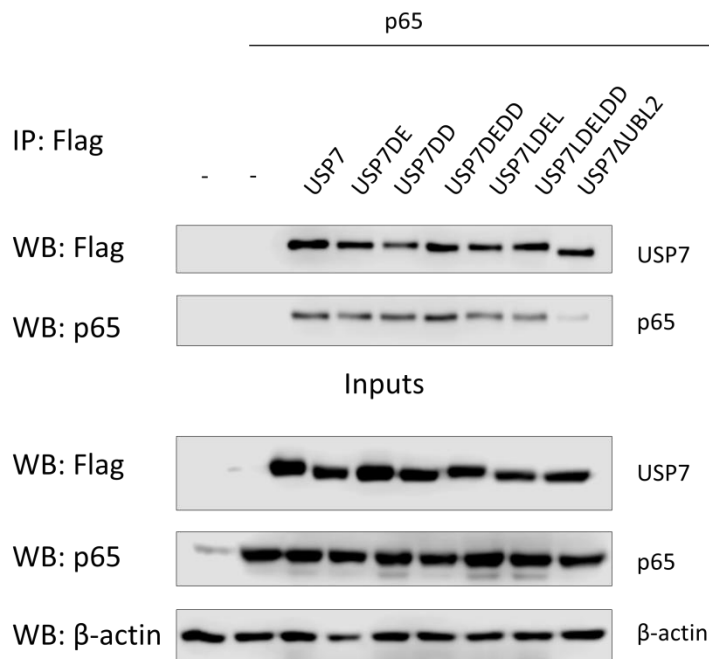


Figure 5-4 Mutation of USP7 757-LDEL-760 762D and 764D to alanine is not sufficient to abolish USP7-p65 interaction. HEK293T cells were co-transfected with USP7 WT, USP7 DE, USP7 DD, USP7 DEDD, USP7 LDEL, USP7 LDELDD and USP7ΔUBL2 FLAG-tagged plasmids along with p65-HA plasmid. Cellular lysates were immunoprecipitated with an anti-FLAG antibody and immunoblotted with anti-FLAG and anti-p65 antibodies. None of the mutations was sufficient to abolish USP7-p65 interaction. The figure is a representative of three independent experiments.

5.3.2 USP7 ΔUBL2 does not reverse p65 ubiquitination.

USP7ΔUBL2 mutant abolishes the interaction with p65, however, the ability of the mutant to inhibit p65 deubiquitination was still unknown. To study the effect of USP7ΔUBL2 deubiquitinase activity on p65 we performed a cellular ubiquitination assay with USP7 WT and USP7ΔUBL2 mutant. In order to be able to detect p65 ubiquitination status, we co-transfected HEK293T cells with USP7 WT and USP7ΔUBL2 FLAG-tagged plasmids along with p65 and ubiquitin-HA plasmids.

In the first place we cloned human p65-HA plasmid into an empty pCDNA3.1 expression vector (see appendix 8.2). Cellular lysates from the co-transfected HEK293T cells were denatured prior to immunoprecipitated with an anti-p65 antibody and immunoblotted with anti-FLAG, anti-p65 and anti-HA antibodies (see Figure 5-5). In contrast to USP7 WT, which effectively blocked p65 ubiquitination, USP7ΔUBL2 is not able to deubiquitinate p65 protein. These data further support the interaction with p65 in order to regulate p65 deubiquitination.

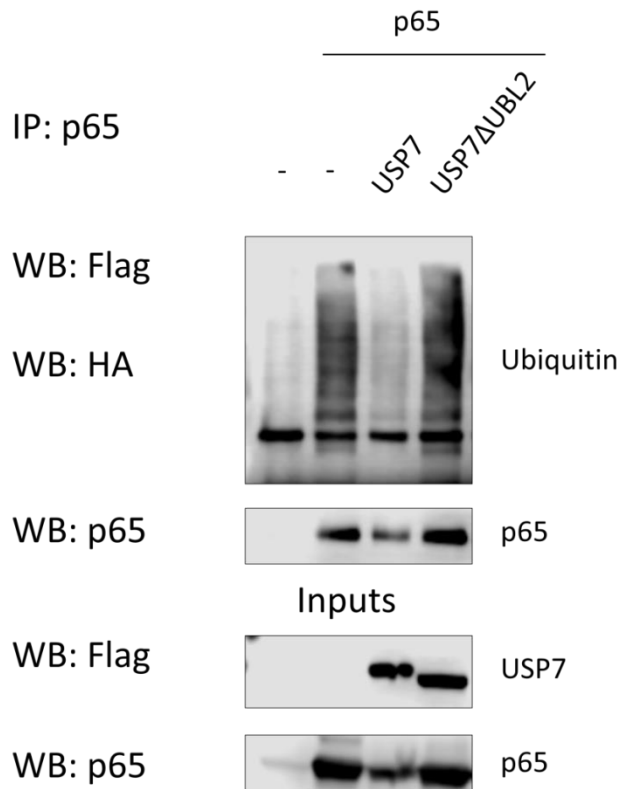


Figure 5-5 USP7 Δ UBL2 mutant is not able to deubiquitinate p65 protein. HEK293T cells were co-transfected with USP7 WT and USP7 Δ UBL2 FLAG-tagged plasmids along with p65 and ubiquitin-HA plasmids. Cellular lysates were immunoprecipitated with p65 antibody and immunoblotted with anti-FLAG, anti-HA and anti-p65 antibodies. Deletion of UBL2 blocks the ability of USP7 to deubiquitinate p65 protein. The figure is a representative of three independent experiments.

5.3.3 USP7 substrate specificity

USP7 acts in several biological processes through the stabilisation or regulation of cellular localisation of proteins involved in those processes [287, 418, 431, 477]. In order to further study the role of UBL2 in regulating substrate interaction, we investigated the effect of USP7 Δ UBL2 mutant on several different substrates interactions.

USP7 is known to interact with all NF- κ B members [287]. These NF- κ B members contain a high sequence similarity and structural homology. However, only RelB, c-Rel and p65 contain a TAD domain so we decided to analyse the interaction of USP7 Δ UBL2 only with RelB and c-Rel. HEK293T cells were co-transfected with USP7 WT and USP7 Δ UBL2 FLAG-tagged plasmids along with RelB and c-Rel respectively. Cellular lysates were immunoprecipitated with anti RelB and anti c-Rel respectively and immunoblotted for USP7 and c-Rel or RelB. RelB interaction with USP7 is not affected by the deletion of USP7 UBL2, while c-Rel

interaction is abolished when USP7 UBL2 is deleted (see Figure 5-6). Protein-protein interactions are regulated by the 3D structure of proteins involved in the interaction; therefore, we performed a structural alignment of the five NF- κ B members to detect structural differences. All NF- κ B subunits when structurally aligned show clear differences between p50 (PDB: 1SVC), p52 (PDB: 3D07), RelB (3D07), c-Rel (PDB: 1GJI) and p65 (PDB: 1VKX). p50 and p52 contain an α -helix not present on RelB, c-Rel and p65 (see Figure 5-7). This α -helix is located in the N-terminal region, where the RHD domain is located. Analysis of the domain composition of all family members showed that p50 and p52 are formed by the RHD domain and a GRR region; while RelB, c-Rel and p65 are formed by the RHD domain and the TAD domain. RelB also contains a leucine zipper domain in the N-terminal region of the protein. These differences in the protein structure would be sufficient to determine a different mechanism for substrate recognition by USP7.

One of the most studied substrates of USP7 is the p53 tumour suppressor protein. We decided to analyse the effect of USP7 UBL2 deletion on the interaction with p53 protein. HEK293T cells were co-transfected with USP7 WT or USP7 Δ UBL2 FLAG-tagged plasmids along with p53 plasmid. Cellular lysates were immunoprecipitated with anti-FLAG antibody and immunoblotted with anti-FLAG and anti-p53 antibodies (see Figure 5-6). This data demonstrated that interaction of USP7 with p53 was not disrupted by the deletion of USP7 UBL2.

USP7 also interacts with several viral proteins including the Epstein Barr viral protein, EBNA1. HEK293T cells were co-transfected with USP7 WT or USP7 Δ UBL2 FLAG-tagged plasmids along with EBNA1-FLAG-HA-tagged plasmid. Cellular lysates were immunoprecipitated with anti-HA antibody and immunoblotted with anti-FLAG and anti-USP7 antibodies (see Figure 5-6). Similar to the interaction with p53 protein, deletion of UBL2 has no effect on EBNA1 interaction with USP7.

We next analysed the ability of USP7 Δ UBL2 to interact with DAXX. HEK293T cells were co-transfected with USP7 WT and USP7 Δ UBL2 FLAG-tagged plasmids along with DAXX-FLAG tagged plasmid. Cellular lysates were immunoprecipitated with anti-DAXX antibody and immunoblotted with anti-FLAG and anti-DAXX antibodies

(see Figure 5-6). This revealed that deletion of UBL2 does not inhibit DAXX interaction with USP7.

Together these results suggest that there is a selective requirement of UBL2 for the interaction of USP7 with its substrates. Deletion of UBL2 disrupts interaction with specific substrates like p65 and c-Rel; but has no effect on the interaction with other substrates such as RelB, DAXX, p53 and EBNA1.

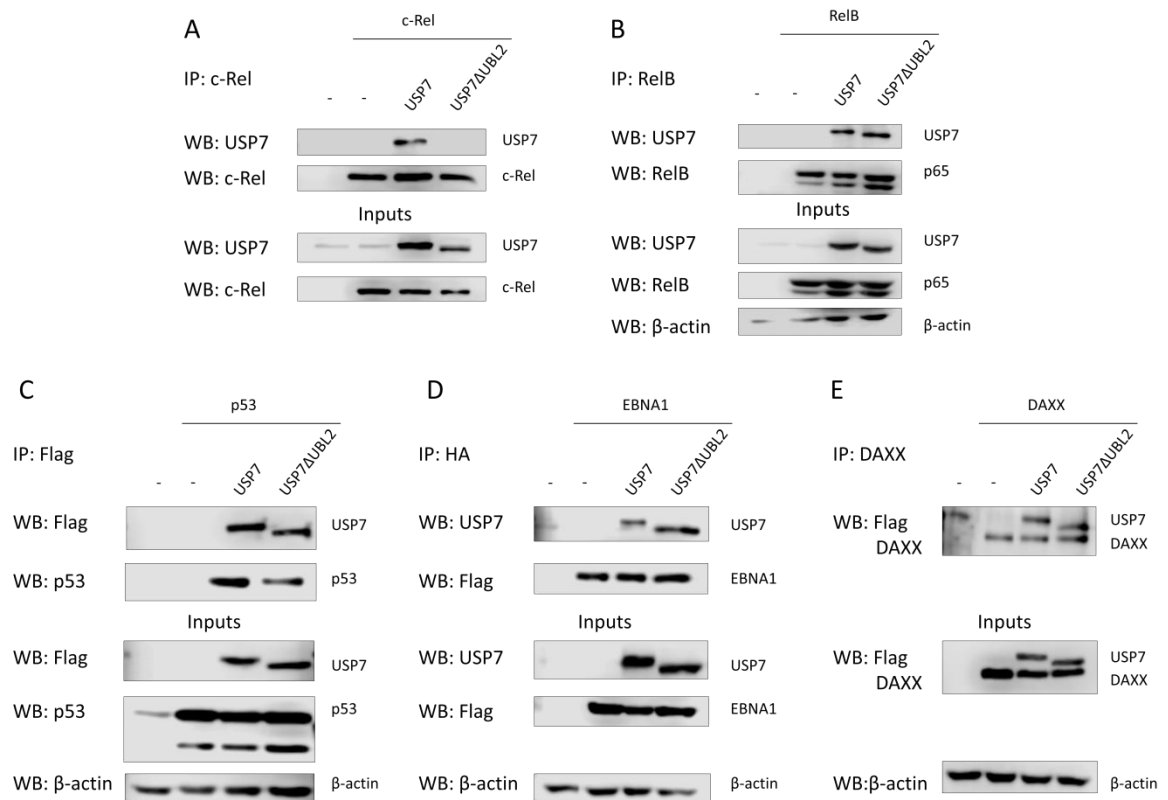


Figure 5-6 USP7 substrate recognition specificity. **A)** HEK293T cells were co-transfected with USP7 WT and USP7 Δ UBL2 FLAG-tagged plasmids along with c-Rel. Cellular lysates were immunoprecipitated with anti-c-Rel and immunoblotted with anti-USP7 and anti-c-Rel antibodies. USP7 Δ UBL2 inhibits c-Rel interaction. The figure is a representative of three independent experiments. **B)** HEK293T cells were co-transfected with USP7 WT and USP7 Δ UBL2 FLAG-tagged plasmids along with RelB. Cellular lysates were immunoprecipitated with anti-RelB and immunoblotted with anti-USP7 and anti-RelB antibodies. USP7 Δ UBL2 has no effect on RelB recognition. The figure is a representative of three independent experiments. **C)** HEK293T cells were co-transfected with USP7 WT and USP7 Δ UBL2 FLAG-tagged plasmids along with p53. Cellular lysates were immunoprecipitated with anti-FLAG antibody and immunoblotted for FLAG and p53 antibodies. USP7 Δ UBL2 is not able to disrupt p53 interaction. The figure is a representative of three independent experiments. **D)** HEK293T cells were co-transfected with USP7 WT and USP7 Δ UBL2 FLAG-tagged plasmids along with EBNA1-HA-FLAG-tagged plasmid. Cellular lysates were immunoprecipitated with anti-HA and immunoblotted with anti-USP7 and anti-FLAG antibodies. USP7 Δ UBL2 was not sufficient to disrupt EBNA1 recognition. The figure is a representative of three independent experiments. **E)** HEK293T cells were co-transfected with USP7 WT and USP7 Δ UBL2 FLAG-tagged plasmids along with DAXX-FLAG plasmid. Cellular lysates were immunoprecipitated with anti-DAXX and immunoblotted with anti-DAXX and anti-FLAG antibodies. USP7 Δ UBL2 is still able to interact with DAXX. The figure is a representative of three independent experiments.

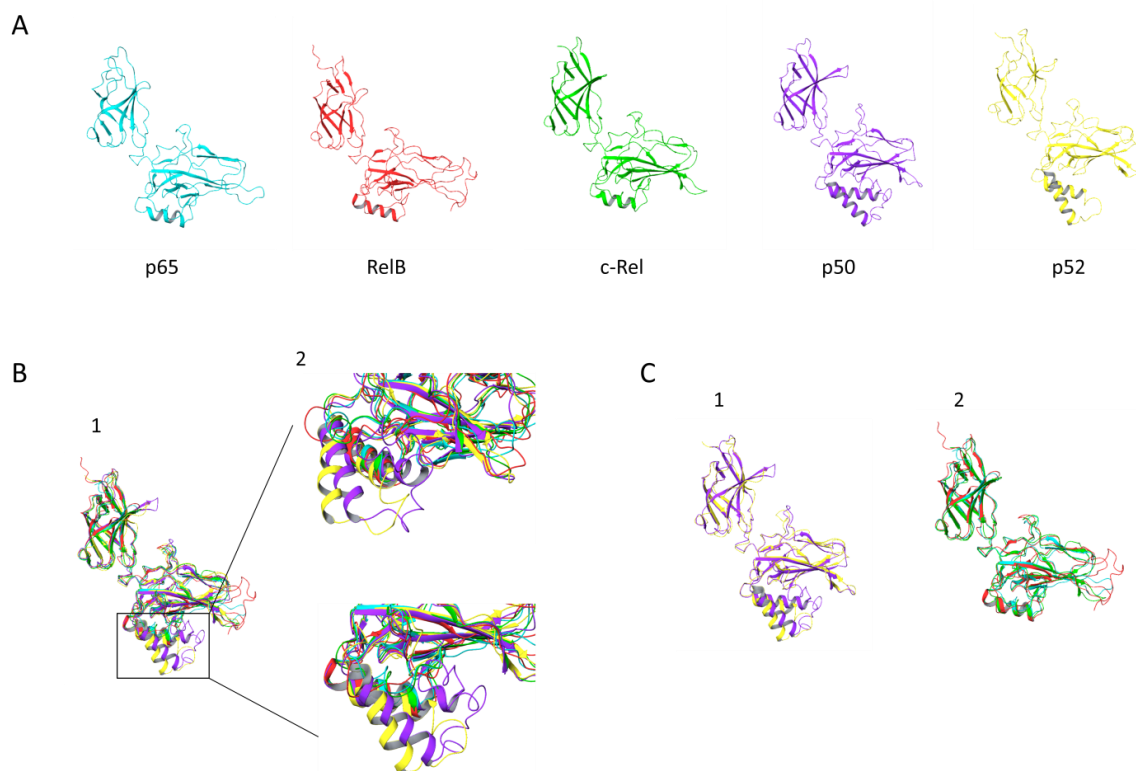


Figure 5-7 Structural alignment of the NF- κ B subunits. **A)** 3D structures of the different subunits forming the NF- κ B transcription factor family. p65 (1VKX) is coloured in blue, RelB (3DO7) in red, c-Rel (1GJI) in green, p50 (1SVC) in purple and p52 (3DO7) in yellow. **B)** Structural alignment of NF- κ B subunits. 1) p65 (1VKX) is coloured in blue, RelB (3DO7) in red, c-Rel (1GJI) in green, p50 (1SVC) in purple and p52 (3DO7) in yellow. The black box marks the differences between NF- κ B members. 2) Zoom-in of the α -helix present on p50 and p52 but missing on p65, RelB and c-Rel. p65 (1VKX) is coloured in blue, RelB (3DO7) in red, c-Rel (1GJI) in green, p50 (1SVC) in purple and p52 (3DO7) in yellow. **C)** Structural alignment of NF- κ B members based on the two different groups existing. 1) p50 and p52 alignment. p50 (1SVC) in purple and p52 (3DO7) in yellow. 2) p65, RelB and c-Rel structural alignment. p65 (1VKX) is coloured in blue, RelB (3DO7) in red, c-Rel (1GJI) in green. All structures were analysed with Maestro Schrodinger software.

5.4 Discussion

USP7 deubiquitinase enzyme interacts with and subsequently deubiquitinates a wide range of different substrates [287, 407, 431, 432]. The specific substrate recognition is required for a tight regulation of its deubiquitinase activity. Our results identified UBL2 of USP7 as essential for the interaction with p65. This domain has also been identified to play a key role in recognition of GMPS, UHRF1 and ICP0 [41, 418]. On the other hand, substrates as p53 and EBNA1 have been identified to interact with a binding site on the N-terminal MATH/TRAF domain [41, 418]. Thus, we may classify USP7 substrates by N-terminal MATH/TRAF domain recognised substrates and C-terminal region recognised substrates. Mutations within the C-terminal region do not interfere with the interaction of substrates recognised by the N-terminal MATH/TRAF domain, same as deletion of

the MATH/TRAF domain is not able to abolish the interaction with p65. Consistently, our results show that EBNA1 and p53 interaction is not altered by the deletion of UBL2. Our data also demonstrates that other substrates such as DAXX and RelB, are not disrupted by UBL2 deletion which suggests that they are recognised by the N-terminal MATH/TRAF domain.

Recent studies on the binding interface between USP7 and ICP0, UHRF1 and GMPS identified two aspartates (D762 and D764) in USP7 sequence, as important residues for the interaction [41]. UBL2 of USP7 recognises a positively charged motif (K/RxKxxxK) on substrates [41, 418], creating electrostatic intermolecular interactions between the carboxylate ion of D762 and D764, and the ammonium ion of the K or R present in K/RxKxxxK motif [41, 476]. Electrostatic interactions are the strongest non-covalent intermolecular interaction and the best potential target to disrupt the binding interface between two proteins [476]. Our peptide array data identified 757-LDEL-760 as amino-acids of USP7 that interact with p65. Combining our peptide array data and the crucial role of D762 and D764 on ICP0 recognition, we studied the interaction with p65 when those amino-acids are mutated; however, there is no inhibition of the interaction. One explanation could be that the negatively charged patch is involved in the interaction but is not essential for the interaction. Mutants D762R, D764R disrupt the interaction with GMPS, UHRF1 and ICP0 [41]. This probably occurs because the presence of two positively charged amino-acids instead of two negatively charged amino-acids is creating a repulsion force between both proteins. As stated before, the UBL2 binding pocket recognises a positively charged motif on substrates. The interaction between two proteins is driven by steric complementarity and attractive intermolecular forces created between both proteins. When any of these characteristics is disrupted, so is the interaction. The mutation to alanine of D762 and D764 showed different levels of inhibition on GMPS, UHRF1 and ICP0 [41]. This suggests that these amino-acids are involved in recognising the three substrates, but not with the same importance. This theory applies to the mutants created here. They might not include the key amino-acids which are essential for the interaction or a bigger disruption of the force field created in the protein interface might be needed to abolish the interaction. The possibility of different amino-acids being essential for different substrate recognition requires further investigation. Structural models of the interacting complexes

could be really useful to detect differences in the binding mechanism of each substrate. Another explanation for these results could be that the binding pocket containing D762 and D764 recognises different substrates; however, disruption of the electrostatic interactions within USP7 D762 and D764 and p65 is not sufficient to detect visible differences on the interaction levels. Thus, it should be taken into account that disruption of the binding interface of UBL2 not only would inhibit p65 interaction but also DNMT1, UHRF1, GMPS, ICPO and some other substrates recognised by UBL2 domain as well.

The NF- κ B members are known to interact with USP7 but the mechanism by which each different NF- κ B member is recognised is unknown [287]. The comparison of their domain composition and structural analysis show two clear groups. One group is formed by p50 and p52, which are not able to activate transcription and when forming homodimers act as repressors, are composed by the shared N-terminal RHD followed by a GRR. Whereas the second group is composed by RelB, c-Rel and p65; which are formed by the amino RHD and a C-terminal TAD. RelB differs from p65 and c-Rel, by the additional presence of a LZ domain. This LZ and dimerisation with p50 or p52 is required to bind to the DNA and for its transactivation ability [1, 40, 52, 478-481]. These differences are reflected in the 3D structure of the proteins and in the interaction with USP7. RelB interacts with the USP7 Δ UBL2 mutant while c-Rel, which contains the same structural domains as p65 is not able to interact with it. The presence of the LZ domain on RelB could affect the mechanism by which USP7 recognises RelB as a substrate. When comparing structural conformation of the proteins, RelB is not as similar to p65 as c-Rel is. There is a loop on the N-terminal region which is not aligned with p65 or c-Rel. On the other hand, c-Rel protein is organised in the same way as p65 protein, containing exactly the same domains. Structural alignment of both proteins shows almost perfect assembly between both proteins. These results reflect the importance of structure for protein-protein interactions. Different 3D structures will determine different protein interaction partners and mechanisms, which will finally determine the different biological role of each protein on the cell. The design of an anti-inflammatory drug based on USP7 deubiquitinase activity on NF- κ B members would inhibit specifically p65 and c-Rel activity, canonical activation of the NF- κ B pathway, while the non-canonical activation would be intact due to RelB being able to interact with

USP7. This drug would specifically target the expression of genes involved in inflammation, cell survival and innate immunity, while expression of genes involved in the lymphoid organogenesis, adaptive immunity, anti-inflammatory properties, B-cell maturation and osteoclastogenesis would be intact. p65 and c-Rel subunits sharing a binding mechanism with USP7, highlights the pro-inflammatory potential of a specific drug based on the disruption of the interaction. Further investigation of the effects of USP7 Δ UBL2 on p50 and p52 is required to analyse that this strategy would not affect the repressive function of p50 and p52 homodimers.

Deletion of UBL2 not only abolishes the interaction with p65 subunit but also USP7 deubiquitinase activity on p65. This lack of activity is hypothesised to be due to a lack of interaction, as USP7 is not able to interact with p65 it cannot deubiquitinate p65 subunit. However, the impact of UBL2 deletion of USP7 deubiquitinase activity has not been assessed here and further investigation of the activity of USP7 UBL2 deletion on interacting substrates should be required. USP7 catalytic activity is regulated by conformational rearrangements upon substrate binding [408]. The location of UBL12 with respect to the CD has an effect on the ability of UBL45 to contact the catalytic domain and place the CTP of USP7 in the active cleft. When eliminating UBL2, flexibility between UBL domains is kept, but UBL45 might not be at a proper distance to be able to place the CTP on the active cleft. Therefore, further investigation on the effects of UBL2 deletion on USP7 activity is required.

New therapeutic strategies are targeting the binding interface of interacting proteins [476]. Defining the specific binding site for p65 will reduce the potential side effects derived from a catalytic inhibition of USP7. In this chapter we discovered that the binding pocket of USP7 for p65 is located in UBL2 of USP7. However, not every USP7 substrate is recognised by UBL2; substrates such as p53, EBNA1, RelB and DAXX do not required the presence of UBL2 to interact with USP7. Supporting that the interaction is required for USP7 deubiquitinase activity on its substrates, USP7 UBL2 deletion inhibits USP7 deubiquitinase activity on p65. Our data suggest that design of a substrate specific inhibitory compound to inhibit p65 inflammatory response is possible, reducing the unwanted effects of USP7 catalytic inhibition.

Chapter Six

Structural modelling of USP7-p65 interaction

6 Structural modelling of USP7-p65 interaction

6.1 Abstract

3D structure of proteins is a key determinant of the biological function of proteins and regulates the possible interactions with other proteins. There has been a huge development of techniques to elucidate 3D structure of proteins and protein-protein complexes; but still, a high number of protein complexes and proteins are not solved. Molecular modelling is a series of computational techniques which helps to elucidate the 3D structure of proteins and protein complexes. There are different types of molecular modelling, including de novo modelling and template based modelling. As for protein complexes, the technique denominated docking has been developed. Molecular docking is the computational technique use to predict the 3D structure of a protein-protein complex from the 3D structures of the proteins involved in the interaction. In order to dock two proteins manually, knowledge of the amino-acids present in the binding site is required. Recent studies have identified a binding pocket located in UBL2 of USP7 which is important for recognising specific substrates. This binding pocket encompasses the amino-acids identified by our experimental data as important for the interaction with p65. In addition, a substrate pattern motif is recognised by USP7 consisting of positively charged amino-acids which can be found on p65 sequence. For this reason, we used the docking technique to generate models of the different possible USP7-p65 interactions leading to the generation of stable USP7-p65 complexes. These models were generated in order to elucidate the amino-acids regulating this interaction. Experimental investigation of the contribution of these residues to the interaction will in turn help to enlighten the accuracy of the model.

6.2 Introduction

Inhibition of USP7 deubiquitinase activity on p65 leads to a termination of the NF- κ B response [287]. However, inhibition of the catalytic activity of USP7 leads to a wide range of effects on different biological processes. Thus, new drug discovery strategies are focus on targeting binding interfaces, which are substrate specific [482-484]. To develop a compound able to inhibit the interaction between USP7 and p65, understanding of their 3D structures is required.

The 3D structure of proteins plays a key role in the function and activity of a protein. The biological function of proteins is intimately related to their ability to interact with other proteins, and these interactions are determined by the protein 3D structure [476, 485-487]. Therefore, the forces controlling the 3D structure of a protein are key for its biological function [476]; and consist of intramolecular bonds. Amino-acid side chains interact with each other through an attractive or a repulsive force. Due to these interactions, proteins will rearrange their conformation in order to obtain their most stable structure [476]. Intramolecular interactions include; attraction forces as, electrostatic or ionic bonds, hydrogen bonds, Van der Waals interactions and dipoles; and repulsive forces [476]. Even though separately electrostatics or ionic bonds are the strongest interaction and Van der Waals the weakest; in the overall of a protein, Van der Waals are more important because there is a greater number of Van der Waals interactions in comparison to electrostatics or ionic bonds [476].

Protein interactions are regulated in a structurally specific way [485, 488, 489]. Protein recognition takes place in a crowded environment; hence, the specificity and regulation of the process is highly important [488]. Regulation of the interaction between proteins depends on the flexibility of the proteins involved and the conformational rearrangements underwent by those proteins, in order to get steric and physicochemical complementarity at the protein-protein interface [485, 488-490]. The 3D structure of a protein or a protein complex can be analysed experimentally and computationally [490-492]. The number of resolved protein 3D structures is increasing with the development of new methods for this purpose; but there are thousands of proteins still with no available 3D structure. In some cases getting the 3D structure of a protein through NMR or X-Ray

crystallography is impeded by experimental constraints and is also time consuming and cost expensive [491].

3D structure of USP7-p65 complex is important when studying the interaction interface. There is no available 3D structure of USP7-p65 complex, but there are a number of X-Ray structures from p65 protein sequence and USP7 protein sequence as explained in sections 1.2.2.1 and 1.4.3.1. When X-Ray crystallisation or NMR is not possible, computational molecular modelling is a useful tool. It can provide the experimental insights required for subsequent experiments such as site directed mutagenesis or co-immunoprecipitation assays in order to study the molecular determinants of two proteins involved in their interaction. Molecular modelling consists on all theoretical and computational methods used to describe the atomic and molecular interactions within molecules [493]. Thanks to the development of molecular modelling techniques, conformational flexibility and plasticity over a range of space and time scale can be simulated [491, 493]. Molecular modelling techniques can be divided into two groups; de novo modelling or template based modelling. De novo molecular modelling predicts the 3D structure of a protein from its primary amino acid sequence. It does not use a 3D structure of a homolog protein as a template. It is normally used to determine the folding of small molecules [491, 494]. Rosetta method is the method used by ROBETTA software (Baker Lab). ROBETTA software is able to design protein structural models with a given amino-acid sequence of a maximum of 600 amino-acids when a template structure is found on the PDB files. Rosetta is among the de novo methods but is not a truly de novo method [487, 491]. Rosetta combines different small peptide fragments obtained from the PDB and assembles them to get the complete protein structure following a relaxation process [491]. Template based modelling uses a known protein structure as the template for the structural modelling. The sequence identity between the target and the template has to be greater than 30%. When the template used is from an homologous protein it is called homologous modelling [491, 494-498]. Once the proteins have been modelled a relaxation process of the model has to be performed in order to study the accuracy of the model. This process allows the molecules to move and find the most stable state. Molecular Dynamics (MD) program is usually used to mimic the

movement of atoms within the protein in space and time and looks for possible collisions [476, 490].

Protein-protein complex modelling is also possible. Molecular docking is the computational technique used to predict the 3D structure of a protein-protein complex from the 3D structures of the proteins involved in the interaction [476, 488, 491, 499-501]. An accurate docking requires an optimal binding orientation with steric and physicochemical complementarity at the protein-protein interface [488, 491]. When the binding site is known, the more relevant docking method is the manual docking. The binding pocket is characterised conformationally and by its amino-acid composition [501]. The user manually pairs the binding site of the protein into the complementary binding pocket of the interacting protein and defines the ideal binding distance for each potential interaction [476].

The amino-acids forming the binding interface on USP7-p65 interaction are still unknown. However, USP7 ubiquitin recognition pocket has been identified and certain regions of USP7 bound to ubiquitin have been solved as for example PDB: 5JTV and 5JTJ [299]. p65 protein is known to be ubiquitinated by several E3 ligases such as PPAR γ , ING4, SOCS1 [380, 383, 502, 503] at 10 different K residues in the human protein (K28, K56, K62, K79, K122, K123, K195, K310, K314 and K315) [372, 380, 381, 383, 388]. However, USP7 is the only known deubiquitinase enzyme in charge of p65 deubiquitination. This fact makes the modelling process even more difficult by the addition of more than one possible model in which different K residues could be ubiquitinated. These ubiquitinated lysines are supposed to be at close distance from USP7 catalytic triad so it can deubiquitinate p65.

As Box and Draper said, “essentially all models are wrong, but some are useful” (Empirical Model Building and Response Surfaces, Box and Draper 1987). Modelling the interaction between USP7 and p65 is a useful tool for the design of subsequent experiments which will allow us to define the specific amino-acids involved in the interaction and the accuracy of the model as well. In this chapter we modelled a full length p65 protein and a full length USP7 protein 3D structure. Besides, we modelled the interaction between both proteins,

investigating the possible complexes for the interaction between USP7-p65 based on our biochemical data and previously determined interacting pockets.

6.3 Results

6.3.1 p65 full length protein 3D structure model

There is no full length p65 available structure, hence we used the truncated p65 structure from 1VKX (amino-acids 19-291 forming the RHD) (see Figure 6-1) and the ROBETTA software to design a full length p65 protein 3D structure. We submitted the murine amino-acid sequence of p65 to ROBETTA software (<http://robetta.bakerlab.org/>). As a result, we got 5 different models (see Figure 6-2 and Figure 6-3). From these 5 models, comparing them to the p65 1VKX protein structure, we chose the more similar one and continue the full length p65 model with that one (ROBETTA model 1).

For our full length p65 to be more consistent with the structure of the solved p65 on 1VKX, we structurally aligned the models to p65 1VKX (see Figure 6-4). Following the alignment, we spliced amino-acids 20-291 from 1VKX into the model. For amino-acids 1-20 splicing, we aligned structures manually and subsequently spliced amino-acids 1-20 into amino-acids 21-551 from 1VKX and p65 ROBETTA model 1, getting a full length p65 protein structure (see Figure 6-5 and Figure 6-6).

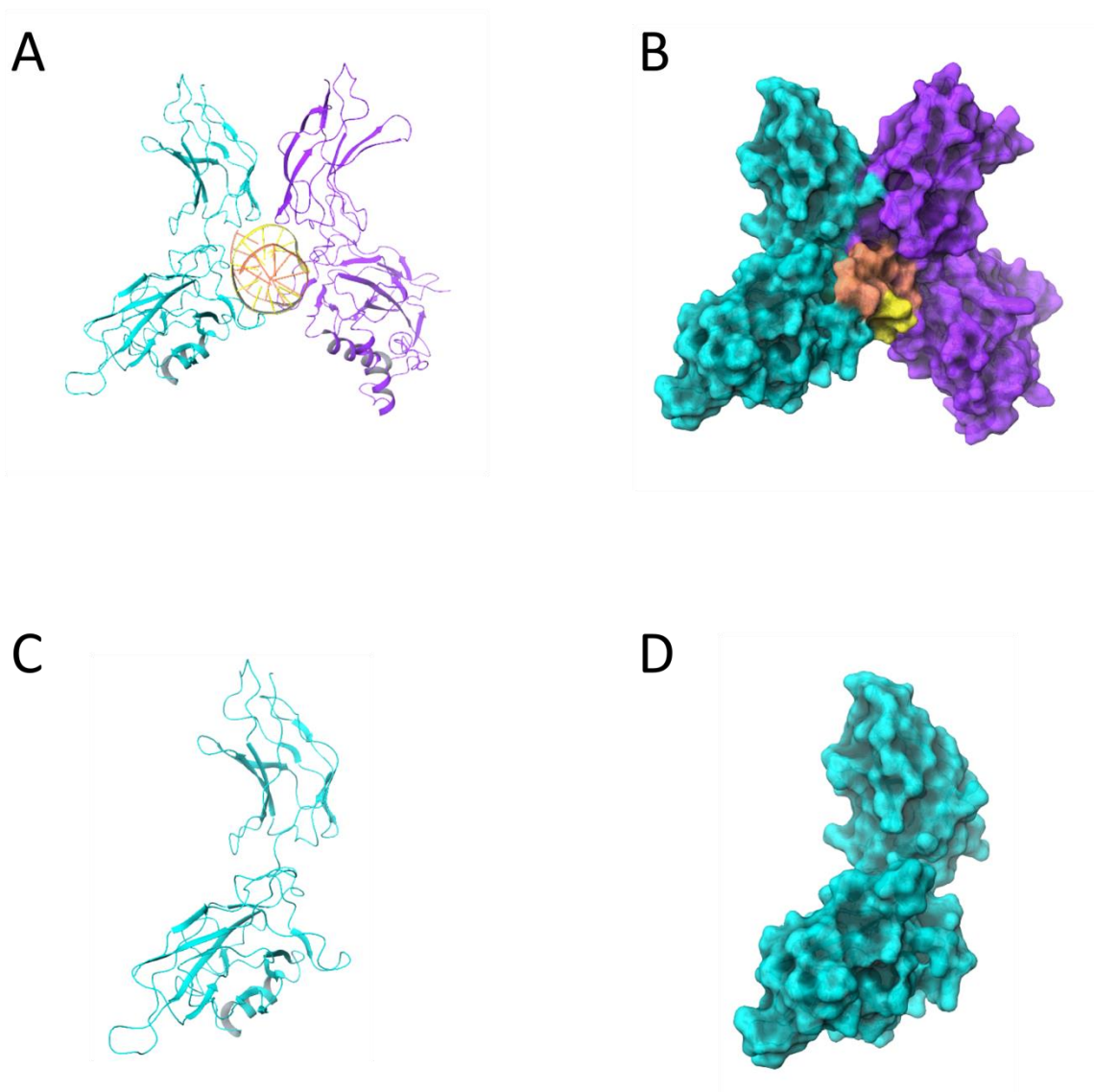
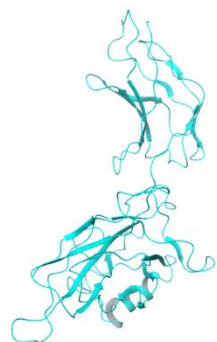


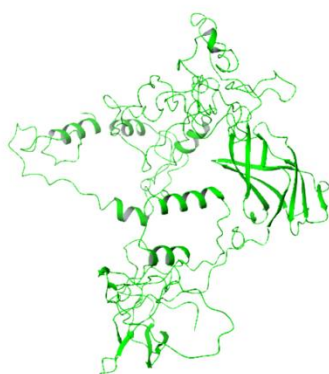
Figure 6-1 1VKX PDB crystal structures. **A)** Ribbon of the crystal structure of the heterodimer p50-p65 (p50 amino-acids 39-364 and p65 amino-acids 19-291) in complex with the DNA helix from 1VKX. p65 is coloured in blue, p50 in purple and the DNA helix in yellow and pink. **B)** Compact surface of the crystal structure of the heterodimer p50-p65 in complex with the DNA helix from 1VKX. p65 is coloured in blue, p50 in purple and the DNA helix in yellow and pink. **C)** Ribbon of the truncated p65 protein (RHD amino-acids 19-291) structure from 1VKX. **D)** Surface of the truncated p65 protein (RHD amino-acids 19-291) structure from 1VKX. All structures were analysed with Maestro Schrodinger software.



1VKX



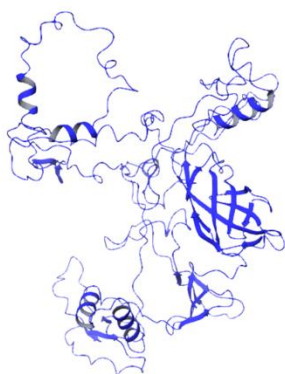
Model 1



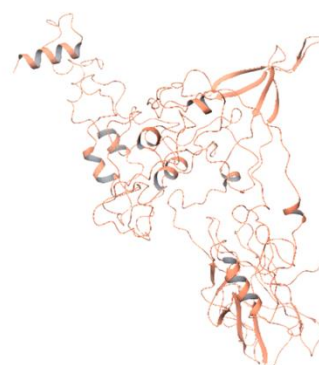
Model 2



Model 3

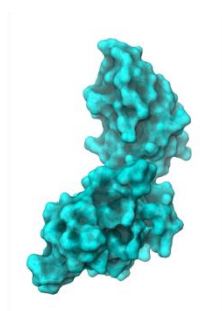


Model 4

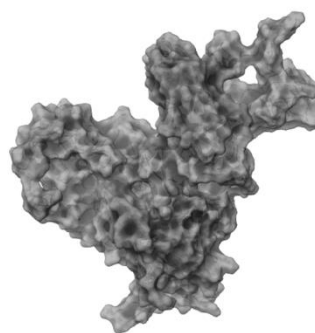


Model 5

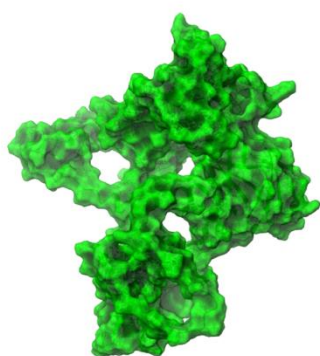
Figure 6-2 Ribbon structures of p65 protein modelled with ROBETTA software in comparison with p65 protein structure from 1VKX. Ribbon of the crystal structure of p65 from 1VKX (RHD amino-acids 19-291) and full length models developed by ROBETTA software. Each structure is labelled on the figure. The view of all models tries to keep amino-acids 225-290 beta-sheet secondary structure in the same place as p65 beta-sheet secondary structure in 1VKX. All 3D structures were analysed with Maestro Schrodinger Software.



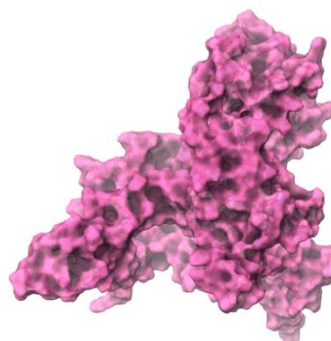
1VKX



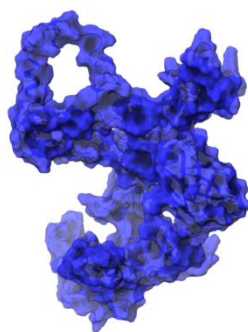
Model 1



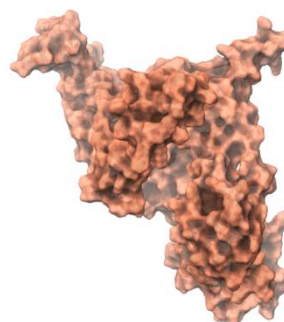
Model 2



Model 3



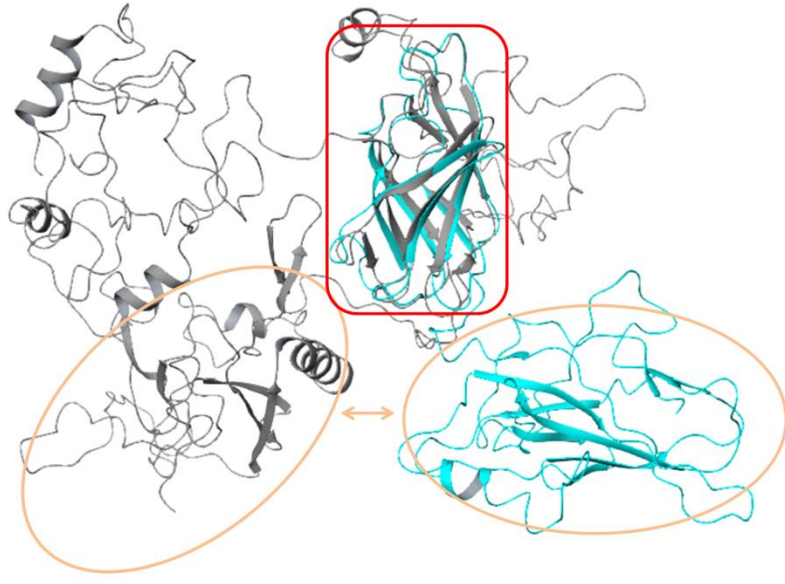
Model 4



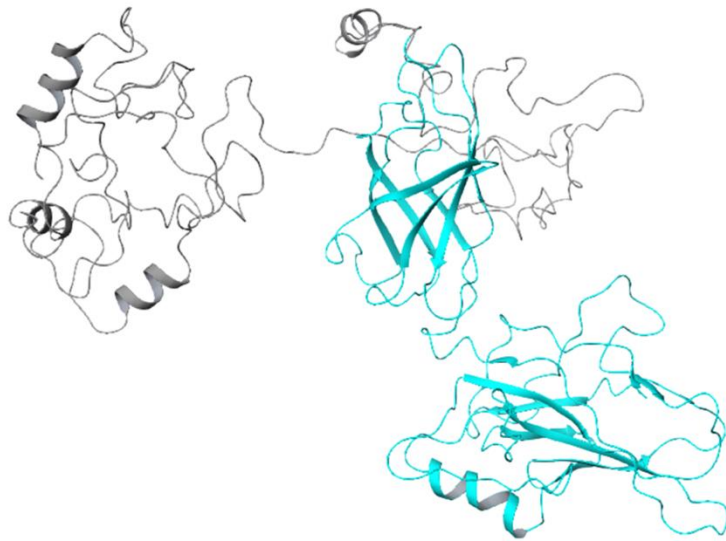
Model 5

Figure 6-3 Surface structures of p65 protein modelled with ROBETTA software in comparison with p65 protein structure from 1VKX. Surface of the crystal structure of p65 from 1VKX (RHD amino-acids 19-291) and full length models of full length p65 protein developed by ROBETTA software. Each structure is labelled on the figure. Colours are maintained for each structure. The view of all models tries to keep amino-acids 225-290 beta-sheet secondary structure in the same place as p65 beta-sheet secondary structure in 1VKX. All structures were analysed with Maestro Schrodinger software.

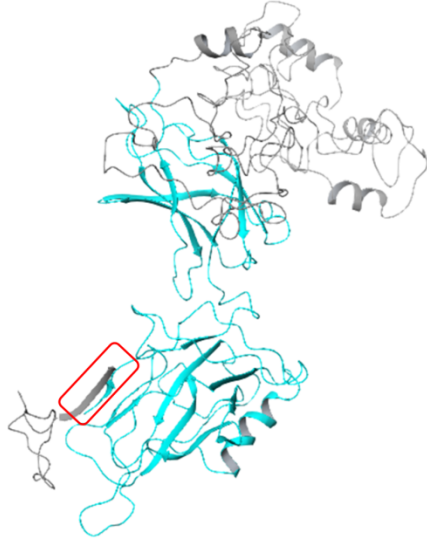
A



B



C



Splicing

D



Figure 6-4 p65 full length protein model generation. **A)** Structural alignment of p65 structure from 1VKX (RHD amino-acids 19-291, coloured in blue) and p65 full length ROBETTA model 1 (grey). The box in red highlights the aligned secondary structure from both structures; amino-acids 225-290 (most conserved secondary structure among the models). Orange circles mark the homologous region between both proteins (amino-acids 20-190), which is not structurally aligned. **B)** Structure from the splicing of 1VKX protein structure (RHD amino-acids 19-291, coloured in blue) into amino-acids 292-551 of ROBETTA model 1 (grey). **C)** Manual structural alignment of amino-acids 20-26 from ROBETTA model 1 (grey) and the newly modelled amino-acids 21-551 p65 structure. Parts of the model from 1VKX are coloured in blue (amino-acids 21-291), while parts from ROBETTA model 1 are coloured in grey (amino-acids 292-551). The red box highlights the structural alignment of amino-acids 20-26. **D)** p65 full length structural model resulting from the splicing of amino-acids 1-20 from ROBETTA model 1 (grey) into the previously modelled 21-551 amino-acids p65 structure. Parts of the model from 1VKX are coloured in blue (amino-acids 21-291), while parts from ROBETTA model 1 are coloured in grey (amino-acids 1-20 and 292-551). All structures were analysed with Maestro Schrodinger software.

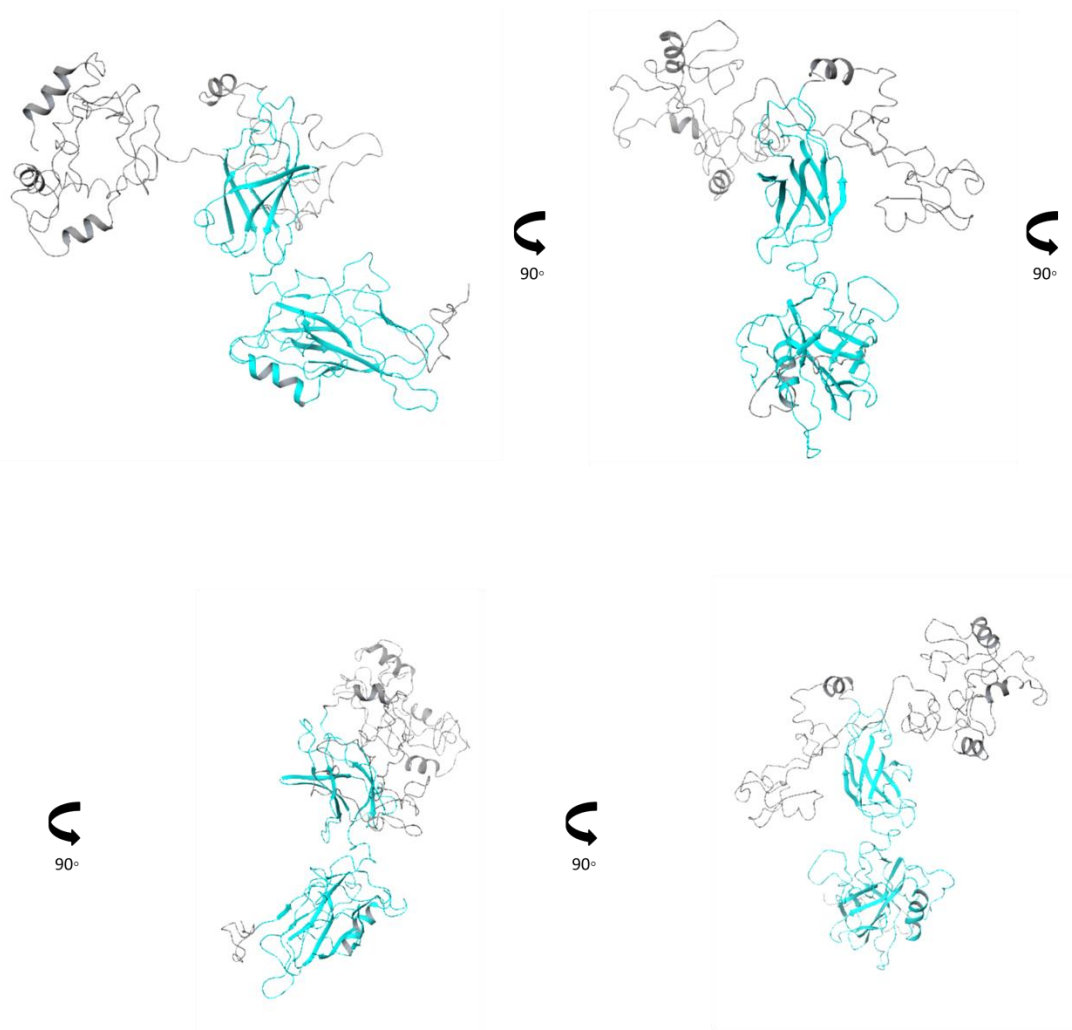


Figure 6-5 Ribbon of p65 full length protein structural model. Different views of p65 protein modelled structure. The original amino-acid structure from 1VKX (amino-acids 20-291) is coloured in blue, while the original amino-acid structure from ROBETTA model 1 (amino-acids 1-19 and 292-551) is coloured in grey. All 3D structures were analysed with Maestro Schrodinger Software.

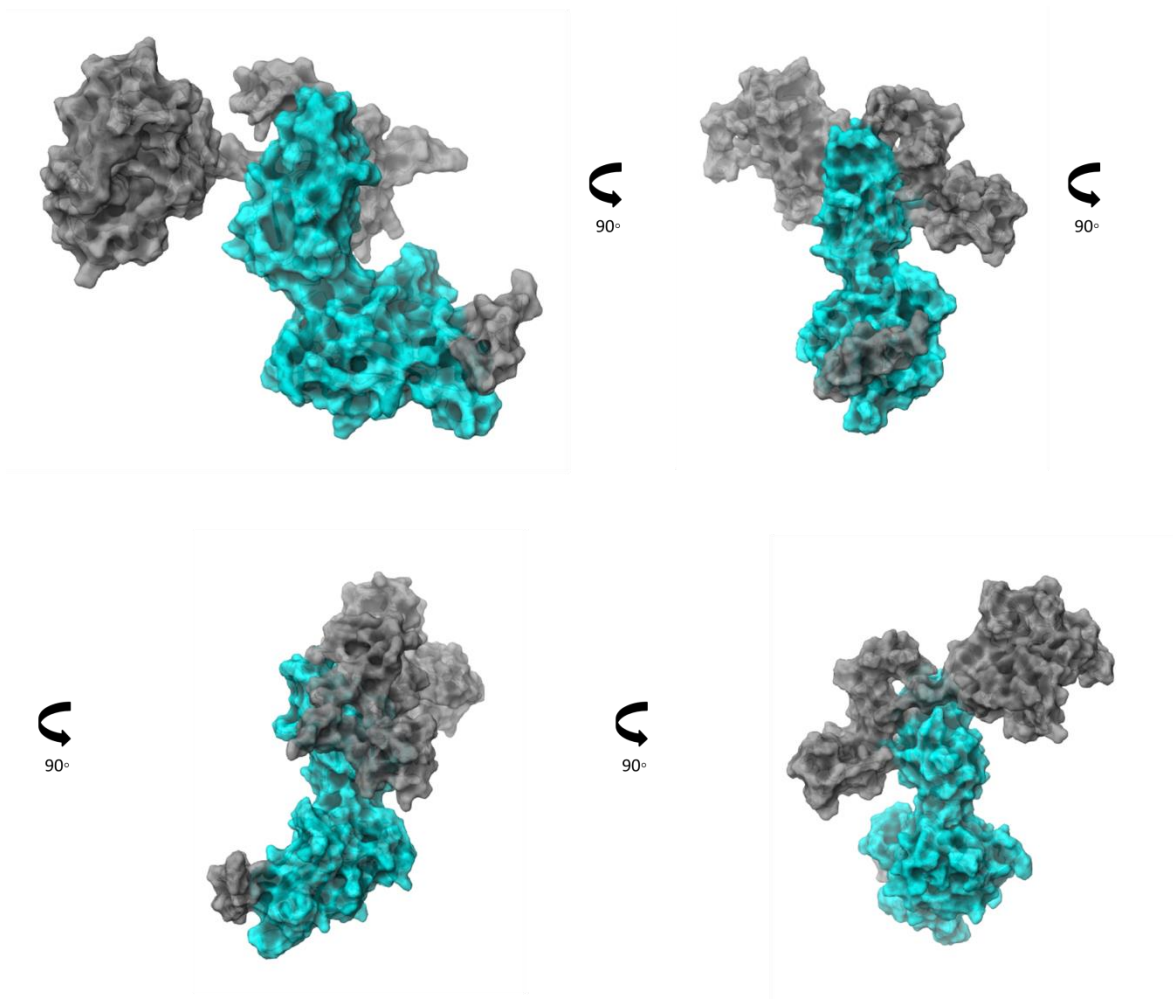


Figure 6-6 Surface of p65 full length protein structural model. Surface of the full length p65 protein model. Different views of the protein modelled structure. The original amino-acid structure from 1VKX (amino-acids 20-291) is coloured in blue, while the original amino-acid structure from ROBETTA model 1 (amino-acids 1-19 and 292-551) is coloured in grey. All structures were analysed by Maestro Schrodinger software.

6.3.2 USP7 full length protein 3D structure model

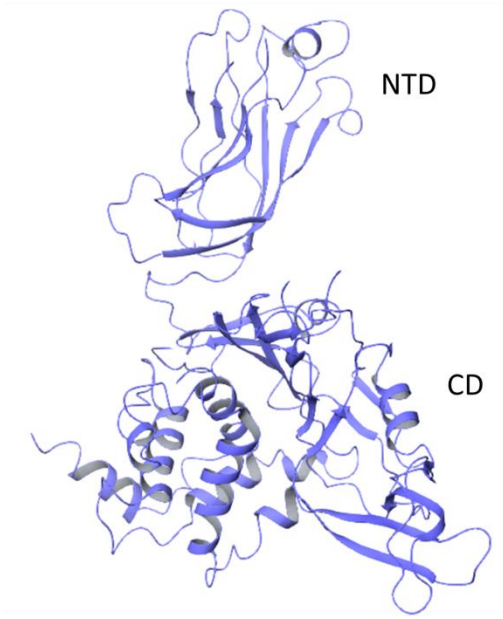
A full length USP7 protein has not been crystallised, however, a recent study proposed a full length structural model of USP7 using structures of smaller USP7 regions or domains [299]. We modelled a full length USP7 3D structure following their model. Modelling of the full length USP7 was carried out in collaboration with Dr Matti Lepistö and Dr Christian Tyrchan (AstraZeneca, Sweden).

The full length USP7 computational modelling was carried out with sequential structure alignments and splicing of different structures of USP7. The PDB files used were 5JTV, 5J7T, 4YOC, 5JTJ and 2F1Z (see Table 6-1, and Figure 6-7). Subsequently, atomic distances and any disrupted secondary structure were

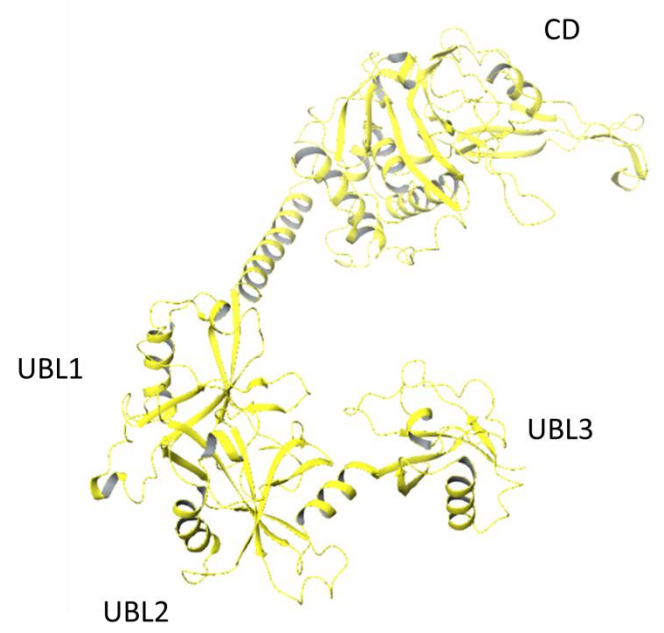
repaired and the complex was minimised and relaxed by a molecular dynamics process.

Table 6-1 Structures contained in each PDB file

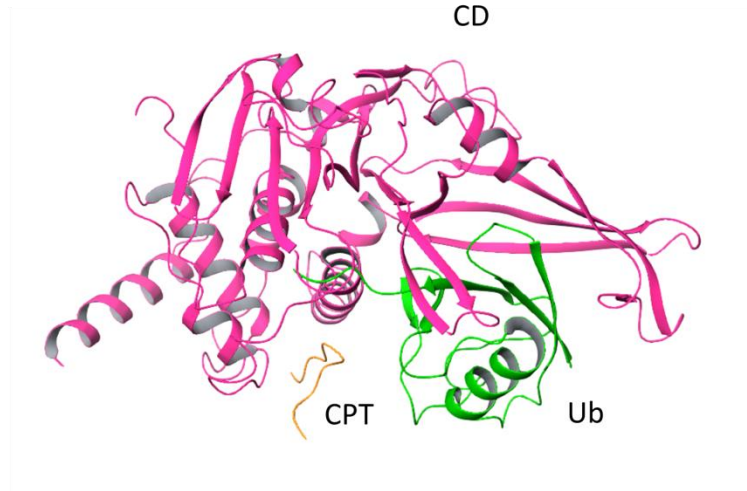
PDB File	Structure
5JTV	USP7 CD and UBL45 and ubiquitin
5J7T	USP7 CD and UBL123
4YOC	USP7 UBL12345 and DNMT1
5JTJ	USP7 CD and CTP and Ubiquitin
2F1Z	USP7 NTD and CD



2F1Z



5J7T



5JTJ

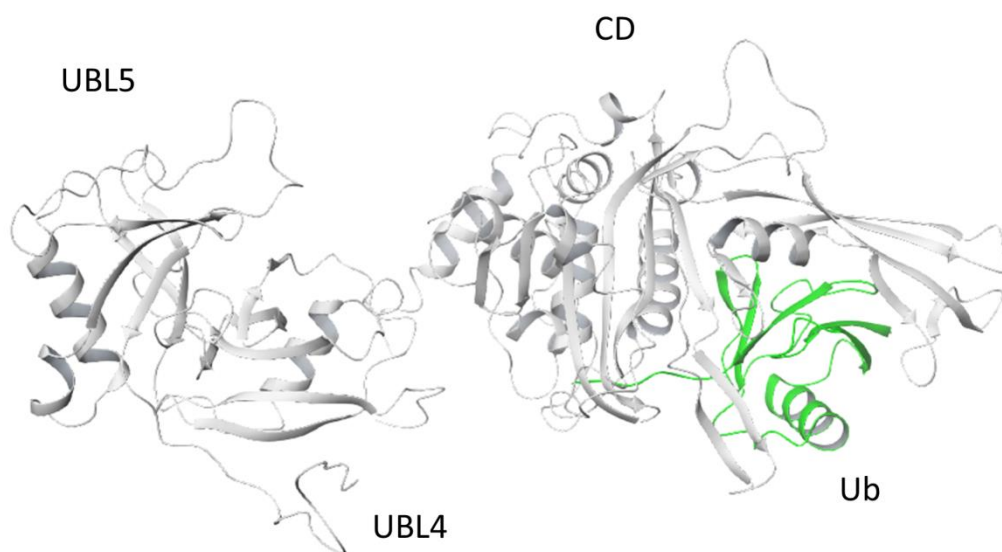
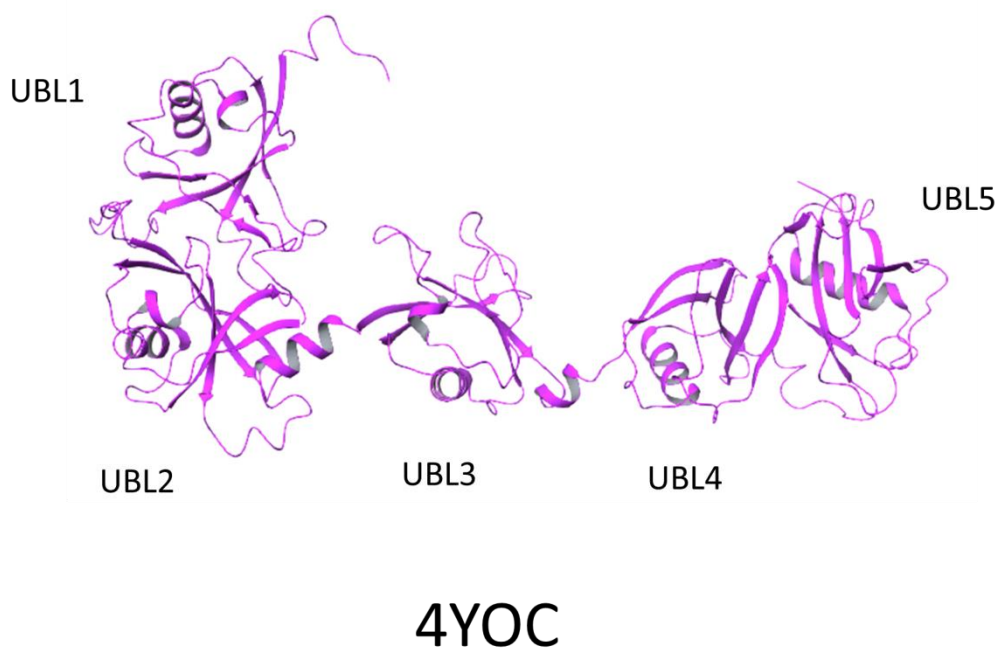


Figure 6-7 Crystal structures of human USP7 used to develop a USP7 full length model. 2F1Z contains the NTD and CD in its inactive form of USP7 and is coloured in purple. 4YOC encloses the five UBLs of USP7 and is coloured in violet. 5J7T comprises the CD and UBL123 from USP7 and is coloured in yellow. 5JTJ is formed by the active CD (pink) and CTP (orange) of USP7 and a ubiquitin molecule (green). 5JTV encompasses the CD and UBL45 from USP7 (light grey) and a ubiquitin molecule (green). All structures were analysed with Maestro Schrodinger software. Each domain is labelled on the structures.

We started with 2F1Z, the only USP7 structure from the PDB files selected containing the NTD. 2F1Z lacks certain loops in its USP7 NTD 3D structure. For this task MOE software was used to model the loops from the real sequence of USP7 and a minimisation process was performed to look for possible rearrangements that would maximise the stability of the protein and to avoid atomic collisions, which were not found (see Figure 6-8).

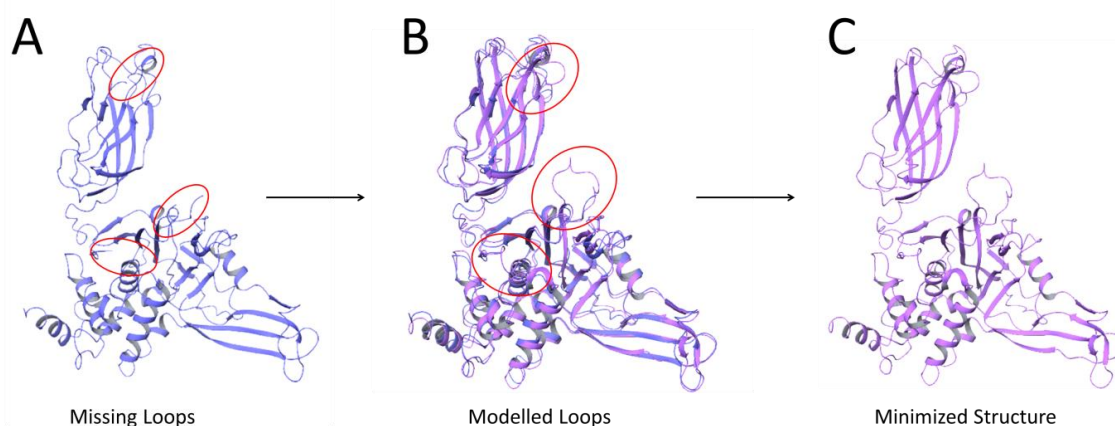


Figure 6-8 USP7 NTD modelling. **A)** Location of the missing loops on 2F1Z 3D structure. Red boxes highlight the location of the missing loops in the 3D structure. **B)** Alignment of the 2F1Z structure (dark purple) with the new modelled NTD-CD structure of USP7 containing the missing loops (light purple). The red boxes mark the overlap between the missing loops and the modelled loops. Loops were modelled with MOE software. **C)** Final modelled structure of USP7 NTD-CD. All structures were analysed with Maestro Schrodinger software.

From structural analysis of USP7 in the absence and presence of ubiquitin, USP7 is known to exist in an inactive and in an active state [299-301]. We structurally aligned the structures of the new modelled USP7 NTD-CD and 5JTJ (see Figure 6-9). 5JTJ structure is in the active conformation of USP7, containing the CTP, which has an important role on USP7 deubiquitinase activity, in the correct location. The crystallised CD on 5JTJ is on the active conformation of USP7 due to its interaction with the ubiquitin molecule. On the other hand, the CD crystallised with the NTD is on its apo conformation (with no substrate interacting with USP7) (see Figure 6-9 and Figure 6-10). In order to create a functionally active model of USP7 3D structure, we required the protein to be on its halo conformation; that is, bound to its ligand. For this reason, we needed to splice the NTD into the active CD conformation. Once the NTD was spliced into the active CD-CTP we looked for possible collisions. There was a loop in the active CD colliding with the NTD (see Figure 6-10). We decided to sculpt the loop in order to avoid the collision. For this purpose, we splitted the new structural

model composed by the NTD-CD-CTP and ubiquitin molecule and continue only with the NTD-CD modelled structure, keeping the CTP and ubiquitin molecule for their addition later on. After sculpting the loop, the new structure was minimised to relax the molecule and look for possible atomic collisions (see Figure 6-11 and Figure 6-12).

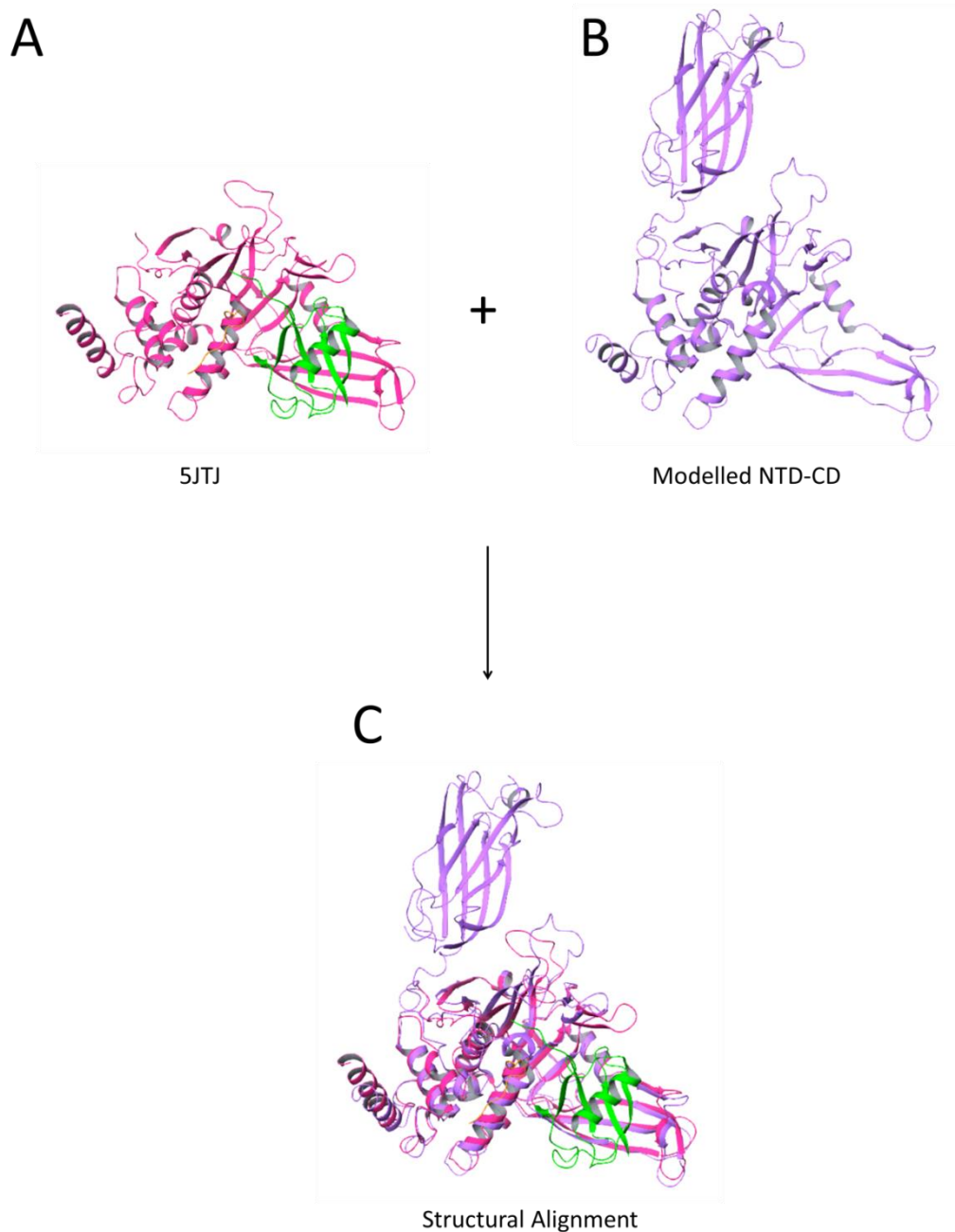


Figure 6-9 Structural alignment of the new modelled NTD-CD USP7 structure and 5JTJ. A) Active CD structure (pink) in complex with USP7 CTP (orange) and a ubiquitin molecule (green) from 5JTJ PDB file. **B)** Structure of the modelled NTD-CD USP7. **C)** Structural alignment of modelled NTD-CD and 5JTJ. Ubiquitin molecule is coloured in green, 5JTJ active CD in pink, 5JTJ CTP in orange and 5JTJ ubiquitin in green. All structures were analysed on Maestro Schrodinger software.

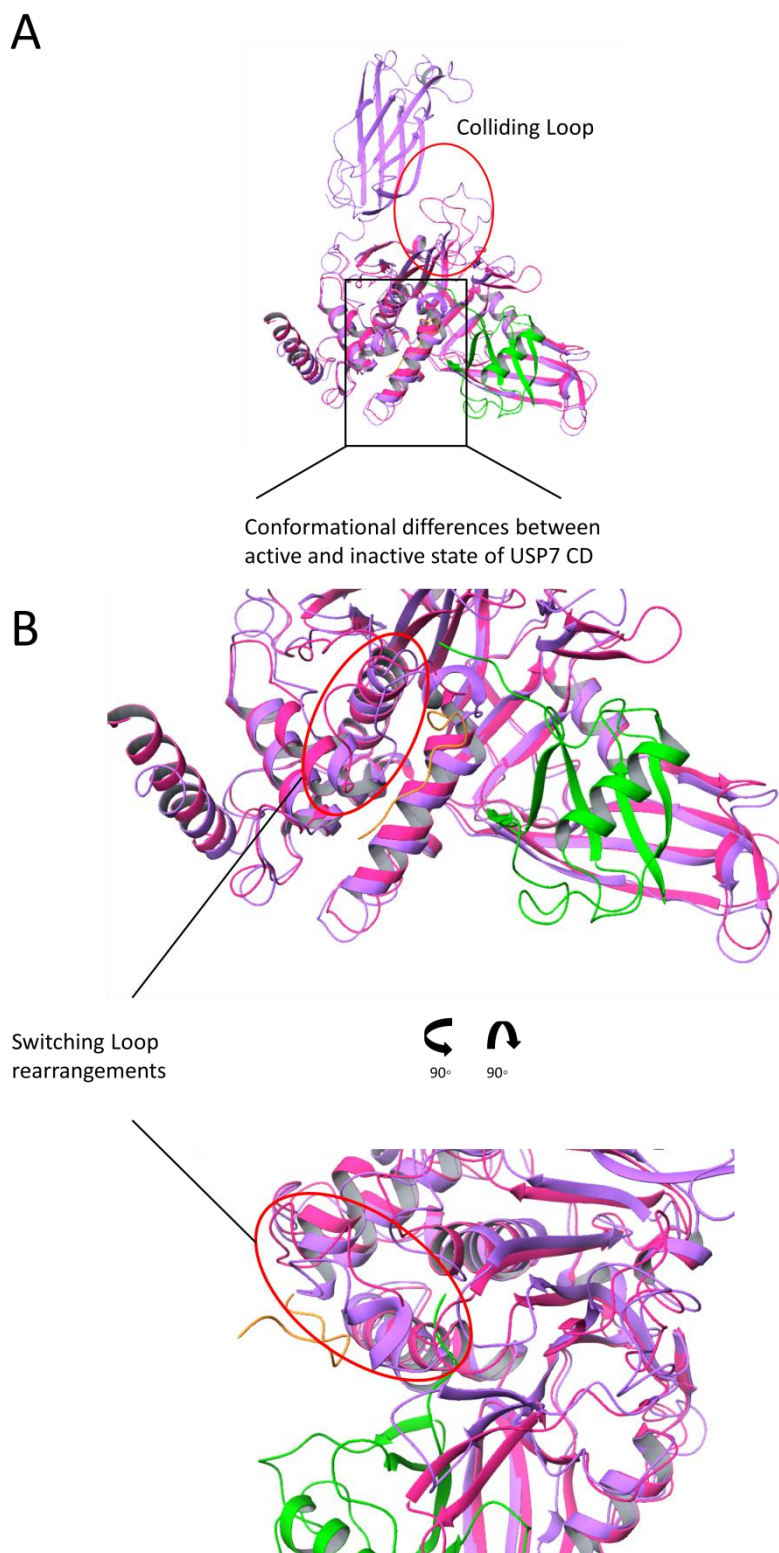


Figure 6-10 Differences between 2F1Z active CD and modelled NTD inactive CD structural conformation. A) General overview of the alignment of both 3D structures. The red circle marks differences in a loop, which collides with the NTD when present. The black box highlights the structural rearrangements on the CD of USP7 due to the conformational rearrangements upon activation. Modelled NTD-CD USP7 is coloured in purple, 2F1Z CD is coloured in pink, 2F1Z CTP in orange and 2F1Z ubiquitin in green. **B)** Zoom-in of the conformational rearrangements of the CD upon activation. Move of the switching loop from an in-conformation to an out-conformation, highlighted in red circles. Location of the CTP on the active cleft. Modelled NTD-CD USP7 is coloured in purple, 2F1Z CD is coloured in pink, 2F1Z CTP in orange and 2F1Z ubiquitin in green. All structures were analysed on Maestro Schrodinger software.

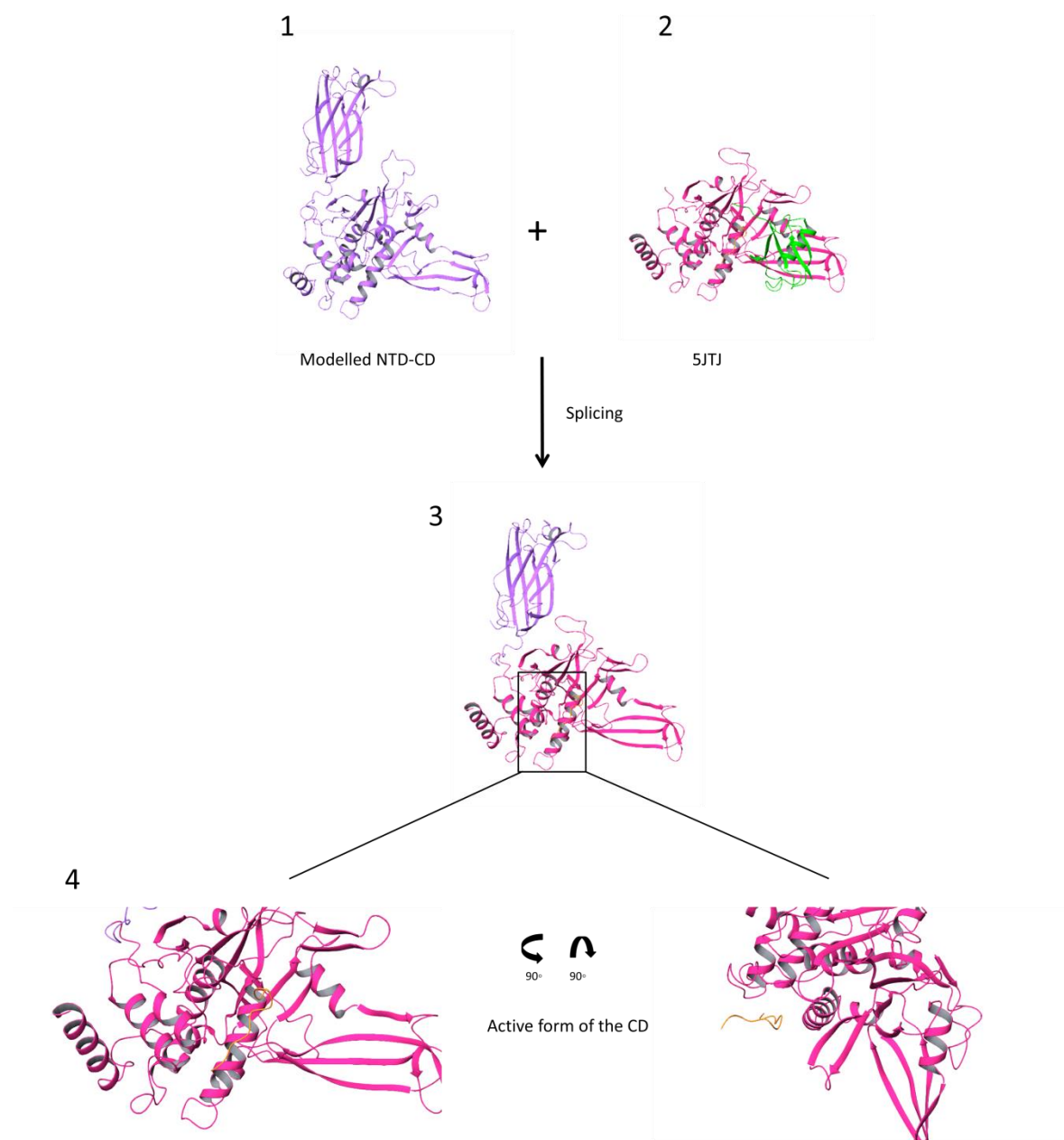


Figure 6-11 USP7 NTD active CD structure modelling. NTD splicing into active CD conformation. 1) Modelled NTD-CD structure coloured in purple. 2) 5JTJ 3D structure containing the active CD of USP7 (pink), the CTP of USP (orange) and a ubiquitin molecule (green). 3) Splicing of NTD (purple) into the active CD of USP7 from 2F1Z (pink). The black box marks the switching loop conformation. 4) Zoom-in of the switching loop out-conformation, active state of the CD of USP7. Active CD part from 2F1Z is coloured in pink, the CTP from 2F1Z is coloured in orange and the NTD-CD from the modelled NTD-CD is coloured in purple. All structures were analysed on Maestro Schrodinger software.

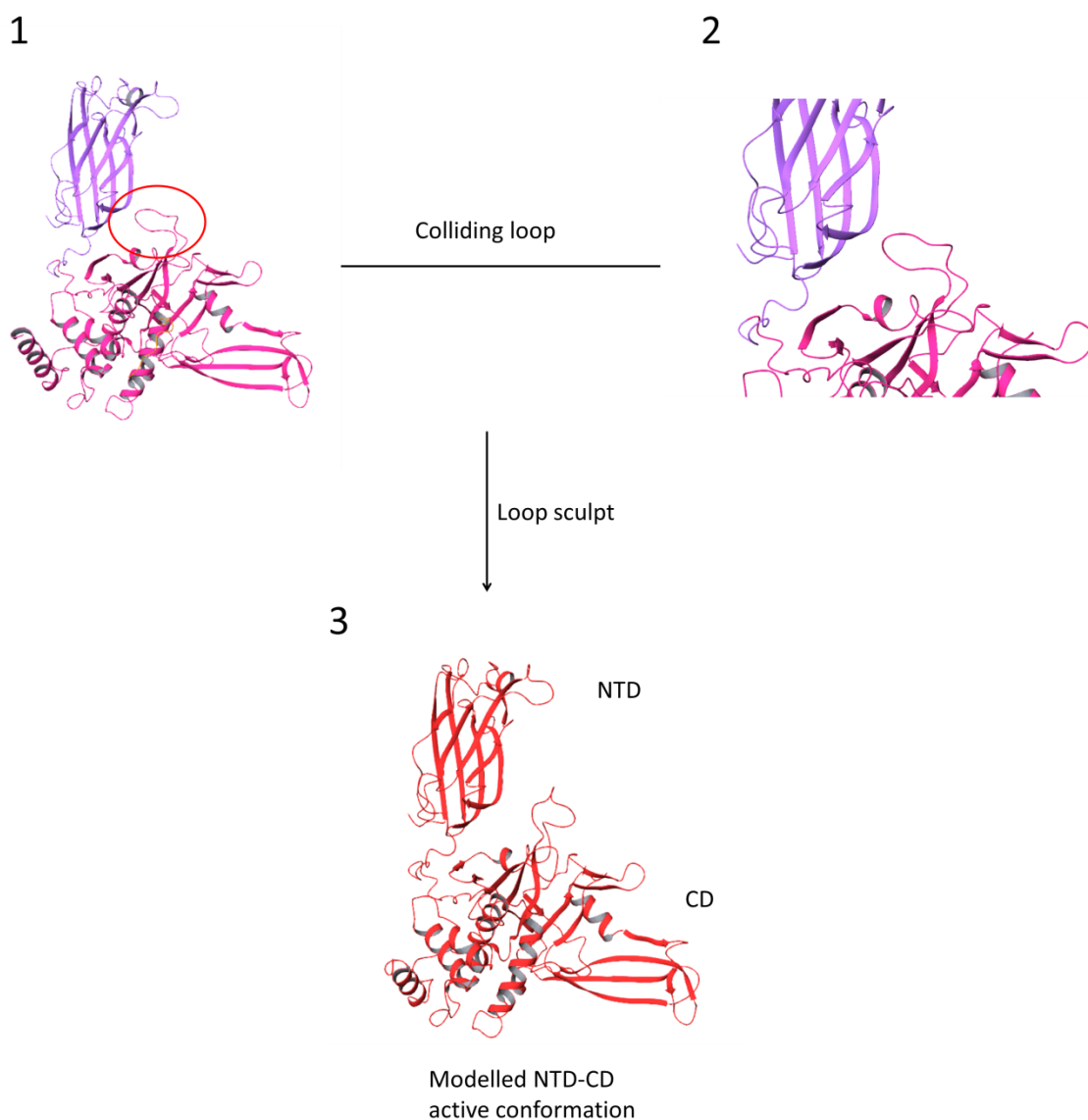
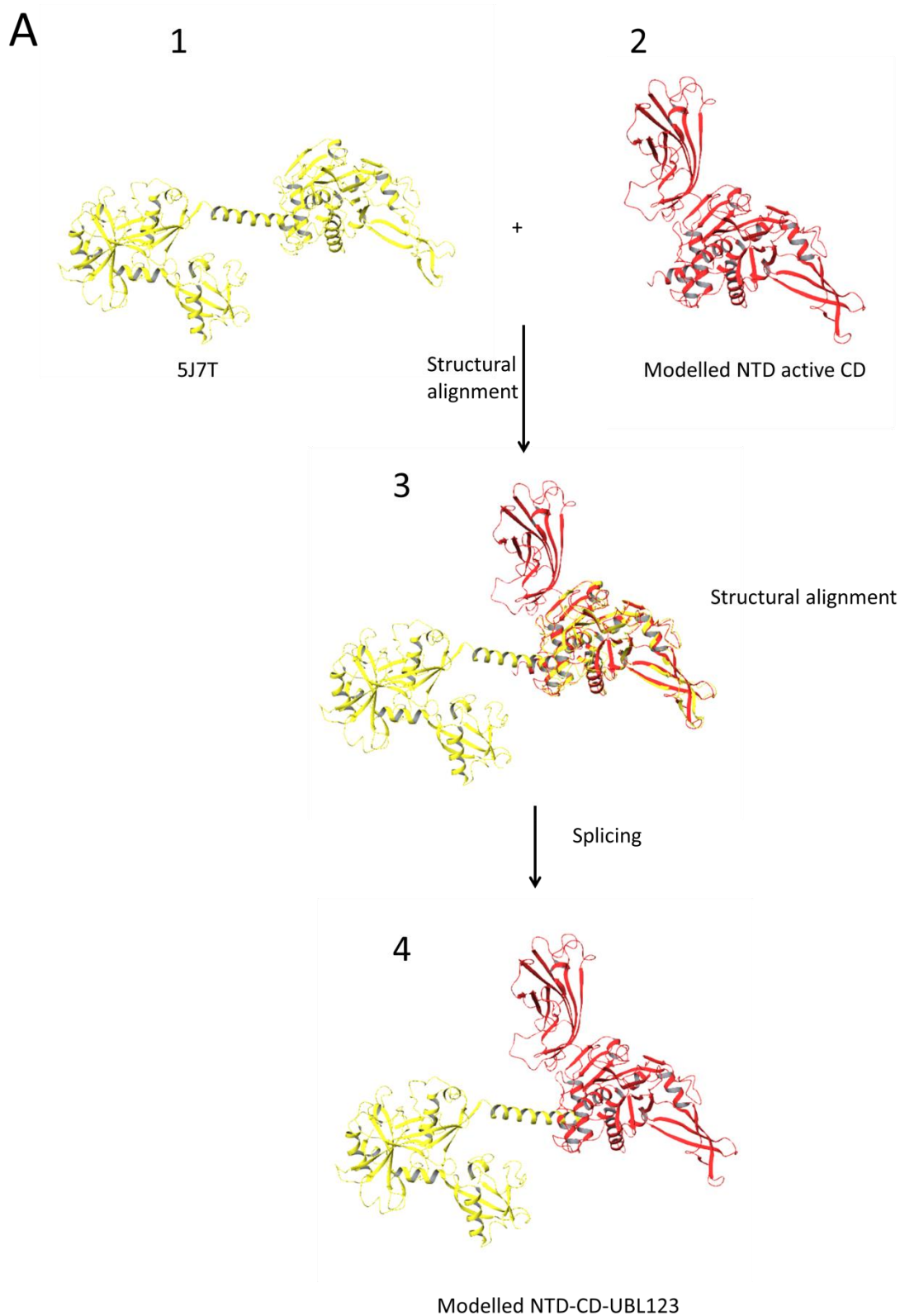


Figure 6-12 Reproduction of the colliding loop from the active CD with the NTD. 1) General overview of the new modelled NTD active CD USP7. Red circle points the colliding loop present on the CD. Active CD part from 2F1Z is coloured in pink, the CTP from 2F1Z is coloured in orange and the NTD-CD from the modelled NTD-CD is coloured in purple. 2) Zoom-in of the colliding loop. Active CD part of 2F1Z is coloured in pink, the CTP from 2F1Z is coloured in orange and the NTD-CD from the modelled NTD-CD is coloured in purple. 3) Loop sculpt, not colliding anymore. Each domain of USP7 is labelled. New modelled NTD active CD is coloured in red. All structures were analysed with Maestro Schrodinger software.

After the minimisation process we continued modelling the C-terminal region of USP7. Therefore, the next step was the addition of the UBLs to the NTD-CD USP7 structure. We first added UBL123 to the model. 5J7T PDB file encompasses the CD of USP7 and UBL123. We aligned the new model NTD-CD with 5J7T structure and spliced the NTD-CD into UBL123 from 5J7T. The structure resulted was formed by USP7 NTD-CD-UBL123 (see Figure 6-13). After relaxing the newly formed structure and confirming no collisions between atoms, we continued modelling the full length USP7. Next step was to add the UBL45 region. For UBL45 we had two different conformations; an elongated arrangement (4YOC) and a more compact arrangement (5JTV). We aligned both structures with the new modelled USP7 NTD-CD-UBL123 (see Figure 6-14 and Figure 6-15). The alignment with 4YOC, kept UBL45 far away from the catalytic triad and the CTP. Moreover, alignment with 5JTV contained UBL45 in a compact form close to the CD but far away from UBL123. Following the model from Rouge et al [299], we spliced the new NTD-CD-UBL123 into UBL45 of 4YOC PDB structure and ran a minimisation process to relax the new structure (see Figure 6-16). Having USP7 NTD-CD-UBL12345 the only part missing was the C-terminal region. PDB file 5JTJ contains the CTP in the active form, located in the activation cleft. The next step was to bond the newly created structure with the CTP from 5JTJ. There was a gap of 9 amino-acids (KAPKRSRYT) between the end of UBL5 and the CTP (see Figure 6-17). However, the distance between the end of UBL5 and the CTP was bigger than the distance covered by the addition of the nine amino-acids missing. For this reason, distance constraints were used to get UBL45 closer to the CD and a minimisation process was performed. During the process some secondary structures of UBL45 were disrupted (see Figure 6-17). The disrupted secondary structures of UBL45 were fixed through the addition of some distance and angles constraints, to maintain the appropriate helical turn, during a minimisation process. Once the distance was appropriate; the missing amino-acids were added following the USP7 sequence and taking into account the presence of the ubiquitin molecule for CTP's proper location within USP7 active structural conformation (see Figure 6-17). Then, the newly created structure was spliced into the CTP to give a full length (except the first 63 amino-acids) USP7 structural model (see Figure 6-17). To make sure the model was in a stable conformation with no atoms colliding; we run a minimisation process to relax the molecule. Subsequently, a molecular dynamics process was performed to

identify the most stable conformation for the new USP7 structure (see Figure 6-18). After this process, full length USP7 structure was ready for future docking experiments.



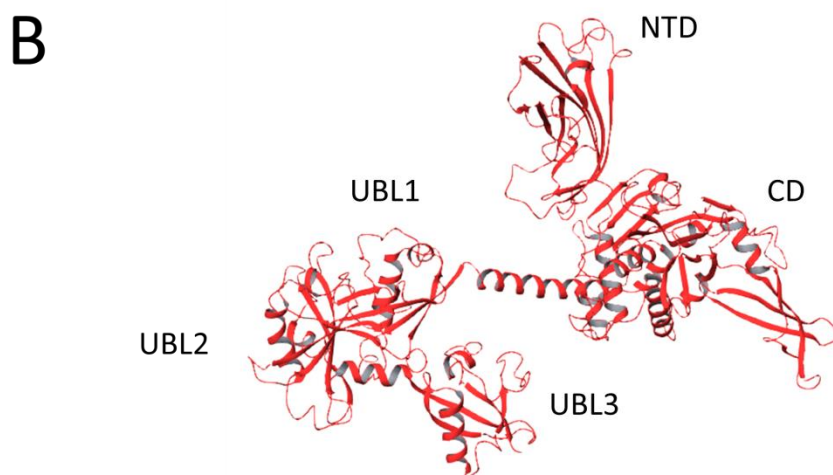


Figure 6-13 USP7 NTD-CD-UBL123 structural modelling. A) Modelling steps to create USP7 NTD-CD-UBL123 structure. 1) 5J7T structure containing the CD and UBL123 of USP7. 5J7T structure is coloured in yellow. 2) Modelled NTD active CD structure coloured in red. 3) Alignment of 5J7T structure (yellow) and modelled USP7 NTD active CD (red). 4) Splicing of modelled USP7 NTD active CD (red) into UBL123 from 5J7T (yellow) to form the new USP7 NTD-CD-UBL123 structure. **B)** Newly modelled USP7 NTD-CD-UBL123 structure with each USP7 domain labelled. All structures were analysed with Maestro Schrodinger software.

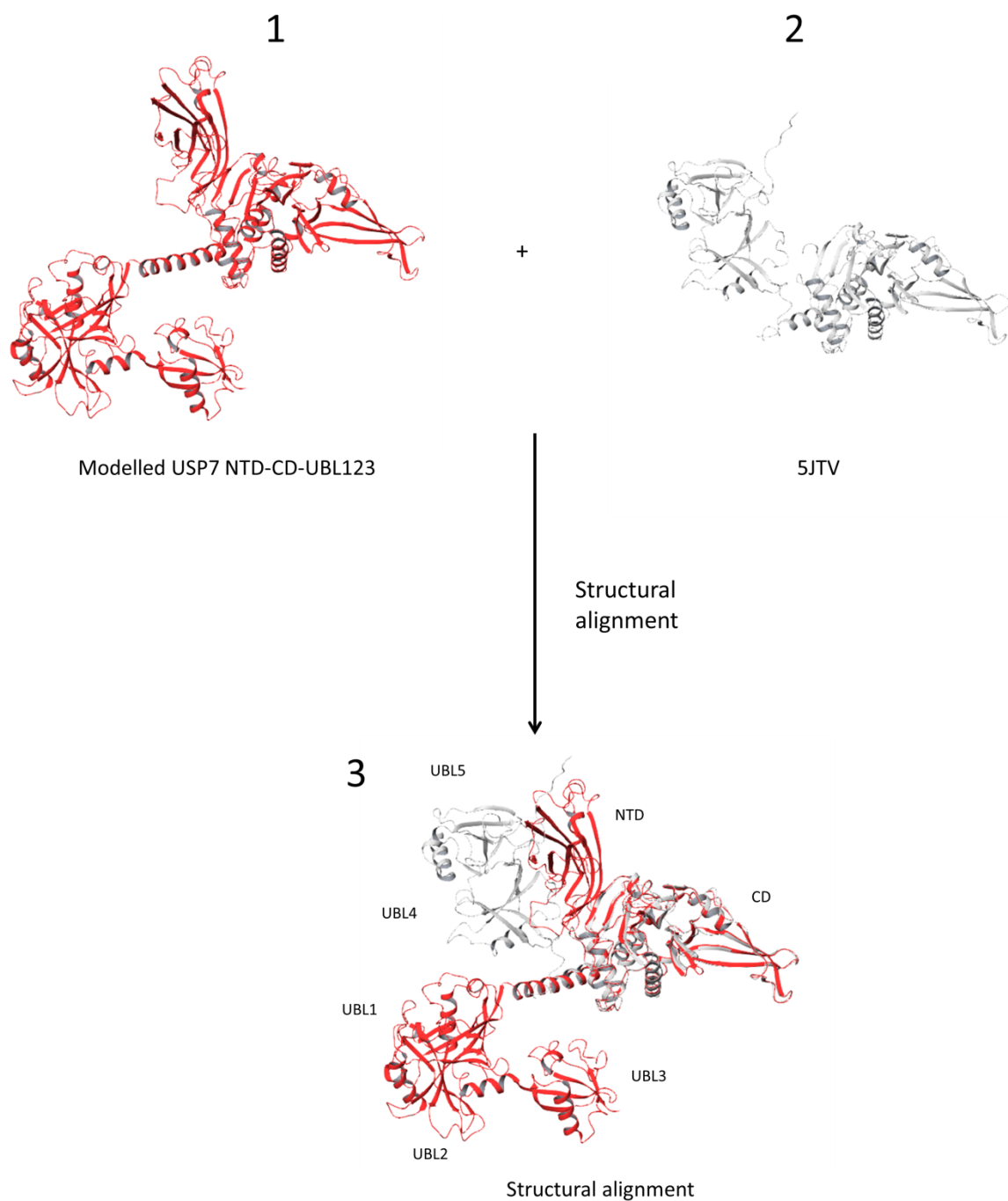


Figure 6-14 Modelled USP7 NTD-CD-UBL123 alignment with 5JTV. 1) Modelled USP7 NTD-CD-UBL123 structure coloured in red. 2) 5JTV structure coloured in grey. It contains USP7 CD and UBL45. 3) Modelled USP7 NTD-CD-UBL123 (red) structural alignment with 5JTV (grey). Each domain of USP7 is labelled on the structure. All 3D structures were analysed with Maestro Schrodinger Software.

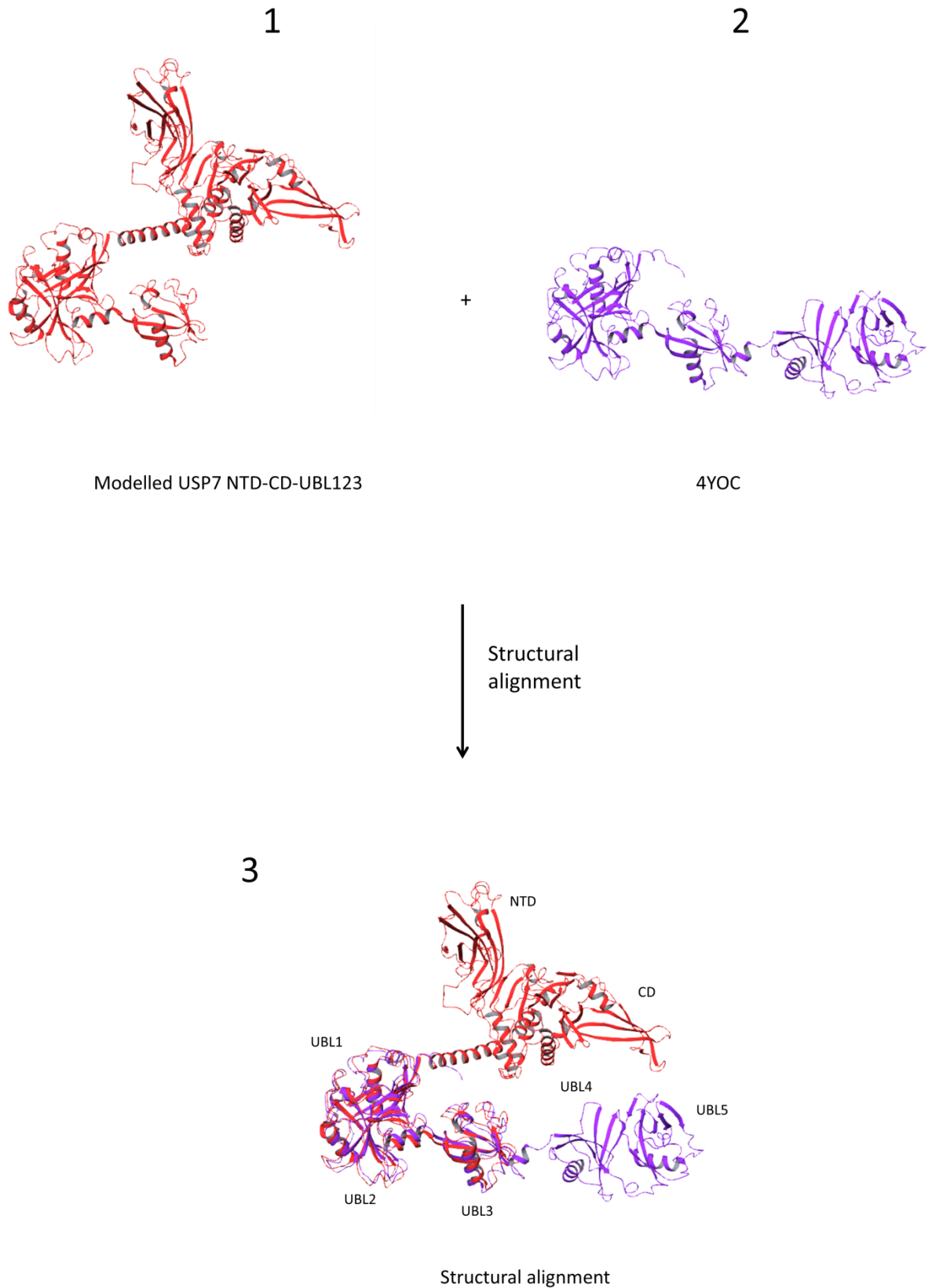


Figure 6-15 Modelled USP7 NTD-CD-UBL123 alignment with 4YOC. 1) Modelled USP7 NTD-CD-UBL123 structure coloured in red. 2) 4YOC USP7 UBL12345 coloured in violet. 3) Modelled USP7 NTD-CD-UBL123 (red) structural alignment with 4YOC (violet). Each domain of USP7 is labelled on the structure. All structures were analysed with Maestro Schrodinger software.

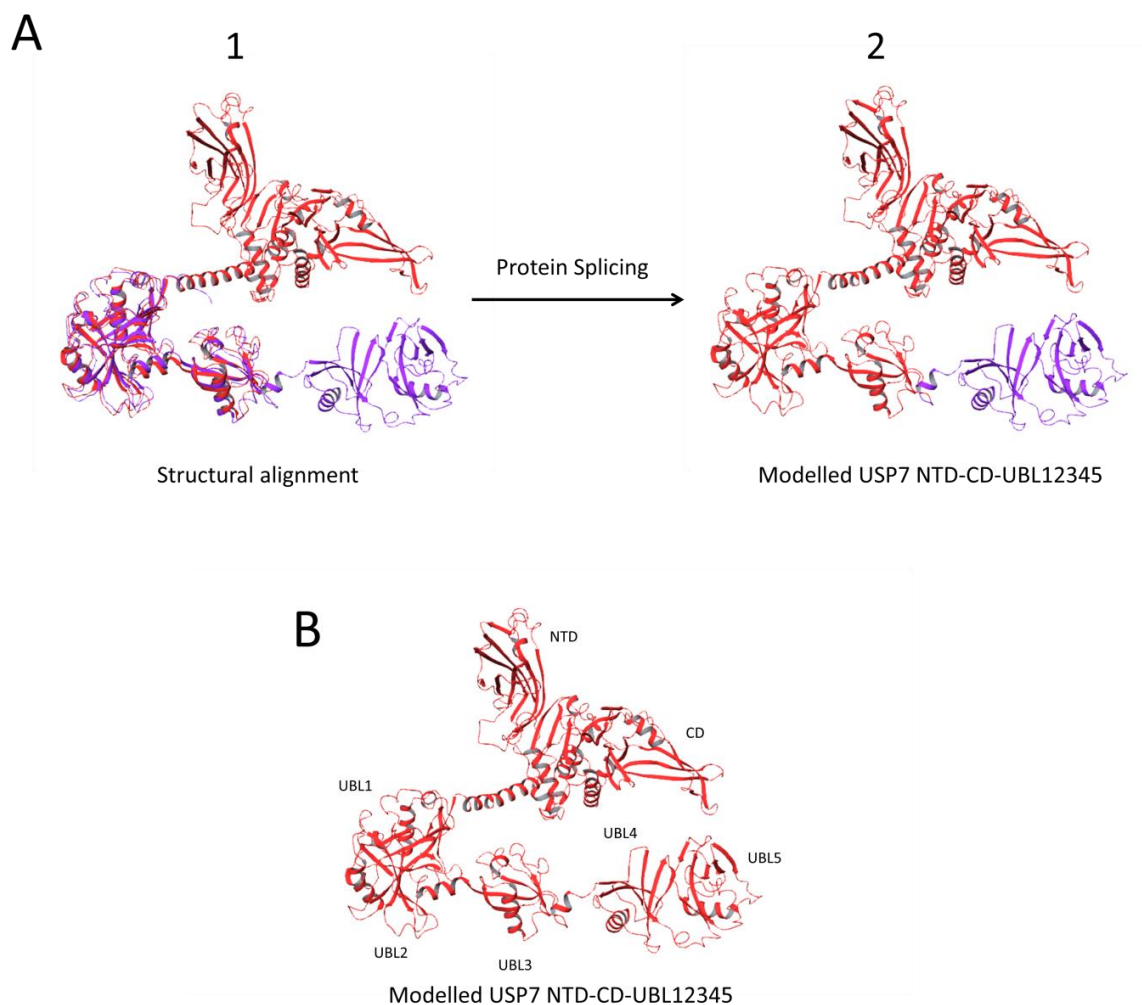
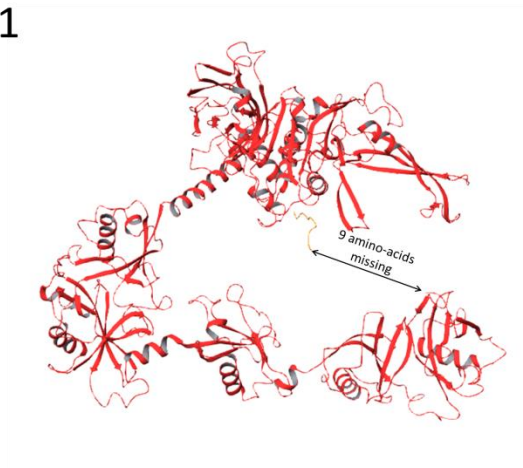


Figure 6-16 USP7 NTD-CD-UBL12345 structural modelling. A) Modelling steps to create USP7 NTD-CD-UBL12345 structure. 1) Structural alignment of 4YOC (USP7 UBL12345) structure (violet) and modelled NTD-CD-UBL123 (red). 2) Splicing of modelled USP7 NTD-CD-UBL123 (red) and 4YOC USP7 UBL12345 (violet). **B)** Modelled USP7 NTD-CD-UBL12345 coloured in red. Each domain of USP7 is labelled. All structures were analysed with Maestro Schrodinger software.

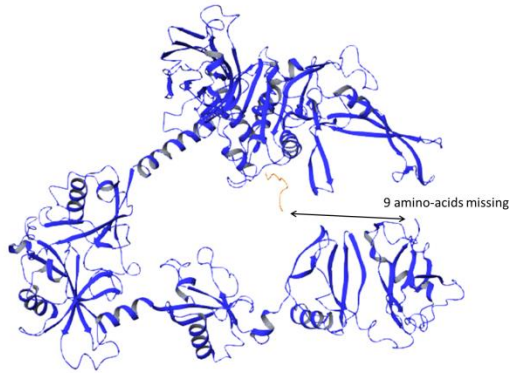
A

1



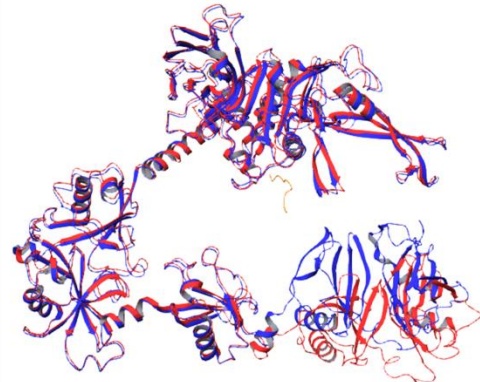
Distance
constraints

2



Differences

3



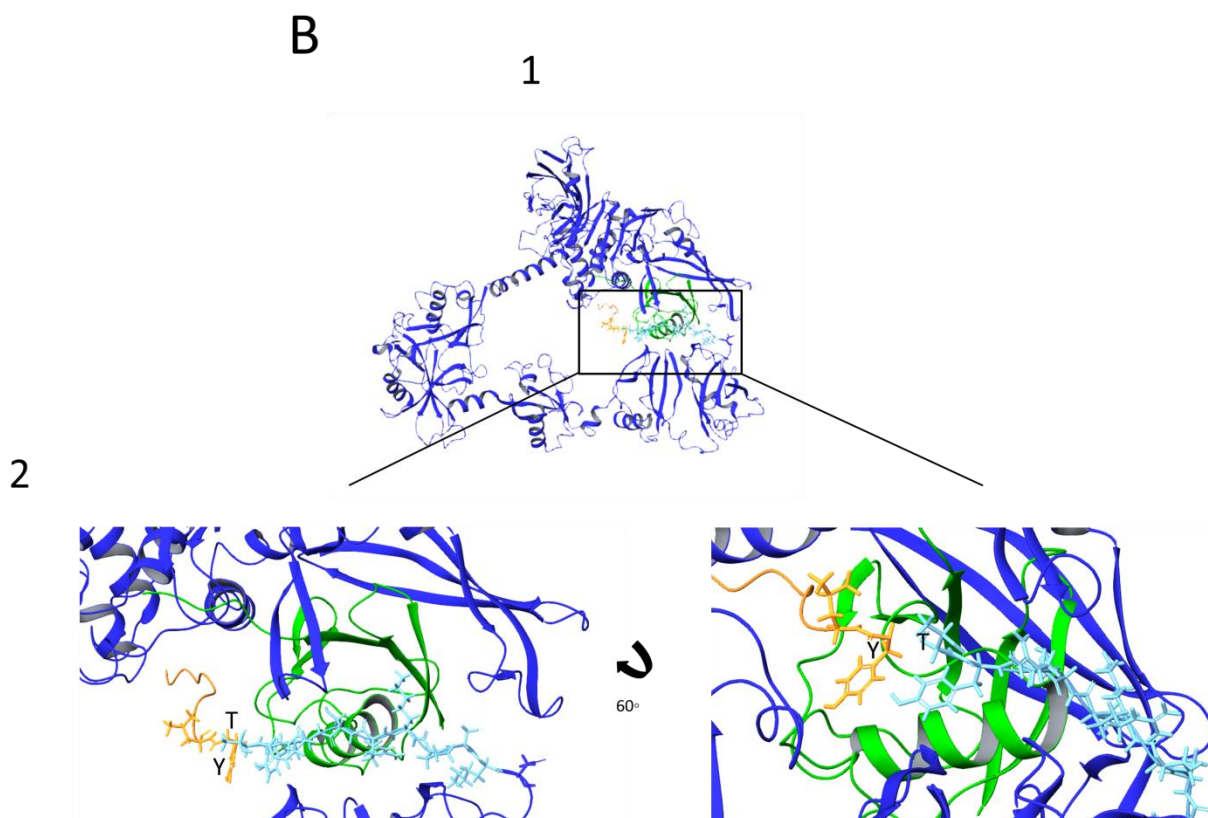
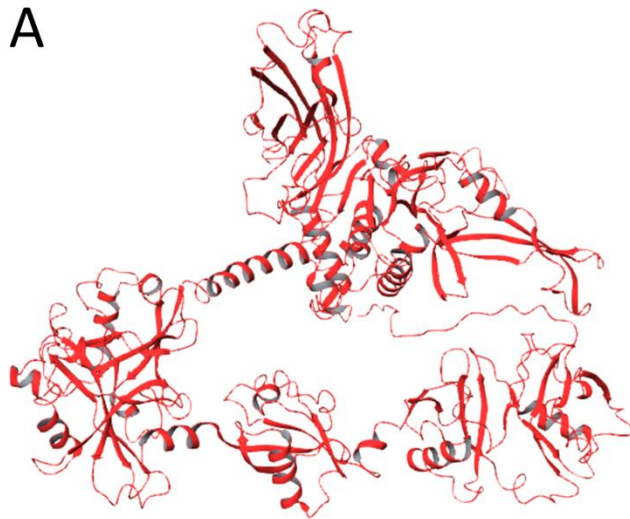
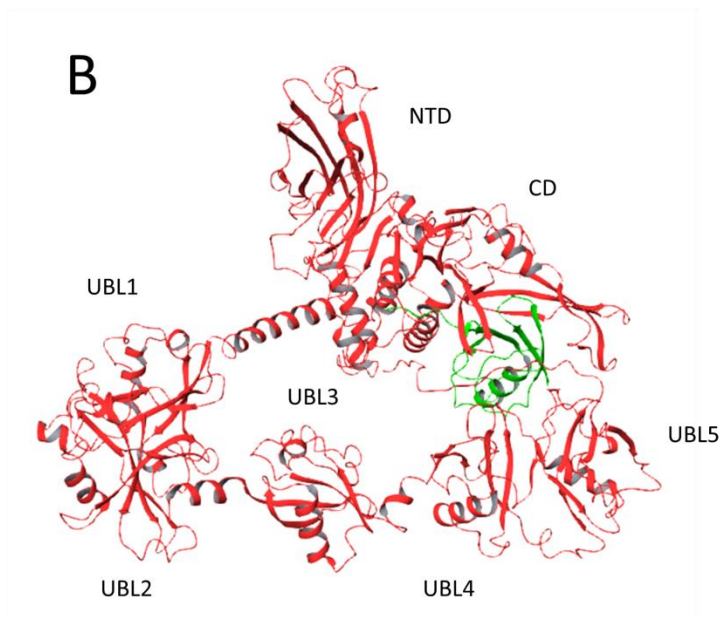


Figure 6-17 USP7 CTP connection to modelled USP7 NTD, CD, UBL12345. **A)** UBL45 approach to the CD. 1) Modelled NTD-CD-UBL12345 USP7 (red) among with the CTP (orange). 2) UBL45 converge to CD. USP7 NTD-CD-UBL12345 structure is coloured in blue and USP7 CTP in orange. 3) Comparison of the secondary structure differences between modelled USP7 NTD-CD-UBL12345 before (red) and after (blue) the UBL45 approach to the CD. USP7 CTP is coloured in orange. **B)** Addition of the 9 missing amino-acids (KAPKRSRYT) to the molecule. 1) General overview of the addition of the 9 missing amino-acids. The box in black marks the distance between last added amino-acid (T) and the first amino-acid from the CTP (Y). USP7 NTD-CD-UBL12345 is coloured in dark blue, the CTP in orange, the added amino-acids in light blue and ubiquitin in green. 2) Zoom-in of the distance between last added amino-acid (T) and the first amino-acid from the CTP (Y). USP7 NTD-CD-UBL12345 is coloured in dark blue, the CTP in orange, the added amino-acids in light blue and ubiquitin in green. All structures were analysed with Maestro Schrodinger software.



Full length USP7

MD
↓



MD of the full length USP7 in complex with ubiquitin

Figure 6-18 Molecular Dynamics of the full length USP7 model structure in complex with ubiquitin. **A)** Full length USP7 molecule. **B)** Relaxed full length USP7 molecule in complex with ubiquitin as the result of the molecular dynamics process. USP7 molecule is coloured in red and ubiquitin in green. Each domain of USP7 is labelled on the structure. All structures were analysed with Maestro Schrodinger software.

6.3.3 USP7-p65 complex model

Considering the previous data about USP7 binding pockets and the number of possible p65 ubiquitinated lysines, we designed three different models. As the full length USP7 was modelled taking into account the 3D structure of a ubiquitin molecule (which in nature will correspond with the ubiquitin bound to the ubiquitinated substrate) located in the appropriate position for USP7 deubiquitinase activity, we incorporated the ubiquitin molecule structure to USP7 full length model. For the first model, we incorporated the possible ubiquitinated lysines of p65; bonding the lysine to the ubiquitin molecule present on USP7 full length structural model. The other two models were based on the positively charged motif (R/KxR/KxxxR/K) of p65 and USP7 UBL2 binding pocket, forming part of the binding interface.

6.3.3.1 No lysine specificity detected on USP7 deubiquitinase activity

We studied the preference of USP7 to deubiquitinate various ubiquitinated lysines on p65 as K56, K62 and K123. p65 K56, K62 and K123 were selected according to sequence homology between NF- κ B members of the homologous regions surrounding those lysines (see appendix 8.6). Mutation of these lysines to arginine maintains the physicochemical properties of the protein but prevents ubiquitination at those sites. If USP7 specifically recognises a ubiquitinated lysine, when that lysine is mutated to arginine the interaction between USP7 and p65 will be affected.

We cloned murine p65 WT, p65K56R, p65K62R and p65K123R into pCDNA3.1 in order to remove the FLAG-tag from the original plasmids (see appendix 8.2). HEK293T cells were co-transfected with murine p65 WT, p65 K56R, p65 K62R and p65 K123R plasmids along with USP7 FLAG-tagged plasmid. Cellular extracts were immunoprecipitated with an anti-FLAG antibody and immunoblotted with antibodies anti-p65 protein and anti-FLAG tag. The interaction between USP7 and p65 mutants is equivalent between WT and K56R, K62R and K123R mutants; there is no affinity for any of the lysines (see Figure 6-19). This result suggests that USP7 acts on several different ubiquitinated lysines on p65; therefore, USP7 does not have a preference for interaction with p65 ubiquitinated at specific lysines.

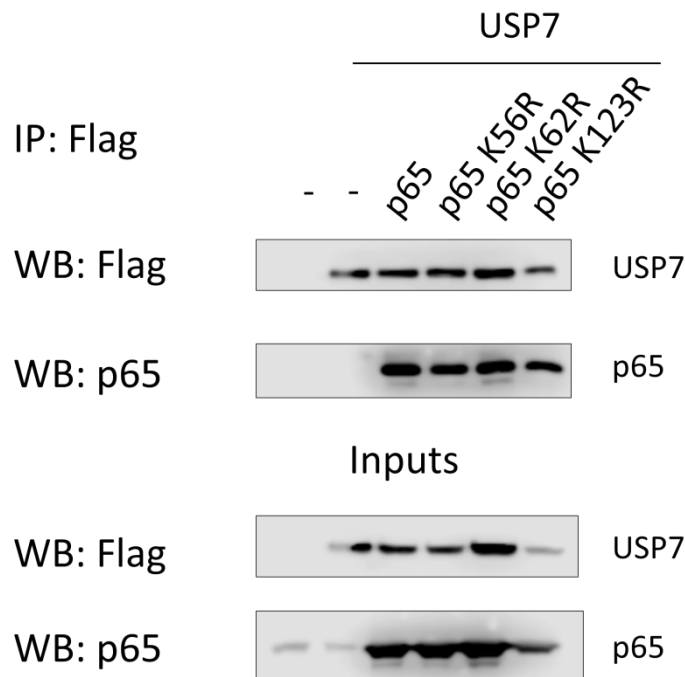


Figure 6-19 USP7 has no specificity for K56, K62 or K123. HEK293T cells were co-transfected with murine p65 WT, p65 K56R, p65 K62R and p65 K123R plasmids along with FLAG-tagged USP7. Cellular lysates were immunoprecipitated with anti-FLAG antibody and immunoblotted with anti-FLAG and anti-p65 antibodies. USP7 has no preference for ubiquitinated K56, K62 or K123. The figure is a representative of three independent experiments.

6.3.3.2 Model of USP7-p65 interaction when p65 is ubiquitinated at K62

PDB files 5JTV and 5JTJ used in USP7 full length modelling contain a ubiquitin molecule. Merging both structures, the location of the possible ubiquitinated lysine is quite well defined. The lysine of p65 which would be ubiquitinated has to bind the G76 residue of ubiquitin molecule, and be at a feasible distance from the catalytic triad as it would happen when the ubiquitin bound to p65 locates in the appropriate location for USP7 deubiquitinase activity (see Figure 6-20). Based on the steric conformation of p65, K62 is the most accessible ubiquitinated site on p65 (see Figure 6-20). Hence, we decided to dock the p50-p65-DNA complex structure on USP7 full length structure where p65 is ubiquitinated at K62.

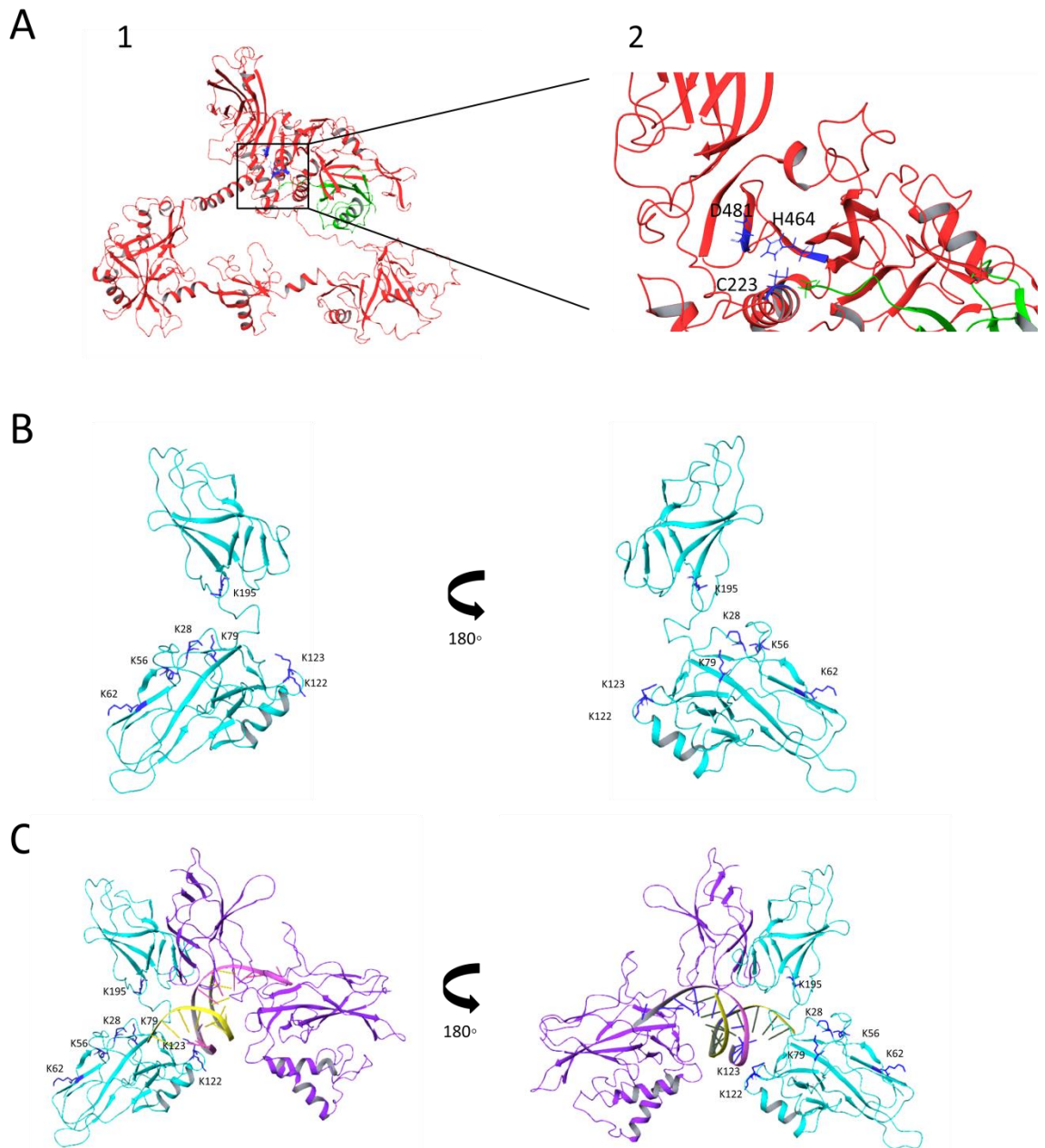


Figure 6-20 Definition of the interacting site of USP7 with p65 ubiquitinated lysine. A) Location of the catalytic triad on USP7 and ubiquitin molecule. 1) General overview of USP7 catalytic triad and ubiquitin molecule location on USP7 full length molecule (coloured in red). USP7 catalytic triad (C223, H464, D481) is coloured in blue and ubiquitin molecule is coloured in green. The black box marks the location of the catalytic triad and ubiquitin G76. Zoom-in of the catalytic triad and ubiquitin G76 location. USP7 full length model is coloured in red, USP7 catalytic triad (C223, H464, D481) is coloured in blue and ubiquitin molecule is coloured in green. **B)** Different views of truncated p65 structure from PDB file 1VKX (amino-acids 19-291) with the known ubiquitinated lysines coloured in dark blue. **C)** Different views of p50-p65 heterodimer in complex with DNA structure from PDB file 1VKX (p50 amino-acids 39-364 and p65 amino-acids 19-291). p65 is coloured in light blue with the known ubiquitinated lysines coloured in dark blue. p50 is coloured in purple and the DNA helix in yellow and pink. All structures were analysed with Maestro Schrodinger software.

6.3.3.2.1 K62

Lysine 62 of p65 is ubiquitinated by the E3 ligase ING4 promoting p65 degradation [39]. Due to steric characteristics of the heterodimer in complex with the DNA helix, K62 is the most accessible lysine. As both binding interfaces were defined, we next performed manual docking. K62 has to form a bond with G76 of ubiquitin and be at an appropriate distance from the catalytic triad of USP7. One obstacle on the docking was the presence of the DNA helix. The DNA helix was elongated and bent into the appropriate conformation to fit in the model (see Figure 6-21). In this model, K62 forms a bond with G76 of ubiquitin and is located in the centre of the USP7 full length molecule (see Figure 6-22). We hypothesised that the DNA helix bends in a way that also goes in between the USP7 molecule (see Figure 6-23). We proposed a mechanism for this model in which the heterodimer in complex with the DNA binds to USP7 and USP7 undergoes conformational rearrangements to locate the heterodimer in the centre. More specifically, USP7 molecule is in an open conformation and when p65 binds to the molecule it closes; getting UBL45 and the CTP closer to the CD, and surrounding the p50-p65-DNA complex which stays in the middle of USP7 molecule. If the mechanism is correct, contacts between USP7 and the DNA may be important in the interaction. Structurally, this model is quite compact, with almost no gaps in between molecules (see Figure 6-23). The presence of gaps in the interaction interface leads to the presence of solvent molecules which could interfere with the interaction. One disadvantage of the model is the missing part of p65. The missing region of p65 contains K310, K314 and K315, three possible ubiquitination sites [468]. If we focus on the p65 structure, most of the contacts between USP7 and p65 are located on UBL1 and UBL3, while UBL45 is in contact with the DNA helix. The full complex, once modelled, was relaxed by a minimisation process. The minimisation process helped to detect the presence of any atomic collisions and select the most stable conformation of the structure of the complex.

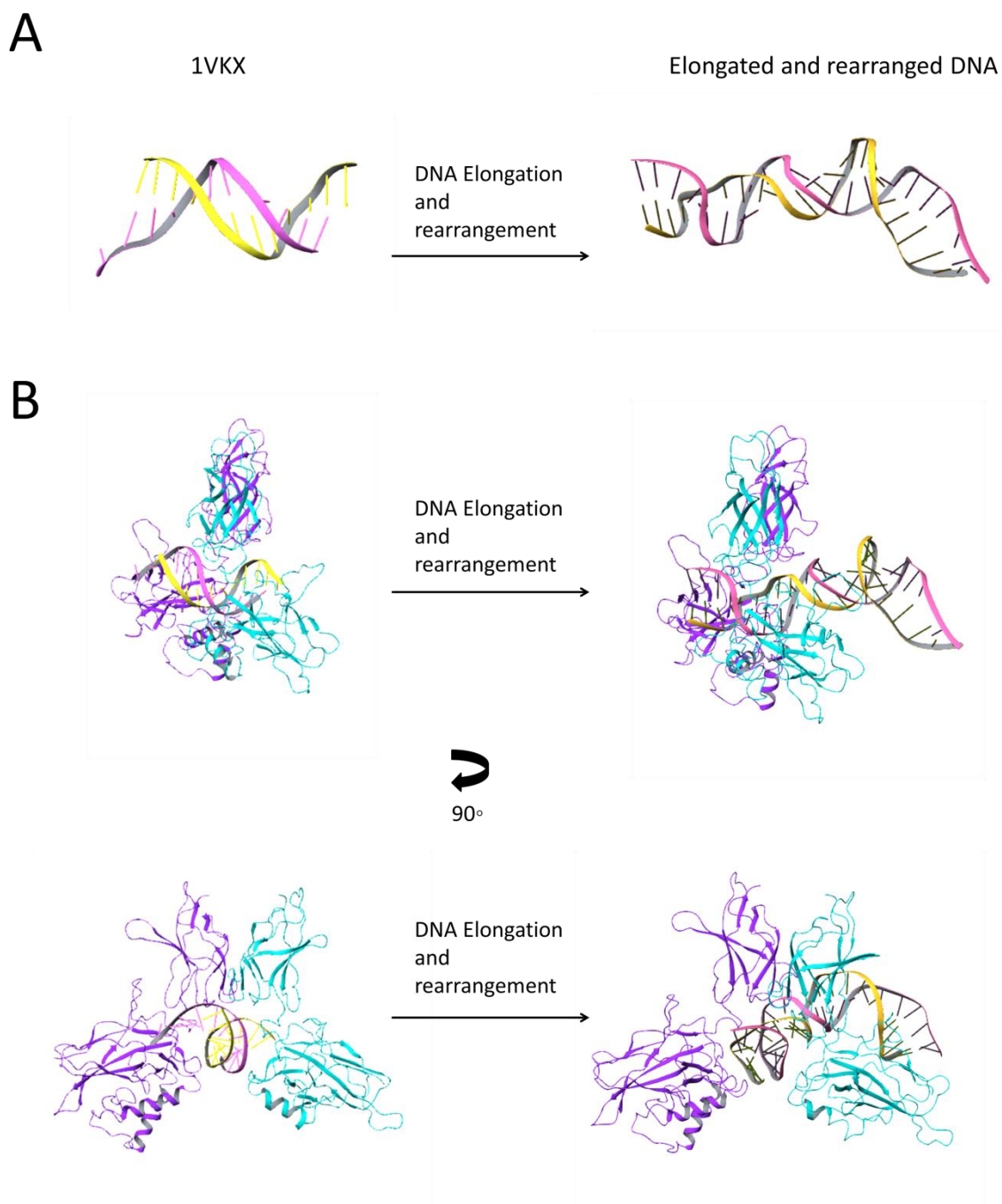


Figure 6-21 DNA helix elongation and rearrangement. A) Comparison of the DNA helix solved in the crystal structure of 1VKX with the DNA helix modelled to fit in the model. The DNA helix is coloured in yellow and pink. The DNA helix was elongated to model possible interactions with USP7 molecule. In order to fit in the model, the DNA helix was bent. **B)** Comparison of p50-p65 heterodimer (p50 amino-acids 39-364 and p65 amino-acids 19-291) in complex with the DNA helix solved in 1VKX and the heterodimer in complex with the modelled DNA helix. Different views of the complex. p65 protein is coloured in blue, p50 in purple and the DNA helix in yellow and pink. The DNA helix was elongated to model possible interactions with USP7 molecule. In order to fit in the model, the DNA helix was bent. All structures were analysed with Maestro Schrodinger software.

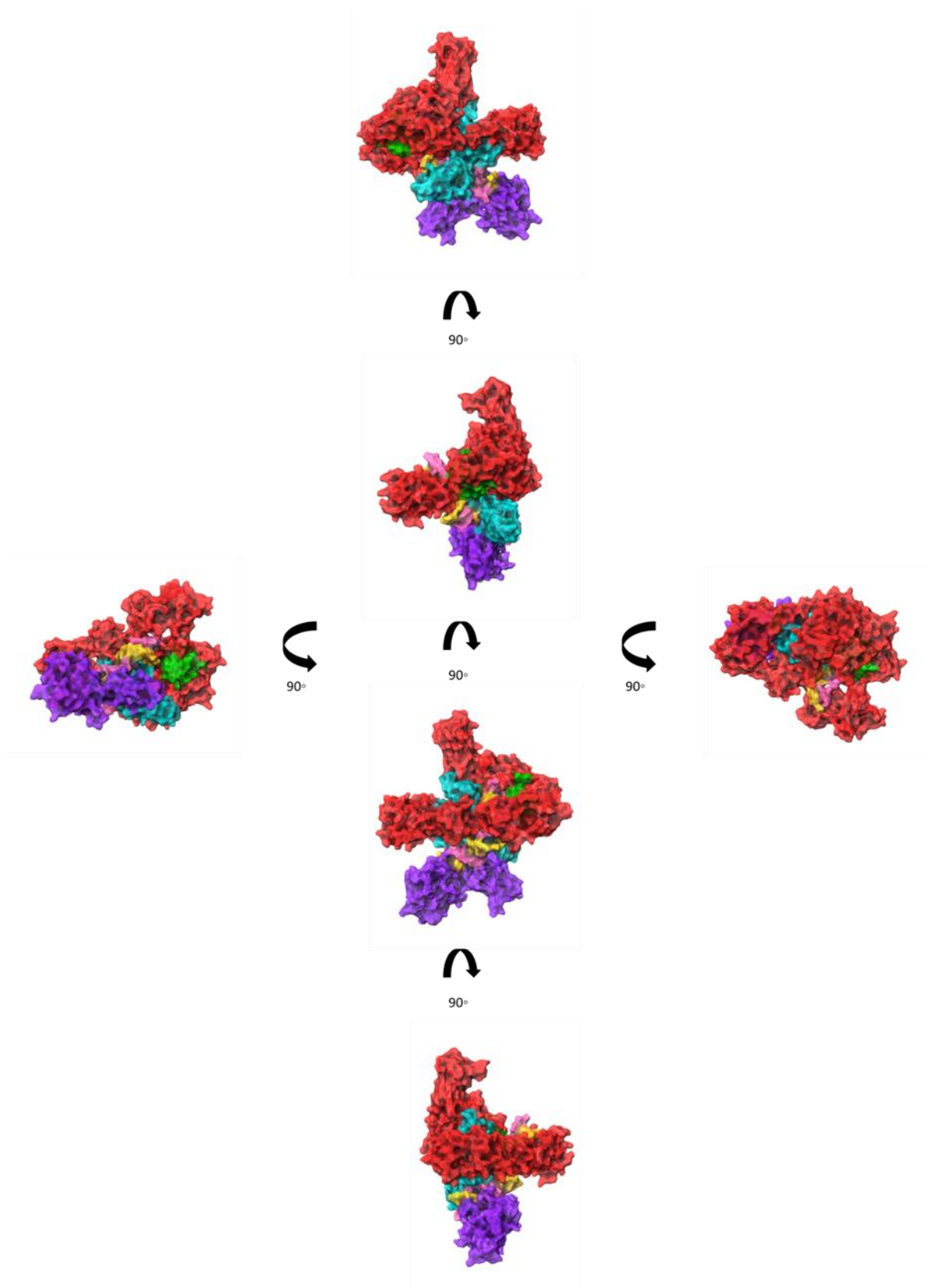


Figure 6-23 Surface model of the USP7-p65/p50/DNA complex based on ubiquitination of p65 K62. Different views of the complex. USP7 is coloured in red, p65 in blue, p50 in purple, ubiquitin in green and the DNA helix in yellow and pink. All structures were analysed with Maestro Schrodinger software.

6.3.3.3 Model of USP7-p65 interaction based on p65 R/KxR/KxxxR/K motif interaction with USP7 UBL2 binding pocket

Recent studies on USP7 substrate recognition identified the binding site on UBL2 of USP7 for substrates recognised by the C-terminal region [20, 21]. Pfoh et al described a peptidic sequence on ICP0 containing a KxxK motif required for USP7 binding [41]. The complementary region identified on USP7 which form part of the binding site was composed by amino-acids 758-DELMDGD-764, being D762 and D764 the amino-acids forming the interacting bonds with the lysines on KxxxK motif of ICP0 [41]. D762 and D764 when mutated to alanine or arginine are able to disrupt the interaction with ICP0, GMPS and UHRF1 [41]. Kim and Sixma investigated the positively charged motif present on the substrates binding to the C-terminal region of USP7 [418]. They identified a R/KxKxxxK motif on ICP0, DNMT1 and UHRF1 [418]. Using peptidic sequences of each substrate containing this motif they crystallised them in interaction with UBL2 of USP7 [418]. Comparing the interaction between the three substrate peptidic sequences with UBL2 we designed a binding pocket on USP7. This binding pocket is formed by amino-acids 627-ARSNGTK-633, 736-EEVKPNLTER-745 and 757-LDELMDGD-764 (see Figure 6-24 and Figure 6-25). Comparing the amino-acids forming the binding pocket to those identified as important by our experimental data from the peptide array and subsequent alanine scan, we found that the identified K633, L757, D758, E759 and L760 amino-acids are located within the binding pocket. From the co-immunoprecipitation assays data, we know that mutation on L757, D758, E759 and L760 does not inhibit the interaction. We modelled the interaction in that binding pocket in order to provide more details on the possibility of those amino-acids participating in the interaction.

Having the binding pocket defined in USP7 we needed to define the interacting amino-acids on p65. As discovered by Pfoh et al and Kim and Sixma [41, 418], the interaction of USP7 with ICP0, DNMT1, UHRF1 and GMPS takes place through a positively charged region on the substrates. We analysed the p65 sequence for the presence of a similar motif on p65 (human and murine) sequence with Geneious software. This analysis identified two similarly positively charged motifs on p65. The first identified motif is 35-RYKCECR-41, and the second motif is 295-RHRIEEK-301 (see Figure 6-26). Using these motifs of p65 and the binding

pocket of USP7, we manually docked them in order to get a model of USP7-p65 interaction which could help defining future experiments. Identification of these positively charged motifs within different USP7 substrates' sequence is shown on appendix 8.7.

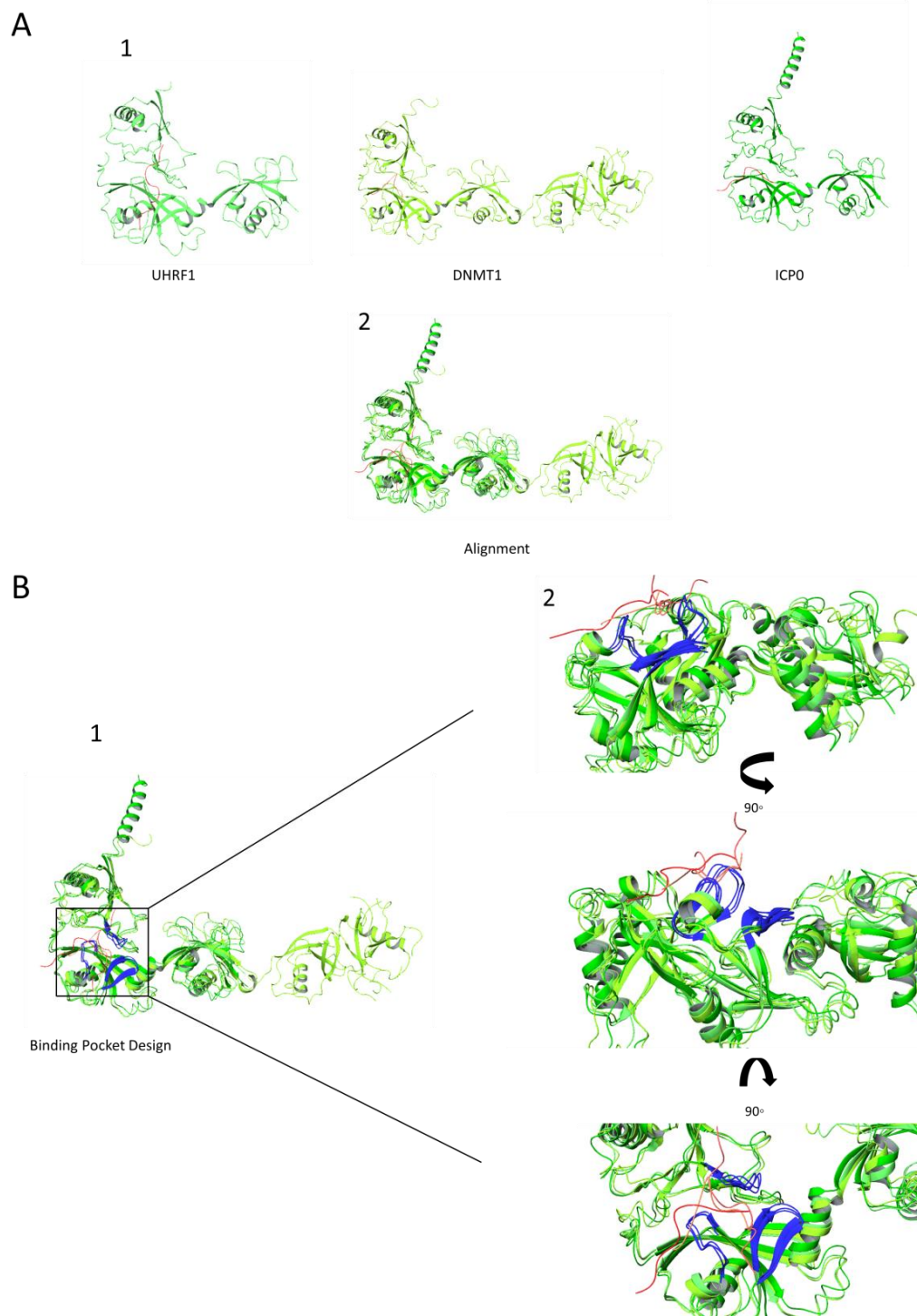


Figure 6-24 Binding pocket on USP7. **A)** Alignment of the crystal structures of USP7 co-crystallised with the positively charged peptidic sequences of UHRF1 (amino-acids 652-664, PDB: 5C6D), DNMT1 (amino-acids 1108-1115, PDB: 4Z96) and ICP0 (amino-acids 617-626, PDB: 4WPI). 1) Structures of USP7 co-crystallised with the positively charged peptidic sequences of UHRF1 (5C6D), DNMT1 (4Z96) and ICP0 (4WPI). Each structure is coloured in a different grade of green (USP7) and red (substrate peptidic sequence). 2) Alignment of the three structures to visualise the binding pocket in which the peptides are bound. **B)** Definition of the amino-acids forming the binding pocket (627-ARSNGTK-633, 736-EEVKPNLTER-745 and 757-LDELMDGD-764). 1) General overview of the structural alignment. USP7 structures are coloured in different grades of green, substrate peptidic sequences in different grades of red and amino-acids forming the binding pocket are coloured in blue. The black box highlights the binding pocket location. 2) Zoom-in of the binding pocket on USP7. USP7 structures are coloured in different grades of green, substrate peptidic sequences in different grades of red and amino-acids forming the binding pocket are coloured in blue. All structures were analysed with Maestro Schrodinger software.

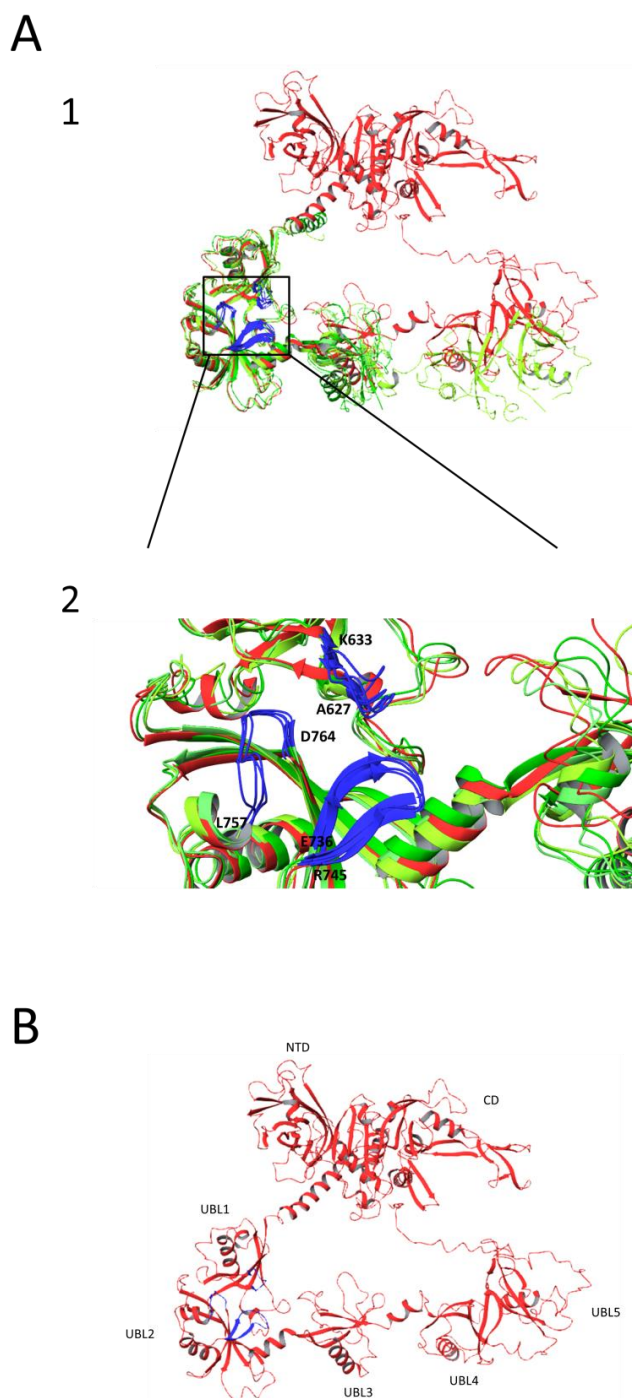


Figure 6-25 Binding pocket location in full length USP7 model. A) Alignment of the full length USP7 model with USP7 structures from 4Z96 (amino-acids 556-1083), 4WPI (amino-acids 538-882) and 5C6D (amino-acids 560-881) PDB files. 1) General overview of the structural alignment of full length USP7 model with USP7 structures 4Z96, 4WPI, 5C6D. USP7 structures from 4Z96, 4WPI, 5C6D are coloured in different grades of green, substrate peptidic sequences in different grades of red, amino-acids forming the binding pocket are coloured in blue and USP7 full length structure in red. The black box marks the location of the binding pocket. 2) Zoom-in on the binding pocket structural conformation. USP7 structures 4Z96, 4WPI, 5C6D are coloured in different grades of green, substrate peptidic sequences in different grades of red, amino-acids forming the binding pocket are coloured in blue and USP7 full length structure in red. The black box marks the location of the binding pocket. **B)** Binding pocket located in the full length USP7 model. Each domain is labelled on the structure. USP7 structure is coloured in red and binding pocket amino-acids are coloured in blue. All structures were analysed with Maestro Schrodinger software.

Human p65



Murine p65



Figure 6-26 R/KxxR/K motif presence on p65 human and murine sequences. Location on the sequence of human p65 and murine p65 proteins of R/KxxR/K motifs. Sequences were analysed with Geneius Software.

6.3.3.3.1 p65 amino-acids 35-RYKCECR-41 as part of the binding interface

This model was developed by a manual docking and subsequent minimisation process to relax the structure of the complex. The interface of the interaction was formed by amino-acids 627-ARNGTK-633, 736-EEVKPNLTER-745 and 757-LDELMDGD-764 of USP7 and amino-acids 35-RYKECR-41 from p65. Motif 35-RYKECR-41 of p65 is present on the solved crystal structure of p65, 1VKX. Thus, we used the same p50-p65-DNA complex structure as it was used for the K62

model. The DNA helix in this model is also elongated and rearranged in comparison to the DNA helix solved in 1VKX. In this case, the binding site was defined but the need of a ubiquitinated lysine in close proximity to G76 of ubiquitin and the catalytic triad of USP7 was also considered. K28 is the most accessible ubiquitinated lysine in this model (see Figure 6-27). PPAR γ promotes ubiquitination of p65 at K28 [380], and is also a substrate of USP7 [504]. K56 is also located in the area of the catalytic triad and the ubiquitin molecule; but some conformational rearrangements on p65 would be required for a proper interaction between K56, the catalytic triad and the ubiquitin molecule (see Figure 6-27). The study of the binding site in the model shows how amino-acids involved in the interaction are far from each other (see Figure 6-27). For this model to work properly, full length p65 structure and flexibility of the molecules should be taken into account. Conformational rearrangements of both proteins; USP7 and p65, after binding, will play an important role in the interactive complex structure. Another disadvantage of this model is that the model is not as compact as K62 model. Several gaps are observed, which would be filled with solvent molecules (see Figure 6-28). These solvent molecules may interfere with the interaction. On the other hand, a general overview of the model shows interactions between USP7 and p65 on UBL3 while the DNA helix interacts with the NTD and the α -helix connecting the CD with UBL1 (see Figure 6-28). In this case, the role of UBL45 may be to properly activate the deubiquitinase activity of USP7.

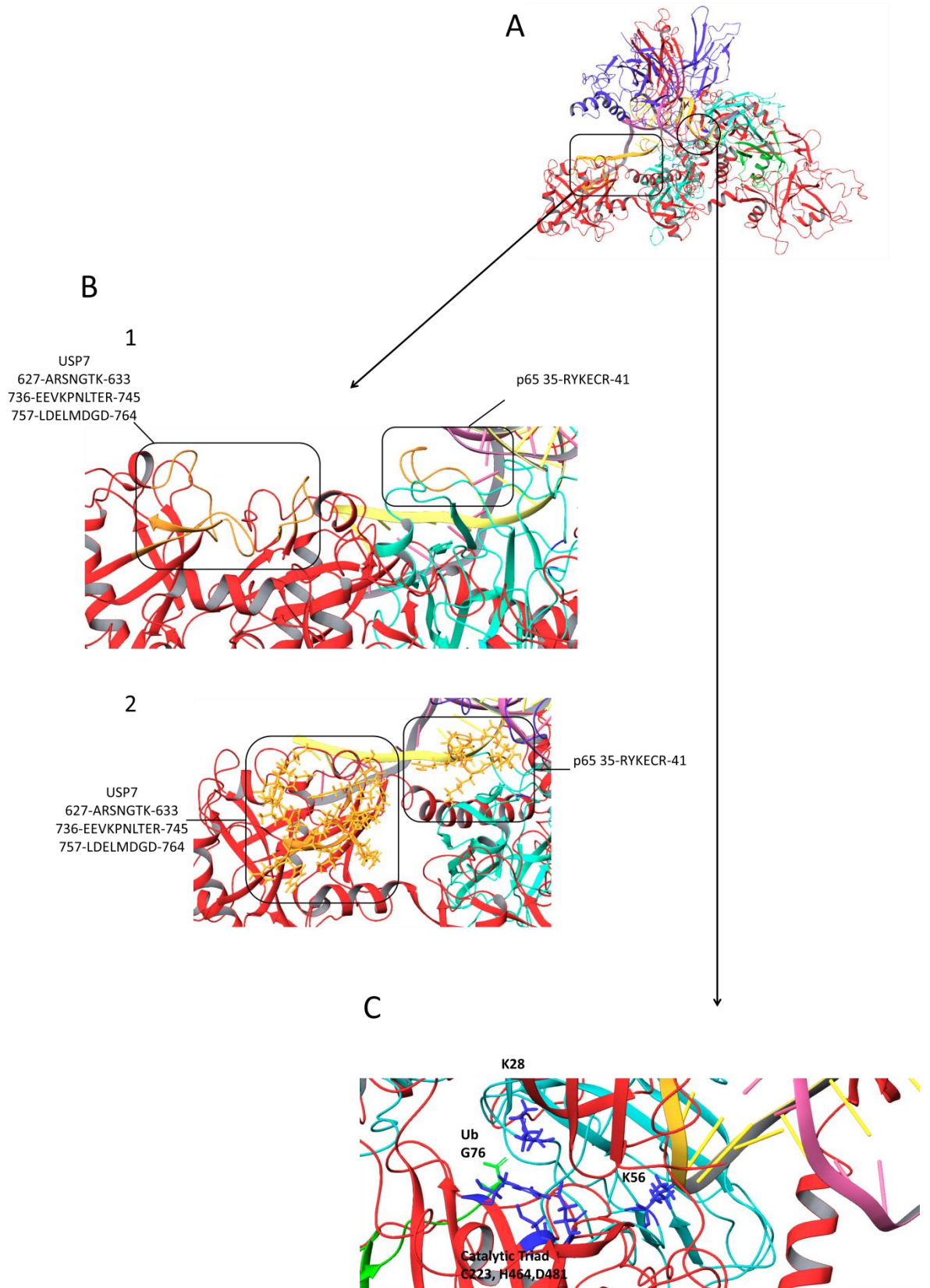


Figure 6-27 Model based on the interaction with the motif 35-RYKECR-41 of p65. A) Overall overview of the ribbon structure of the model. USP7 molecule is coloured in red, ubiquitin in green, p65 in blue, p50 in purple, DNA helix in yellow and pink, the binding site amino-acids in orange (amino-acids 627-ARSNGTK-633, 736-EEVKPNLTER-745 and 757-LDELMDGD-764 of USP7 and amino-acids 35-RYKECR-41 from p65) and the K-ubiquitinated accessible (K28 and K56) and catalytic triad (C223, H464 and D481) in dark blue. The black box marks the location of the binding interface. The black circle highlights the location of USP7 catalytic triad and possible p65 ubiquitinated lysines. **B)** Zoom-in of the binding site region. USP7 molecule is coloured in red, ubiquitin in green, p65 in blue, p50 in purple, DNA helix in yellow and pink, the binding site amino-acids in orange (amino-acids 627-ARSNGTK-633, 736-EEVKPNLTER-745 and 757-LDELMDGD-764 of USP7 and amino-acids 35-RYKECR-41 from p65) and the K-ubiquitinated accessible (K28 and K56) and catalytic triad (C223, H464 and D481) in dark blue. Black boxes show the location of USP7 binding pocket and p65 binding motif and their amino-acidic composition. 1) Amino-acids involved in the binding interface backbone coloured in orange. 2) Amino-acids involved in the binding interface backbone and side chains coloured in orange. **C)** Zoom-in of the catalytic triad (C223, H464 and D481) region. USP7 molecule is coloured in red, ubiquitin in green, p65 in blue, p50 in purple, DNA helix in yellow and pink, the binding site amino-acids in orange and the K-ubiquitinated accessible and catalytic triad in dark blue. Catalytic triad, possible p65 ubiquitinated lysines amino-acids side chains are coloured in dark blue and ubiquitin G76 side chain coloured in green. All structures were analysed with Maestro Schrodinger software.

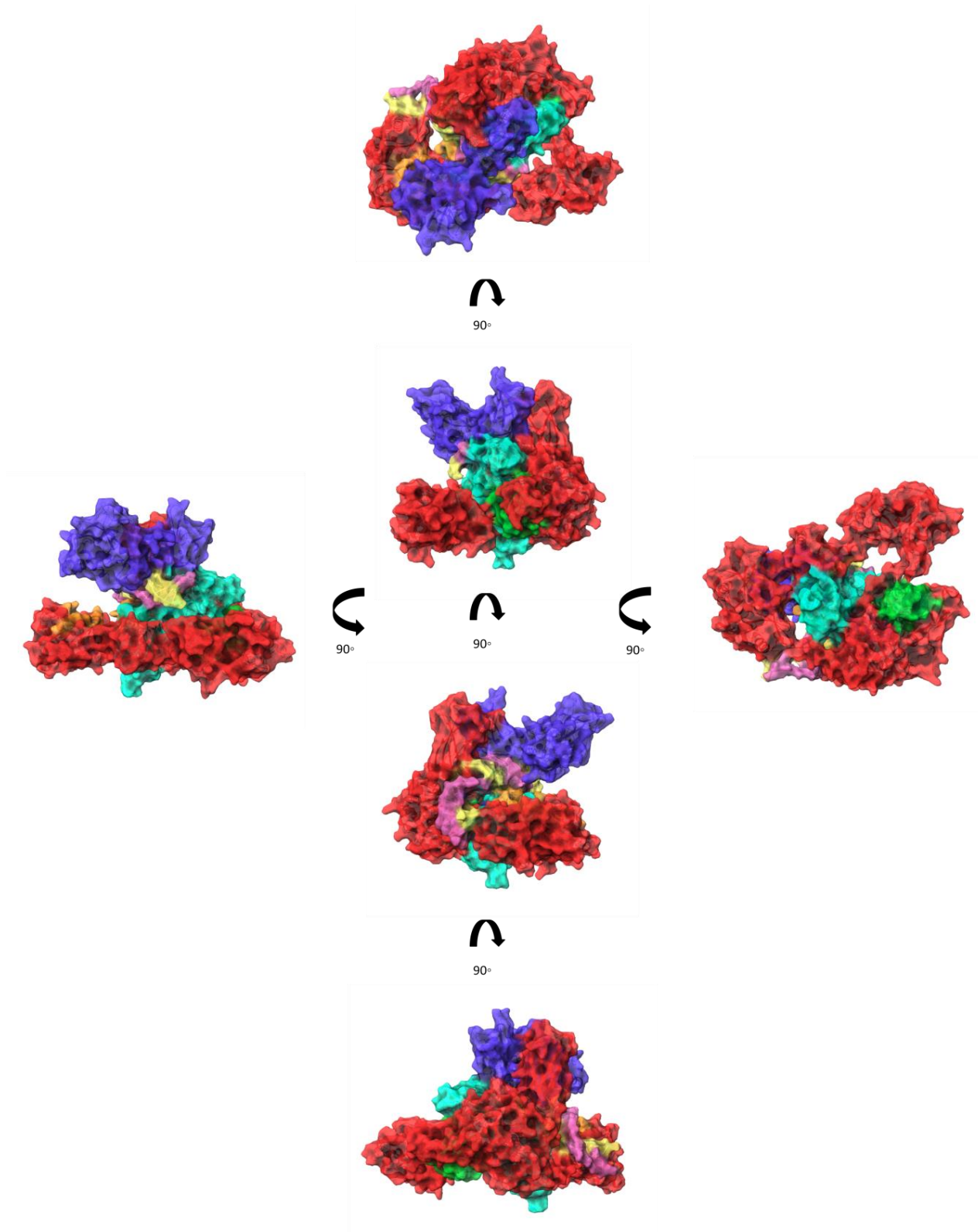


Figure 6-28 Surface of the USP7-p65/p50/DNA complex, modelled based on the interaction with motif 35-RYKECR-41. Different views of the complex. USP7 is coloured in red, p65 in blue, p50 in purple, ubiquitin in green, the DNA helix in yellow and pink and amino-acids involved in the interaction in orange. All structures were analysed with Maestro Schrodinger software.

6.3.3.3.2 p65 amino-acids 295-RHRIEEK-301 as part of the binding interface

This model was also docked manually and subsequently relaxed by a minimisation process. The binding pocket on USP7 was the same as for motif 35-RYKCECR-41 model, amino-acids 627-ARSNGTK-633, 736-EEVKPNLTER-745 and 757-LDELMDGD-764 of USP7 and in this case, amino-acids 295-RHRIEEK-301 from p65. Amino-acids 295-RHRIEEK-301 are not present in the crystal structure of 1VKX and so we used the full length p65 structure modelled with a combination of 1VKX structure and model 1 from ROBETTA software (see Figure 6-29). The motif 295-RHRIEEK-301 is located in an α -helix conformation followed by a flexible loop in this model. Comparing the five ROBETTA models, the α -helix containing the 295-RHRIEEK-301 motif is conserved, but the remaining flexible loop form a different rearrangement in each model. In order for the model to be more consistent, we used a truncated p65 structure, amino-acids 1-317, which contains the motif 295-RHRIEEK-301 in the conserved α -helix conformation within ROBETTA models (keeping K310, K314 and K315 as well in the model) (see Figure 6-29).

We also added the p50 structure from 1VKX and the elongated and bent DNA helix as for the K62 model (see Figure 6-29). The location of the p65 motif on an α -helix in a flexible loop area facilitated a docking focusing only on the binding site. The motif sterically fits in the binding pocket allowing the p65 molecule to move (see Figure 6-30). This ability to move after binding, agrees with the notion of molecules going through conformational rearrangements upon binding. In this model, there is no single ubiquitinated lysine in close proximity to the catalytic triad, but most of them are facing the catalytic triad and the ubiquitin molecule as well (see Figure 6-30). We hypothesised that p65 and USP7 conformational rearrangements will lead to the proximity of the target ubiquitinated lysine to the catalytic triad. This model fits the fact that USP7 is not specific for a certain ubiquitinated lysine (see Figure 6-30).

This model works as follows. In the first place the motif 295-RHRIEEK-301 of p65 will bind to the binding pocket present on USP7. Then both molecules will go through conformational rearrangements, accommodating the p65 molecule appropriately, depending on which lysine is ubiquitinated, allowing USP7 to

deubiquitinate p65 protein. This model has the same disadvantage as the model based on the interaction with 35-RYKCECR-41 motif on p65; it contains several gaps and is not as compact as the model based on K62 ubiquitination (see Figure 6-31). Those gaps may be filled with solvent molecules which may interfere with the interaction. A general overview of the model shows interactions between USP7 and p65 through UBL12 and the N-terminal of p65 may interact with UBL3, but no interactions between DNA and USP7. UBL45 will likely be involved in the approximation of p65 molecule to the catalytic triad proximity in this model. See Figure 6-31.

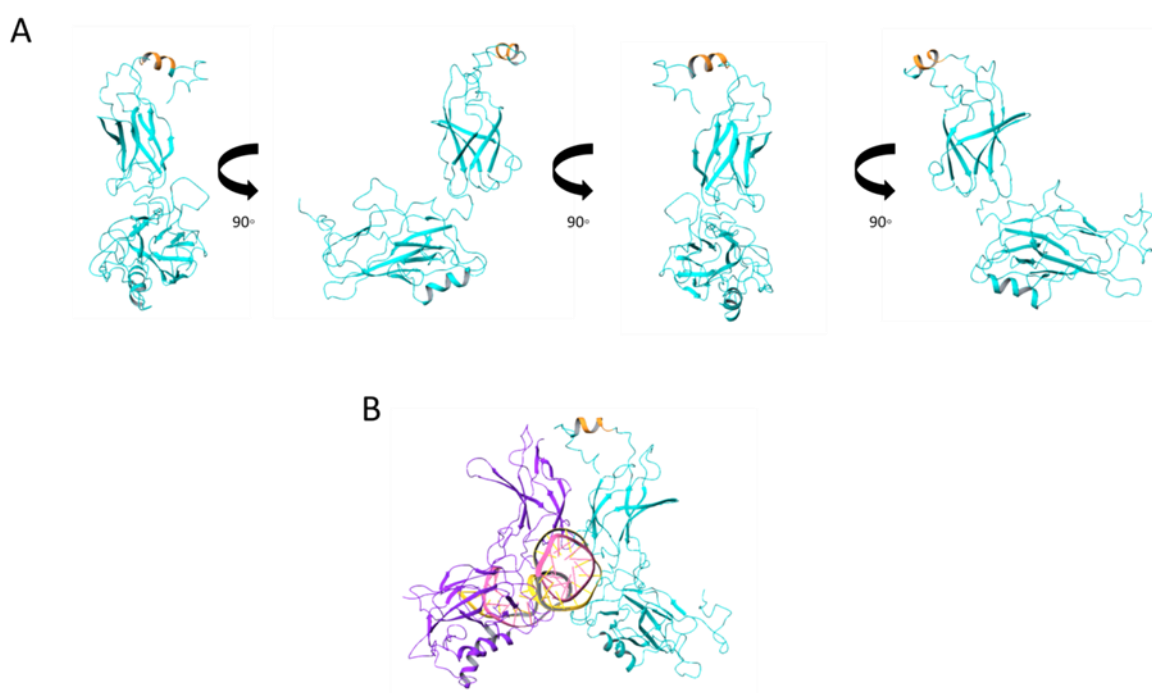


Figure 6-29 Model of p65 amino-acids 1-317 structure. A) Different views of the p65 molecule structure with the motif 295-301 coloured in orange. **B)** Heterodimer p50-p65 in complex with the elongated rearranged DNA helix 3D structure from 1VKX. p65 is coloured in blue, the motif 295-301 is coloured in orange, p50 is coloured in purple and the DNA helix is coloured in yellow and pink. All 3D structures were analysed with Maestro Schrodinger Software.

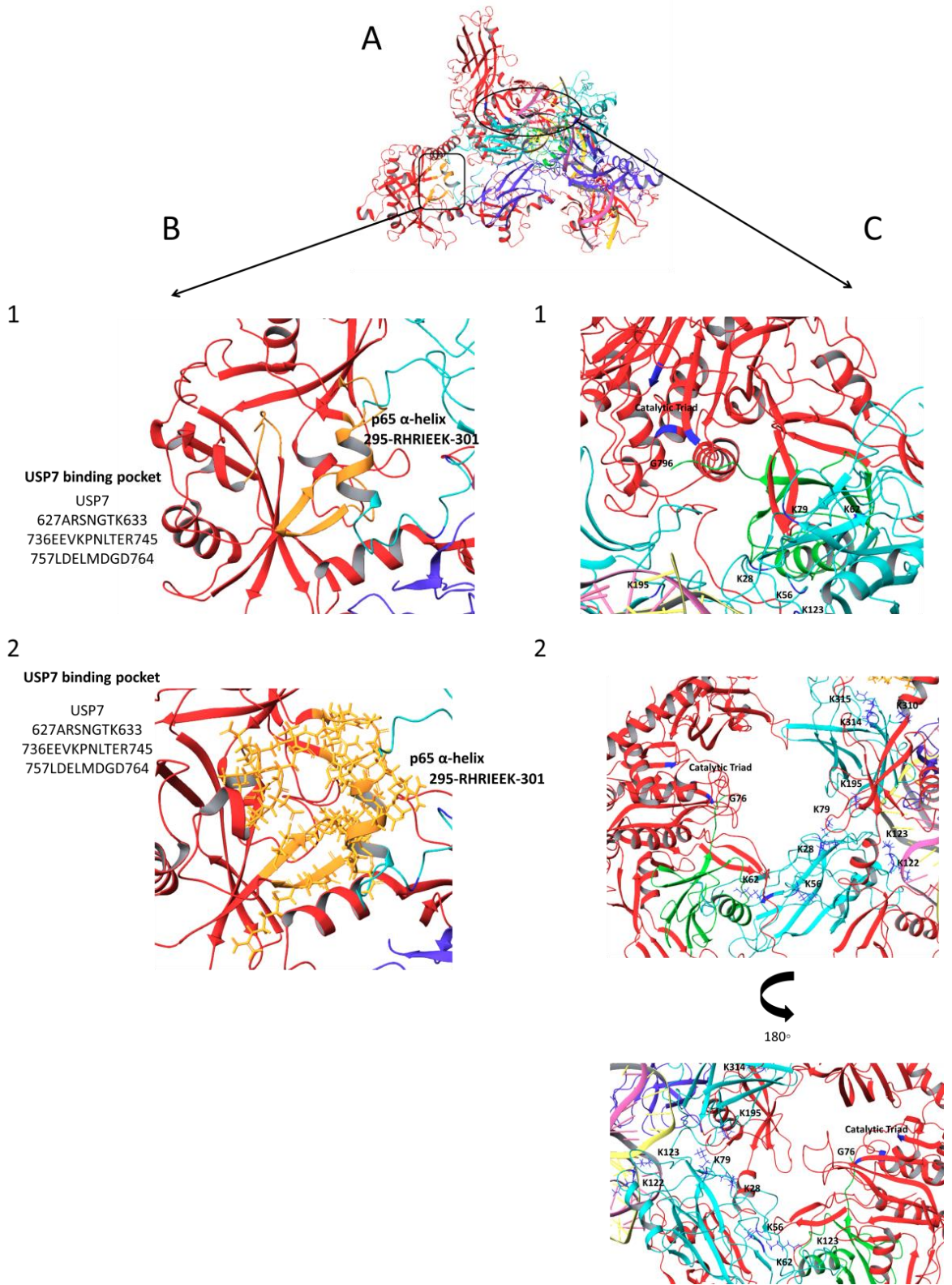


Figure 6-30 Model based on the interaction with the motif 295-RHRIEEK-301 of p65. A) Overview of the ribbon structure of the model. USP7 is coloured in red, ubiquitin in green, p65 in blue, p50 in purple, DNA helix in yellow and pink, the binding site amino-acids in orange (amino-acids 627-ARSNGTK-633, 736-EEVKPNLTER-745 and 757-LDELMDGD-764 of USP7 and amino-acids 295-RHRIEEK-301 from p65) and the accessible K-ubiquitinated and catalytic triad (C223, H464 and D481) in dark blue. The black box marks the location of the binding interface. The black circle highlights the location of USP7 catalytic triad and possible p65 ubiquitinated lysines. p50 protein structure is from 1VKX, p65 is from 1VKX and ROBETTA model 1, the DNA helix was elongated and rearranged from the DNA helix of 1VKZ, and full length USP7 and ubiquitin are from 5JTV, 5J7T, 4YOC, 5JTJ and 2F1Z. **B)** Zoom-in of the binding site region. USP7 molecule is coloured in red, ubiquitin in green, p65 in blue, p50 in purple, DNA helix in yellow and pink, the binding site amino-acids in orange (amino-acids 627-ARSNGTK-633, 736-EEVKPNLTER-745 and 757-LDELMDGD-764 of USP7 and amino-acids 295-RHRIEEK-301 from p65) and the accessible K-ubiquitinated and catalytic triad (C223, H464 and D481) in dark blue. 1) Amino-acids involved in the binding interface backbone coloured in orange. 2) Amino-acids involved in the binding interface backbone and side chains coloured in orange. **C)** Zoom-in of the catalytic triad region (C223, H464 and D481). USP7 molecule is coloured in red, ubiquitin in green, p65 in blue, p50 in purple, DNA helix in yellow and pink and the accessible K-ubiquitinated (K28, K56, K62, K79, K122, K123, K195, K310, K314 and K315) and catalytic triad (C223, H464 and D481) in dark blue. Catalytic triad, possible p65 ubiquitinated lysines amino-acids side chains are coloured in dark blue and ubiquitin G76 side chain coloured in green. 1) Zoom-in of the catalytic triad and accessible K-ubiquitinated on p65. 2) Zoom-out of the catalytic triad and accessible K-ubiquitinated on p65. All structures were analysed with Maestro Schrodinger software.

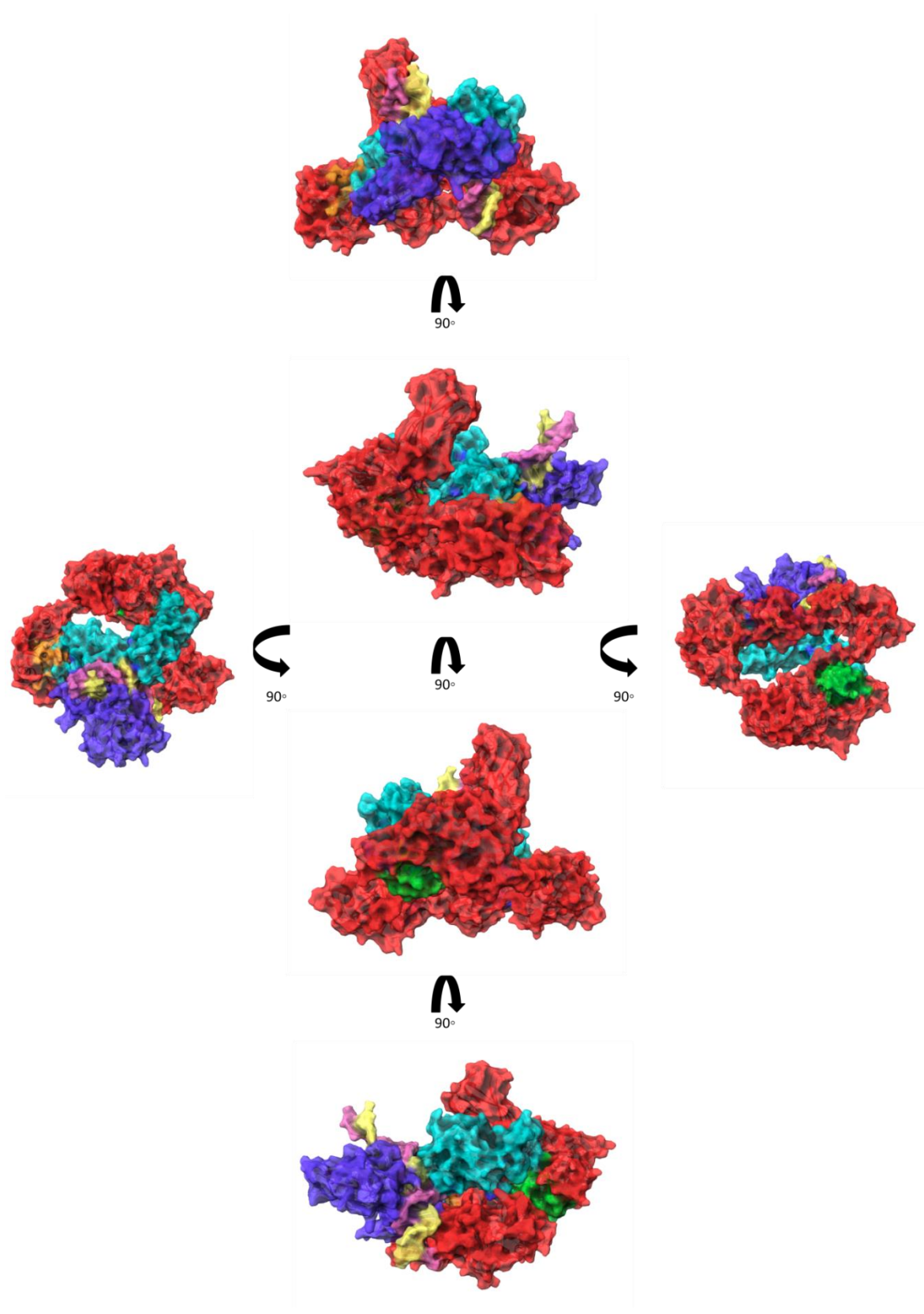


Figure 6-31 Surface of the USP7-p65/p50/DNA complex modelled based on the interaction with motif 295-RHRIEEK-301. Different views of the complex. USP7 is coloured in red, p65 in blue, p50 in purple, ubiquitin in green, the DNA helix in yellow and pink and amino-acids involved in the interaction in orange. All structures were analysed with Maestro Schrodinger software.

6.4 Discussion

There are no available 3D structures of USP7 full length protein, p65 full length protein or the complex formed by USP7-p65, thus we modelled them with the help of computational chemistry softwares.

p65 protein has been solved in a truncated version containing amino-acids 19-291 from the RHD and missing the TAD. Normally, the flexible regions of a protein are less stable and a huge number of proteins are solved in a truncated version. NMR experiments of p65 TAD, shows a disordered region with some more conserved helical turns [27, 28], which correlates with the different rearrangements of p65 protein TAD domain when modelled with ROBETTA. Flexible loops do not have a conserved conformation, so this part might not have a defined structure, what makes really difficult to characterise the 3D structure of that area. Mutations stabilising the area would be a good approach to solve the crystal structure of that region. However, certain amino-acid mutations could totally disrupt the whole 3D structure of the protein. The p65 full length model helps to locate possible amino-acids involved in USP7 interaction. Within structural conformations, α -helices and β -sheets are conserved conformations, while loops are flexible and not conserved. The presence of the α -helix within the flexible loops identifies a conserved region which may be important for p65 protein. The role of this α -helix, as it is formed by the positively charged motif R/KxR/KxxxR/K identified in USP7 substrates, may be essential to form the binding interface with USP7 protein. The full length p65 protein model helps us to identify possible interacting interfaces.

On the other hand, USP7 is a 130KDa protein, which makes difficult the process of purification, the bigger the protein the more difficult to purify. In these cases, structural experiments are too cost expensive and time consuming [487]. For this reason, molecular modelling is the best option to combine all information from different techniques. The full length USP7 model takes into account the molecular rearrangements that USP7 undergoes upon substrate binding [299-301]. Therefore, it takes into account USP7 flexibility. As for p65 protein full length model, USP7 full length model helps to identify possible protein-protein interaction interfaces. Furthermore, knowledge of the specific binding pocket identified in UBL2 makes the screening for potential inhibitory

compounds possible. A virtual compound screening is a useful tool in the design of new therapeutic drugs. Knowing the binding pocket structure, compounds can be identified by a steric filter and subsequently by its physicochemical properties. However, further research should be done on the determination of the amino-acids involved in the interaction and the actual structural model of the interaction for the development of new therapeutic specific drugs targeting the interface of the interaction between USP7-p65.

The USP7-p65 models described in this chapter have been manually done. In the manual docking the flexibility of the molecules relies in the possible changes the user does on proteins. However, considering all the information about the interaction from the experimental data (UBL2 is required for the interaction, p65 is ubiquitinated, USP7 does not have specificity for a unique lysine, p65 needs to be bound to the DNA [287]), one unique state of the interaction is not enough to explain the interaction mechanism with p65.

UBL2 is involved in the substrate recognition not only of p65 but also of DNMT1, ICP0, UHRF1, GMPS [41, 418]. These USP7 substrates do not share a large homology on their sequences and subsequently on their structures. However, they are recognised by the same binding pocket on USP7, which recognises an amino-acidic pattern on substrates. For this reason the motif proposed as the motif recognised by USP7 is a general motif composed by a 7 amino-acids sequence containing 3 positively charge amino-acids in a conserved order [41, 418]. To be a conserved pattern necessary for the interaction, the hypothesis would be that it is present in a conserved structural conformation. The crystallised structures used to understand USP7 binding pocket conformation, only used a peptidic sequence of each substrate. These peptidic sequences are rearranged as a flexible loop; thus, these 3D structures give insights on USP7 binding pocket but not on any conserved 3D structure on substrates binding the pocket. Comparison of both motifs found on p65 detects a flexible loop structure for amino-acids 35-41 and an α -helix structure for amino-acids 295-301. It is more likely to form the binding site with motif 295-301 due to the presence of the conserved secondary structure on the motif. In this secondary structure positively charge amino-acids will face the binding pocket generating electrostatic interactions with the negatively charge amino-acids from USP7

binding pocket. If the motif is present in a flexible loop, flexibility of the molecule makes more than one conformation of the flexible loop possible to bind the pocket. Molecules are dynamic in nature, but the interaction interface is generally conserved. We hypothesised that the recognised motif is more likely to be present on a conserved stable structural conformation instead of being on a flexible loop. Therefore, we hypothesised that once the molecule forms the interaction, the rest of the molecule undergoes conformational rearrangements; flexibility would be required upon binding.

As well as having substrate specificity, USP7 recognises ubiquitinated lysines within a protein. p65 protein is known to be ubiquitinated in 9 different lysines within its sequence [468] and USP7 is the only known DUB which deubiquitinates p65 [287]. This suggests a general mechanism in which USP7 is able to deubiquitinate different ubiquitination sites within p65. We studied the ability of USP7 to interact with three different ubiquitination sites of p65 when mutated to arginine. There is no specificity for any of the lysine, as the interaction level with all three mutants is the same as for the WT. Flexibility of USP7 C-terminal region correlates with this concept. USP7 might have a unique binding site for p65; once p65 binds USP7, the UBLs go through some conformational rearrangements to accommodate p65 K-ubiquitinated in the correct space to be deubiquitinated by the catalytic triad. This hypothesis should be studied with further experiments such as SDM to describe the unique binding site. This hypothesis fits with the motif 295-RHRIEEK-301 model. In the model the motif is bound to USP7 and most of the lysines are facing the catalytic triad in the area above UBL45. UBL45 have a specific role on USP7 deubiquitinase activity. They could also have a role on accommodation of the specific ubiquitinated molecule in the exact site to be deubiquitinated. USP7 C-terminal region is composed by the 5 UBL domains which form a dimeric-monomeric-dimeric conformation. Flexibility of UBL12 is quite reduced, UBL3 has more flexibility grades than UBL12, but it is the UBL45 dimer the one containing higher flexibility level. In the inactive state, UBL45 are in an open conformation and once the substrate binds, they get closer letting the CTP connect with the activation cleft. This movement could be in charge of the appropriate movements needed by p65 to properly fit the ubiquitinated lysine on the catalytic triad. Further investigation in the activation mechanism of USP7

should be done to surely confirm the conformational changes suffered upon p65 binding like hydrogen/deuterium exchange experiments followed by mass spectrometry analysis. Hydrogen/deuterium experiments have been used to detect binding interfaces between two interacting proteins [505]. Besides, it has been described that hydrogen/deuterium exchange experiments followed by a mass spectrometry analysis detected structural rearrangements on viral capsids [506]. Thus, hydrogen/deuterium exchange experiments followed by mass spectrometry analysis of USP7 full length alone, p65 full length alone and USP7 and p65 together in order to form the USP7-p65 complex could help elucidating the interacting mechanism of both proteins.

Lastly, the interaction with USP7 of a DNA binding defective mutant of p65 is reduced [287]; however, the role of DNA on USP7-p65 binding is still unknown. The DNA helix could have a proper job in the interaction as it is proposed in the first model (ubiquitination of K62). According to this model, the double stranded DNA helix would make contacts with USP7 molecule and stabilise the complex. Or this reduction could be due to a reduction on p65 ubiquitination level on that DNA binding defective mutant. Further investigation on the role of DNA helix should be performed to confirm its active role on the interaction or its indirect effect.

To summarise, we designed three different models for USP7-p65 interaction. The first model designed was the one based on K62 ubiquitination. This model identifies the DNA helix forming contacts with USP7 as well. Further investigation on the contribution of the DNA helix is required. This model also helps us to study the specificity of USP7 on ubiquitinated lysines. If USP7 deubiquitinase activity was specific of only a ubiquitinated lysine, the model should be performed using that lysine as the one bound to the ubiquitin molecule. As we expected, USP7 has no specificity for lysines, therefore a binding pocket on USP7 may recognise a binding motif on p65. The last two models are based on two possible interactive motifs on p65, and give us more information for subsequent mutational experiments. Mutation of both motifs of p65 could give us information on the molecular determinants of p65 involved in the interaction. Mutational experiments on the binding pocket amino-acids of USP7, would allow the identification of the amino-acids involved in p65 binding.

Molecular modelling is a helpful tool for subsequent experiments. It gives a different point of view of the same question; which are the amino-acids involved in this interaction?

Chapter Seven

General discussion

7 General discussion

The main aim of this thesis was to investigate the recognition of p65 by USP7 towards the ultimate goal of developing a p65 specific USP7 deubiquitinase activity inhibitor. We identified USP7 UBL2 as essential for p65 recognition and subsequent USP7 deubiquitinase activity in a substrate specific way.

USP7 interacts with a wide variety of substrates by different mechanisms [418]. However, the main focus developing a USP7 inhibitor is based on inhibition of USP7 catalytic activity [445, 453]. Hence, these inhibitors would have effects in a plethora of biological processes [287, 407, 418]. The potential of a substrate based compound inhibitor means that USP7 inhibition of p65 would not affect its deubiquitinating activity of substrates like p53, EBNA1, DAXX and RelB. This signifies that the pro-inflammatory role of USP7 through its p65 deubiquitinase activity would be suppressed while its roles on viral infection through EBNA1 [429, 430], its roles on apoptosis, cell survival and tumourigenesis through p53 and DAXX [417, 423] and its anti-inflammatory properties through RelB would be intact. On the opposite side, targeting the interaction with p53 for anti-cancer therapies would not affect the pro-inflammatory role of USP7. This new generation of USP7 inhibitors will be targeting specific roles of USP7 instead of targeting the catalytic activity of USP7. USP7 deletion in mice has a lethal effect on embryos [444]; therefore, the catalytic inhibition of USP7 activity may potentially lead to undesired consequences.

These data also implicate that p53, EBNA1, DAXX and RelB are recognised by USP7 in a different way to p65 and c-Rel. p53 and EBNA1 have been identified as N-terminal interacting substrates [418] while p65 has been identified as a C-terminal interacting substrate [287]. The recognition domain for RelB, DAXX and c-Rel has not yet been identified; however, our data suggest that RelB and DAXX are recognised by the N-terminal MATH/TRAF domain and c-Rel is recognised by the C-terminal UBL2. The majority of the structural work on USP7-substrate binding has been performed with peptide sequences of the substrates [41, 418]. These peptide sequences acquire a flexible loop conformation; hence, they are useful tools for USP7 binding pocket recognition, although no structural information on USP7 substrates is described.

RelB, c-Rel and p65 are members of the NF- κ B family of proteins sharing high structural homology on their RHDs [1, 15]. Protein-protein interactions are driven by the different 3D structures of the proteins involved in the interaction [476, 485-487]; the data from this thesis show that RelB uses a different recognition mechanism than p65 and c-Rel in the interaction with USP7. RelB structurally differs from p65 and c-Rel by the presence of a LZ domain in its N-terminal domain and a more prominent linker between the two immunoglobulin like domains of the RHD [1, 31]. Besides, RelB is only transcriptionally active when bound to p50 or p52, and drives the NF- κ B transcriptional response through the non-canonical pathway [1]. These structural differences on its RHD might be the reason why RelB has a different USP7 interaction mechanism than p65 and c-Rel. Taking this into account, USP7 might be able to distinctly regulate the pro-inflammatory and anti-inflammatory effects of NF- κ B.

From our data, we showed that USP7 Δ UBL2 does not deubiquitinate p65 as USP7 WT does, correlating interaction inhibition with deubiquitinase activity inhibition. Nonetheless, the majority of the structural experiments performed on USP7 suggested that the flexibility of the HUBL is a requirement for its full catalytic activity [408]. The CD and HUBL of USP7 are connected through a helical turn which when shortened decreases the catalytic activity of USP7 [300]. This helical turn is crucial for proper UBL12 location and subsequently, UBL45 and CTP location on the active cleft [300]. UBL3 is bound to UBL12 and UBL45 through flexible linkers that permit USP7 to undergo conformational rearrangements on the HUBL and accommodate each UBL in the correct structural conformation for a proper deubiquitinase activity [300, 418, 422]. According to these experiments, deletion of the whole UBL2 might have the same effect as shortening the helical turn connecting the CD and HUBL. UBL3 would locate closer to the helical turn and the flexibility of its linkers might not be sufficient to accommodate the CTP on the active cleft. To further investigate if the deubiquitinase activity of USP7 Δ UBL2 on p65 was inhibited by the inhibition of the interaction between USP7 and p65 or by the disruption of the HUBL proper structural conformation, a cellular ubiquitination assay of RelB was performed by Jennifer Mitchell (Carmody Group) which is described on appendix 8.8. The data show that USP7 Δ UBL2 mutant deubiquitinates RelB protein, confirming that p65 deubiquitination inhibition was due to an inhibition of the

interaction with p65. It is important to keep in mind that our data have been obtained from in vivo experiments, in other words from a functional cellular environment. This means that USP7 HUBL might be more flexible than it was thought, and might be able to accommodate UBL45 and the CTP to gain a full catalytic activity even when UBL2 is removed.

On the other hand, we also encountered some surprising results. Most of the amino-acidic contacts identified on the peptide array and subsequent alanine scan experiments take part through USP7 UBL3 although UBL3 is not crucial for the interaction. This suggests that UBL3 plays a role stabilising USP7-substrate complexes. Previous studies identified UBL12 as the region of HUBL needed for substrate recognition and a functional role for UBL45, which when deleted, reduces the catalytic activity of USP7 [408, 418]; however, the role of UBL3 has not yet been defined. Our data suggest that UBL3 is important for the interaction of USP7 with p65, to stabilise the complex between both proteins. Moreover, USP7 has no specificity for any of the possible ubiquitination sites on p65, meaning that there is not a unique USP7-p65 complex. Depending on which lysine is ubiquitinated, once USP7 and p65 interact, they will undergo the necessary conformational rearrangements to accommodate the ubiquitinated lysine in the proper location for the catalytic triad to be able to deubiquitinate it. These data suggest that USP7 has a unique p65 recognition mechanism and depending on the structural rearrangements undertaken by the complex, USP7 would deubiquitinate each specific lysine. Following this result, we defined USP7 amino-acids 627-ARSNGTK-633, 736-EEVKPNLTER-745 and 757-LDELMDGD-764 as a potential USP7 binding pocket for p65 recognition, which recognises a positively charged pattern on p65 (R/KxR/KxxxR/K). In this way, we discovered two possible motifs on p65 sequence. The first motif, 35-RYKCECR-41, is composed by a flexible loop, and the second motif, 295-RHRIEEK-301, is not present on available 3D structures. If the interaction mechanism is conserved by different substrates as our data suggest, the binding interface has to be composed by conserved structural regions. When modelling the full length p65 protein, the disordered TAD 295-RHRIEEK-301 was placed on a conserved α -helix secondary structure. This location suggests that 295-RHRIEEK-301 is more likely to be the pattern recognised by USP7 binding pocket. Besides, the α -helix conformation will face the positively charged amino-acids on the pattern

towards the USP7 binding pocket and the negatively charged amino-acids facing the opposite direction. These unexpected results have important implications on the explanation of USP7-p65 interaction. This mechanism is in turn more complicated than we initially thought, and likely explains why a p65 mimetic peptide strategy was not sufficient to inhibit the interaction.

Although we identified UBL2 as the UBL regulating p65 interaction, further investigation is required to develop a p65-specific USP7 inhibitor. Based on our binding pocket identification, a virtual compound screening could be performed. The compound screening would firstly filter compounds by their steric conformation, and those who fit in the binding pocket would then be filtered according to their physicochemical properties. The selected compounds could be tested in *in vivo* inflammatory models to study their effect on the pro-inflammatory role of NF- κ B. At the same time, mutational analysis on both p65 and USP7 proteins would be useful to identify the contribution of USP7 binding pocket (627-ARSNGTK-633, 736-EEVKPNLTER-745 and 757-LDELMDGD-764) and p65 motifs (35-RYKCECR-41 and 295-RHRIEEK-301) to the interaction. On the other hand, immunoprecipitation assays with different substrates, which have not been tested already, could be performed to analyse the possibility of substrate specificity. As for the role of USP7 inhibition on different NF- κ B members, repression of the transcriptional activity of NF- κ B members could be tested by a promoter activity reporter assay.

Together the data presented in this thesis demonstrate that USP7 specific roles on different biological processes could be specifically targeted. In addition to identification of USP7 UBL2 as the domain regulating p65 interaction, we described substrate selectivity even between NF- κ B members. Deletion of USP7 UBL2 targets p65 along with c-Rel; therefore, it just inhibits the pro-inflammatory role of the NF- κ B response. Furthermore, the identification of a potential USP7 binding pocket provides an excellent basis for a virtual compound screening to identify inhibitors specific for the inhibition of p65 deubiquitination by USP7.

Chapter Eight

Appendixes

8 Appendixes

8.1 Amino-acids abbreviations

Alanine	Ala	A
Arginine	Arg	R
Asparagine	Asn	N
Aspartic acid	Asp	D
Cysteine	Cys	C
Glutamine	Gln	Q
Glutamic acid	Glu	E
Glycine	Gly	G
Histidine	His	H
Isoleucine	Ile	I
Leucine	Leu	L
Lysine	Lys	K
Methionine	Met	M
Phenylalanine	Phe	F
Proline	Pro	P
Serine	Ser	S
Threonine	Thr	T

Tryptophan	Trp	W
------------	-----	---

Tyrosine	Tyr	Y
----------	-----	---

Valine	Val	V
--------	-----	---

8.2 Cloning

Primers amplifying p65 protein were designed (see Table 2-14). p65 protein cDNA was amplified by PCR, gel extracted and purified. Amplified cDNA following digestion by the correspondent restriction enzymes was ligated into the new empty vector (see section 2.2.7). To study the success of the cloning strategy, several colonies resulted from the transformation of the ligation product were amplified by PCR and subsequently sequenced. Successful cloned plasmids were selected for subsequent experiments. See Figure 8-1.

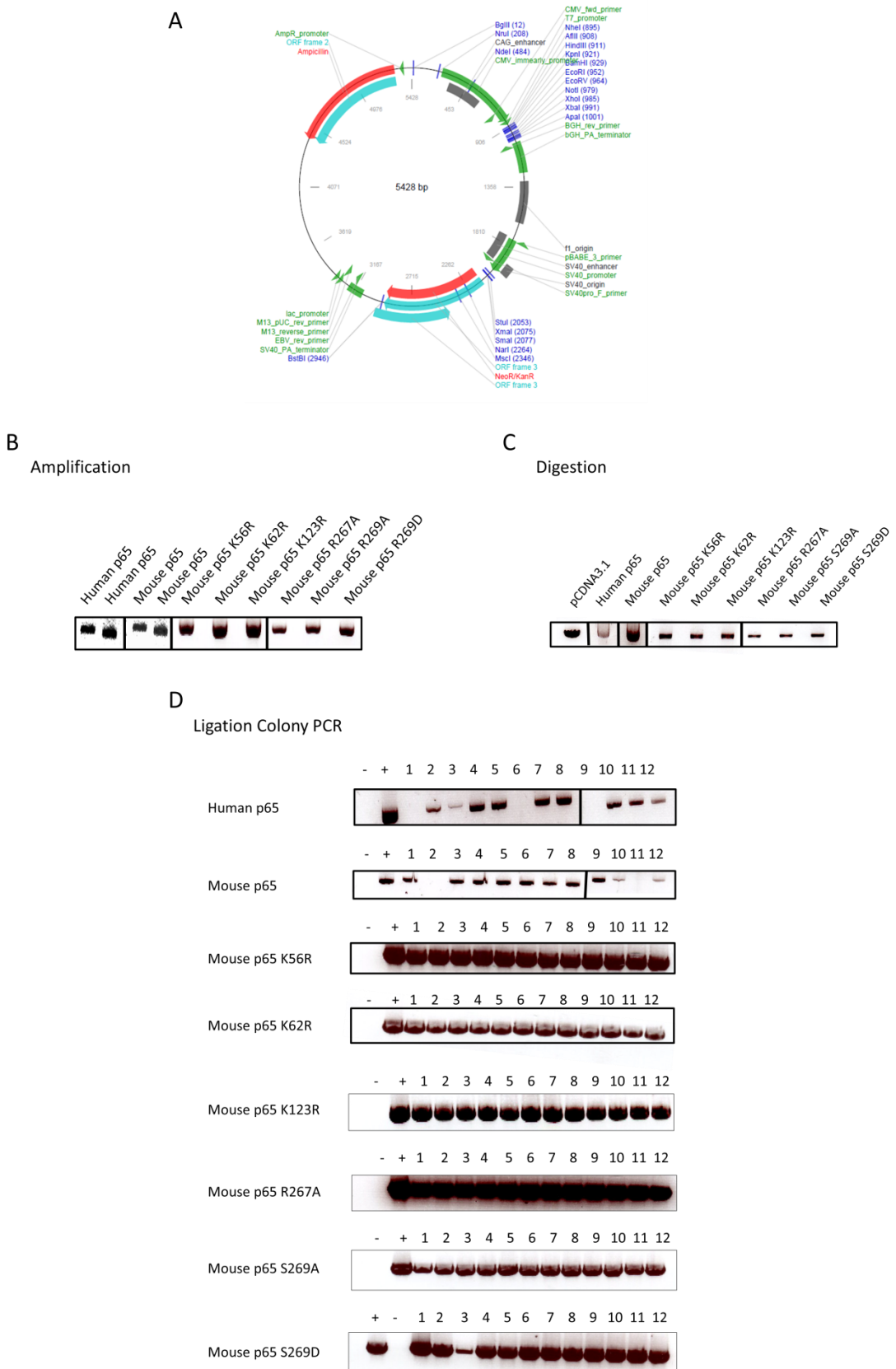


Figure 8-1 p53 WT and mutants cloning into an empty pCDNA3.1 expression vector. A) pCDNA3.1 expression vector map (Plasmid map from Addgene, Cambridge, USA). **B)** PCR amplification of p53 protein (WT (human and mouse) and mutants (mouse)). **B)** p53 protein PCR amplification product. **C)** p53 protein and pCDNA3.1 empty vector digestion product by the enzymes XbaI and HindIII. **D)** Ligation product colony PCR for each of the new cloned plasmids.

8.3 Peptide array sequences

Sequences of the peptide arrays used for USP7 C-terminal peptide array experiment (see Table 8-1).

Table 8-1 Peptide array sequences.

Name	Sequence	Location
A1	VERLQEEKRIEAQKRKER	541-558
A2	QEEKRIEAQKRKERQEAH	545-562
A3	RIEAQKRKERQEAHLYMQ	549-566
A4	QKRKERQEAHLYMQVQIV	553-570
A5	ERQEAHLYMQVQIVAEDQ	557-574
A6	AHLYMQVQIVAEDQFCGH	561-578
A7	MQVQIVAEDQFCGHQGND	565-582
A8	IVAEDQFCGHQGNDMYDE	569-586
A9	DQFCGHQGNDMYDEEKVK	573-590
A10	GHQGNDMYDEEKVKYTVF	577-594
A11	NDMYDEEKVKYTVFKVLK	581-598
A12	DEEKVKYTVFKVLKNSSL	585-602
A13	VKYTVFKVLKNSSLAEFV	589-606
A14	VFKVLKNSSLAEFVQSLS	593-610
A15	LKNSSLAEFVQSLSQTMG	597-614
A16	SLAEFVQSLSQTMGFPQD	601-618
A17	FVQSLSQTMGFPQDQIRL	605-622
A18	LSQTMGFPQDQIRLWPMQ	609-626
A19	MGFPQDQIRLWPMQARSN	613-630
A20	QDQIRLWPMQARSNGTKR	617-634
A21	RLWPMQARSNGTKRPAML	621-638
A22	MQARSNGTKRPAMLDNEA	625-642
A23	SNGTKRPAMLDNEADGNK	629-646
A24	KRPAMLDNEADGNKTMIE	633-650
A25	MLDNEADGNKTMIELSDN	637-654
A26	EADGNKTMIELSDNENPW	641-658

Name	Sequence	Location
A27	NKTMIELSDNENPWTIFL	645-662
A28	IELSDNENPWTIFLETVD	649-666
A29	DNENPWTIFLETVDPELA	653-670
A30	PWTIFLETVDPELAASGA	657-674
B1	FLETVDPELAASGATLPK	661-678
B2	VDPELAASGATLPKFDKD	665-682
B3	LAASGATLPKFDKDHVDM	669-686
B4	GATLPKFDKDHVDMFLK	673-690
B5	PKFDKDHVDMFLKMYDP	677-694
B6	KDHVDMFLKMYDPKTRS	681-698
B7	VMLFLKMYDPKTRSLNYC	685-702
B8	LKMYDPKTRSLNYCGHIY	689-706
B9	DPKTRSLNYCGHIYTPIS	693-710
B10	RSLNYCGHIYTPISCKIR	697-714
B11	YCGHIYTPISCKIRDLLP	701-718
B12	YTPISCKIRDLLPVMCD	706-722
B13	ISCKIRDLLPVMCDRAGF	709-726
B14	IRDLLPVMCDRAGFIQDT	713-730
B15	LPVMCDRAGFIQDTSLIL	717-734
B16	CDRAGFIQDTSLILYEEV	721-738
B17	GFIQDTSLILYEEVKPNL	725-742
B18	DTSLILYEEVKPNLTERI	729-746
B19	ILYEEVKPNLTERIQDYD	733-750
B20	EVKPNLTERIQDYDVSLD	737-754
B21	NLTERIQDYDVSLDKALD	741-758
B22	RIQDYDVSLDKALDELMD	745-762
B23	YDVSLDKALDELMDGDII	749-766
B24	LDKALDELMDGDIIVFQK	753-770
B25	LDELMDGDIIVFQKDDPE	757-774
B26	MDGDIIVFQKDDPENDNS	761-778
B27	IIVFQKDDPENDNSELPT	765-782
B28	QKDDPENDNSELPTAKEY	769-786

Name	Sequence	Location
B29	PENDNSELPTAKEYFRDL	773-790
B30	NSELPTAKEYFRDLYHRV	777-794
C1	PTAKEYFRDLYHRVDVIF	781-798
C2	EYFRDLYHRVDVIFCDKT	785-802
C3	DLYHRVDVIFCDKTIPND	789-806
C4	RVDVIFCDKTIPNDPGFV	793-810
C5	IFCDKTIPNDPGFVVTLS	797-814
C6	KTIPNDPGFVVTLNRMN	801-817
C7	NDPGFVVTLNRMNYFQV	805-822
C8	FVVTLNRMNYFQVAKTV	809-826
C9	LSNRMNYFQVAKTVAQRL	813-830
C10	MNYFQVAKTVAQRLNTDP	817-834
C11	QVAKTVAQRLNTDPMLLQ	821-838
C12	TVAQRLNTDPMLLQFFKS	825-842
C13	RLNTDPMLLQFFKSQGYR	829-846
C14	DPMLLQFFKSQGYRDGPG	833-850
C15	LQFFKSQGYRDGPGNPLR	837-854
C16	KSQGYRDGPGNPLRHNYE	841-858
C17	YRDGPGNPLRHNYEGTLR	845-862
C18	PGNPLRHNYEGTLRDLLQ	849-866
C19	LRHNYEGTLRDLLQFFKP	853-870
C20	YEGTLRDLLQFFKPRQPK	857-874
C21	LRDLLQFFKPRQPKKLYY	861-878
C22	LQFFKPRQPKKLYYQQLK	865-882
C23	KPRQPKKLYYQQLKMKIT	869-886
C24	PKKLYYQQLKMKITDFEN	873-890
C25	YYQQLKMKITDFENRRSF	877-894
C26	LKMKITDFENRRSFKCIW	881-898
C27	ITDFENRRSFKCIWLNSQ	885-902
C28	ENRRSFKCIWLNSQFREE	889-906
C29	SFKCIWLNSQFREEEITL	893-910
C30	IWLNSQFREEEITLYPDK	897-914

Name	Sequence	Location
D1	SQFREEEITLYPDKHGCV	901-918
D2	EEEITLYPDKHGCVRDLL	905-922
D3	TLYPDKHGCVRDLLLEECK	909-926
D4	DKHGCVRDLLLEECKKAVE	913-930
D5	CVRDLEEECKKAVELGEK	917-934
D6	LLEECKKAVELGEKASGK	921-938
D7	CKKAVELGEKASGKLRLL	925-942
D8	VELGEKASGKLRLLLEIVS	929-946
D9	EKASGKLRLLLEIVSYKII	933-950
D10	GKLRLLLEIVSYKIIICLSP	N/A
D11	LLEIVSYKIIICLSPATSR	N/A
D12	VSYKIIICLSPATSRTFRI	N/A
D13	IICLSPATSRTFRIIEIP	N/A
D14	SPATSRTFRIEEIPLDQV	963-980
D15	SRTFRIEEIPLDQVDIDK	967-984
D16	RIEEIPLDQVDIDKENEM	971-988
D17	IPLDQVDIDKENEMLVTV	975-992
D18	QVDIDKENEMLVTVAHFH	979-996
D19	DKENEMLVTVAHFHKEVF	983-1000
D20	EMLVTVAHFHKEVFGTFG	987-1004
D21	TVAHFHKEVFGTFGIPFL	991-1008
D22	FHKEVFGTFGIPFLRIH	995-1012
D23	VFGTFGIPFLRIHQGEH	999-1016
D24	FGIPFLRIHQGEHFREV	1003-1020
D25	FLLRIHQGEHFREVMKRI	1007-1024
D26	IHQGEHFREVMKRIQSLL	1011-1028
D27	EHFREVMKRIQSLLDIQE	1015-1032
D28	EVMKRIQSLLDIQEKEFE	1019-1036
D29	RIQSLLDIQEKEFEKFKF	1023-1040
D30	LLDIQEKEFEKFKFAIVM	1027-1044
E1	QEKEFEKFKFAIVMMGRH	1031-1048
E2	FEKFKFAIVMMGRHQYIN	1035-1052

Name	Sequence	Location
E3	KFAIVMMGRHQYINEDEY	1039-1056
E4	VMMGRHQYINEDEYEVNL	1043-1060
E5	RHQYINEDEYEVNLKDFE	1047-1064
E6	INEDEYEVNLKDFEPQPG	1051-1068
E7	EYEVNLKDFEPQPGNMSH	1055-1072
E8	NLKDFEPQPGNMSHPRPW	1059-1076
E9	FEPQPGNMSHPRPWLGLD	1063-1080
E10	PGNMSHPRPWLGLDHFNK	1067-1084
E11	SHPRPWLGLDHFNKAPKR	1071-1088
E12	PWLGLDHFNKAPKRSRYT	1075-1092
E13	LDHFNKAPKRSRYTYLEK	1079-1096
E14	NKAPKRSRYTYLEKAIKI	1083-1100
E15	APKRSRYTYLEKAIKIH	1085-1101
F1	ASGKLRLLEIVSYKIIGV	935-952
F2	LRLLEIVSYKIIGVHQED	939-956
F3	EIVSYKIIGVHQEDELLE	943-960
F4	YKIIGVHQEDELLECLSP	947-964
F5	GVHQEDELLECLSPATSR	951-968
F6	EDELLECLSPATSRTFRI	955-972
F7	LECLSPATSRTRFRIEIP	959-976

8.4 Alanine scanning peptide array sequences

Sequences of the peptide arrays used for the alanine scanning peptide array experiment (see Table 8-2).

Table 8-2 Alanine scanning peptide array sequences.

Peptide	Location	Sequence
A11	1	NDMYDEEKVKYTVFKVLK
A11	2	ADMYDEEKVKYTVFKVLK
A11	3	NAMYDEEKVKYTVFKVLK
A11	4	NDAYDEEKVKYTVFKVLK
A11	5	NDMADEEKVKYTVFKVLK
A11	6	NDMYAEEKVKYTVFKVLK
A11	7	NDMYDAEKVKYTVFKVLK
A11	8	NDMYDEAKVKYTVFKVLK
A11	9	NDMYDEEAVKYTVFKVLK
A11	10	NDMYDEEKAKYTVFKVLK
A11	11	NDMYDEEKVAYTVFKVLK
A11	12	NDMYDEEKVKATVFKVLK
A11	13	NDMYDEEKVKYAVFKVLK
A11	14	NDMYDEEKVKYTAFKVLK
A11	15	NDMYDEEKVKYTVAKVLK
A11	16	NDMYDEEKVKYTVFAVLK
A11	17	NDMYDEEKVKYTVFKALK
A11	18	NDMYDEEKVKYTVFKVAK
A11	19	NDMYDEEKVKYTVFKVLA
A20	1	QDQIRLWPMQARSNGTKR
A20	2	ADQIRLWPMQARSNGTKR
A20	3	QAQIRLWPMQARSNGTKR
A20	4	QDAIRLWPMQARSNGTKR
A20	5	QDQARLWPMQARSNGTKR
A20	6	QDQIALWPMQARSNGTKR
A20	7	QDQIRAWPMQARSNGTKR

Peptide	Location	Sequence
A20	8	QDQIRLAPMQARSNGTKR
A20	9	QDQIRLWAMQARSNGTKR
A20	10	QDQIRLWPAQARSNGTKR
A20	11	QDQIRLWPMMAARSNGTKR
A20	12	QDQIRLWPMQARSNGTKR
A20	13	QDQIRLWPMQAASNGTKR
A20	14	QDQIRLWPMQARANGTKR
A20	15	QDQIRLWPMQARSAGTKR
A20	16	QDQIRLWPMQARSNATKR
A20	17	QDQIRLWPMQARSNGAKR
A20	18	QDQIRLWPMQARSNGTAR
A20	19	QDQIRLWPMQARSNGTKA
A23	1	SNGTKRPAMLDNEADGNK
A23	2	ANGTKRPAMLDNEADGNK
A23	3	SAGTKRPAMLDNEADGNK
A23	4	SNATKRPAMLDNEADGNK
A23	5	SNGAKRPAMLDNEADGNK
A23	6	SNGTARPAMLDNEADGNK
A23	7	SNGTKAPAMLDNEADGNK
A23	8	SNGTKRAAMLDNEADGNK
A23	9	SNGTKRPAMLDNEADGNK
A23	10	SNGTKRPAALDNEADGNK
A23	11	SNGTKRPAMADNEADGNK
A23	12	SNGTKRPAMLANEADGNK
A23	13	SNGTKRPAMLDAEADGNK
A23	14	SNGTKRPAMLDNAADGNK
A23	15	SNGTKRPAMLDNEADGNK
A23	16	SNGTKRPAMLDNEAAGNK
A23	17	SNGTKRPAMLDNEADANK
A23	18	SNGTKRPAMLDNEADGAK
A23	19	SNGTKRPAMLDNEADGNA
B24	1	LDKALDELMDGDIIVFQK

Peptide	Location	Sequence
B24	2	ADKALDELMDGDIIVFQK
B24	3	LAKALDELMDGDIIVFQK
B24	4	LDAALDELMDGDIIVFQK
B24	5	LDKALDELMDGDIIVFQK
B24	6	LDKAADELMDGDIIVFQK
B24	7	LDKALAELMDGDIIVFQK
B24	8	LDKALDALMDGDIIVFQK
B24	9	LDKALDEAMDGDIIVFQK
B24	10	LDKALDELADGDIIVFQK
B24	11	LDKALDELMAGDIIVFQK
B24	12	LDKALDELMDADIIVFQK
B24	13	LDKALDELMDGAIIVFQK
B24	14	LDKALDELMDGDAIVFQK
B24	15	LDKALDELMDGDIIVFQK
B24	16	LDKALDELMDGDIIVFQK
B24	17	LDKALDELMDGDIIVFQK
B24	18	LDKALDELMDGDIIVFQK
B24	19	LDKALDELMDGDIIVFQK
C13	1	RLNTDPMLLQFFKSQGYR
C13	2	ALNTDPMLLQFFKSQGYR
C13	3	RANTDPMLLQFFKSQGYR
C13	4	RLATDPMLLQFFKSQGYR
C13	5	RLNADPMLLQFFKSQGYR
C13	6	RLNTAPMLLQFFKSQGYR
C13	7	RLNTDAMLLQFFKSQGYR
C13	8	RLNTDPALLQFFKSQGYR
C13	9	RLNTDPMALQFFKSQGYR
C13	10	RLNTDPMLAQFFKSQGYR
C13	11	RLNTDPMLLAFFKSQGYR
C13	12	RLNTDPMLLQAFKSQGYR
C13	13	RLNTDPMLLQFAKSQGYR
C13	14	RLNTDPMLLQFFASQGYR

Peptide	Location	Sequence
C13	15	RLNTDPMLLQFFKAQGYR
C13	16	RLNTDPMLLQFFKSAGYR
C13	17	RLNTDPMLLQFFKSQAYR
C13	18	RLNTDPMLLQFFKSQGAR
C13	19	RLNTDPMLLQFFKSQGYA
C15	1	LQFFKSQGYRDGPGNPLR
C15	2	AQFFKSQGYRDGPGNPLR
C15	3	LAFFKSQGYRDGPGNPLR
C15	4	LQAFKSQGYRDGPGNPLR
C15	5	LQFAKSQGYRDGPGNPLR
C15	6	LQFFASQGYRDGPGNPLR
C15	7	LQFFKAQGYRDGPGNPLR
C15	8	LQFFKSAGYRDGPGNPLR
C15	9	LQFFKSQAYRDGPGNPLR
C15	10	LQFFKSQGARDGPGNPLR
C15	11	LQFFKSQGYADGPGNPLR
C15	12	LQFFKSQGYRAGPGNPLR
C15	13	LQFFKSQGYRDAPGNPLR
C15	14	LQFFKSQGYRDGAGNPLR
C15	15	LQFFKSQGYRDGPANPLR
C15	16	LQFFKSQGYRDGPGAPLR
C15	17	LQFFKSQGYRDGPGNALR
C15	18	LQFFKSQGYRDGPGNPAR
C15	19	LQFFKSQGYRDGPGNPLA
C17	1	YRDGPGNPLRHNYEGTLR
C17	2	ARDGPGNPLRHNYEGTLR
C17	3	YADGPGNPLRHNYEGTLR
C17	4	YRAGPGNPLRHNYEGTLR
C17	5	YRDAPGNPLRHNYEGTLR
C17	6	YRDGAGNPLRHNYEGTLR
C17	7	YRDGPANPLRHNYEGTLR
C17	8	YRDGPGAPLRHNYEGTLR

Peptide	Location	Sequence
C17	9	YRDGPGNALRHNYEGTLR
C17	10	YRDGPGNPARHNYEGTLR
C17	11	YRDGPGNPLAHNYEGTLR
C17	12	YRDGPGNPLRANYEGTLR
C17	13	YRDGPGNPLRHAYEGTLR
C17	14	YRDGPGNPLRHNAEGTLR
C17	15	YRDGPGNPLRHNYAGTLR
C17	16	YRDGPGNPLRHNYEATLR
C17	17	YRDGPGNPLRHNYEGALR
C17	18	YRDGPGNPLRHNYEGTAR
C17	19	YRDGPGNPLRHNYEGTLA
C20	1	YEGTLRDLLQFFKPRQPK
C20	2	AEGTLRDLLQFFKPRQPK
C20	3	YAGTLRDLLQFFKPRQPK
C20	4	YEATLRDLLQFFKPRQPK
C20	5	YEGALRDLLQFFKPRQPK
C20	6	YEGTARDLLQFFKPRQPK
C20	7	YEGTLADLLQFFKPRQPK
C20	8	YEGTLRALLQFFKPRQPK
C20	9	YEGTLRDALQFFKPRQPK
C20	10	YEGTLRDLAQFFKPRQPK
C20	11	YEGTLRDLLAFFKPRQPK
C20	12	YEGTLRDLLQAFKPRQPK
C20	13	YEGTLRDLLQFAKPRQPK
C20	14	YEGTLRDLLQFFAPRQPK
C20	15	YEGTLRDLLQFFKARQPK
C20	16	YEGTLRDLLQFFKPAQPK
C20	17	YEGTLRDLLQFFKPRAPK
C20	18	YEGTLRDLLQFFKPRQAK
C20	19	YEGTLRDLLQFFKPRQPA
C25	1	YYQQLKMKITDFENRRSF
C25	2	AYQQLKMKITDFENRRSF

Peptide	Location	Sequence
C25	3	YAQQLKMKITDFENRRSF
C25	4	YYAQLKMKITDFENRRSF
C25	5	YYQALKMKITDFENRRSF
C25	6	YYQQAKMKITDFENRRSF
C25	7	YYQQLAMKITDFENRRSF
C25	8	YYQQLKAKITDFENRRSF
C25	9	YYQQLKMAITDFENRRSF
C25	10	YYQQLKMKATDFENRRSF
C25	11	YYQQLKMKIADFENRRSF
C25	12	YYQQLKMKITAFENRRSF
C25	13	YYQQLKMKITDAENRRSF
C25	14	YYQQLKMKITDFANRRSF
C25	15	YYQQLKMKITDFEARRSF
C25	16	YYQQLKMKITDFENARSF
C25	17	YYQQLKMKITDFENRASf
C25	18	YYQQLKMKITDFENRRAF
C25	19	YYQQLKMKITDFENRRSA
C30	1	IWLNSQFREEEITLYPDK
C30	2	AWLNSQFREEEITLYPDK
C30	3	IALNSQFREEEITLYPDK
C30	4	IWANSQFREEEITLYPDK
C30	5	IWLASQFREEEITLYPDK
C30	6	IWLNAQFREEEITLYPDK
C30	7	IWLNSAFREEEITLYPDK
C30	8	IWLNSQAREEEITLYPDK
C30	9	IWLNSQFAEEEITLYPDK
C30	10	IWLNSQFRAEEITLYPDK
C30	11	IWLNSQFREAEITLYPDK
C30	12	IWLNSQFREEAITLYPDK
C30	13	IWLNSQFREEEATLYPDK
C30	14	IWLNSQFREEEIALYPDK
C30	15	IWLNSQFREEEITAYPDK

Peptide	Location	Sequence
C30	16	IWLNSQFREEEITLAPDK
C30	17	IWLNSQFREEEITLYADK
C30	18	IWLNSQFREEEITLYPAK
C30	19	IWLNSQFREEEITLYPDA
D15	1	SRTFRIEEIPLDQVDIDK
D15	2	ARTFRIEEIPLDQVDIDK
D15	3	SATFRIEEIPLDQVDIDK
D15	4	SRAFRIEEIPLDQVDIDK
D15	5	SRTARIEEIPLDQVDIDK
D15	6	SRTFAIEEIPLDQVDIDK
D15	7	SRTFRAEEIPLDQVDIDK
D15	8	SRTFRIAEIPLDQVDIDK
D15	9	SRTFRIEAIPLDQVDIDK
D15	10	SRTFRIEEAPLDQVDIDK
D15	11	SRTFRIEEIALDQVDIDK
D15	12	SRTFRIEEIPADQVDIDK
D15	13	SRTFRIEEIPLAQVDIDK
D15	14	SRTFRIEEIPLDAVDIDK
D15	15	SRTFRIEEIPLDQADIDK
D15	16	SRTFRIEEIPLDQVAIDK
D15	17	SRTFRIEEIPLDQVDADK
D15	18	SRTFRIEEIPLDQVDIAK
D15	19	SRTFRIEEIPLDQVDIDA
D25	1	FLLRIHQGEHFREVMKRI
D25	2	ALLRIHQGEHFREVMKRI
D25	3	FALRIHQGEHFREVMKRI
D25	4	FLARIHQGEHFREVMKRI
D25	5	FLLAIHQGEHFREVMKRI
D25	6	FLLRAHQGEHFREVMKRI
D25	7	FLLRIAQGEHFREVMKRI
D25	8	FLLRIHQGEHFREVMKRI
D25	9	FLLRIHQAEHFREVMKRI

Peptide	Location	Sequence
D25	10	FLLRIHQGAHFREVMKRI
D25	11	FLLRIHQGEAFREVMKRI
D25	12	FLLRIHQGEHAREVMKRI
D25	13	FLLRIHQGEHFAEVMKRI
D25	14	FLLRIHQGEHFRAVMKRI
D25	15	FLLRIHQGEHFREAMKRI
D25	16	FLLRIHQGEHFREVAKRI
D25	17	FLLRIHQGEHFREVMARI
D25	18	FLLRIHQGEHFREVMKAI
D25	19	FLLRIHQGEHFREVMKRA
E10	1	PGNMSHPRPWLGLDHFNK
E10	2	AGNMSHPRPWLGLDHFNK
E10	3	PANMSHPRPWLGLDHFNK
E10	4	PGAMSHPRPWLGLDHFNK
E10	5	PGNASHPRPWLGLDHFNK
E10	6	PGNMAHPRPWLGLDHFNK
E10	7	PGNMSAPRPWLGLDHFNK
E10	8	PGNMSHARPWLGLDHFNK
E10	9	PGNMSHPAPWLGLDHFNK
E10	10	PGNMSHPRAWLGLDHFNK
E10	11	PGNMSHPRPALGLDHFNK
E10	12	PGNMSHPRPWAGLDHFNK
E10	13	PGNMSHPRPWLALDHFNK
E10	14	PGNMSHPRPWLGLADHFNK
E10	15	PGNMSHPRPWLGLAHFNK
E10	16	PGNMSHPRPWLGLDAFNK
E10	17	PGNMSHPRPWLGLDHANK
E10	18	PGNMSHPRPWLGLDHFAK
E10	19	PGNMSHPRPWLGLDHFNA
E15	1	APKRSRYTYLEKAIKIH
E15	2	APKRSRYTYLEKAIKIH
E15	3	AAKRSRYTYLEKAIKIH

Peptide	Location	Sequence
E15	4	APARSRYTYLEKAIKIH
E15	5	APKASRYTYLEKAIKIH
E15	6	APKRARYTYLEKAIKIH
E15	7	APKRSAYTYLEKAIKIH
E15	8	APKRSRATYLEKAIKIH
E15	9	APKRSRYAYLEKAIKIH
E15	10	APKRSRYTALEKAIKIH
E15	11	APKRSRYTYAEKAIKIH
E15	12	APKRSRYTYLAKAIKIH
E15	13	APKRSRYTYLEAAIKIH
E15	14	APKRSRYTYLEKAIKIH
E15	15	APKRSRYTYLEKAAKIH
E15	16	APKRSRYTYLEKAIKAIH
E15	17	APKRSRYTYLEKAIKAH
E15	18	APKRSRYTYLEKAIKIA

8.5 Structural model of USP7-p65 complex based mutants

Structural model designed during a stay at AstraZeneca Sweden with the help and in collaboration with Dr Matti Lepistö and Dr Christian Tyrchan. In this model UBL1 and UBL2 from USP7 make direct contacts with p65 protein (see Figure 8-2).

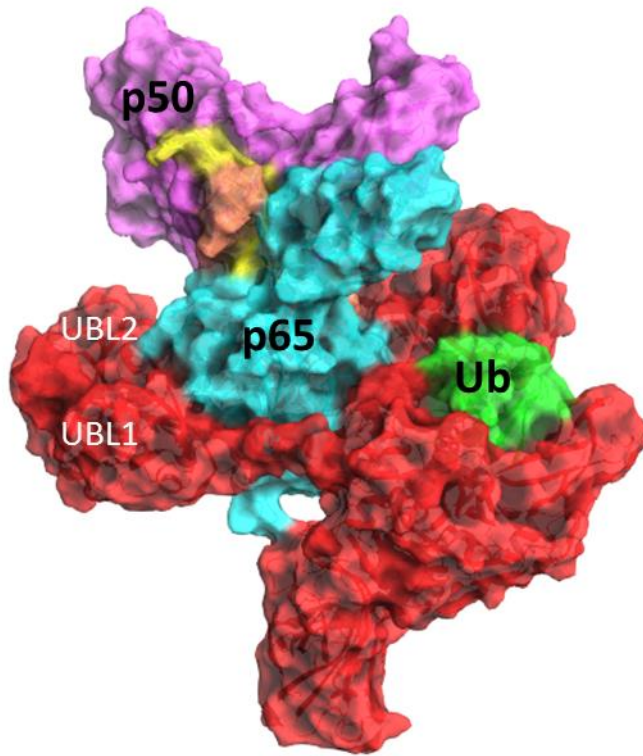


Figure 8-2 USP7-p65 complex structural model. Structural model of the interaction generated during a stay at AstraZeneca Sweden with the help of Dr Christian Tyrchan and Dr Matti Lepistö. Direct contacts between UBL1 and UBL2 of USP7 with p65. USP7 is coloured in red, ubiquitin in green, p65 in blue, p50 in purple and the DNA helix in yellow and pink.

8.6 NF- κ B members sequence homology for K56, K62 and K123 of p65

Sequence homology in the amino-acids surrounding K56 residue shared by the NF- κ B members (see Table 8-3), K62 residue (see Table 8-4) and K123 residue (see Table 8-5). Amino-acids coloured in red represents homology within subunits; amino-acids in blue, homology between some subunits but no with p65; amino-acids in green, homology between negatively charged amino-acids; and maroon, homology between positively charged amino-acids.

Table 8-3 p65 K56 sequence homology within NF- κ B members.

Subunit	K56									
p65	S	T	F	T	T	K	T	H	P	T
c-Rel	S	T	D	N	N	K	T	F	P	S
RelB	S	T	E	A	S	K	T	Q	P	A
p52	S	E	K	G	R	K	T	Y	P	T
p50	S	E	K	N	K	K	S	Y	P	Q

Table 8-4 p65 K62 sequence homology within NF- κ B members.

Subunit	K62								
p65	T	H	P	T	I	K	I	N	G
c-Rel	T	F	P	S	I	Q	I	L	N
RelB	T	Q	P	A	I	E	L	R	D
p52	T	Y	P	T	V	K	I	C	N
p50	S	Y	P	Q	V	K	I	C	N

Table 8-5 p65 K123 sequence homology within NF- κ B members.

Subunit	K123								
p65	Q	C	V	K	K	R	D	L	E
c-Rel	Q	C	V	K	K	K	D	L	K
RelB	Q	C	V	R	K	K	E	I	E
p52	L	H	V	T	K	K	N	M	M
p50	L	H	V	T	K	K	K	V	F

8.7 R/KxR/KxxxR/K motif identification within different USP7 substrates' sequences

Identification of R/KxR/KxxxR/K positively charged motifs within different USP7 substrates' sequence through Geneious software (see Figure 8-3).

UHRF1



ICPO



DNMT1



DNMT1



Figure 8-3 R/KxR/KxxxR/K motif presence on USP7 different substrates' sequences. Location on the sequence of UHRF1, ICP0 and DNMT1 proteins of R/KxR/KxxxR/K motifs. Sequences were analysed with Geneius Software.

8.8 RelB ubiquitination assay

RelB ubiquitination assay was performed by Jennifer Mitchell (Carmody Group). To study the effect of UBL2 deletion of USP7 deubiquitinase activity on a different substrate than p65 we selected RelB NF- κ B member. RelB shares homology with p65 but is still able to interact with USP7 Δ UBL2. A cellular ubiquitination assay with USP7 WT and USP7 Δ UBL2 mutant was performed. In order to be able to detect RelB ubiquitination status, HEK293T cells were co-transfected with USP7 WT and USP7 Δ UBL2 FLAG-tagged plasmids along with RelB and ubiquitin-HA plasmids.

Cellular lysates from the co-transfected HEK293T cells were denatured prior to immunoprecipitated with an anti-RelB antibody and immunoblotted with anti-RelB and anti-HA antibodies (see Figure 8-4). In contrast to USP7 Δ UBL2 inability to deubiquitinate p65, USP7 Δ UBL2 deubiquitinates RelB protein (see Figure 8-4). These data further support the requirement of interaction with the substrate in order to regulate substrate deubiquitination.

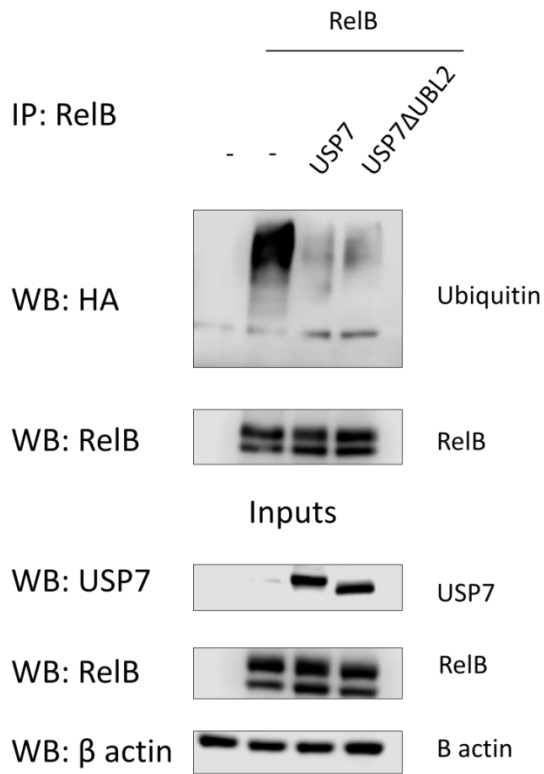


Figure 8-4 USP7ΔUBL2 mutant deubiquitinates RelB protein. HEK293T cells were co-transfected with USP7 WT and USP7ΔUBL2 FLAG-tagged plasmids along with RelB and Ubiquitin-HA plasmids. Cellular lysates were immunoprecipitated with RelB antibody and immunoblotted with HA-tag and USP7 and RelB proteins antibodies. Deletion of UBL2 has no impact on USP7 ability to deubiquitinate RelB protein. The figure is a representative of three independent experiments. RelB ubiquitination assay was performed by Jennifer Mitchell (Carmody Group).

List of references

1. Baeuerle PA, Henkel T (1994) Function and activation of NF- κ B in the immune system. *Annual Review of Immunology* 12:141-179
2. Herrington FD, Carmody RJ, Goodyear CS (2016) Modulation of NF- κ B signaling as a therapeutic target in autoimmunity. *Journal of Biomolecular Screening* 21:223-242
3. Foo SY, Nolan GP (1999) NF- κ B to the rescue. RELs, apoptosis and cellular transformation. *Trends in Genetics: TIG* 15:229-235
4. Singh H, Sen R, Baltimore D, Sharp PA (1986) A nuclear factor that binds to a conserved sequence motif in transcriptional control elements of immunoglobulin genes. *Nature* 319:154-158
5. Den R, Baltimore D (1986) Multiple nuclear factors interact with the immunoglobulin enhancer sequences. *Cell* 46:705-716
6. Lee J-I, Burckart GJ (1998) Nuclear Factor Kappa B: Important transcription factor and therapeutic target. *Journal of clinical pharmacology* 38:981-993
7. Bonizzi G, Karin M (2004) The two NF- κ B activation pathways and their role in innate and adaptive immunity. *Trends in Immunology* 25:280-288
8. May MJ, Ghosh S (1998) Signal transduction through NF- κ B. *Immunology Today* 19:80-88
9. Mercurio F, Manning AM (1999) Multiple signals converging on NF- κ B. *Current Opinion in Cell Biology* 11:226-232
10. Perkins ND (2000) The Rel NF- κ B family friend and foe. *Trends in Biological Sciences* 25:434-440
11. Aggarwal BB (2004) Nuclear Factor- κ B: The enemy within. *Cancer Cell* 6:203-208
12. Hayden MS, Ghosh S (2012) NF-kappaB, the first quarter-century: remarkable progress and outstanding questions. *Genes and Development* 26:203-234
13. Bhatt D, Ghosh S (2014) Regulation of the NF- κ B-mediated transcription of inflammatory genes. *Frontiers in Immunology* 5:71
14. Gasparini C, Feldmann M (2012) NF- κ B as a target for modulating inflammatory responses. *Current Pharmaceutical Design* 18:5735-5745
15. Carmody RJ, Chen YH (2007) Nuclear Factor- κ B activation and regulation

- during Toll-like receptor signaling. *Cellular and Molecular Immunology* 4:31-41
16. Dixit V, Mak TW (2002) NF- κ B signaling: Many roads lead to Madrid. *Cell* 111:615-619
 17. Christian F, Smith EL, Carmody RJ (2016) The Regulation of NF- κ B subunits by phosphorylation. *Cells* 5
 18. Iwai K (2014) Diverse roles of the ubiquitin system in NF- κ B activation. *Biochimica et Biophysica Acta: Molecular Cell Research* 1843:129-136
 19. Collins PE, Kiely PA, Carmody RJ (2014) Inhibition of transcription by B cell leukemia 3 (Bcl-3) protein requires interaction with Nuclear Factor κ B (NF- κ B) p50. *The Journal of Biological Chemistry* 289:7059-7067
 20. Brady G, Bowie AG (2014) Innate immune activation of NF- κ B and its antagonism by poxviruses. *Cytokine and Growth Factors Review* 25:611-620
 21. Ghosh S, Hayden MS (2008) New regulators of NF- κ B in inflammation. *Nature Reviews Immunology* 8:837-848
 22. Chen FE, Huang D-B, Chen Y-Q, Ghosh G (1998) Crystal structure of p50/p65 heterodimer of transcription factor NF- κ B bound to DNA. *Nature* 391:410-413
 23. Hayden MS, Ghosh S (2008) Shared principles in NF- κ B signaling. *Cell* 132:344-362
 24. May MJ, Ghosh S (1997) Rel NF- κ B and I κ B proteins an overview. *Seminars in Cancer Biology* 8:63-73
 25. Hoffmann A, Natoli G, Ghosh G (2006) Transcriptional regulation via the NF- κ B signaling module. *Oncogene* 25:6706-6716
 26. Burstein E, Duckett CS (2003) Dying for NF- κ B? Control of cell death by transcriptional regulation of the apoptotic machinery. *Current Opinion in Cell Biology* 15:732-737
 27. Mukherjee SP, Behar M, Birnbaum HA, et al (2013) Analysis of the RelA:CBP/p300 interaction reveals its involvement in NF- κ B-driven transcription. *PLoS Biology* 11:e1001647
 28. Lecoq L, Raiola L, Chabot PR, et al (2017) Structural characterization of interactions between transactivation domain 1 of the p65 subunit of NF- κ B and transcription regulatory factors. *Nucleic Acids Research* 45:5564-5576
 29. Stroud JC, Oltman A, Han A, et al (2009) Structural basis of HIV-1 activation by NF- κ B-A higher-order complex of p50:RelA bound to the HIV-

- 1 LTR. *Journal of Molecular Biology* 393:98-112
30. Huang DB, Chen YQ, Ruetsche M, et al (2001) X-ray crystal structure of proto-oncogene product c-Rel bound to the CD28 response element of IL-2. *Structure* 9:669-678
 31. Moorthy AK, Huang D Bin, Wang VYF, et al (2007) X-ray structure of a NF- κ B p50/RelB/DNA complex reveals assembly of multiple dimers on tandem κ B sites. *Journal of Molecular Biology* 373:723-734
 32. Müller CW, Rey F a, Sodeoka M, et al (1995) Structure of the NF-kappa B p50 homodimer bound to DNA. *Nature* 373:311-317
 33. Borjigin Wang, Michael M J, Snyder SH (1995) Structure of NF- κ B p50 homodimer bound to a κ B site. *Nature* 378:783-785
 34. Cramer P, Larson CJ, Verdine GL, Müller CW (1997) Structure of the human NF-kappaB p52 homodimer-DNA complex at 2.1 Å resolution. *The EMBO Journal* 16:7078-7090
 35. Chen YQ, Ghosh S, Ghosh G (1998) A novel DNA recognition mode by the NF-kappa B p65 homodimer. *Nature Structural and Molecular Biology* 5:67-73
 36. Huxford T, Huang DB, Malek S, Ghosh G (1998) The crystal structure of the I κ B α /NF- κ B complex reveals mechanisms of NF- κ B inactivation. *Cell* 95:759-770
 37. Berkowitz B, Huang D Bin, Chen-Park FE, et al (2002) The X-ray crystal structure of the NF- κ B p50-p65 heterodimer bound to the interferon β - κ B site. *The Journal of Biological Chemistry* 277:24694-24700
 38. Escalante CR, Shen L, Thanos D, Aggarwal AK (2002) Structure of NF- κ B p50/p65 heterodimer bound to the PRDII DNA element from the interferon- β promoter. *Structure* 10:383-391
 39. Panne D, Maniatis T, Harrison SC (2007) An atomic model of the interferon- β enhanceosome. *Cell* 129:1111-1123
 40. O'Shea JM, Perkins ND (2008) Regulation of the RelA (p65) transactivation domain. *Biochemical Society Transactions* 36:603-608
 41. Pfoh R, Lacdao IK, Georges AA, et al (2015) Crystal structure of USP7 ubiquitin-like domains with an ICP0 peptide reveals a novel mechanism used by viral and cellular proteins to target USP7. *PLoS Pathogens* 11:e1004950
 42. Perkins ND (2006) Post-translational modifications regulating the activity

- and function of the nuclear factor kappa B pathway. *Oncogene* 25:6717-6730
43. Huxford T, Ghosh G (2009) A structural guide to proteins of the NF- κ B signaling module. *Cold Spring Harbor Perspectives in Biology* 1:a000075
 44. Nolan GP, Ghosh S, Liou H-C, et al (1991) DNA binding and I κ B inhibition of the cloned p65 Subunit of NF- κ B, a rel-related polypeptide. *Cell* 64:961-969
 45. Kawai T, Akira S (2007) Signaling to NF- κ B by Toll-like receptors. *Trends in Molecular Medicine* 13:460-469
 46. Hoesel B, Schmid JA (2013) The complexity of NF- κ B signaling in inflammation and cancer. *Molecular Cancer* 12:86
 47. Campbell KJ, Rocha S, Perkins ND (2004) Active repression of antiapoptotic gene expression by RelA(p65) NF- κ B. *Molecular Cell* 13:853-865
 48. Spencer E, Jiang J, Chen ZJ (1999) Signal-induced ubiquitination of I κ B α by the F-box protein Slimb/B- TrCP. *Genes and Development* 13:284-294
 49. Yaron A, Hatzubai A, Davis M, et al (1998) Identification of the receptor component of the I κ B α -ubiquitin ligase. *Nature* 396:590-594
 50. Amir RE, Haecker H, Karin M, Ciechanover A (2004) Mechanism of processing of the NF- κ B2 p100 precursor: Identification of the specific polyubiquitin chain-anchoring lysine residue and analysis of the role of NEDD8-modification on the SCFB-TrCP ubiquitin ligase. *Oncogene* 23:2540-2547
 51. Fong A, Sun SC (2002) Genetic evidence for the essential role of β -transducin repeat-containing protein in the inducible processing of NF- κ B2/p100. *Journal of Biological Chemistry* 277:22111-22114
 52. Oeckinghaus A, Ghosh S (2009) The NF- κ B family of transcription factors and its regulation. *Cold Spring Harbor Perspectives in Biology* 1:a000034
 53. Mankan AK, Lawless MW, Gray SG, et al (2009) NF- κ B regulation: the nuclear response. *Journal of Cellular and Molecular Medicine* 13:631-643
 54. Huang B, Yang X-D, Lamb A, Chen L-F (2010) Posttranslational modifications of NF- κ B: another layer of regulation for NF- κ B signaling pathway. *Cell Signaling* 22:1282-1290
 55. Ghos S, Hayden M (2013) Celebrating 25 years of NF- κ B research. *Immunological Reviews* 246:5-13
 56. Renner F, Moreno R, Schmitz ML (2010) SUMOylation-dependent

- localization of IKK ϵ in PML nuclear bodies is essential for protection against DNA-damage-triggered cell death. *Molecular Cell* 37:503-515
57. Buss H, Dörrie A, Schmitz ML, et al (2004) Constitutive and interleukin-1-inducible phosphorylation of p65 NF- κ B at serine 536 is mediated by multiple protein kinases including I κ B kinase (IKK)- α , IKKB, IKK ϵ , TRAF family member-associated (TANK)-binding kinase 1 (TBK1), and an unknown kinase and couples p65 to TATA-binding protein associated factor IL-31-mediated IL-8 transcription. *Journal of Biological Chemistry* 279:55633-55643
 58. Anrather J, Racchumi G, Iadecola C (2005) cis-acting element-specific transcriptional activity of differentially phosphorylated nuclear factor- κ B. *Journal of Biological Chemistry* 280:244-252
 59. Ju J, Naura AS, Errami Y, et al (2010) Phosphorylation of p50 NF- κ B at a single serine residue by DNA-dependent protein kinase is critical for VCAM-1 expression upon TNF treatment. *Journal of Biological Chemistry* 285:41152-41160
 60. Authier H, Billot K, Derudder E, et al (2014) IKK phosphorylates RelB to modulate its promoter specificity and promote fibroblast migration downstream of TNF receptors. *Proceedings of the National Academy of Sciences of U.S.A.* 111:14794-14799
 61. Starczynowski DT, Reynolds JG, Gilmore TD (2005) Mutations of tumor necrosis factor α -responsive serine residues within the C-terminal transactivation domain of human transcription factor REL enhance its in vitro transforming ability. *Oncogene* 24:7355-7368
 62. Milanovic M, Kracht M, Schmitz ML (2014) The cytokine-induced conformational switch of nuclear factor κ B p65 is mediated by p65 phosphorylation. *The Biochemical Journal* 457:401-413
 63. Zhong H, Voll RE, Ghosh S (1998) Phosphorylation of NF- κ B p65 by PKA stimulates transcriptional activity by promoting a novel bivalent interaction with the coactivator CBP/p300. *Molecular Cell* 1:661-671
 64. Mertins P, Mani DR, Ruggles K V., et al (2016) Proteogenomics connects somatic mutations to signalling in breast cancer. *Nature* 534:55-62
 65. Xing D, Gong K, Feng W, et al (2011) O-GlcNAc modification of nfkb p65 inhibits tnf- α -induced inflammatory mediator expression in rat aortic smooth muscle cells. *PLoS One* 6:e24021

66. Zhong H, SuYang H, Erdjument-Bromage H, et al (1997) The transcriptional activity of NF- κ B is regulated by the I κ B- associated PKAc subunit through a cyclic AMP-independent mechanism. *Cell* 89:413-424
67. Buss H, Dörrie A, Schmitz ML, et al (2004) Phosphorylation of Serine 468 by GSK-3B Negatively Regulates Basal p65 NF- κ B Activity. *Journal of Biological Chemistry* 279:49571-49574
68. Lanucara F, Lam C, Mann J, et al (2016) Dynamic phosphorylation of RelA on Ser42 and Ser45 in response to TNF α stimulation regulates DNA binding and transcription. *Open Biology* 6
69. Sharma K, D'Souza RCJ, Tyanova S, et al (2014) Ultradeep human phosphoproteome reveals a distinct regulatory nature of Tyr and Ser/Thr-based signaling. *Cell Reports* 8:1583-1594
70. Mertins P, Yang F, Liu T, et al (2014) Ischemia in Tumors Induces Early and Sustained Phosphorylation Changes in Stress Kinase Pathways but Does Not Affect Global Protein Levels. *Molecular and Cell Proteomics* 13:1690-1704
71. Mertins P, Qiao JW, Patel J, et al (2013) Integrated proteomic analysis of post-translational modifications by serial enrichment. *Nature Methods* 10:634-637
72. Klammer M, Kaminski M, Zedler A, et al (2012) Phosphosignature predicts dasatinib response in non-small cell lung cancer. *Molecular and Cellular Proteomics* 11:651-668
73. Beli P, Lukashchuk N, Wagner SA, et al (2012) Proteomic investigations reveal a role for RNA processing factor THRAP3 in the DNA damage response. *Molecular Cell* 46:212-225
74. Ishinaga H, Jono H, Lim JH, et al (2007) TGF- β induces p65 acetylation to enhance bacteria-induced NF- κ B activation. *The EMBO Journal* 26:1150-1162
75. Vermeulen L, Wilde G De, Damme P Van, et al (2003) Transcriptional activation of the NF- κ B p65 subunit by mitogen- and stress-activated protein kinase-1. *The EMBO Journal* 22:1313-1324
76. Reber L, Vermeulen L, Haegeman G, Frossard N (2009) Ser276 phosphorylation of NF- κ B p65 by MSK1 controls SCF expression in inflammation. *PLoS One* 4:e4393
77. Jamaluddin M, Tian B, Boldogh I, et al (2009) Respiratory syncytial virus infection induces a reactive oxygen species-MSK1-phospho-Ser-276 RelA

- pathway required for cytokine expression. *Journal of Virology* 83:10605-10615
78. Jacks KA, Koch CA (2010) Differential regulation of mitogen- and stress-activated protein kinase-1 and -2 (MSK1 and MSK2) by CK2 following UV radiation. *Journal of Biological Chemistry* 285:1661-1670
 79. Nihira K, Ando Y, Yamaguchi T, et al (2010) Pim-1 controls NF- κ B signalling by stabilizing RelA/p65. *Cell Death and Differentiation* 17:689-698
 80. Wang H, Moreau F, Hirota CL, MacNaughton WK (2010) Proteinase-activated receptors induce interleukin-8 expression by intestinal epithelial cells through ERK/RSK90 activation and histone acetylation. *The FASEB Journal* 24:1971-1980
 81. Wang Y, Mo X, Piper MG, et al (2011) M-CSF induces monocyte survival by activating NF- κ B p65 phosphorylation at Ser276 via protein kinase C. *PLoS One* 6:e28081
 82. Hochrainer K, Racchumi G, Anrather J (2013) Site-specific phosphorylation of the p65 protein subunit mediates selective gene expression by differential NF- κ B and RNA polymerase II promoter recruitment. *Journal of Biological Chemistry* 288:285-293
 83. Ma Z, Chalkley RJ, Vosseller K (2017) Hyper-O-GlcNAcylation activates nuclear factor κ -light-chain enhancer of activated B cells (NF- κ B) signaling through interplay with phosphorylation and acetylation. *Journal of Biological Chemistry* 292:9150-9163
 84. Duran A, Diaz-Meco MT, Moscat J (2003) Essential role of RelA Ser311 phosphorylation by zetaPKC in NF- κ B transcriptional activation. *The EMBO Journal* 22:3910-3918
 85. Zhang TT, Kang TH, Ma B, et al (2012) LAH4 enhances CD8⁺ T cell immunity of protein/peptide-based vaccines. *Vaccine* 30:784-793
 86. Levy D, Kuo AJ, Chang Y, et al (2011) Lysine methylation of the NF- κ B subunit RelA by SETD6 couples activity of the histone methyltransferase GLP at chromatin to tonic repression of NF- κ B signaling. *Nature Immunology* 12:29-36
 87. Chang Y, Levy D, Horton JR, et al (2011) Structural basis of SETD6-mediated regulation of the NF- κ B network via methyl-lysine signaling. *Nucleic Acids Research* 39:6380-6389
 88. Wang B, Wei H, Prabhu L, et al (2015) Role of novel serine 316

- phosphorylation of the p65 subunit of NF- κ B in differential gene regulation. *Journal of Biological Chemistry* 290:20336-20347
89. O'Shea JM, Perkins ND (2010) Thr435 phosphorylation regulates RelA (p65) NF- κ B subunit transactivation. *Biochemical Journal* 426:345-354
 90. Yeh PY, Yeh KH, Chuang SE, et al (2004) Suppression of MEK/ERK signaling pathway enhances cisplatin-induced NF- κ B activation by protein phosphatase 4-mediated NF- κ B p 65 Thr dephosphorylation. *Journal of Biological Chemistry* 279:26143-26148
 91. Mattioli I, Geng H, Sebald A, et al (2006) Inducible phosphorylation of NF- κ B p65 at serine 468 by T cell costimulation is mediated by IKK ϵ . *Journal of Biological Chemistry* 281:6175-6183
 92. Campbell KJ, Witty JM, Rocha S, Perkins ND (2006) Cisplatin mimics ARF tumor suppressor regulation of RelA (p65) nuclear factor- κ B transactivation. *Cancer Research* 66:929-935
 93. Msaki A, Sanchez AM, Koh LF, et al (2011) The role of RelA (p65) threonine 505 phosphorylation in the regulation of cell growth, survival, and migration. *Molecular Biology of the Cell* 22:3032-3040
 94. Bird TA, Schooley K, Dower SK, et al (1997) Activation of nuclear transcription factor NF- κ B by interleukin-1 is accompanied by casein kinase II-mediated phosphorylation of the p65 subunit. *Journal of Biological Chemistry* 272:32606-32612
 95. Wang D, Westerheide SD, Hanson JL, Baldwin A.S. J (2000) Tumor necrosis factor α -induced phosphorylation of RelA/p65 on Ser529 is controlled by casein kinase II. *Journal of Biological Chemistry* 275:32592-32597
 96. Wang D, Baldwin a S (1998) Activation of nuclear factor- κ B-dependent transcription by tumor necrosis factor- α is mediated through phosphorylation of RelA/p65 on serine 529. *Journal of Biological Chemistry* 273:29411-29416
 97. Bristow CL, Wolkowicz R, Trucy M, et al (2007) NF- κ B signaling, elastase localization, and phagocytosis differ in HIV-1 permissive and nonpermissive U937 clones. *Journal of Immunology* 180:92-499
 98. Sakurai H, Chiba H, Miyoshi H, et al (1999) I κ B kinases phosphorylate NF- κ B p65 subunit on serine 536 in the transactivation domain. *Journal of Biological Chemistry* 274:30353-30356
 99. Sizemore N, Lerner N, Dombrowski N, et al (2002) Distinct roles of the I κ B

- kinase α and β subunits in liberating nuclear factor κ B (NF- κ B) from I κ B and in phosphorylating the p65 subunit of NF- κ B. *Journal of Biological Chemistry* 277:3863-3869
100. Haller D, Russo MP, Balfour Sartor R, Jobin C (2002) IKKB and phosphatidylinositol 3-kinase/Akt participate in non-pathogenic gram-negative enteric bacteria-induced RelA phosphorylation and NF- κ B activation in both primary and intestinal epithelial cell lines. *Journal of Biological Chemistry* 277:38168-38178
 101. Yoboua F, Martel A, Duval A, et al (2010) Respiratory syncytial virus-mediated NF- κ B p65 phosphorylation at serine 536 is dependent on RIG-I, TRAF6, and IKK. *Journal of Virology* 84:7267-7277
 102. Bao X, Indukuri H, Liu T, et al (2013) IKK ϵ MODULATES RSV-INDUCED NF- κ B-DEPENDENT GENE TRANSCRIPTION. *Virology* 6:224-231
 103. Kiernan R, Brès V, Ng RWM, et al (2003) Post-activation turn-off of NF- κ B-dependent transcription is regulated by acetylation of p65. *Journal of Biological Chemistry* 278:2758-2766
 104. Chen L feng, Mu Y, Greene WC (2002) Acetylation of RelA at discrete sites regulates distinct nuclear functions of NF- κ B. *The EMBO Journal* 21:6539-6548
 105. Chen L, Williams S a, Mu Y, et al (2005) NF- κ B RelA Phosphorylation Regulates RelA Acetylation NF- κ B RelA Phosphorylation Regulates RelA Acetylation. *Molecular and Cellular Biology* 25:7966-7975
 106. Rothgiesser KM, Fey M, Hottiger MO (2010) Acetylation of p65 at lysine 314 is important for late NF- κ B-dependent gene expression. *BMC Genomics* 11:22
 107. Lu T, Jackson MW, Wang B, et al (2010) Regulation of NF- κ B by NSD1/FBXL11-dependent reversible lysine methylation of p65. *Proceedings of the National Academy of Sciences of U.S.A.* 107:46-51
 108. Ea C-K, Baltimore D (2009) Regulation of NF- κ B activity through lysine monomethylation of p65. *Proceedings of the National Academy of Sciences of U.S.A.* 106:18972-18977
 109. Yang XD, Huang B, Li M, et al (2009) Negative regulation of NF- κ B action by Set9-mediated lysine methylation of the relA subunit. *The EMBO Journal* 28:1055-1066
 110. Seeler JS, Dejean A (2003) Nuclear and unclear functions of sumo. *Nature*

Reviews Molecular Cell Biology 4:690-699

111. Mabb AM, Miyamoto S (2007) SUMO and NF- κ B ties. *Cellular and Molecular Life Sciences* 64:1979-1996
112. Leidner J, Voogdt C, Niedenthal R, et al (2014) SUMOylation attenuates the transcriptional activity of the NF- κ B subunit Rel B. *Journal of Cellular Biochemistry* 115:1430-1440
113. Liu Y, Bridges R, Wortham A, Kulesz-Martin M (2012) NF- κ B repression by PIAS3 mediated ReLA SUMOylation. *PLoS One* 7: e37636
114. Chen LF, Greene WC (2003) Regulation of distinct biological activities of the NF- κ B transcription factor complex by acetylation. *Journal of Molecular Medicine* 81:549-557
115. Mitchell S, Vargas J, Hoffmann A (2016) Signaling via the NF κ B system. *WIREs Systems Biology and Medicine* 8:227-241
116. Orange JS, May MJ (2008) Cell penetrating peptide inhibitors of Nuclear Factor-kappa B. *Cellular and Molecular Life Sciences* 65:3564-3591
117. Madani F, Lindberg S, Langel Ü, et al (2011) Mechanisms of cellular uptake of cell-penetrating peptides. *Biophysical Journal* 2011:1-10
118. Rizzuti M, Nizzardo M, Zanetta C, et al (2015) Therapeutic applications of the cell-penetrating HIV-1 Tat peptide. *Drug Discovery Today* 20:76-85
119. Bechara C, Sagan S (2013) Cell-penetrating peptides: 20 years later, where do we stand? *FEBS Letters* 587:1693-1702
120. Guo Z, Peng H, Kang J, Sun D (2016) Cell-penetrating peptides: Possible transduction mechanisms and therapeutic applications. *Biomedical Reports* 4:528-534
121. Delcroix M, Riley LW (2010) Cell-penetrating peptides for antiviral drug development. *Pharmaceuticals* 3:448-470
122. Gros E, Deshayes S, Morris MC, et al (2006) A non-covalent peptide-based strategy for protein and peptide nucleic acid transduction. *Biochimica et Biophysica Acta - Biomembranes* 1758:384-393
123. Joliot A, Prochiantz A (2004) Transduction peptides: from technology. *Nature Cell Biology* 6:189-196
124. Kaplan IM, Wadia JS, Dowdy SF (2005) Cationic TAT peptide transduction domain enters cells by macropinocytosis. *Journal of Controlled Release* 102:247-253
125. Song XR, Torphy TJ, Griswold DE, et al (2002) Coming of Age : anti

- cytokine therapies. *Molecular Interventions* 2:36-46
126. Bradley JR, Pober JS (2001) Tumor necrosis factor receptor-associated factors (TRAFs). *Oncogene* 20:6482-91
 127. Rho SB, Park SY (2010) (WO2010041827) NF- κ B inhibitor containing ARH1 protein or gene encoding the same.
 128. Hsu H, Shu HB, Pan MG, Goeddel D V. (1996) TRADD-TRAF2 and TRADD-FADD interactions define two distinct TNF receptor 1 signal transduction pathways. *Cell* 84:299-308
 129. Cao Z, Xiong J, Takeuchi M, et al (1996) TRAF6 is a signal transducer for interleukin-1. *Nature* 383:443-446
 130. Horng T, Barton GM, Medzhitov R (2001) TIRAP: an adapter molecule in the Toll signaling pathway. *Nature Immunology* 98:12654-12658
 131. Jeyaseelan S, Manzer R, Young SK, et al (2005) Toll-IL-1 receptor domain-containing adaptor protein is critical for early lung immune responses against Escherichia coli lipopolysaccharide and viable Escherichia coli. *Journal of Immunology* 175:7484-7495
 132. Song HY, Régnier CH, Kirschning CJ, et al (1997) Tumor necrosis factor (TNF)-mediated kinase cascades: bifurcation of nuclear factor-kappaB and c-jun N-terminal kinase (JNK/SAPK) pathways at TNF receptor-associated factor 2. *Proceedings of the National Academy of Sciences of the U.S.A.* 94:9792-9796
 133. Malinin NL, Boldin MP, Kovalenko AV, Wallach D (1997) MAP3K-related kinase involved in NF- κ B induction by TNF, CD95 and IL-1. *Nature* 385:540-544
 134. Scheidereit C (2006) I κ B kinase complexes: Gateways to NF- κ B activation and transcription. *Oncogene* 25:6685-6705
 135. Logeat F, Israel N, Ten R, et al (1991) Inhibition of transcription factors belonging to the rel / NF- κ B family by a transdominant negative mutant. *The EMBO Journal* 10:1827-1832
 136. DiDonato J a, Hayakawa M, Rothwarf DM, et al (1997) A cytokine-responsive I κ B kinase that activates the transcription factor NF- κ B. *Nature* 388:548-54
 137. Mercurio F, Zhu H, Murray BW, et al (1997) IKK-1 and IKK-2: Cytokine-activated I κ B kinases essential for NF- κ B activation. *Science* 278:860-866
 138. Ling L, Cao Z, Goeddel D V. (1998) NF- κ B-inducing kinase activates IKK-

- α by phosphorylation of Ser-176. *Proceedings of the National Academy of Sciences of U.S.A.* 95:3792-3797
139. Régnier CH, Song HY, Gao X, et al (1997) Identification and characterization of an I κ B kinase. *Cell* 90:373-383
 140. Woronicz JD, Gao X, Cao Z, et al (1997) I κ B kinase- β : NF- κ B activation and complex formation with I κ B kinase- α and NIK. *Science* 278:866-869
 141. Zandi E, Rothwarf DM, Delhase M, et al (1997) The I κ B kinase complex (IKK) contains two kinase subunits, IKK β 1; and IKK β 2; necessary for I κ B phosphorylation and NF κ B activation. *Cell* 91:243-252
 142. Karin M, Yamamoto Y, Wang QM (2004) The IKK NF- κ B system: A treasure trove for drug development. *Nature Reviews Drug Discovery* 3:17-26
 143. Pande V, Ramos M (2005) NF- κ B in human disease: current inhibitors and prospects for de novo structure based design of inhibitors. *Current Medicinal Chemistry* 12:357-374
 144. Burke JR, Pattoli MA, Gregor KR, et al (2003) BMS-345541 is a highly selective inhibitor of I κ B kinase that binds at an allosteric site of the enzyme and blocks NF- κ B-dependent transcription in mice. *Journal of Biological Chemistry* 278:1450-1456
 145. Kapahi P, Takahashi T, Natoli G, et al (2000) Inhibition of NF- κ B activation by arsenite through reaction with a critical cysteine in the activation loop of I κ B kinase. *Journal of Biological Chemistry* 275:36062-36066
 146. Kwok BHB, Koh B, Ndubuisi MI, et al (2001) The anti-inflammatory natural product parthenolide from the medicinal herb Feverfew directly binds to and inhibits I κ B kinase. *Chemistry and Biology* 8:759-766
 147. Liang M-C, Bardhan S, Li C, et al (2003) Jesterone dimer, a synthetic derivative of the fungal metabolite jesterone, blocks activation of transcription factor nuclear factor kappaB by inhibiting the inhibitor of kappaB kinase. *Molecular Pharmacology* 64:123-31
 148. Liang MC, Bardhan S, Pace EA, et al (2006) Inhibition of transcription factor NF- κ B signaling proteins IKK β and p65 through specific cysteine residues by epoxyquinone a monomer: Correlation with its anti-cancer cell growth activity. *Biochemical Pharmacology* 71:634-645
 149. Zhou L, Yeo AT, Ballarano C, et al (2014) Disulfide-mediated stabilization of the I κ B kinase binding domain of NF- κ B essential modulator (NEMO). *Biochemistry* 53:7929-7944

150. Li W, Yu B, Li M, et al (2010) NEMO-binding domain peptide promotes osteoblast differentiation impaired by tumor necrosis factor alpha. *Biochemical and Biophysical Research Communication* 391:1228-1233
151. May MJ, D'Acquisto F, Madge LA, et al (2005) Selective inhibition of NF- κ B activation by a peptide that blocks the interaction of NEMO with the I κ B kinase complex. *Science* 5177:2070-2072
152. Tilstra J, Rehman KK, Hennon T, et al (2007) Protein transduction: identification, characterization and optimization. *Biochemical Society Transactions* 35:811-815
153. Choi M, Rolle S, Wellner M, et al (2003) Inhibition of NF- κ B by a TAT-NEMO-binding domain peptide accelerates constitutive apoptosis and abrogates LPS-delayed neutrophil apoptosis. *Blood* 102:2259-2267
154. Dai S, Hirayama T, Abbas S, Abu-Amer Y (2004) The I κ B kinase (IKK) inhibitor, NEMO-binding domain peptide, blocks osteoclastogenesis and bone erosion in inflammatory arthritis. *Journal of Biological Chemistry* 279:37219-37222
155. Clohisy JC, Yamanaka Y, Faccio R, Abu-Amer Y (1991) Inhibition of IKK activation, through sequestering NEMO, blocks PMMA-induced osteoclastogenesis and calvarial inflammatory osteolysis. *Journal of Orthopaedic Research* 11:1609-1612
156. Rehman KK, Bertera S, Bottino R, et al (2003) Protection of islets by in Situ peptide-mediated transduction of the I κ B kinase inhibitor nemo-binding domain peptide. *Journal of Biological Chemistry* 278:9862-9868
157. Swinney DC, Xu YZ, Scarafia LE, et al (2002) A small molecule ubiquitination inhibitor blocks NF- κ B-dependent cytokine expression in cells and rats. *Journal of Biological Chemistry* 277:23573-23581
158. Yaron A, Gonen H, Alkalay I, et al (1997) Inhibition of NF-kappa-B cellular function via specific targeting of the I-kappa-B-ubiquitin ligase. *The EMBO Journal* 16:6486-94
159. Cusack JC, Liu R, Houston M, et al (2001) Enhanced chemosensitivity to CPT-11 with proteasome inhibitor PS-341: implications for systemic Nuclear Factor- κ B inhibition advances in brief. *Cancer* 61:3535-3540
160. Hideshima T, Chauhan D, Richardson P, et al (2002) NF- κ B as a therapeutic target in multiple myeloma. *Journal of Biological Chemistry* 277:16639-16647

161. Chauhan D, Hideshima T, Anderson KC (2005) Proteasome inhibition in multiple myeloma: Therapeutic Implication. *Annual Reviews of Pharmacology and Toxicology* 45:465-476
162. Torgerson TR, Colosia a D, Donahue JP, et al (1998) Regulation of NF- κ B, AP-1, NFAT, and STAT1 nuclear import in T Lymphocytes by non-invasive delivery of peptide carrying the nuclear localization sequence of NF-kappa B p50. *Journal of Immunology* 161:6084-92
163. Lin YZ, Yao S, Veach RA, et al (1995) Inhibition of nuclear translocation of transcription factor NF- κ B by a synthetic peptide containing a cell membrane-permeable motif and nuclear localization sequence. *Journal of Biological Chemistry*. 270:14255-14258
164. Dev IK, Subbiah V (2008) Enriched fractions from clary sage for the treatment of cancer, cardiovascular and inflammatory diseases.
165. Dev IK, Subbiah V (2007) Triterpene derivatives for the treatment of cancer and inflammatory disease by inhibition of NF- κ B.
166. Morishita R, Sugimoto T, Aoki M, et al (1997) In vivo transfection of cis element "decoy" against nuclear factor- κ B binding site prevents myocardial infarction. *Nature Medicine* 3:894-899
167. Kupatt C, Wichels R, Deiß M, et al (2002) Retroinfusion of NF κ B decoy oligonucleotide extends cardioprotection achieved by CD18 inhibition in a preclinical study of myocardial ischemia and retroinfusion in pigs. *Gene Therapy* 9:518-526
168. Isomura I, Morita A (2006) Regulation of NF- κ B Signaling by Decoy oligodeoxynucleotides. *Review Literature Arts of America* 50:559-563
169. García-Piñeres AJ, Lindenmeyer MT, Merfort I (2004) Role of cysteine residues of p65/NF- κ B on the inhibition by the sesquiterpene lactone parthenolide and N-ethyl maleimide, and on its transactivating potential. *Life Sciences* 75:841-856
170. Zhang S, Won Y-K, Ong C-N, Shen H-M (2005) Anti-cancer potential of sesquiterpene lactones: bioactivity and molecular mechanisms. *Current Medicinal Chemistry* 5:239-249
171. Chaicharoenpong C, Umezawa K (2002) Synthesis and structure -activity relationship of dehydroxymethylepoxyquinomicin analogues as inhibitors of NF- κ B functions. *Bioorganic and Medicinal Chemistry* 10:3933-3939
172. Yamamoto M, Horie R, Takeiri M, et al (2008) Inactivation of NF- κ B

- components by covalent binding of (-)-dehydroxymethylepoxyquinomicin to specific cysteine residues. *Journal of Medicinal Chemistry* 51:5780-5788
173. Ariga A, Namekawa J, Matsumoto N, et al (2002) Inhibition of TNF- α -induced nuclear translocation and activation of NF- κ B by dehydroxymethylepoxyquinomicin. *Journal of Biological Chemistry* 277:24625-24630
174. Watanabe M, Nakashima M, Togano T, et al (2008) Identification of the RelA domain responsible for action of a new NF- κ B inhibitor DHMEQ. *Biochemical and Biophysical Research Communications* 376:310-314
175. Takada Y, Singh S, Aggarwal BB (2004) Identification of a p65 peptide that selectively inhibits NF- κ B activation induced by various inflammatory stimuli and its role in down-regulation of NF- κ B-mediated gene expression and up-regulation of apoptosis. *Journal of Biological Chemistry* 279:15096-15104
176. Aggarwal S, Takada Y, Singh S, et al (2004) Inhibition of growth and survival of human head and neck squamous cell carcinoma cells by curcumin via modulation of nuclear factor- κ B signaling. *International Journal of Cancer* 111:679-692
177. Zhou H, Monack DM, Kayagaki N, et al (2005) *Yersinia* virulence factor YopJ acts as a deubiquitinase to inhibit NF- κ B activation. *The Journal of Experimental Medicine* 202:1327-1332
178. Schesser K, Spiik AK, Dukuzumuremyi JM, et al (1998) The yopJ locus is required for *Yersinia*-mediated inhibition of NF- κ B activation and cytokine expression: YopJ contains a eukaryotic SH2-like domain that is essential for its repressive activity. *Molecular Microbiology* 28:1067-1079
179. Collier-Hyams LS, Zeng H, Sun J, et al (2002) Cutting edge: Salmonella AvrA effector inhibits the key proinflammatory, anti-apoptotic NF- κ B pathway. *Journal of Immunology* 169:2846-2850
180. Pahl HL, Krauss B, Schulze-Osthoff K, et al (1996) The immunosuppressive fungal metabolite gliotoxin specifically inhibits transcription factor NF- κ B. *The Journal of Experimental Medicine* 183:1829-1840
181. Erkel G, Anke T, Sterner O (1996) Inhibition of NF- κ B activation by panepoxydone. *Biochemical and Biophysical Research Communications* 226:214-221
182. Hiscott J, Nguyen TLA, Arguello M, et al (2006) Manipulation of the nuclear

- factor- κ B pathway and the innate immune response by viruses. *Oncogene* 25:6844-6867
183. Staal FJ, Roederer M, Herzenberg LA (1990) Intracellular thiols regulate activation of nuclear factor kappa B and transcription of human immunodeficiency virus. *Proceedings of the National Academy of Sciences of U.S.A.* 87:9943-9947
 184. Mihm S, Ennen J, Pessara U, et al (1991) Inhibition of HIV-1 replication and NF- κ B activity by cysteine and cysteine derivatives. *AIDS* 5:497-503
 185. McDade TP, Perugini R a, Vittimberga FJ, et al (1999) Salicylates inhibit NF- κ B activation and enhance TNF- α -induced apoptosis in human pancreatic cancer cells. *Journal of Surgical Research* 83:56-61
 186. De Bosscher K, Vanden Berghe W, Haegeman G (2006) Cross-talk between nuclear receptors and nuclear factor κ B. *Oncogene* 25:6868-6886
 187. Venkataraman L, Burakoff SJ, Sen R (1995) FK506 Inhibits antigen receptor-mediated induction of c-tel in B and T lymphoid cells. *Journal of Experimental Medicine* 181:1091-1099
 188. Serfling E, Avots A, Neumann M (1995) The architecture of the interleukin-2 promoter: a reflection of T lymphocyte activation. *Biochimica et Biophysica Acta - Gene Structure and Expression* 1263:181-200
 189. Frantz B, Nordby EC, Bren G, et al (1994) Calcineurin acts in synergy with PMA to inactivate I kappa B/MAD3, an inhibitor of NF-kappa B. *The EMBO Journal* 13:861-870
 190. Kwak JH, Jung JK, Lee H (2011) Nuclear factor-kappa B inhibitors; a patent review (2006-2010). *Expert Opinion on Therapeutic Pattern* 21:1897-1910
 191. Bergmann M, Hart L, Lindsay M, et al (1998) IkappaBalpha degradation and nuclear factor-kappaB DNA binding are insufficient for interleukin-1beta and tumor necrosis factor-alpha-induced kappaB-dependent transcription. Requirement for an additional activation pathway. *Journal of Biological Chemistry* 273:6607-6610
 192. Reddy S a G, Huang JH (1997) Phosphatidylinositol 3-kinase in interleukin 1 signaling. *Journal of Biological Chemistry* 272:29167-29173
 193. Sizemore N, Leung S, Stark GR (1999) Activation of phosphatidylinositol 3-kinase in response to interleukin-1 leads to phosphorylation and activation of the NF- κ B p65/RelA subunit. *Molecular and Cellular Biology* 19:4798-4805

194. Fujihara S, Jaffray E, Farrow SN, et al (2005) Inhibition of NF- κ B by a cell permeable form of I κ B α induces apoptosis in eosinophils. *Biochemical and Biophysical Research Communication* 326:632-637
195. Kabouridis PS, Hasan M, Newson J, et al (2002) Inhibition of NF- κ B activity by a membrane-transducing mutant of I κ B α . *Journal of Immunology* 169:2587-2593
196. Cabal-Hierro L, Lazo PS (2012) Signal transduction by tumor necrosis factor receptors. *Cell Signal* 24:1297-1305
197. Muppidi JR, Tschopp J, Siegel RM (2004) Life and death decisions: secondary complexes and lipid rafts in TNF receptor family signal transduction. *Immunity* 21:461-465
198. Ha H, Han D, Choi Y (2009) TRAF-mediated TNFR-family signaling. *Current Protocols in Immunology Chapter 11* 1-19
199. Hochstrasser M (1996) Ubiquitin-dependent protein degradation. *Annual Review of Genetics* 30:405-439
200. Ciechanover A, Iwai K (2004) The ubiquitin system: from basic mechanisms to the patient bed. *IUBMB Life* 56:193-201
201. Kloetzel PM (2004) The proteasome and MHC class I antigen processing. *Biochimica et Biophysica Acta* 1695:217-225
202. McDonough H, Patterson C (2003) CHIP: a link between the chaperone and proteasome systems. *Cell Stress Chaperones* 8:303-308
203. Kostova Z, Wolf DH (2003) For whom the bell tolls: protein quality control of the endoplasmic reticulum and the ubiquitin-proteasome connection. *The EMBO Journal* 22:2309-2317
204. Ward CL, Omura S, Kopito RR (1995) Degradation of CFTR by the ubiquitin-proteasome pathway. *Cell* 83:121-127
205. Karin M, Ben-neriah Y (2000) Phosphorylation meets ubiquitination: the control of NF- κ B activity. *Annual Reviews in Immunology* 18:621-663
206. Hoeller D, Dikic I (2009) Targeting the ubiquitin system in cancer therapy. *Nature* 458:438-444
207. Corn PG (2007) Role of the ubiquitin proteasome system in renal cell carcinoma. *BMC Biochemistry* 8:1-10
208. Herrmann J, Ciechanover A, Lerman LO, Lerman A (2004) The ubiquitin-proteasome system in cardiovascular diseases - a hypothesis extended. *Cardiovascular Research* 61:11-21

209. Petroski MD (2008) The ubiquitin system, disease, and drug discovery. *BMC Biochemistry* 9:1-15
210. Lehman NL (2009) The ubiquitin proteasome system in neuropathology. *Acta Neuropathology* 118:329-347
211. Nandi D, Tahiliani P, Kumar A, Chandu D (2006) The ubiquitin-proteasome system. *Journal of Biosciences* 31:137-155
212. Bedford L, Lowe J, Dick LR, et al (2011) Ubiquitin-like protein conjugation and the ubiquitin-proteasome system as drug targets. *Nature Reviews Drug Discovery* 10:29-46
213. Schreiber A, Peter M (2014) Substrate recognition in selective autophagy and the ubiquitin-proteasome system. *Biochimica et Biophysica Acta* 1843:163-181
214. Kleiger G, Mayor T (2014) Perilous journey: a tour of the ubiquitin-proteasome system. *Trends in Cell Biology* 24:352-359
215. Andersen KA, Martin LJ, Prince JM, Raines RT (2015) Intrinsic site-selectivity of ubiquitin dimer formation. *Protein Science* 24:182-189
216. Strieter ER, Korasick DA (2012) Unraveling the complexity of ubiquitin signaling. *ACS Chemical Biology* 7:52-63
217. Schmukle AC, Walczak H (2012) No one can whistle a symphony alone - how different ubiquitin linkages cooperate to orchestrate NF- κ B activity. *Journal of Cell Science* 125:549-559
218. Chau V, Tobias JW, Bachmair A, et al (1989) A multiubiquitin chain is confined to specific lysine in a targeted short-lived protein. *Science* 243:1576-1583
219. Thrower JS, Hoffman L, Rechsteiner M, Pickart CM (2000) Recognition of the polyubiquitin proteolytic signal. *The EMBO Journal* 19:94-102
220. Van Nocker S, Vierstra RD (1993) Multiubiquitin chains linked through lysine 48 are abundant in vivo and are competent intermediates in the ubiquitin proteolytic pathway. *Journal of Biological Chemistry* 268:24766-24773
221. Meyer HJ, Rape M (2014) Enhanced protein degradation by branched ubiquitin chains. *Cell* 157:910-921
222. Morris JR, Solomon E (2004) BRCA1: BARD1 induces the formation of conjugated ubiquitin structures, dependent on K6 of ubiquitin, in cells during DNA replication and repair. *Human Molecular Genetics* 13:807-817

223. Nishikawa H, Ooka S, Sato K, et al (2004) Mass spectrometric and mutational analyses reveal Lys-6-linked polyubiquitin chains catalyzed by BRCA1-BARD1 ubiquitin ligase. *Journal of Biological Chemistry* 279:3916-3924
224. Gatti M, Pinato S, Maiolica A, et al (2015) RNF168 promotes noncanonical K27 ubiquitination to signal DNA damage. *Cell Reports* 10:226-238
225. Hoege C, Pfander B, Moldovan GL, et al (2002) RAD6-dependent DNA repair is linked to modification of PCNA by ubiquitin and SUMO. *Nature* 419:135-141
226. Sun L, Deng L, Ea C-KCK, et al (2004) The TRAF6 ubiquitin ligase and TAK1 kinase mediate IKK activation by BCL10 and MALT1 in T lymphocytes. *Molecular Cell* 14:289-301
227. Al-Hakim AK, Zagorska A, Chapman L, et al (2008) Control of AMPK-related kinases by USP9X and atypical Lys 29 /Lys 33 -linked polyubiquitin chains. *Biochemistry Journal* 411:249-260
228. Ordureau A, Sarraf SA, Duda DM, et al (2014) Quantitative proteomics reveal a feedforward mechanism for mitochondrial PARKIN translocation and ubiquitin chain synthesis. *Molecular Cell* 56:1-16
229. Ordureau A, Heo J-M, Duda DM, et al (2015) Defining roles of PARKIN and ubiquitin phosphorylation by PINK1 in mitochondrial quality control using a ubiquitin replacement strategy. *Proceedings of the National Academy of Sciences of U.S.A.* 112:6637-6642
230. Geisler S, Holmström KM, Skujat D, et al (2010) PINK1/Parkin-mediated mitophagy is dependent on VDAC1 and p62/SQSTM1. *Nature Cell Biology* 12:119-131
231. Glauser L, Sonnay S, Stafa K, Moore DJ (2011) Parkin promotes the ubiquitination and degradation of the mitochondrial fusion factor mitofusin 1. *Journal of Neurochemistry* 118:636-645
232. Mukhopadhyay D, Riezman H (2007) Proteasome-independent functions of ubiquitin in endocytosis and signaling. *Science* 315:201-205
233. Tokunaga F, Sakata SI, Saeki Y, et al (2009) Involvement of linear polyubiquitylation of NEMO in NF- κ B activation. *Nature Cell Biology* 11:123-132
234. Walczak H, Iwai K, Dikic I (2012) Generation and physiological roles of linear ubiquitin chains. *BMC Biology* 10:23

235. Kirisako T, Kamei K, Murata S, et al (2006) A ubiquitin ligase complex assembles linear polyubiquitin chains. *The EMBO Journal* 25:4877-4887
236. Gerlach B, Cordier SM, Schmukle AC, et al (2011) Linear ubiquitination prevents inflammation and regulates immune signalling. *Nature* 471:591-596
237. Ikeda F, Deribe YL, Skånland SS, et al (2011) SHARPIN forms a linear ubiquitin ligase complex regulating NF- κ B activity and apoptosis. *Nature* 471:637-641
238. Rahighi S, Ikeda F, Kawasaki M, et al (2009) Specific recognition of linear ubiquitin chains by NEMO is important for NF- κ B activation. *Cell* 136:1098-1109
239. Matsumoto ML, Wickliffe KE, Dong KC, et al (2010) K11-linked polyubiquitination in cell cycle control revealed by a K11 linkage-specific antibody. *Molecular Cell* 39:477-484
240. Xu P, Duong DM, Seyfried NT, et al (2009) Quantitative proteomics reveals the function of unconventional ubiquitin chains in proteasomal degradation. *Cell* 137:133-145
241. Kirkpatrick DS, Hathaway NA, Hanna J, et al (2006) Quantitative analysis of in vitro ubiquitinated cyclin B1 reveals complex chain topology. *Nature Cell Biology* 8:700-710
242. Bremm A, Komander D (2011) Emerging roles for Lys11-linked polyubiquitin in cellular regulation. *Trends in Biochemical Sciences* 36:355-363
243. Hay-Koren A, Caspi M, Zilberberg A, Rosin-Arbesfeld R (2011) The EDD E3 ubiquitin ligase ubiquitinates and up-regulates β -catenin. *Molecular Biology of the Cell* 22:399-411
244. Okumura F, Hatakeyama S, Matsumoto M, et al (2004) Functional regulation of FEZ1 by the U-box-type ubiquitin ligase E4B contributes to neuritogenesis. *Journal of Biological Chemistry* 279:53533-53543
245. Peng D-J, Zeng M, Muromoto R, et al (2011) Noncanonical K27-Linked polyubiquitination of TIEG1 regulates Foxp3 expression and tumor growth. *Journal of Immunology* 186:5638-5647
246. Chastagner P, Israël A, Brou C (2006) Itch/AIP4 mediates Deltex degradation through the formation of K29-linked polyubiquitin chains. *EMBO Reports* 7:1147-1153
247. Huang H, Jeon M shin, Liao L, et al (2010) K33-linked polyubiquitination of

- T cell receptor- ζ regulates proteolysis-independent T cell signaling.
Immunity 33:60-70
248. Yuan WC, Lee YR, Lin SY, et al (2014) K33-Linked polyubiquitination of coronin 7 by Cul3-KLHL20 ubiquitin E3 ligase regulates protein trafficking. *Molecular Cell* 54:1-15
 249. Zhang L, Xu M, Scotti E, et al (2013) Both K63 and K48 ubiquitin linkages signal lysosomal degradation of the LDL receptor. *The Journal of Lipid Research* 54:1410-1420
 250. Arnason T, Ellison MJ (1994) Stress resistance in *Saccharomyces cerevisiae* is strongly correlated with assembly of a novel type of multiubiquitin chain. *Molecular and Cellular Biology* 14:7876-7883
 251. Cohen-Kaplan V, Livneh I, Avni N, et al (2016) The ubiquitin-proteasome system and autophagy: Coordinated and independent activities. *International Journal of Biochemistry and Cell Biology* 79:403-418
 252. Ravid T, Hochstrasser M (2008) Degradation signal diversity in the ubiquitin-proteasome system. *Nature Reviews Molecular Cell Biology* 9:679-690
 253. Jacobson AD, Zhang NY, Xu P, et al (2009) The lysine 48 and lysine 63 ubiquitin conjugates are processed differently by the 26S proteasome. *Journal of Biological Chemistry* 284:35485-35494
 254. Lee BH, Lee MJ, Park S, et al (2010) Enhancement of proteasome activity by a small-molecule inhibitor of USP14. *Nature* 467:179-184
 255. Lam YA, Xu W, DeMartino GN, Cohen RE (1997) Editing of ubiquitinating conjugates by an isopeptidase in the 26S proteasome. *Nature* 385:737-740
 256. Koulich E, Li X, DeMartino GN (2008) Relative structural and functional roles of multiple deubiquitylating proteins associated with mammalian 26S proteasome. *Molecular Biology of the Cell* 19:1072-1082
 257. Clague MJ, Coulson JM, Urbe S (2012) Cellular functions of the DUBs. *Journal of Cell Science* 125:277-286
 258. Katz EJ, Isasa M, Crosas B (2010) A new map to understand deubiquitination. *Biochemical Society Transactions* 38:21-28
 259. Hagai T, Levy Y (2010) Ubiquitin not only serves as a tag but also assists degradation by inducing protein unfolding. *Proceedings of the National Academy of Sciences of U.S.A.* 107:2001-2006
 260. Berndsen CE, Wolberger C (2014) New insights into ubiquitin E3 ligase

- mechanism. *Nature Structural and Molecular Biology* 21:301-307
261. Metzger MB, Hristova VA, Weissman AM (2010) HECT and RING finger families of E3 ubiquitin ligases at a glance. *Journal of Cell Science* 125:531-537
 262. Scheffner M, Kumar S (2013) Mammalian HECT ubiquitin-protein ligases: biological and pathophysiological aspects. *Biochimica et Biophysica Acta* 1843:61-74
 263. Metzger MB, Pruneda JN, Klevit RE, Weissman AM (2013) RING-type E3 ligases: master manipulators of E2 ubiquitin-conjugating enzymes and ubiquitination. *Biochimica et Biophysica Acta* 1843:47-60
 264. Hua Z, Vierstra RD (2011) The Cullin-RING ubiquitin-protein ligases. *Annual Review of Plant Biology* 62:299-334
 265. Komada M (2008) Controlling receptor downregulation by ubiquitination and deubiquitination. *Current Drug Discovery Technologies* 5:78-84
 266. Huang OW, Cochran AG (2013) Regulation of deubiquitinase proteolytic activity. *Current Opinion in Structural Biology* 23:806-811
 267. Komander D, Clague MJ, Urbe S (2009) Breaking the chains: structure and function of the deubiquitinases. *Nature Reviews Molecular Cell Biology* 10:550-563
 268. Lim K-H, Ramakrishna S, Baek K-H (2013) Molecular mechanisms and functions of cytokine-inducible deubiquitinating enzymes. *Cytokine and Growth Factor Reviews* 24:427-431
 269. Eletr ZM, Wilkinson KD (2014) Regulation of proteolysis by human deubiquitinating enzymes. *Biochimica et Biophysica Acta* 1843:114-128
 270. Nijman SMB, Luna-vargas MPA, Velds A, et al (2005) Review A Genomic and Functional Inventory of Deubiquitinating Enzymes. *Cell* 773-786
 271. Rehman SAA, Kristariyanto YA, Choi S-Y, et al (2016) MINDY-1 is a member of an evolutionarily conserved and structurally distinct new family of deubiquitinating enzymes. *Molecular Cell* 63:146-155
 272. Grou CP, Pinto MP, Mendes A V., et al (2015) The de novo synthesis of ubiquitin: identification of deubiquitinases acting on ubiquitin precursors. *Scientific Reports* 5:1-16
 273. Yao T, Cohen RE (2002) A cryptic protease couples deubiquitination and degradation by the proteasome. *Nature* 419:403-407
 274. Reyes-Turcu FE, Horton JR, Mullally JE, et al (2006) The ubiquitin binding

- domain ZnF UBP recognizes the C-terminal diglycine motif of unanchored ubiquitin. *Cell* 124:1197-1208
275. Verma R, Aravind L, Oania R, et al (2002) Role of Rpn11 metalloprotease in deubiquitination and degradation by the 26S proteasome. *Science* 298:611-615
276. Clague MJ, Urbé S (2006) Endocytosis: the DUB version. *Trends in Cell Biology* 16:551-559
277. Henderson MJ, Vij N, Zeitlin PL (2010) Ubiquitin C-terminal hydrolase-L1 protects cystic fibrosis transmembrane conductance regulator from early stages of proteasomal degradation. *Journal of Biological Chemistry* 285:11314-11325
278. McCullough J, Clague MJ, Urbé S (2004) AMSH is an endosome-associated ubiquitin isopeptidase. *The Journal of Cell Biology* 166:487-492
279. Macdonald E, Urbé S, Clague MJ (2014) USP8 controls the trafficking and sorting of lysosomal enzymes. *Traffic* 15:879-888
280. van Loosdregt J, Fleskens V, Fu J, et al (2013) Stabilization of the transcription factor Foxp3 by the deubiquitinase USP7 increases Treg-cell-suppressive capacity. *Immunity* 39:259-271
281. Nicassio F, Corrado N, Vissers JHA, et al (2007) Human USP3 is a chromatin modifier required for S phase progression and genome stability. *Current Biology* 17:1972-1977
282. Bhattacharya S, Ghosh MK (2014) Cell death and deubiquitinases: perspectives in cancer. *Biomedicine Research International* 2014:435197
283. Mtango NR, Stovsky M, VandeVoort CA, et al (2012) Essential role of ubiquitin C-terminal hydrolases UCHL1 and UCHL3 in mammalian oocyte maturation. *Journal of Cell Physiology* 227:2022-2029
284. Kovalenko A, Chable-Bessia C, Cantarella G, et al (2003) The tumour suppressor CYLD negatively regulates NF- κ B signalling by deubiquitination. *Nature Letters* 424:801-805
285. Boone DL, Turer EE, Lee EG, et al (2004) The ubiquitin-modifying enzyme A20 is required for termination of Toll-like receptor responses. *Nature Immunology* 5:1052-1060
286. Enesa K, Zakkar M, Chaudhury H, et al (2008) NF- κ B suppression by the deubiquitinating enzyme cezanne: a novel negative feedback loop in pro-inflammatory signaling. *Journal of Biological Chemistry* 283:7036-7045

287. Colleran A, Collins PE, O'Carroll C, et al (2013) Deubiquitination of NF- κ B by Ubiquitin-Specific Protease-7 promotes transcription. *Proceedings of the National Academy of Sciences of U.S.A.* 110:618-623
288. Park Y, Jin HS, Aki D, et al (2014) The ubiquitin system in immune regulation. *Advances in Immunology* 124:17-66
289. Shimizu Y, Taraborrelli L, Walczak H (2015) Linear ubiquitination in immunity. *Immunological Reviews* 266:190-207
290. Reyes-Turcu FE, Ventii KH, Wilkinson KD (2009) Regulation and cellular roles of ubiquitin-specific deubiquitinating enzymes. *Annual Review of Biochemistry* 78:363-397
291. Kessler BM, Edelman MJ (2011) PTMs in conversation: activity and function of deubiquitinating enzymes regulated via post-translational modifications. *Cell Biochemistry and Biophysics* 60:21-38
292. Cohn MA, Kee Y, Haas W, et al (2009) UAF1 is a subunit of multiple deubiquitinating enzyme complexes. *Journal of Biological Chemistry* 284:5343-5351
293. Kee Y, Yang K, Cohn MA, et al (2010) WDR20 regulates activity of the USP12·UAF1 deubiquitinating enzyme complex. *Journal of Biological Chemistry* 285:11252-11257
294. Clague MJ (2013) Oxidation controls the DUB step. *Nature* 497:49-50
295. Row PE, Prior IA, McCullough J, et al (2006) The ubiquitin isopeptidase UBPY regulates endosomal ubiquitin dynamics and is essential for receptor down-regulation. *Journal of Biological Chemistry* 281:12618-12624
296. Blagoev B, Ong SE, Kratchmarova I, Mann M (2004) Temporal analysis of phosphotyrosine-dependent signaling networks by quantitative proteomics. *Nature Biotechnology* 22:1139-1145
297. Endo A, Matsumoto M, Inada T, et al (2009) Nucleolar structure and function are regulated by the deubiquitylating enzyme USP36. *Journal of Cell Science* 122:678-686
298. Nakamura N, Hirose S (2008) Regulation of mitochondrial morphology by USP30, a deubiquitinating enzyme present in the mitochondrial outer membrane. *Molecular Biology of the Cell* 19:1903-1911
299. Rouge L, Bainbridge TW, Kwok M, et al (2016) Molecular understanding of USP7 substrate recognition and C-Terminal activation. *Structure* 24:1335-1345

300. Kim RQ, van Dijk WJ, Sixma TK (2016) Structure of USP7 catalytic domain and three Ubl-domains reveals a connector alpha-helix with regulatory role. *Journal of Structural Biology* 195:11-18
301. Hu M, Li P, Li M, et al (2002) Crystal structure of a UBP-family deubiquitinating enzyme in isolation and in complex with ubiquitin aldehyde. *Cell* 111:1041-1054
302. Huang X, Dixit VM (2016) Drugging the undruggables: exploring the ubiquitin system for drug development. *Cell Research* 26:484-498
303. Zhang W, Sidhu SS (2014) Development of inhibitors in the ubiquitination cascade. *FEBS Letters* 588:356-367
304. Tsubuki S, Saito Y, Tomioka M, et al (1996) Differential inhibition of calpain and proteasome activities by peptidyl aldehydes of di-leucine and tri-leucine. *Journal of Biochemistry* 119:572-576
305. Guo N, Peng Z (2013) MG132, a proteasome inhibitor, induces apoptosis in tumor cells. *Asia-Pacific Journal of Clinical Oncology* 9:6-11
306. Nalepa G, Rolfe M, Harper JW (2006) Drug discovery in the ubiquitin-proteasome system. *Nature Reviews Drug Discovery* 5:596-613
307. Rentsch A, Landsberg D, Brodmann T, et al (2013) Synthesis and pharmacology of proteasome inhibitors. *Angew Chemie - International Edition* 52:5450-5488
308. Hideshima T, Richardson P, Chauhan D, et al (2001) The proteasome inhibitor PS-341 inhibits growth, induces apoptosis, and overcomes drug resistance in human multiple myeloma cells. *Cancer Research* 61:3071-3076
309. Chauhan D, Hideshima T, Mitsiades C, et al (2005) Proteasome inhibitor therapy in multiple myeloma. *Molecular Cancer Therapeutics* 4:686-692
310. Pei X-Y, Dai Y, Grant S (2004) Synergistic induction of oxidative injury and apoptosis in human multiple myeloma cells by the proteasome inhibitor bortezomib and histone deacetylase inhibitors. *Clinical Cancer Research* 10:3839-3852
311. Kortuem KM, Stewart a K (2013) Carfilzomib. *Blood* 121:893-897
312. Meng L, Mohan R, Kwok BHB, et al (1999) Epoxomicin, a potent and selective proteasome inhibitor, exhibits in vivo antiinflammatory activity. *Proceedings of the National Academy of Sciences of U.S.A.* 96:10403-10408
313. Groll M, Kim KB, Kairies N, et al (2000) Crystal structure of epoxomicin:20S

- proteasome reveals a molecular basis for selectivity of α' , β' -epoxyketone proteasome inhibitors. *Journal of the American Chemical Society* 122:1237-1238
314. Demo SD, Kirk CJ, Aujay MA, et al (2007) Antitumor activity of PR-171, a novel irreversible inhibitor of the proteasome. *Cancer Research* 63:6383-6391
315. Kupperman E, Lee EC, Cao Y, et al (2010) Evaluation of the proteasome inhibitor MLN9708 in preclinical models of human cancer. *Cancer Research* 70:1970-1980
316. Yang Y, Kitagaki J, Dai RM, et al (2007) Inhibitors of ubiquitin-activating enzyme (E1), a new class of potential cancer therapeutics. *Cancer Research* 67:9472-9481
317. Xu GW, Ali M, Wood TE, et al (2010) The ubiquitin-activating enzyme E1 as a therapeutic target for the treatment of leukemia and multiple myeloma. *Blood* 115:2251-2259
318. Kitagaki J, Yang Y, Saavedra JE, et al (2009) Nitric oxide prodrug JS-K inhibits ubiquitin E1 and kills tumor cells retaining wild-type p53. *Oncogene* 28:619-624
319. Soucy TA, Smith PG, Rolfe M (2009) Targeting NEDD8-activated cullin-RING ligases for the treatment of cancer. *Clinical Cancer Research* 15:3912-3916
320. Soucy TA, Smith PG, Milhollen MA, et al (2009) An inhibitor of NEDD8-activating enzyme as a new approach to treat cancer. *Nature* 458:732-736
321. Chiba T, Tanaka K (2004) Cullin-based ubiquitin ligase and its control by NEDD8-conjugating system. *Current Protein and Peptide Science* 5:177-184
322. Goldenberg SJ, Cascio TC, Shumway SD, et al (2004) Structure of the Cand1-Cul1-Roc1 complex reveals regulatory mechanisms for the assembly of the multisubunit cullin-dependent ubiquitin ligases. *Cell* 119:517-528
323. Petroski MD, Deshaies RJ (2005) Function and regulation of cullin-RING ubiquitin ligases. *Nature Reviews Molecular Cell Biology* 6:9-20
324. Brownell JE, Sintchak MD, Gavin JM, et al (2010) Substrate-assisted inhibition of ubiquitin-like protein-activating enzymes: the NEDD8 E1 inhibitor MLN4924 forms a NEDD8-AMP mimetic in situ. *Molecular Cell* 37:102-111
325. Ye Y, Rape M (2009) Building ubiquitin chains: E2 enzymes at work. *Nature Reviews Molecular Cell Biology* 10:755-764

326. Ceccarelli DF, Tang X, Pelletier B, et al (2011) An allosteric inhibitor of the human Cdc34 ubiquitin-conjugating enzyme. *Cell* 145:1075-1087
327. Pierce JW, Schoenleber R, Jesmok G, et al (1997) Novel inhibitors of cytokine-induced I κ B α phosphorylation and endothelial cell adhesion molecule expression show anti-inflammatory effects in vivo. *Journal of Biological Chemistry* 272:21096-21103
328. Pulvino M, Liang Y, Oleksyn D, et al (2012) Inhibition of proliferation and survival of diffuse large B-cell lymphoma cells by a small-molecule inhibitor of the ubiquitin-conjugating enzyme Ubc13-Uev1A. *Blood* 120:1-33
329. Deng L, Wang C, Spencer E, et al (2000) Activation of the I κ B kinase complex by TRAF6 requires a dimeric ubiquitin-conjugating enzyme complex and a unique polyubiquitin chain. *Cell* 103:351-361
330. Souers AJ, Levenson JD, Boghaert ER, et al (2013) ABT-199, a potent and selective BCL-2 inhibitor, achieves antitumor activity while sparing platelets. *Nature Medicine* 19:202-208
331. Wu L, Grigoryan A V., Li Y, et al (2012) Specific small molecule inhibitors of Skp2-mediated p27 degradation. *Chemistry and Biology* 19:1515-1524
332. Chan CH, Morrow JK, Li CF, et al (2013) Pharmacological inactivation of Skp2 SCF ubiquitin ligase restricts cancer stem cell traits and cancer progression. *Cell* 154:556-568
333. Ito T, Ando H, Suzuki T, et al (2010) Identification of a primary target of thalidomide teratogenicity. *Science* 327:1345-1351
334. Dimopoulos MA, Richardson PG, Moreau P, Anderson KC (2014) Current treatment landscape for relapsed and/or refractory multiple myeloma. *Nature Reviews Clinical Oncology* 12:1-13
335. Yang B, Yu R, Chi X, Lu X (2013) Lenalidomide treatment for multiple myeloma: systematic review and meta-analysis of randomized controlled trials. *PLoS One* 8:1-9
336. Vassilev LT, Vu BT, Craves B, et al (2004) In vivo activation of the p53 pathway by small-molecule antagonists of MDM2. *Science* 303:844-848
337. Shangary S, Qin D, McEachern D, et al (2008) Temporal activation of p53 by a specific MDM2 inhibitor is selectively toxic to tumors and leads to complete tumor growth inhibition. *Proceedings of the National Academy of Sciences of U.S.A.* 105:3933-3938

338. Issaeva N, Bozko P, Enge M, et al (2004) Small molecule RITA binds to p53, blocks p53-HDM-2 interaction and activates p53 function in tumors. *Nature Medicine* 10:1321-1328
339. Verma R, Peters NR, D'Onofrio M, et al (2014) Ubistatins inhibit proteasome-dependent degradation by binding the ubiquitin chain. *Science* 306:117-120
340. Oeckinghaus A, Wegener E, Welteke V, et al (2007) Malt1 ubiquitination triggers NF- κ B signaling upon T-cell activation. *The EMBO Journal* 26:4634-4645
341. Kanarek N, London N, Schueler-Furman O, Ben-Neriah Y (2010) Ubiquitination and degradation of the inhibitors of NF- κ B. *Cold Spring Harbor Perspectives in Biology* 2:1-16
342. Sun SC (2011) Non-canonical NF- κ B signaling pathway. *Cell Research* 21:71-85
343. Matsuzawa A, Tseng PH, Vallabhapur S, et al (2008) Essential cytoplasmic translocation of a cytokine receptor-assembled signaling complex. *Science* 321:663-668
344. Vallabhapur S, Matsuzawa A, Zhang W, et al (2008) Non-redundant and complementary functions of adaptor proteins TRAF2 and TRAF3 in a ubiquitination cascade that activates NIK-dependent alternative NF- κ B signaling. *Nature Immunology* 9:1364-1370
345. Zarnegar B, Yamazaki S, He JQ, Cheng G (2008) Control of canonical NF- κ B activation through the NIK-IKK complex pathway. *Proceedings of the National Academy of Sciences of U.S.A.* 105:3503-3508
346. Wajant H, Scheurich P (2011) TNFR1-induced activation of the classical NF- κ B pathway. *The FEBS Journal* 278:862-876
347. Haas TL, Emmerich CH, Gerlach B, et al (2009) Recruitment of the linear ubiquitin chain assembly complex stabilizes the TNF-R1 signaling complex and is required for TNF-mediated gene induction. *Molecular Cell* 36:831-844
348. Ea CK, Deng L, Xia ZP, et al (2006) Activation of IKK by TNF α requires site-specific ubiquitination of RIP1 and polyubiquitin binding by NEMO. *Molecular Cell* 22:245-257
349. Kanayama A, Seth RB, Sun L, et al (2004) TAB2 and TAB3 activate the NF- κ B pathway through binding to polyubiquitin chains. *Molecular Cell* 15:535-

548

350. Lee TH, Shank J, Cusson N, Kelliher MA (2004) The kinase activity of Rip1 is not required for tumor necrosis factor- α -induced I κ B kinase or p38 MAP kinase activation or for the ubiquitination of Rip1 by Traf2. *Journal of Biological Chemistry* 279:33185-33191
351. Wu CJ, Conze DB, Li T, et al (2006) Sensing of Lys 63-linked polyubiquitination by NEMO is a key event in NF- κ B activation. *Nature Cell Biology* 8:398-406
352. Tokunaga F, Iwai K (2012) LUBAC, a novel ubiquitin ligase for linear ubiquitination, is crucial for inflammation and immune responses. *Microbes and Infection* 14:563-572
353. Laplantine E, Fontan E, Chiaravalli J, et al (2009) NEMO specifically recognizes K63-linked poly-ubiquitin chains through a new bipartite ubiquitin-binding domain. *The EMBO Journal* 28:2885-2895
354. Yoshikawa A, Sato Y, Yamashita M, et al (2009) Crystal structure of the NEMO ubiquitin-binding domain in complex with Lys 63-linked di-ubiquitin. *FEBS Letters* 583:3317-3322
355. Schmidt C, Peng B, Li Z, et al (2003) Mechanisms of proinflammatory cytokine-induced biphasic NF- κ B activation. *Molecular Cell* 12:1287-1300
356. Wang C, Deng L, Hong M, et al (2001) TAK1 is a ubiquitin-dependent kinase of MKK and IKK. *Nature Letters* 412:346-351
357. Yang Y, Xia F, Hermance N, et al (2011) A cytosolic ATM/NEMO/RIP1 complex recruits TAK1 to mediate the NF- κ B and p38 mitogen-activated protein kinase (MAPK)/MAPK-activated protein 2 responses to DNA damage. *Molecular and Cellular Biology* 31:2774-2786
358. Gautheron J, Courtois G (2010) "Without Ub I am nothing": NEMO as a multifunctional player in ubiquitin-mediated control of NF- κ B activation. *Cellular and Molecular Life Sciences* 67:3101-3113
359. Zhu G, Wu CJ, Zhao Y, Ashwell JD (2007) Optineurin negatively regulates TNF α -induced NF- κ B activation by competing with NEMO for ubiquitinated RIP. *Current Biology* 17:1438-1443
360. Mauro C, Pacifico F, Lavorgna A, et al (2006) ABIN-1 binds to NEMO/IKK γ and co-operates with A20 in inhibiting NF- κ B. *Journal of Biological Chemistry* 281:18482-18488
361. Wagner S, Carpentier I, Rogov V, et al (2008) Ubiquitin binding mediates

- the NF- κ B inhibitory potential of ABIN proteins. *Oncogene* 27:3739-3745
362. Dynek JN, Goncharov T, Dueber EC, et al (2010) c-IAP1 and Ubch5 promote K11-linked polyubiquitination of RIP1 in TNF signalling. *The EMBO Journal* 29:4198-4209
363. Arimoto K, Takahashi H, Hishiki T, et al (2007) Negative regulation of the RIG-I signaling by the ubiquitin ligase RNF125. *Proceedings of the National Academy of Sciences of U.S.A.* 104:7500-7505
364. Tang ED, Wang CY, Xiong Y, Guan KL (2003) A role for NF- κ B essential modifier/I κ B kinase- γ (NEMO/IKK γ) ubiquitination in the activation of the I κ B kinase complex by tumor necrosis factor- α . *Journal of Biological Chemistry* 278:37297-37305
365. Nakasone MA, Livnat-Levanon N, Glickman MH, et al (2013) Mixed-linkage ubiquitin chains send mixed messages. *Structure* 21:727-740
366. Saccani S, Marazzi I, Beg AA, Natoli G (2004) Degradation of promoter-bound p65/RelA is essential for the prompt termination of the NF- κ B response. *Journal of Experimental Medicine* 200:107-113
367. Bosisio D, Marazzi I, Agresti A, et al (2006) A hyper-dynamic equilibrium between promoter-bound and nucleoplasmic dimers controls NF- κ B-dependent gene activity. *The EMBO Journal* 25:798-810
368. Carmody RJ, Ruan Q, Palmer S, et al (2007) Negative regulation of toll-like receptor signaling by NF- κ B p50 ubiquitination blockade. *Science* 317:675-678
369. Matthews JR, Nicholson J, Jaffray E, et al (1995) Conformational changes induced of nDNA binding NF- κ B. *Nucleic Acids Research* 23:3393-3402
370. Hay RT, Nicholson J (1993) DNA binding alters the protease susceptibility of the p50 subunit of NF- κ B. *Nucleic Acids Research* 21:4592-4598
371. Kim W, Bennett EJ, Huttlin EL, et al (2011) Systematic and quantitative assessment of the ubiquitin-modified proteome. *Molecular Cell* 44:325-340
372. Udeshi ND, Svinkina T, Mertins P, et al (2013) Refined preparation and use of anti-diglycine remnant (K- ϵ -GG) antibody enables routine quantification of 10,000s of ubiquitination sites in single proteomics experiments. *Molecular and Cellular Proteomics* 12:825-831
373. Lumpkin RJ, Gu H, Zhu Y, et al (2017) Site-specific identification and quantitation of endogenous SUMO modifications under native conditions. *Nature Communications* 8:1171

374. Zhang J, Wang K, Wang S, Zheng C (2013) Herpes simplex virus 1 E3 ubiquitin ligase ICP0 protein inhibits tumor necrosis factor alpha-induced NF- κ B activation by interacting with p65/RelA and p50/NF- κ B1. *Journal of Virology* 87:12935-12948
375. Hailfinger S, Nogai H, Pelzer C, et al (2011) Malt1-dependent RelB cleavage promotes canonical NF- κ B activation in lymphocytes and lymphoma cell lines. *Proceedings of the National Academy of Sciences of U.S.A.* 108:14596-14601
376. Marienfeld R, Berberich-Siebelt F, Berberich I, et al (2001) Signal-specific and phosphorylation-dependent RelB degradation: a potential mechanism of NF- κ B control. *Oncogene* 20:8142-8147
377. Leidner J, Palkowitsch L, Marienfeld U, et al (2008) Identification of lysine residues critical for the transcriptional activity and polyubiquitination of the NF- κ B family member RelB. *Biochemical Journal* 416:117-127
378. Chang M, Jin W, Chang J-H, et al (2011) The ubiquitin ligase Peli1 negatively regulates T cell activation and prevents autoimmunity. *Nature Immunology* 12:1002-1009
379. Zarnegar BJ, Wang Y, Mahoney DJ, et al (2009) Activation of noncanonical NF- κ B requires coordinated assembly of a regulatory complex of the adaptors cIAP1, cIAP2, TRAF2, TRAF3 and the kinase NIK. *Nature Immunology* 9:1371-1378
380. Hou Y, Moreau F, Chadee K (2012) PPAR γ is an E3 ligase that induces the degradation of NF κ B/p65. *Nature Communications* 3:1300
381. Li H, Wittwer T, Weber A, et al (2012) Regulation of NF- κ B activity by competition between RelA acetylation and ubiquitination. *Oncogene* 31:611-623
382. Hochrainer K, Racchumi G, Zhang S, et al (2012) Monoubiquitination of nuclear RelA negatively regulates NF- κ B activity independent of proteasomal degradation. *Cellular and Molecular Life Sciences* 69:2057-2073
383. Hou Y, Zhang Z, Xu Q, et al (2014) Inhibitor of growth 4 induces NF κ B/p65 ubiquitin-dependent degradation. *Oncogene* 33:1997-2003
384. Ryo A, Suizu F, Yoshida Y, et al (2003) Regulation of NF- κ B signaling by Pin1-dependent prolyl isomerization and ubiquitin-mediated proteolysis of p65/RelA. *Molecular Cell* 12:1413-1426

385. Rodrigues L, Filipe J, Seldon MP, et al (2009) Termination of NF- κ B activity through a gammaherpesvirus protein that assembles an EC5S ubiquitin-ligase. *The EMBO Journal* 28:1283-1295
386. Tanaka T, Grusby MJ, Kaisho T (2007) PDLIM2-mediated termination of transcription factor NF- κ B activation by intranuclear sequestration and degradation of the p65 subunit. *Nature Immunology* 8:584-591
387. Hochrainer K, Pejanovic N, Olaseun VA, et al (2015) The ubiquitin ligase HERC3 attenuates NF- κ B-dependent transcription independently of its enzymatic activity by delivering the RelA subunit for degradation. *Nucleic Acids Research* 43:9889-9904
388. Fan Y, Mao R, Zhao Y, et al (2009) Tumor Necrosis Factor- α induces RelA degradation via ubiquitination at lysine 195 to prevent excessive Nuclear Factor- κ B activation. *Journal of Biological Chemistry* 284:29290-29297
389. Trompouki E, Hatzivassiliou E, Tschirritzis T, et al (2003) CYLD is a deubiquitinating enzyme that negatively regulates NF- κ B activation by TNFR family members. *Nature* 424:793-796
390. Reiley WW, Jin W, Lee AJ, et al (2007) Deubiquitinating enzyme CYLD negatively regulates the ubiquitin-dependent kinase Tak1 and prevents abnormal T cell responses. *Journal of Experimental Medicine* 204:1475-1485
391. Song HY, Rothe M, Goeddel D V. (1996) The tumor necrosis factor-inducible zinc finger protein A20 interacts with TRAF1/TRAF2 and inhibits NF- κ B activation. *Proceedings of the National Academy of Sciences* 93:6721-6725
392. Heyninck K, De Valck D, Vanden Berghe W, et al (1999) The zinc finger protein 20 inhibits TNF-induced NF- κ B-dependent gene expression by interfering with an RIP- or TRAF2-mediated transactivation signal and directly binds to a novel NF- κ B-inhibiting protein ABIN. *Cell* 145:1471-1482
393. Heyninck K, Beyaert R (1999) The cytokine-inducible zinc finger protein A20 inhibits IL-1-induced NF- κ B activation at the level of TRAF6. *FEBS Letters* 442:147-150
394. Evans PC, Smith TS, Lai M-J, et al (2003) A novel type of deubiquitinating enzyme. *Journal of Biological Chemistry* 278:23180-23186
395. Metzigg M, Nickles D, Falschlehner C, et al (2011) An RNAi screen identifies USP2 as a factor required for TNF- α -induced NF- κ B signaling. *International Journal of Cancer* 129:607-618

396. Yamaguchi T, Kimura J, Miki Y, Yoshida K (2007) The deubiquitinating enzyme USP11 controls an I κ B kinase α (IKK α)-p53 signaling pathway in response to tumor necrosis factor α (TNF α). *Journal of Biological Chemistry* 282:33943-33948
397. Sun W, Tan X, Shi Y, et al (2010) USP11 negatively regulates TNF α -induced NF- κ B activation by targeting on I κ B α . *Cell signalling* 22:386-394
398. Meng Q, Cai C, Sun T, et al (2015) Reversible ubiquitination shapes NLRC5 function and modulates NF- κ B activation switch. *The Journal Cell Biology* 211:1-16
399. Schweitzer K, Bozko PM, Dubiel W, Naumann M (2007) CSN controls NF- κ B by deubiquitinylation of I κ B α . *The EMBO Journal* 26:1532-1541
400. Xu G, Tan X, Wang H, et al (2010) Ubiquitin-specific peptidase 21 inhibits tumor necrosis factor α -induced nuclear factor κ B activation via binding to and deubiquitinating receptor-interacting protein 1. *Journal of Biological Chemistry* 285:969-978
401. Liu C, Wang L, Chen W, et al (2015) USP35 activated by miR let-7a inhibits cell proliferation and NF- κ B activation through stabilization of ABIN-2. *Oncotarget* 6:27891-27906
402. Schweitzer K, Naumann M (2015) CSN-associated USP48 confers stability to nuclear NF- κ B/RelA by trimming K48-linked Ub-chains. *Biochimica et Biophysica Acta - Molecular Cell Research* 1853:453-469
403. Lockhart PJ, Hulihan M, Lincoln S, et al (2004) Identification of the human ubiquitin specific protease 31 (USP31) gene: structure, sequence and expression analysis. *DNA Sequence - Journal of DNA Sequencing and Mapping* 15:9-14
404. Tzimas C, Michailidou G, Arsenakis M, et al (2006) Human ubiquitin specific protease 31 is a deubiquitinating enzyme implicated in activation of nuclear factor- κ B. *Cell Signalling* 18:83-92
405. Everett RD, Meredith M, Orr A, et al (1997) A novel ubiquitin-specific protease is dynamically associated with the PML nuclear domain and binds to a herpesvirus regulatory protein. *The EMBO Journal* 16:1519-1530
406. Holowaty MN, Sheng Y, Nguyen T, et al (2003) Protein interaction domains of the ubiquitin-specific protease, USP7/HAUSP. *Journal of Biological Chemistry* 278:47753-47761
407. Nicholson B, Kumar KGS (2011) The multifaceted roles of USP7: new

- therapeutic opportunities. *Cell Biochemistry and Biophysics* 60:61-68
408. Faesen AC, Dirac AM, Shanmugham A, et al (2011) Mechanism of USP7/HAUSP activation by its C-terminal ubiquitin-like domain and allosteric regulation by GMP-synthetase. *Molecular Cell* 44:147-159
409. Zapata JM, Pawlowski K, Haas E, et al (2001) A diverse family of proteins containing tumor necrosis factor receptor-associated factor domains. *Journal of Biological Chemistry* 276:24242-24252
410. Ma J, Martin JD, Xue Y, et al (2010) C-terminal region of USP7/HAUSP is critical for deubiquitination activity and contains a second mdm2/p53 binding site. *Archives of Biochemistry and Biophysics* 503:207-212
411. Cheon KW, Baek K-H (2006) HAUSP as a therapeutic target for hematopoietic tumors (Review). *International Journal of Oncology* 28:1209-1215
412. Frappier L, Verrijzer CP (2011) Gene expression control by protein deubiquitinases. *Current Opinion in Genetics and Development* 21:207-213
413. Schaefer JB, Morgan DO (2011) Protein-linked ubiquitin chain structure restricts activity of deubiquitinating enzymes. *Journal of Biological Chemistry* 286:45186-45196
414. Saridakis V, Sheng Y, Sarkari F, et al (2005) Structure of the p53 binding domain of HAUSP/USP7 bound to Epstein-Barr nuclear antigen 1 implications for EBV-mediated immortalization. *Molecular Cell* 18:25-36
415. Sarkari F, La Delfa A, Arrowsmith CH, et al (2010) Further insight into substrate recognition by USP7: structural and biochemical analysis of the HdmX and Hdm2 interactions with USP7. *Journal of Molecular Biology* 402:825-837
416. Sheng Y, Saridakis V, Sarkari F, et al (2006) Molecular recognition of p53 and MDM2 by USP7/HAUSP. *Nature Structural and Molecular Biology* 13:285-291
417. Hu M, Gu L, Li M, et al (2006) Structural basis of competitive recognition of p53 and MDM2 by HAUSP/USP7: implications for the regulation of the p53-MDM2 pathway. *PLoS Biology* 4:e27
418. Kim RQ, Sixma TK (2017) Regulation of USP7: a high incidence of E3 complexes. *Journal of Molecular Biology* 429:3395-3408
419. Frappier L (2012) The Epstein-Barr Virus EBNA1 Protein. *Scientifica* 2012:438204

420. Cheng J, Yang H, Fang J, et al (2015) Molecular mechanism for USP7-mediated DNMT1 stabilization by acetylation. *Nature Communications* 6:7023
421. Zhang ZM, Rothbart SB, Allison DF, et al (2015) An allosteric interaction links USP7 to deubiquitination and chromatin targeting of UHRF1. *Cell Reports* 12:1400-1406
422. Cheng J, Li Z, Gong R, et al (2015) Molecular mechanism for the substrate recognition of USP7. *Protein Cell* 6:849-852
423. Song MS, Salmena L, Carracedo A, et al (2008) The deubiquitinylation and localization of PTEN are regulated by a HAUSP-PML network. *Nature Letters* 455:813-817
424. Trotman LC, Wang X, Alimonti A, et al (2007) Ubiquitination regulates PTEN nuclear import and tumor suppression. *Cell* 128:141-156
425. Faustrup H, Bekker-Jensen S, Bartek J, et al (2009) USP7 counteracts SCFBTrCP- but not APCCdh1-mediated proteolysis of caspase. *The Journal of Cell Biology* 184:13-19
426. van der Horst A, de Vries-Smits AM, Brenkman AB, et al (2006) FOXO4 transcriptional activity is regulated by monoubiquitination and USP7/HAUSP. *Nature Cell Biology* 8:1064-1073
427. Ma H, Chen H, Guo X, et al (2012) M phase phosphorylation of the epigenetic regulator UHRF1 regulates its physical association with the deubiquitylase USP7 and stability. *Proceedings of the National Academy of Sciences of U.S.A.* 109:4828-4833
428. Tavana O, Li D, Dai C, et al (2017) HAUSP deubiquitinated and stabilizes N-Myc in neuroblastoma. *Nature Medicine* 22:1180-1186
429. Meredith M, Orr A, Everett R (1994) Herpes Simplex Virus Type 1 Immediate-Early Protein Vmw110 binds strongly and specifically to a 135-kDa cellular protein. *Virology* 200:457-469
430. Holowaty MN, Zeghouf M, Wu H, et al (2003) Protein profiling with Epstein-Barr nuclear antigen-1 reveals an interaction with the herpesvirus-associated ubiquitin-specific protease HAUSP/USP7. *Journal of Biological Chemistry* 278:29987-29994
431. Dong P, Ihira K, Hamada J, et al (2015) Reactivating p53 functions by suppressing its novel inhibitor iASPP: a potential therapeutic opportunity in p53 wild-type tumors. *Oncotarget* 6:19968-19975

432. Sarkari F, Sheng Y, Frappier L (2010) USP7-HAUSP promotes the sequence-specific DNA binding activity of p53. *PLoS One* 5:e13040
433. Faesen AC, Luna-Vargas MP, Sixma TK (2012) The role of UBL domains in ubiquitin-specific proteases. *Biochemical Society Transactions* 40:539-545
434. Schwertman P, Vermeulen W, Marteijn JA (2013) UVSSA and USP7, a new couple in transcription-coupled DNA repair. *Chromosoma* 122:275-284
435. Pfoh R, Lacdao IK, Saridakis V (2015) Deubiquitinases and the new therapeutic opportunities offered to cancer. *Endocrine-Related Cancer* 22:35-54
436. Westhoff Smith D, Sugden B (2013) Potential cellular functions of Epstein-Barr Nuclear Antigen 1 (EBNA1) of Epstein-Barr Virus. *Viruses* 5:226-240
437. Marcel V, Dichtel-Danjoy ML, Sagne C, et al (2011) Biological functions of p53 isoforms through evolution: lessons from animal and cellular models. *Cell Death and Differentiation* 18:1815-1824
438. Mendoza M, Mandani G, Momand J (2014) The MDM2 gene family. *Biomolecular Concepts* 5:9-19
439. Tang SY, Wan YP, Wu YM (2015) Death domain associated protein (Daxx), a multi-functional protein. *Cellular and Molecular Biology Letters* 20:788-797
440. Giovinazzi S, Morozov VM, Summers MK, et al (2013) USP7 and Daxx regulate mitosis progression and taxane sensitivity by affecting stability of Aurora-A kinase. *Cell Death and Differentiation* 20:721-731
441. Tang J, Qu L-K, Zhang J, et al (2006) Critical role for Daxx in regulating Mdm2. *Nature Cell Biology* 8:855-862
442. Espada J (2012) Non-catalytic functions of DNMT1. *Epigenetics* 7:115-118
443. Sidhu H, Capalash N (2017) UHRF1: The key regulator of epigenetics and molecular target for cancer therapeutics. *Tumor Biology* 39:1010428317692205
444. Kon N, Kobayashi Y, Li M, et al (2010) Inactivation of HAUSP in vivo modulates p53 function. *Oncogene* 29:1270-1279
445. Turnbull AP, Ioannidis S, Krajewski WW, et al (2017) Molecular basis of USP7 inhibition by selective small-molecule inhibitors. *Nature* 550:481-486
446. Reverdy C, Conrath S, Lopez R, et al (2012) Discovery of specific inhibitors of human USP7/HAUSP deubiquitinating enzyme. *Chemistry and Biology* 19:467-477

447. Fan YH, Cheng J, Vasudevan SA, et al (2013) USP7 inhibitor P22077 inhibits neuroblastoma growth via inducing p53-mediated apoptosis. *Cell Death and Disease* 4:1-10
448. Chauhan D, Tian Z, Nicholson B, et al (2012) A small molecule inhibitor of ubiquitin-specific protease-7 induces apoptosis in multiple myeloma cells and overcomes Bortezomib resistance. *Cancer Cell* 22:345-358
449. Colland F, Formstecher E, Jacq X, et al (2009) Small-molecule inhibitor of USP7/HAUSP ubiquitin protease stabilizes and activates p53 in cells. *Molecular Cancer Therapeutics* 8:2286-2295
450. Ritorto MS, Ewan R, Perez-Oliva AB, et al (2014) Screening of DUB activity and specificity by MALDI-TOF mass spectrometry. *Nature Communications* 5:1-11
451. Weinstock J, Wu J, Cao P, et al (2012) Selective dual inhibitors of the cancer-related deubiquitylating proteases USP7 and USP47. *ACS Medicinal Chemistry Letters* 3:789-792
452. Altun M, Kramer HB, Willems LI, et al (2011) Activity-based chemical proteomics accelerates inhibitor development for deubiquitylating enzymes. *Chemistry and Biology* 18:1401-1412
453. Kategaya L, Di Lello P, Rouge L, et al (2017) USP7 small-molecule inhibitors interfere with ubiquitin binding. *Nature* 550:534-538
454. Lamberto I, Liu X, Seo H, et al (2017) Structure-guided development of a potent and selective non-covalent active-site inhibitor of USP7. *Cell Chemical Biology* 24:1-11
455. Di Lello P, Pastor R, Murray JM, et al (2017) Discovery of small-molecule inhibitors of ubiquitin specific protease 7 (USP7) using integrated NMR and in silico techniques. *Journal of Medicinal Chemistry* 60:10056-10070
456. Livak KJ, Schmittgen TD (2001) Analysis of relative gene expression data using real-time quantitative PCR and the 2- $\Delta\Delta$ CT method. *Methods* 25:402-408
457. Baldwin AS (2001) The transcription factor NF- κ B and human disease. *Journal of Clinical Investigation* 107:3-6
458. Kumar A, Takada Y, Boriek AM, Aggarwal BB (2004) Nuclear factor- κ B: its role in health and disease. *Journal of Molecular Medicine* 82:434-448
459. Rayet B, Gelinas C (1999) Aberrant rel/nfkb genes and activity in human cancer. *Oncogene* 18:6938-6947

460. Ramsey JD, Flynn NH (2015) Cell-penetrating peptides transport therapeutics into cells. *Pharmacology and Therapeutics* 154:78-86
461. Brooks H, Lebleu B, Vives E (2005) Tat peptide-mediated cellular delivery: back to basics. *Advanced Drug Delivery Review* 57:559-577
462. Frankel AD, Pabo CO (1988) Cellular uptake of Tat protein from human immunodeficiency virus. *Cell* 55:1189-1193
463. Mann DA, Frankel AD (1991) Endocytosis and targeting exogenous HIV-1 Tat protein. *The EMBO Journal* 10:1733-1739
464. Fawell S, Seery J, Daikh Y, et al (1994) Tat-mediated delivery of heterologous proteins into cells. *Proceedings of the National Academy of Sciences of U.S.A.* 91:664-668
465. Vives E, Brodin P, Lebleu B (1997) A truncated HIV-1 Tat protein basic domain rapidly translocates through the plasma membrane and accumulates in the cell nucleus. *Journal of Biological Chemistry* 272:16010-16017
466. Collins PE, Grassia G, Colleran A, et al (2015) Mapping the interaction of B cell leukemia 3 (BCL-3) and Nuclear Factor κ B (NF- κ B) p50 identifies a BCL-3-mimetic anti-inflammatory peptide. *Journal of Biological Chemistry* 290:15687-15696
467. Prasad RC, Wang XL, Law BK, et al (2009) Identification of genes, including the gene encoding p27Kip1, regulated by serine 276 phosphorylation of the p65 subunit of NF- κ B. *Cancer Letters* 275:139-149
468. Collins PE, Mitxitorena I, Carmody RJ (2016) The ubiquitination of NF- κ B subunits in the control of transcription. *Cells* 5:23
469. Geysen HM, Rodda SJ, Mason TJ, et al (1987) Strategies for epitope analysis using peptide synthesis. *Journal of Immunological Methods* 102:259-274
470. Frank R, Overwin H (1996) SPOT Synthesis. Epitope analysis with arrays of synthetic peptides prepared on cellulose membranes. *Methods in Molecular Biology* 66:149-169
471. Reineke U, Volkmer-Engert R, Schneider-Mergener J (2001) Applications of peptide arrays prepared by the SPOT-technology. *Current Opinion in Biotechnology* 12:59-64
472. Frank R (1992) SPOT synthesis: an easy technique for the positionally addressable, parallel chemical synthesis on a membrane support.

Tetrahedron 48:9217-9232

473. Frank R, Heikens W, Heisterberg-Moutsis G, Blocker H (1983) A new general approach for the simultaneous chemical synthesis of large numbers of oligonucleotides: segmental solid supports. *Nucleic Acids Research* 11:4365-4377
474. Anand P, Nagarajan D, Mukherjee S, Chandra N (2014) ABS-Scan: In silico alanine scanning mutagenesis for binding site residues in protein-ligand complex. *F1000 Research* 3:214
475. Kiely PA, Baillie GS, Barrett R, et al (2009) Phosphorylation of RACK1 on tyrosine 52 by c-Abl is required for insulin-like growth factor I-mediated regulation of focal adhesion kinase. *Journal of Biological Chemistry* 284:20263-20274
476. Patrick GL (2013) *An Introduction to Medicinal Chemistry*, 5th ed. Oxford University Press
477. Ozen A, Rouge L, Bashore C, et al (2018) Selectively modulating conformational states of USP7 catalytic domain for activation. *Structure* 26:72-84
478. Gilmore TD, Gerondakis S (2011) The c-Rel transcription factor in development and disease. *Genes and Cancer* 2:695-711
479. Ghosh S, May MJ, Kopp EB (1998) NF- κ B and Rel proteins: Evolutionarily conserved mediators of immune responses. *Annual Review of Immunology* 16:225-260
480. Hayden MS, Ghosh S (2011) NF- κ B in immunobiology. *Cell Research* 21:223-244
481. Wan F, Lenardo MJ (2009) Specification of DNA binding activity of NF- κ B proteins. *Cold Spring Harbor Perspectives in Biology* 1:a000067
482. Bakail M, Ochsenbein F (2016) Targeting protein-protein interactions, a wide open field for drug design. *Comptes Rendus Chimie* 19:19-27
483. Rosell M, Fernández-Recio J (2018) Hot-spot analysis for drug discovery targeting protein-protein interactions. *Expert Opinion on Drug Discovery* 13:327-338
484. Chene P (2006) Drugs targeting protein-protein interactions. *ChemMedChem* 400-411
485. Hospital A, Goni JR, Orozco M, Gelpi JL (2015) Molecular dynamics simulations: advances and applications. *Advances and Applications in*

Bioinformatics and Chemistry 8:37-47

486. Lee B, Richards FM (1971) The interpretation of protein structures: estimation of static accessibility. *Journal of Molecular Biology* 55:379-4000
487. Das R, Baker D (2008) Macromolecular modeling with rosetta. *Annual Review of Biochemistry* 77:363-382
488. Vakser IA (2014) Protein-protein docking: from interaction to interactome. *Biophysical Journal* 107:1785-1793
489. Grinter SZ, Zou X (2014) Challenges, applications, and recent advances of protein-ligand docking in structure-based drug design. *Molecules* 19:10150-10176
490. Terentiev AA, Moldogazieva NT, Shaitan K V (2010) Dynamic proteomics in modeling of the living cell. Protein-protein interactions. *Biochemistry* 74:1586-1607 . doi: 10.1134/s0006297909130112
491. Bender BJ, Cisneros A, Duran AM, et al (2016) Protocols for molecular modeling with Rosetta3 and RosettaScripts. *Biochemistry* 55:4748-4763
492. Medina-Franco JL, Mendez-Lucio O, Martinez-Mayorga K (2014) The interplay between molecular modeling and chemoinformatics to characterize protein-ligand and protein-protein interactions landscapes for drug discovery. *Advances in Protein Chemistry and Structural Biology* 96:1-37
493. Meneksedag-Erol D, Tang T, Uludag H (2014) Molecular modeling of polynucleotide complexes. *Biomaterials* 35:7068-7076
494. Houry GA, Smadbeck J, Kieslich CA, Floudas CA (2014) Protein folding and de novo protein design for biotechnological applications. *Trends in Biotechnology* 32:99-109
495. Schwede T (2013) Protein modeling: what happened to the “protein structure gap”? *Structure* 21:1531-1540
496. Fiser A (2010) Template-based protein structure modeling. *Methods in Molecular Biology* 673:73-94
497. Qu X, Swanson R, Day R, Tsai J (2009) A Guide to Template Based Structure Prediction. *Current Protein and Peptide Science* 10:270-285
498. Szilagyi A, Zhang Y (2014) Template-based structure modeling of protein-protein interactions. *Current Opinion in Structural Biology* 24:10-23
499. Moreira IS, Fernandes PA, Ramos MJ (2010) Protein-protein docking dealing with the unknown. *Journal of Computational Chemistry* 31:317-342

500. Sousa SF, Fernandes PA, Ramos MJ (2006) Protein-ligand docking: current status and future challenges. *Proteins* 65:15-26
501. Bottegoni G (2011) Protein-ligand docking. *Frontiers in Bioscience* 16:2289-2306
502. Li H, Chan L, Bartuzi P, et al (2014) Copper metabolism domain-containing 1 represses genes that promote inflammation and protects mice from colitis and colitis-associated cancer. *Gastroenterology* 147:1-12
503. Maine GN, Mao X, Komarck CM, Burstein E (2007) COMMD1 promotes the ubiquitination of NF- κ B subunits through a cullin-containing ubiquitin ligase. *The EMBO Journal* 26:436-447
504. Lee KW, Cho JG, Kim CM, et al (2013) Herpesvirus-associated ubiquitin-specific protease (HAUSP) modulates peroxisome proliferator-activated receptor γ (PPAR γ) stability through its deubiquitinating activity. *Journal of Biological Chemistry* 288:32886-32896
505. Percy AJ, Rey M, Burns KM, Schriemer DC (2012) Probing protein interactions with hydrogen/deuterium exchange and mass spectrometry-A review. *Analytica Chimica Acta* 721:7-21
506. Wang L, Lane LC, Smith DL (2001) Detecting structural changes in viral capsids by hydrogen exchange and mass spectrometry. *Protein Science* 10:1234-1243